

1-1-2009

# An air dispersion model for the city of Toronto, Ontario, Canada

Barbara Sylvestre-Williams  
*Ryerson University*

Follow this and additional works at: <http://digitalcommons.ryerson.ca/dissertations>



Part of the [Climate Commons](#)

---

## Recommended Citation

Sylvestre-Williams, Barbara, "An air dispersion model for the city of Toronto, Ontario, Canada" (2009). *Theses and dissertations*. Paper 941.

This Thesis is brought to you for free and open access by Digital Commons @ Ryerson. It has been accepted for inclusion in Theses and dissertations by an authorized administrator of Digital Commons @ Ryerson. For more information, please contact [bcameron@ryerson.ca](mailto:bcameron@ryerson.ca).

61108-7000  
4C  
880.4  
1D44  
595  
2009

# **AN AIR DISPERSION MODEL FOR THE CITY OF TORONTO, ONTARIO, CANADA**

by

Barbara Sylvestre-Williams, Bachelor of Applied Science (Chemical Engineering),

University of Toronto, June 2000

A thesis

Presented to Ryerson University

In partial fulfillment of the requirements for the degree of

Master of Applied Science

in the Program of

Environmental Applied Science and Management

Toronto, Ontario, Canada, 2009

© (Barbara Sylvestre-Williams) 2009

## AUTHOR'S DECLARATION PAGE

I hereby declare that I am the sole author of this thesis.

I authorize Ryerson University to lend this thesis to other institutions or individuals for the purpose of scholarly research.

I further authorize Ryerson University to reproduce this thesis or dissertation by photocopying or by other means, in total or in part, at the request of other institutions or individuals for the purpose of scholarly research.

## ABSTRACT

### AN AIR DISPERSION MODEL FOR THE CITY OF TORONTO, ONTARIO, CANADA

By: Barbara Sylvestre-Williams

Environmental Applied Science and Management

Master of Applied Science, 2009, Ryerson University

Air quality is a major concern for the public; therefore, the reliability of models in predicting the air quality accurately is of a major interest. The objective of this study was to develop an air dispersion model and demonstrate that it can be successfully used in place of or in conjunction with ambient air monitoring stations in determining the local Air Quality Index (AQI).

This thesis begins with a review of existing atmospheric dispersion models, specifically, the Gaussian Plume models and their capabilities to handle the atmospheric chemistry of nitrogen oxides ( $\text{NO}_x$ ) and sulfur dioxides ( $\text{SO}_2$ ). It also includes a review of wet deposition in the form of in-cloud, below-cloud, and snow scavenging. Existing dispersion models are investigated to assess their capability of representing atmospheric chemistry, specifically in the context of  $\text{NO}_x$  and  $\text{SO}_{2x}$  substances and their applications to urban areas. A review was completed of previous studies where Gaussian dispersion models were applied to major cities around the world such as London, Helsinki, Kanto, and Prague, to predict ground level concentrations of  $\text{NO}_x$  and  $\text{SO}_2$ .

For the purpose of this thesis, a Gaussian air dispersion model was developed, known as the Air dispersion model for the Road Sources in Urban areaS (ARSUS) model, which is capable of predicting ground level concentrations for a contaminant of interest. The ARSUS model was

validated against the US EPA ISC3 model before it was used to conduct the two studies in this investigation. These two studies simulated weekday morning rush hour tailpipe emissions of CO and predicted ground level concentrations. The first study used the ARSUS model to predict ground level concentrations of CO from the tailpipe emissions of CO for roads and highways located in the vicinity of the Toronto West ambient air monitoring station. The second study involved an expansion of the domain to predict ground level concentrations of CO from tailpipe emissions from highways located in the City of Toronto. The modelled concentrations were then compared to the Toronto West ambient air monitoring station.

ARSUS model's results indicate that air quality in the immediate vicinity of roads or highways is highly impacted by the tailpipe emissions. Higher concentrations are observed for the areas adjacent to the road and highway sources. The tailpipe emissions of CO from highways have a higher contribution to the local air quality.

The predicted ground level concentrations from the ARSUS model do under-predict when compared to the observed data from the monitoring station; however, despite this a predictive model is viable.

## ACKNOWLEDGEMENTS

I would like to thank my thesis supervisor, Dr. Mehrab Mehrvar, for giving me the opportunity to work on this thesis and subsequently gain valuable professional knowledge. Dr. Mehrvar's on- going support, encouragement and patience provided a perfect path. The authors wish to thank the Dr. Bloxam from the Ontario Ministry of the Environment for his valuable comments.



DEDICATION

Finally, I would like to say thank you and dedicate this thesis to my beloved Nicholas, my husband, for his endless support.

TABLE OF CONTENTS

Abstract..... iii

Acknowledgements..... v

Dedication ..... vi

Table of Contents ..... vii

Tables ..... x

Figures..... xii

Appendices ..... xvii

CHAPTER 1. LITERATURE REVIEW..... 1

1.1 Introduction..... 3

1.2 Current Air Dispersion Models..... 6

1.2.1 Gaussian Dispersion Model..... 6

1.2.1.1 Basic Gaussian Plume Model..... 6

1.2.1.2 Dispersion Coefficients..... 9

1.2.1.3 Characterization of Various Emission Sources  
in Gaussian Dispersion Model ..... 12

1.2.1.4 Limitations of Gaussian Plume Dispersion..... 17

1.2.1.5 Chemistry in Gaussian Plume Dispersion..... 17

1.2.1.6 Treatment of Inversion Layers ..... 20

1.3 Atmospheric Chemistry of NO<sub>x</sub> and SO<sub>x</sub>..... 21

1.3.1 Dry Deposition ..... 22

1.3.2 Wet Deposition ..... 23

1.3.3 Cloundwater Deposition ..... 23

1.4 Application of Gaussian Plume Model to Urban Areas ..... 25

1.4.1 Dispersion Modelling of the City of Kanto, Japan..... 25

1.4.2 Dispersion Modelling of the City of London, UK ..... 25

1.4.3 Dispersion Modelling of the City of Helsinki, Finland..... 26

1.4.4 Dispersion Modelling of the City of Prague,  
Czech Republic..... 28

1.4.5 Historical Work Completed on the Simulation of Pollution Type of Studies Completed for the City of Toronto, Canada .....	28
1.4.6 Preliminary Dispersion Modeling of the City of Toronto, Canada .....	29
1.5 Conclusions .....	33
<b>CHAPTER 2. DEVELOPMENT OF THE COMPUTER MODEL.....</b>	<b>39</b>
2.1 The ARSUS Computer Model .....	39
2.2 Limitations of the ARSUS Model .....	40
2.3 Pseudo Code for the ARSUS Model.....	40
2.4 Input / Output Data for the ARSUS Model .....	50
<b>CHAPTER 3. COMPILATION OF THE INPUT DATA REQUIRED FOR THE ARSUS MODEL .....</b>	<b>52</b>
3.1 Meteorological Data.....	52
3.2 Traffic Data .....	54
3.3 Emissions Estimates.....	59
<b>CHAPTER 4. VERIFICATION AND VALIDATION OF ARSUS MODEL.....</b>	<b>63</b>
4.1 Setup of the Validation Exercise: ISC3 versus ARSUS Model .....	63
4.2 Verification Exercise of the ARSUS Model (Response to Change in Wind Direction) .....	67
4.3 Results of the Validation Exercise.....	68
4.4 Results of the Verification of the ARSUS Model's Response to Wind Change .....	72
<b>CHAPTER 5. RESULTS AND DISCUSSION .....</b>	<b>85</b>
5.1 Selection of the Ambient Air Monitoring Station .....	85
5.2 Comparison of Modelled Concentrations: ARSUS Model versus Ambient Air Quality Data from Toronto West Station .....	87
5.2.1 Small Scale Study of Tailpipe Emissions in the Vicinity of the Toronto West Monitoring Station .....	87
5.2.2 Large Scale Study of Tailpipe Emissions for the City of Toronto .....	88

5.3 Discussion of Results .....	92
<b>CHAPTER 6. CONCLUSIONS AND RECOMMENDATIONS.....</b>	<b>97</b>
6.1 Conclusions.....	97
6.2 Recommendations.....	99
<b>Appendices .....</b>	<b>102</b>
<b>References .....</b>	<b>178</b>
<b>Nomenclature .....</b>	<b>185</b>
<b>Abbreviations .....</b>	<b>186</b>

## TABLES

Table 1:	Summary of smog advisories issued from 2002 – 2005 in Ontario, Canada.....	3
Table 2:	Pasquill dispersion classes related to wind speed and insolation (Adopted from Turner 1970) .....	10
Table 3:	Constants g, h, and i for use in McMullen's equations for rural dispersion coefficients.....	11
Table 4:	Constants l, m, and n for estimation of Briggs urban dispersion coefficients.....	12
Table 5:	Initial dimensions for a virtual source .....	13
Table 6:	Power law constants used to calculate the dispersion coefficients.....	16
Table 7:	Typical aerodynamic values for various wind speeds and vegetation.....	23
Table 8:	Below-cloud scavenging constants.....	24
Table 9:	Scavenging coefficients for temperature of 10 °C.....	24
Table 10:	Summary of morning and afternoon peak time average concentrations .....	32
Table 11:	The statistical analysis of the predicted and measured hourly time series of NO <sub>2</sub> concentrations. Morning and afternoon Traffic Peak Hours for February 1-4, 2005.....	32
Table 3-1:	Toronto Lester B. Pearson International Airport location in City of Toronto, Ontario, Canada. The 1 h surface meteorological data was obtained from this station for the 2007 year, Figure 3-1.....	52
Table 3-2:	Summary of seasonal meteorological variations observed at the Toronto Lester B. Pearson International Airport for the year 2007. ....	54
Table 3-3:	Summary of Major Highways From which Emissions were Estimated, City of Toronto, Ontario, Canada. ....	59
Table 3-4:	Summary of traffic composition assumed for the highways and municipal roads.....	62
Table 4-1:	Meteorological parameters used to validate ISC3 and the ARSUS model. ....	63
Table 4-2:	Summary of emission source parameters used to validate ISC3 and the ARSUS model.....	67

Table 4-3:	Summary of emission source parameters used to validate ISC3 and the ARSUS model.....	67
Table 4-4:	Summary of the linear regression conducted on the plots for Cases 1-3 on Figures 4-4 to 4-6.....	68
Table 4-5:	Summary of the linear regression conducted on the plots for Cases 1-3, validation of volume source algorithm, on Figures 4-11 to 4-13. ....	72
Table 5-1:	Summary of Ambient Air Monitoring Stations located in the city of Toronto and corresponding substances each station monitors for.....	87



## FIGURES

Figure 1.	Elevated point source described by Gaussian Plume model.....	7
Figure 2.	Effective stack height of a point source is a sum of the stack height and plume rise. The momentum and thermal rise add up to the physical height of the stack creating an effective stack height.....	8
Figure 3.	Side of image source which allows for the reflection of plume off ground.....	9
Figure 4.	Effect of urban and rural dispersion coefficients. For urban areas a higher maximum ground level concentration, i.e. $C_{max}(\text{urban})$ , is observed and closer to the source. For rural areas a lower maximum ground level concentration, i.e. $C_{max}(\text{rural})$ , is observed and it occurs further from the source. ....	11
Figure 5.	(Upper) Line source represented by adjacent volume source. (Lower) Line source represented by separated volume source.....	12
Figure 6.	A line source of length $L$ and strength $Ql$ . ....	14
Figure 7.	Infinite line source with strength $Ql$ at an oblique angle ( $\theta$ ) to the wind.....	15
Figure 8.	An area source with strength $Qa$ and width $x1$ .....	16
Figure 9.	Fumigation induced by an inversion layer located above the effective stack height. The inversion layer acts similar to a mirror sealing and forces the plume to the group which result in poor dispersion and higher maximum ground level concentrations at the ground level. ....	21
Figure 10.	The preliminary study was conducted by simulating emissions from a 3 block sector around Yonge Street and Finch Avenue intersection located more than 20 km from the nearest source of meteorological data (International Airport). ....	30
Figure 11.	February 1 to 5, 2005 - wind rose from Toronto Lester B. Pearson International Airport (WMO Identifier 6158733) for the period associated with the study of emissions of $NO_x$ from a road network located in the city of Toronto, Ontario, Canada.....	30
Figure 12.	Area of study located in the city of Toronto, Canada, and modeled contour plots of ground level concentrations, $NO_x$ $\mu g/m^3$ (4 PM, February 4, 2005).....	31

Figure 2-1a.	Flow diagram of FUNCTION: Concentration.m. This is the main program which reads input file and meteorological file, utilizes WindCorrection.m and Gaussian.m functions to estimate concentrations and write them into an EXCEL file. ....	41
Figure 2-1b.	Flow diagram of FUNCTION: WindCorrection.m. This function converts the wind angle from North = 00 to North = 900 and returns the corrected value to the main program (Concentration.m). ....	44
Figure 2-1c.	Flow diagram of FUNCTION: Gaussian.m. This function calculates dispersion parameters using Equation (7) which as subsequently used to calculate ground level concentration using Equation (3). The calculated concentration for point (x,y) is returned to the main program: Concentration.m (Figure 2-1a). ....	45
Figure 2-1d.	Flow diagram of FUNCTION: PlumeRise.m. This function calculates effective stack height due to momentum rise and thermal rise as shown in Figures 1 and 2. The solutions were adopted from the Brigg's approach to estimating effective stack height as a function of atmospheric stability class and downwind distance from the source (Beychok, 1994), (US EPA, 1995). ....	46
Figure 2-2.	A conceptual representation of the input data, ARSUS model and output data files.....	51
Figure 3-1.	Modelling domain for the City of Toronto, Ontario, Canada, showing location of the Toronto's Lester B. Pearson International Airport from which the meteorological data was obtained.....	53
Figure 3-2.	Wind rose for the year 2007 showing wind speeds and dominant wind direction. The meteorological data were obtained from the Meteorological Station, Climate I.D. 6158733. ....	55
Figure 3-3.	Annual wind class frequency distribution for the 2007 meteorological data from the Toronto Lester B. Pearson International Airport. Majority of the wind speeds occur between 2.1 and 5.7 m/s and during winter, spring and fall seasons. ....	56
Figure 3-4.	Annual stability class frequency distribution for the 2007 meteorological data from the Toronto Lester B. Pearson International Airport. Stability class D is occurs 56.5% of the time, and from seasonal analysis occurs in winter, spring and fall seasons. ....	57
Figure 3-5.	Summary of road and highway links used to complete the dispersion modelling exercise for the smaller scale exercise. Emissions from the roads and highways in the vicinity of the Toronto West monitoring station were considered in this modelling exercise. ....	60

Figure 3-6.	Summary of road and highway links used to complete the dispersion modelling exercise for the larger scale exercise. Emissions from the highways passing through the city of Toronto were considered in this modelling exercise.....	61
Figure 4-1.	CASE 1 - Simple setup with a single source emitting at 1 g/s and location of selected receptors at which concentrations were modelled. ....	64
Figure 4-2.	CASE 2 – An expansion of CASE 1 with identical sources increased to a total of 11. ....	65
Figure 4-3.	CASE 3 – An expansion of Case 2 with total number of identical sources to a total of 55. ....	66
Figure 4-4.	CASE 1 (Validation of Point Source Algorithm) – A plot of ISC3 modelled concentrations versus ARSUS modelled concentrations showing good agreement. ....	69
Figure 4-5.	CASE 2 (Validation of Point Source Algorithm) – A plot of ISC3 modelled concentrations versus ARSUS modelled concentrations showing good agreement. ....	70
Figure 4-6.	CASE 3 (Validation of Point Source Algorithm) – A plot of ISC3 modelled concentrations versus ARSUS modelled concentrations showing good agreement. ....	71
Figure 4-7.	A plot of concentration isopleths, concentration generated by the ARSUS and ISC3. The ARSUS model slightly under-predicts and does respond well to changes in wind direction. ....	74
Figure 4-8.	CASE 1 (Validation of Point Source Algorithm) - A plot of residuals showing the ARSUS model under-prediction of modelled concentrations.....	75
Figure 4-9.	CASE 2 (Validation of Point Source Algorithm) – A plot of residuals showing the ARSUS model under-prediction of modelled concentrations. ....	76
Figure 4-10.	CASE 3 (Validation of Point Source Algorithm) - A plot of residuals showing the ARSUS model under-prediction of modelled concentrations. ....	77
Figure 4-11.	CASE 1 (Validation of Volume Source Algorithm) – A plot of ISC3 modelled concentrations versus ARSUS modelled concentrations showing good agreement. ....	78
Figure 4-12.	CASE 2 (Validation of Volume Source Algorithm) – A plot of ISC3 modelled concentrations versus ARSUS modelled concentrations showing good agreement.....	79
Figure 4-13.	CASE 3 (Validation of Volume Source Algorithm) – A plot of ISC3 modelled concentrations versus ARSUS modelled concentrations showing good agreement.....	80
Figure 4-14.	CASE 1 (Validation of Volume Source) – A plot of isopleths of concentrations generated by the ISC3 and the ARSUS. ....	81
Figure 4-15.	CASE 1 (Validation of Volume Source Algorithm) - A plot of residuals showing the ARSUS model under-prediction of modelled concentrations. ....	82
Figure 4-16.	CASE 2 (Validation of Volume Source Algorithm) – A plot of residuals showing the ARSUS model under-prediction of modelled concentrations.....	83
Figure 4-17.	CASE 3 (Validation of Volume Source Algorithm) – A plot of residuals showing the ARSUS model under-prediction of modelled concentrations. ....	84
Figure 5-1.	Modelling domain for the City of Toronto, Ontario, Canada, showing location of the Toronto's Lester B. Pearson International Airport from which the meteorological data was obtained from as well as all 4 MOE Ambient Air Monitoring Stations. As well as approximate boundary for which the modelling was completed.....	86
Figure 5-2.	Sample of an isopleths plot for 1 h, CO concentration predicted by the ARSUS model, April 6 at 6 am 2007. Contribution of CO to the ground level concentrations from the local roads and highways, in the vicinity of the Toronto West monitoring station.....	89
Figure 5-3.	Small scale study of tailpipe emissions from roads and highways in the vicinity of the Toronto West monitoring station. Plot of residuals for concentrations of CO predicted by the ARSUS model and the data from the Toronto West ambient air monitoring station, month of April and May 2007, 6 am to 11 am and weekdays.....	90
Figure 5-4.	Small scale study of tailpipe emissions from roads and highways in the city of Toronto. Plot of percentage for concentrations of CO predicted by the ARSUS model and the data from the Toronto West ambient air monitoring station, month of April 2007 and May, 6 am to 11 am and weekdays. ....	91
Figure 5-5.	Sample of a isopleths plot for 1 h, CO concentration predicted by the ARSUS model, April 6 at 6 am 2007. Contribution of CO from tailpipe emissions (highways only) to the ground level concentrations, in the city of Toronto.....	93
Figure 5-6.	Large scale study of tailpipe emissions from highways in the city of Toronto. Plot of residuals for concentrations of CO predicted by the ARSUS model and the data from the Toronto West ambient air monitoring station, month of April 2007, 6 am to 11 am and weekdays.....	94

Figure 5-7. Large scale study of tailpipe emissions from highways in the city of Toronto. Plot of percentage for concentrations of CO predicted by the ARSUS model and the data from the Toronto West ambient air monitoring station, month of April 2007, 6 am to 11 am and weekdays .....95

## APPENDICES

APPENDIX 1:	SAMPLE OF PROCESSED METEOROLOGICAL DATA
APPENDIX 2:	TRAFFIC AND EMISSIONS DATA
APPENDIX 3:	SUMMARY OF UTM COORDINATES FOR BOTH SOURCES AND RECEPTORS USED IN THE VALIDATION EXERCISE
APPENDIX 4:	SAMPLE OF THE ISC3 INPUT FILE FOR VALIDATION OF POINT SOURCE ALGORITHM EXERCISE
APPENDIX 5:	SAMPLE OF THE ISC3 INPUT FILES FOR VALIDATION OF VOLUME SOURCE ALGORITHM EXERCISE
APPENDIX 6:	TABULATED DATA FROM THE VALIDATION EXERCISES OF POINT AND VOLUME SOURCE ALGORITHMS
APPENDIX 7:	AMBIENT AIR MONITORING DATA 2007
APPENDIX 8:	APPENDIX 8: TABULATED DATA FROM THE SMALL AND LARGE SCALE MODELLING EXERCISE
APPENDIX 9:	ARSUS CODE



# CHAPTER 1

## LITERATURE REVIEW

Chapter 1 is a published paper in the International Journal of Engineering, Laskarzewski B., M. Mehrvar, *"Atmospheric Chemistry in Existing Air Atmospheric Dispersion Models and Their Applications: Trends, Advances and Future in Urban Areas in Ontario, Canada and the World"*, International Journal of Engineering, Volume 3, Issue 1, 21-57, March 2009. It is a literature review on Gaussian air dispersion modelling in urban areas.

The format of the paper has been maintained as per the journal's format. Chapter 2 onward is formatted as per the Ryerson's accepted format for a Master's Thesis.

### Atmospheric Chemistry in Existing Air Atmospheric Dispersion Models and Their Applications: Trends, Advances and Future in Urban Areas in Ontario, Canada and in Other Areas of the World

**Barbara Laskarzewski**

Environmental Applied Science and Management  
Ryerson University  
350 Victoria Street, Toronto Ontario, Canada, M5B 2K3

blaskarz@ryerson.ca

**Mehrab Mehrvar**

Department of Chemical Engineering  
Ryerson University  
350 Victoria Street, Toronto Ontario, Canada, M5B 2K3

mmehrvar@ryerson.ca

#### ABSTRACT

Air quality is a major concern for the public. Therefore, the reliability in modeling and predicting the air quality accurately is of a major interest. This study reviews existing atmospheric dispersion models, specifically, the Gaussian Plume models and their capabilities to handle the atmospheric chemistry of nitrogen oxides ( $\text{NO}_x$ ) and sulfur dioxides ( $\text{SO}_2$ ). It also includes a review of wet deposition in the form of in-cloud, below cloud, and snow scavenging. Existing dispersion models are investigated to assess their capability of handling atmospheric chemistry, specifically in the context of  $\text{NO}_x$  and  $\text{SO}_2$  substances and their applications to urban areas. A number of previous studies have been conducted where Gaussian dispersion model was applied to major cities around the world such as London, Helsinki, Kanto, and Prague, to predict ground level concentrations of  $\text{NO}_x$  and  $\text{SO}_2$ . These studies demonstrated a good agreement between the modeled and observed ground level concentrations of  $\text{NO}_x$  and  $\text{SO}_2$ . Toronto, Ontario, Canada is also a heavily populated urban area where a dispersion model could be applied to evaluate ground level concentrations of various contaminants to better understand the air quality. This paper also includes a preliminary study of road emissions for a segment of the city of Toronto and its busy streets during morning and afternoon rush hours. The results of the modeling are compared to the observed data. The small scale test of dispersion of  $\text{NO}_2$  in the city of Toronto was utilized for the local hourly

meteorological data and traffic emissions. The predicted ground level concentrations were compared to Air Quality Index (AQI) data and showed a good agreement. Another improvement addressed here is a discussion on various wet deposition such as in cloud, below cloud, and snow.

**Keywords:** Air quality data, Air dispersion modeling, Gaussian dispersion model, Dry deposition, Wet deposition (in-cloud, below cloud, snow), Urban emissions

## 1. INTRODUCTION

Over the past few years, the smog days in Ontario, Canada have been steadily increasing. Overall, longer smog episodes are observed with occurrences outside of the regular smog season. Air pollution limits the enjoyment of the outdoors and increases the cost of the health care [1] and [2]. To combat this problem, the Ontario Ministry of Environment (MOE) introduced new tools to reduce emissions as well as improved communication with the public on the state of the air quality. The communication policy has been implemented by the introduction of an Air Quality Index (AQI) based on actual pollutant concentrations reported by various monitoring stations across Ontario. One major concern is the spatial distribution of pollutants not captured by monitoring stations.

To further enhance the understanding of pollution in an urban area, studies involving computational fluid dynamics (CFD) for street canyons, the land use regression (LUR), and the use of dispersion models have been conducted [3]. For a number of cities across the world dispersion models were applied to urban areas to understand pollution in a given city [4], [5], [6], [7] and [8]. The objective of these studies was to develop new air quality standards. These studies compared modeled ground level concentrations of  $\text{NO}_x$ ,  $\text{SO}_2$ , and CO to the monitored data and showed a good agreement between observed and predicted data.

Therefore, the main objectives of this study are to review the developments of Gaussian dispersion model, to review the dispersion modeling applied to urban areas, and to conduct a small scale test for the city of Toronto, Ontario, Canada.

Over the years, the dispersion models have been used by the policy makers to develop air quality standards, an approach applicable to the city of Toronto, Ontario, Canada [10] and [11]. In 2005, fifteen smog advisories, a record number covering 53 days, were issued during smog season [12] in Toronto, Ontario, Canada. This is also a record number of days covering smog since the start of the Smog Alert Program in Ontario in 2002. Even more prominent was an episode that lasted 5 days in February 2005 and occurred outside smog season due to elevated levels of particulate matter with diameter less than 2.5 micrometers ( $\text{PM}_{2.5}$ ) followed by the earliest smog advisory ever issued during the normal smog season in April, 2005. As shown in Table 1, there has been an increase in smog advisories since 2002 [12], [13], [14] and [15].

**TABLE 1:** Summary of smog advisories issued from 2002 to 2005 in Ontario, Canada [12-15]

Year	Number of Advisories	Number of Days
2002	10	27
2003	7	19
2004	8	20
2005	15	53

Since 1999, each air quality study completed states that the air quality in Ontario is improving [12-18]. In 2005, the Ontario Medical Association (OMA) announced air pollution costs were estimated to be \$507,000,000 in direct health care costs [1]. The OMA deems the cost to be an underestimate and a better understanding of air pollution and its effect on human health is required. In the past few years, a number of air initiatives have been established by the Ontario Ministry of the Environment (MOE). The initiatives include recently improved means of how the state of air quality is reported to the general public, the implementation of new regulations and mandates to reduce industrial emissions, and the review of the air quality standards for the province. For many that live in and around the Great Toronto Area (GTA), checking the AQI became a daily routine [19]. In recent years, AQI was reported to public using a new scale with a range of 1 to 100, good to very poor, respectively. Along with the quantitative scale, AQI lists the primary contaminant of greatest impact on human health which results in a poor air quality. Furthermore, the public is provided with a brief summary warning of how the pollutants affect vulnerable population so that necessary precautions may be undertaken. At the present time, the Ministry of the Environment utilizes data from Environment Canada's Canadian Regional and Hemispheric Ozone and  $\text{NO}_x$  System (CHRONOS), NOAA's WRF/CHEM and NOAA-EPA NCEP/AQFS models to forecast air quality for the City of Toronto [20]. The primary objective is to forecast smog episodes.

The AQI information is obtained via a network of 44 ambient air monitoring stations and 444 municipalities across Ontario [12] and [21]. In addition to improving public communication on the status of the air quality, the MOE established a set of new regulations targeting industries with the direct objectives to reduce emissions. Since the early 70's, the MOE established a permitting system that set ground level limits. All industrial emitters were required by law, Section 9 of Canadian Environmental Protection Act (CEPA), to utilize an air dispersion model (Appendix A: Ontario Regulation 346 (O.Reg. 346)) and site specific emissions to demonstrate compliance against set ground level concentrations for the contaminants of interest. With time, the tools used to demonstrate compliance were clearly becoming out of date [22]. As the regulation aged, limitations began to slow the approval process and prevent certain applicants from obtaining permission to conduct work. It became apparent that in order to address the public concern, i.e., poor air quality, and pressure from industry, the MOE began to look into alternative solutions. In the 90's, the MOE introduced a number of alternative permits and an Environmental Leaders program. The new permits (i.e. streamline review, the use of conditions in permits, and the comprehensive permits) were becoming ineffective as shown by the internal review of MOE's work. Specifically, work was conducted by Standards Compliance Branch (SCB), former Environmental SWAT Team, and Selected Targets Air Compliance (STAC) department. The SCB's work on regular basis demonstrated that approximately 60% of an industrial sector was found to be in non-compliance with provincial regulations [23]. The Environmental Leaders program is a program where companies are invited to sign up and are included under following conditions [24]:

- commitment to voluntary reduction of emissions; and
- making production and emission data available to the public.

In exchange, Environmental Leaders program members are promised:

- the public acknowledgement in MOE's publications; and
- the recognition on the Ministry's web site.



Currently, there are nine members listed on the MOE's website [24]. As stated by the Industrial Pollution Team, the program was not effective in Ontario [24]. The report prepared by the Industrial Pollution Team specifically addresses the need to update tools (i.e. air dispersion models) utilized in the permitting process. Poor air quality, aging permitting system, and industries not committing to reduce emissions resulted in an overhaul of the system by implementation of the following new regulations:

1. Ontario Regulation 419/05, entitled "Air Pollution – Local Air Quality", (O.Reg. 419/05) replaced O.Reg. 346 allowing companies to utilize new dispersion models: Industrial Source Complex – Short Term Model [Version 3]-Plume Rise Model Enhancements (ISC-PRIME), the American Meteorological Society/Environmental Protection Agency Regulatory Model Improvement Committee's Dispersion Model (AERMOD) along with the establishment of new air standards [25];
2. Ontario Regulation 127/01, entitled "Airborne Contaminant Discharge Monitoring and Reporting", (O.Reg. 127/01) which is an annual emissions reporting program due by June 1st each year [26];
3. Data from annual reporting programs was utilized to implement Ontario Regulation 194/05, entitled "Industrial Emissions – Nitrogen Oxides and Sulphur Dioxide", (O.Reg. 194) which caps NO<sub>x</sub> and SO<sub>x</sub> emissions of very specific industries with set reduction targets [27]. The targets are intensity based. For industries that do not meet their targets, options of trading or paying for the emissions exist;
4. On the federal level, a National Pollutant Release Inventory (NPRI), a program similar to O.Reg. 127/01 which requires industries to submit an annual emissions report by June 1st each year [28];
5. On the federal level, Canadian Environmental Protection Act Section 71 (CEPA S. 71) requires for specific industries, as identified within the reporting requirement, to submit annual emissions by May 31 due [29] with the objective to set future targets that will lower annual emissions. Due May 31st 2008 are the annual 2006 values; and
6. On the federal level, a Greenhouse Gases Release (GHG) inventory was introduced for larger emitters (> 100 ktonnes/year) of CO<sub>2</sub> which requires annual reporting. [30]

With the rise of the poor air quality in Ontario that causes high health costs, the MOE began to update its 30 year old system. This improvement is coming about in forms of various new regulations with objectives to reduce overall emissions. The current reforms and expansion of regulations within the province of Ontario have a goal in common to reduce emissions that have a health impact. Other Canadian provinces such as British Columbia [31] and Alberta [32] are also undergoing reforms to improve their air quality. These provinces are moving to implement advanced air dispersion models to study the air quality.

The annual air quality studies, new regulations, and air standards all published by the MOE do not link together at the present time. The AQI warnings issued to the public in most cases are based on readings from one monitoring station within a region [33]. Uniform air quality across the municipality of interest is the main assumption undertaken with the AQI warnings. Data used to establish the AQI is not processed or reviewed for quality control [33]. Historical data, statistical analysis, decay rate, or predicted future quality of air is not provided. Data used to establish the AQI undergoes minimal review for quality control [33]. Both assumptions of uniformity and minimal quality check have been recognized in the most recent Environmental Commissioner of Ontario report [34] as providing a "false sense of security".

The AQI notification program can be refined by completing air dispersion modeling for a city. This approach incorporates a reduced grid size, utilization of local meteorological conditions, input of actual emissions from surround sources, and predicted concentration contours at various time frames, i.e., sub hourly and hourly, to better represent the state of air quality within the area of interest. There are a number of similar approaches currently conducted in other countries [4], [5], [6], [7], [8] and [9], of which all share the same objective to utilize air dispersion models for a city and use the information to understand air quality and provide information to develop air quality standards for that city.

In order to understand the limitations of the air dispersion models, next section provides an overview of the Gaussian Plume model. Subsequently, a discussion follows with a review of standard methods applied to handle dry and wet deposition specifically in box models. This is followed by a review of other wet deposition (i.e. in-cloud, below cloud, and snow scavenging) not necessarily already implemented in box models. Section 4 takes the knowledge from previous discussion and concentrates on how the dispersion models have been applied up to date to urban areas with a review of five studies. The studies show that Gaussian dispersion model should be used to urban areas and yields good results. Finally, in our own study, a small scale study was conducted for the city of Toronto, Ontario, Canada, utilizing local meteorological and traffic data. This is a preliminary study which confirms Gaussian dispersion could be applied to the city of Toronto and it can be expanded to include other factors, such as wet deposition, scavenging, and reactions, in the model.

## 2. CURRENT AIR DISPERSION MODELS

The atmospheric dispersion modeling has been an area of interest for a long time. In the past, the limitation of studying atmospheric dispersion was limited to the data processing. The original dispersion models addressed very specific situations such as a set of screen models (SCREEN3, TSCREEN, VISCREEN etc.) containing generated meteorological conditions which were not based on measured data. There are also models which apply to specific solution, a single scenario such as point source (ADAM), spill (AFTOX), and road (CALINE3). With the advancement of computing power, the box type of air dispersion models became widely available (ISC-PRIME, AEMOD, CALPUFF). The advantage of the box type models is not only being readily available in most cases but also is capable of handling multiple emission sources. At the present time, the most of the box dispersion models are under the management of the US Environmental Protection Agency (US EPA) [35]. Many of these box models are widely used in other countries and recently a number of environmental governing bodies set these air dispersion models on the preferred list [25], [31], [32] and [36]. The box models allow the user to enter information about meteorology, emission sources, and in some instances topography. The information is processed by the box models to provide concentrations of the pollutant of interest. With the recent expansion of computing speeds and the ability to handle large data, dispersion modeling has been expanded. In many cases, the models are used to simulate urban areas or emergency situations. The new tools allow for the evaluation of past events and the prediction of future events such as poor air quality days (i.e. smog) in the cities. This study concentrates on the revaluation of such dispersion model, Plume model and its capability to handle atmospheric chemistry, specifically how the chemistry of NO<sub>x</sub> and SO<sub>2</sub> contaminants have been treated in a Gaussian Plume model for an urban area.

### 2.1. Gaussian Dispersion Model

The concepts of the Gaussian Plume model, dispersion coefficients, characterization of sources (i.e. volume, line, and area sources), limitations of the model, and the capabilities to handle atmospheric chemistry are discussed in this section. The discussion revolves around concepts that apply to urban type of sources.

#### 2.1.1. Basic Gaussian Plume Model

Between the seventeenth and eighteenth centuries, a bell-shaped distribution called "Gaussian-distribution" was derived by De Moivre, Gauss, and Laplace [37]. Experiments conducted by Shlien and Corrsin [38] related to dispersion of a plume related Gaussian behaviour. This discovery has since been used to provide a method of predicting the turbulent dispersion of air pollutants in the atmosphere. The basic Gaussian Plume is as follows [37]:

$$C(x, y, z) = \frac{Q_p}{2\pi U \sigma_y \sigma_z} \exp\left(-\frac{y^2}{2\sigma_y^2} - \frac{z^2}{2\sigma_z^2}\right) \quad (1)$$

where  $C$ ,  $Q_p$ ,  $\sigma_y$ ,  $\sigma_z$ , and  $U$  are average mass concentration [ $\text{g}/\text{m}^3$ ], strength of the point source [ $\text{g}/\text{s}$ ], dispersion coefficient in y-direction [ $\text{m}$ ], dispersion coefficient in z-direction [ $\text{m}$ ], and wind velocity [ $\text{m}/\text{s}$ ], respectively. This equation applies to an elevated point source located at the origin (0,0) and the height of  $H$ , in a wind-oriented coordinate system where the x-axis is the direction of the wind, as shown in Figure 1.

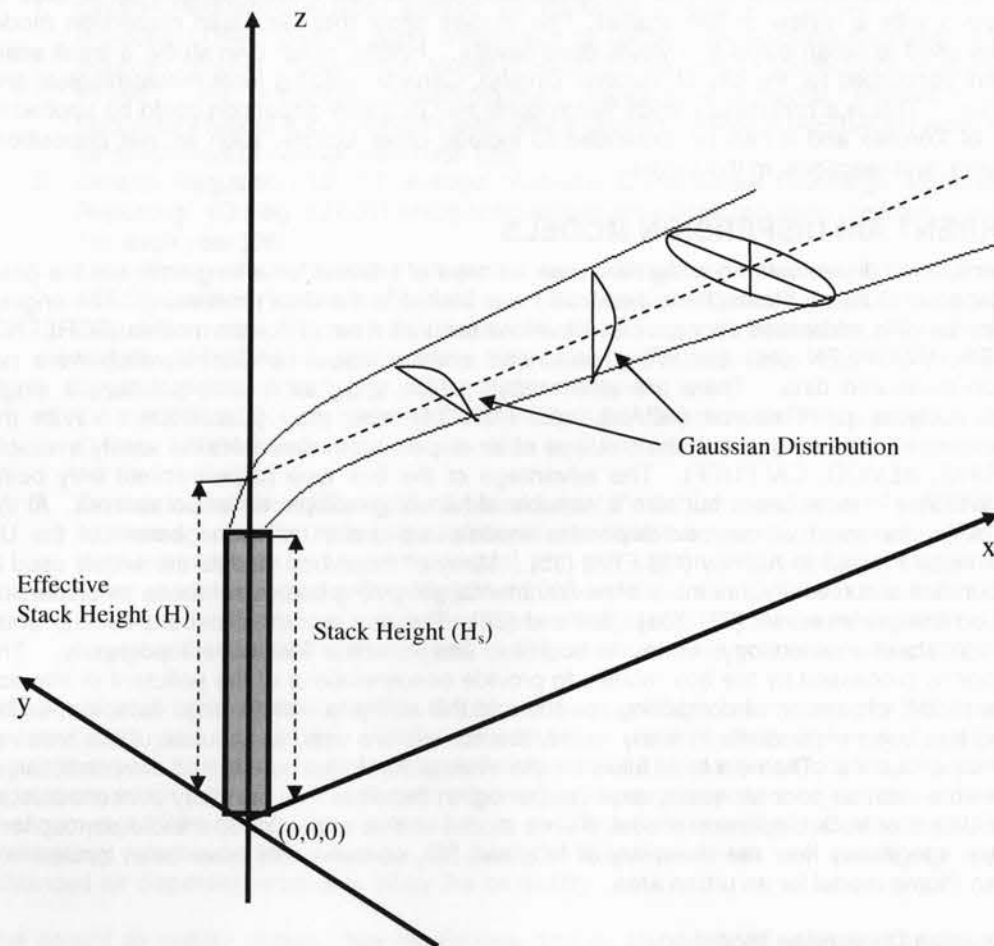


FIGURE 1: Elevated point source described by Gaussian Plume model

is the effective height of the stack, which is equal to the stack's height plus the plume rise (Figures 1 and 2). As dictated by the Gaussian Plume equation, the maximum concentration lies in the centre of the plume.

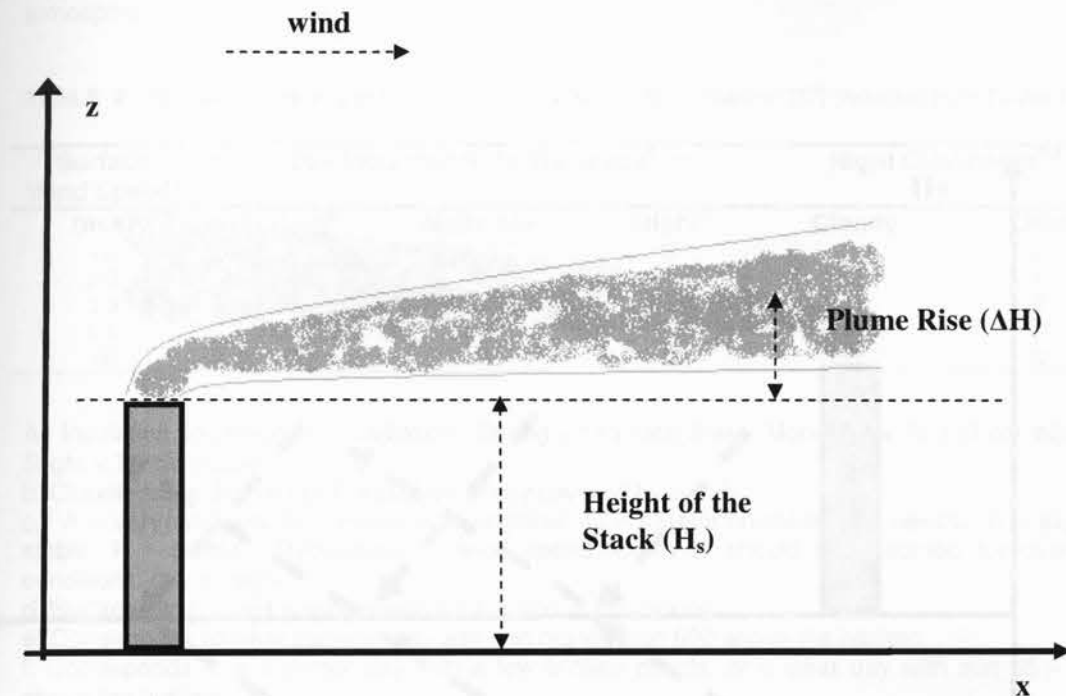


FIGURE 2: Effective stack height of a point source is a sum of the stack height and plume rise. The momentum and thermal rise add up to the physical height of the stack creating an effective stack height

The plume disperses in the horizontal direction following the Gaussian distribution. The distributions are described by the values of  $\sigma_y$  and  $\sigma_z$ . Average wind speed,  $U$ , is a function of the height,  $z$ . If this value is not known, the first estimate could be made utilizing the following power law velocity profile at elevation  $z_1$  [39]:

$$U = U_1 \left( \frac{H}{z_1} \right)^n \quad (2)$$

where  $n$ ,  $U_1$ ,  $z_1$ , and  $H$  are a dimensionless parameter, wind velocity at reference elevation of  $z_1$  [ $\text{m}/\text{s}$ ], elevation [ $\text{m}$ ], and stack height [ $\text{m}$ ], respectively.

The basic Gaussian Plume model is for a point source, i.e., the tall stack in space that emits without set barrier. The ground level concentrations can be evaluated to infinity. At some point in time, the plume disperses in the vertical direction and touches the ground. The basic formula can be further modified to account for the plume reflection from the ground, considered a zero flux or impenetrable surface. This was accomplished by creating an image source component in basic Gaussian Plume formula, as shown in Equation (3).

$$C(x, y, z) = \frac{Q_p}{2\pi U \sigma_y \sigma_z} \exp\left(-\frac{y^2}{2\sigma_y^2}\right) \left\{ \exp\left[-\frac{(z-H)^2}{2\sigma_z^2}\right] + \exp\left[-\frac{(z+H)^2}{2\sigma_z^2}\right] \right\} \quad (3)$$

The reflection source is shown in Figure 3.



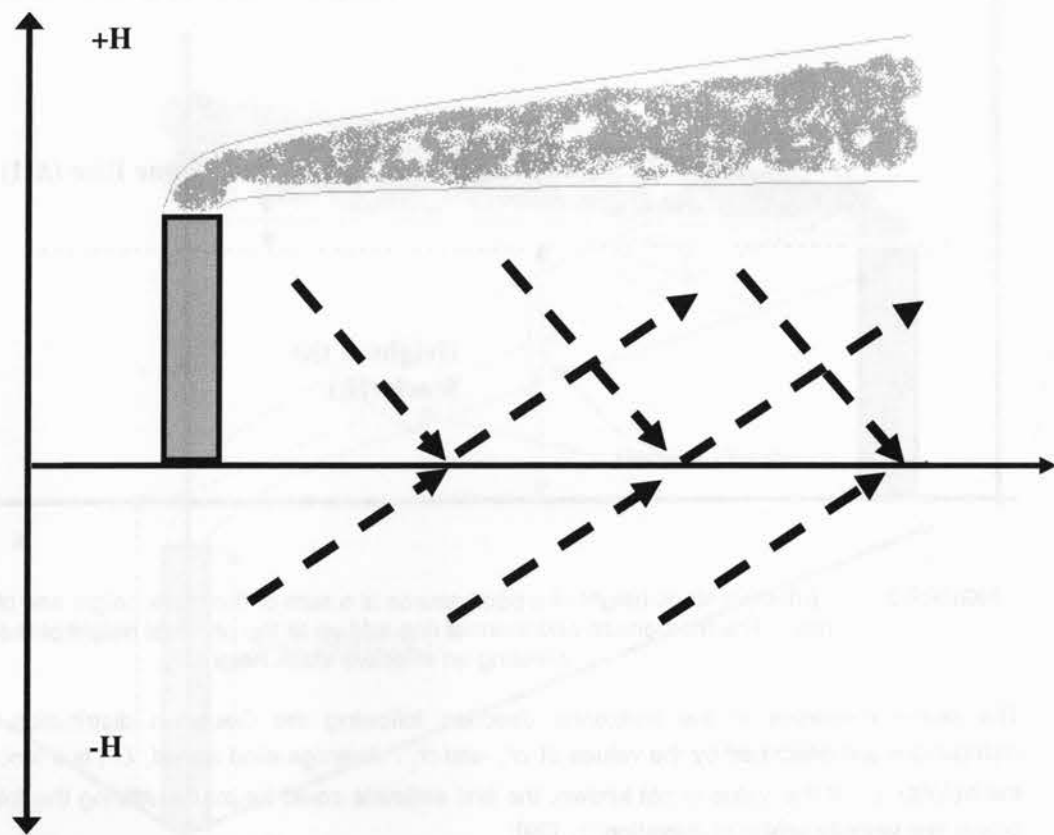


FIGURE 3: Side of image source which allows for the reflection of plume off ground

The result is the Gaussian dispersion equation for a continuous point-source. This equation provides the downwind concentration from an isolated point source located at (0,0,z) to infinity. There are a number of simplified forms of the Gaussian Plume formula for situations such as maximum concentration/first touchdown of the plume and ground level sources [37].

2.1.2. Dispersion Coefficients

The dispersion coefficients,  $\sigma_y$  and  $\sigma_z$  in Equation (1), are used in the dispersion model to provide the dispersion effect of the plume. These coefficients describe how well the atmosphere is mixed. Ideally, high mixing of air in the atmosphere which surrounds a source is sought. High mixing results in good dispersion of the pollutants and thus, lower ground level concentrations. The state of the atmosphere depends on few variables such as mechanical mixing induced by winds and thermal mixing induced by solar insulation. The most commonly used descriptive of the atmosphere's state is provided by Pasquill Stability classes. There are six classes labeled A to F, ranging from unstable or most turbulent to most stable or least turbulent conditions,

respectively [37]. Table 2 provides the Pasquill Stability classes which describe the state of the atmosphere.

TABLE 2: Pasquill dispersion classes related to wind speed and insulation [37] (Adopted from Turner 1970)

Surface Wind Speed <sup>d</sup>	Day Incoming Solar Radiation <sup>a,c</sup>			Night Cloudiness <sup>b,e</sup>	
	Strong <sup>e</sup>	Moderate <sup>f</sup>	Slight <sup>g</sup>	Cloudy	Clear
<2	A	A-B	B	-	-
2-3	A-B	B	C	E	F
3-5	B	B-C	C	D	E
5-6	C	C-D	D	D	D
>6	C	D	D	D	D

- A. Insulation, incoming solar radiation: Strong > 143 cal/m2/sec, Moderate = 72-143 cal/m2/sec, Slight < 72 cal/m2/sec.
- b. Cloudiness is defined as the fraction of sky covered by clouds.
- c. A – very unstable, B – moderately unstable, C – slightly unstable, D – neutral, E – slightly stable, F – stable. Regardless of wind speed, Class D should be assumed for overcast conditions, day or night.
- d. Surface wind speed is measured at 10 m above the ground.
- e. Corresponds to clear summer day with sun higher than 600 above the horizon.
- f. Corresponds to a summer day with a few broken clouds, or a clear day with sun 35 – 600 above the horizon.
- g. Corresponds to a fall afternoon, or a cloudy summer day, or clear summer day with the sun 15 – 350.

The Pasquill dispersion coefficients are based on the field experimental data, flat terrain, and rural areas. The plots allow for the user to read off dispersion coefficient at specific distance for selected stability class extracted from Table 2. The graphical plots of the dispersion coefficients become useless when solving Gaussian dispersion using a box model on a computer platform.

A number of analytical equations have been developed that express dispersion coefficients for rural and urban areas. These algebraic solutions are fitted against the dispersion coefficient plots and provide a few methods to calculate each dispersion factor. One of the methods is the use of power law to describe dispersion coefficients [37] and [40]:

$$\sigma_y = ax^b$$
$$\sigma_z = cx^d + e$$

(4)

where  $x$  and variables  $a$  through  $e$  are distance [m] and dimensionless parameters, respectively. Parameters  $a$  through  $e$  are functions of the atmospheric stability class and the downwind is a function to obtain dispersion coefficients or a combination of power law and another approach. Another approach, most commonly used in dispersion models is shown as follows [40]:

$$\sigma_y = \left( \frac{x}{2.15} \right) \tan \theta$$

(5)

where  $\theta = f - g(\ln x)$  and  $\theta$ ,  $f$  and  $g$  are angle [0] and two dimensionless parameters, respectively. McMullen [41] developed the following dispersion coefficients as the most representative of Turner's version of the rural Pasquill dispersion coefficients for rural areas. The advantage of the McMullen's equation is its application to both vertical and horizontal dispersion coefficients.

$$\sigma = \exp(g + h \ln x + i(\ln x)^2)$$

(6)

Constants  $g$  through  $i$  are dimensionless parameters as provided in Table 3. There also exist dispersion coefficients suitable for urban areas. Experimental data obtained from urban areas result in higher dispersion coefficients [42] and [43]. The plume encounters turbulence due to buildings and relatively warmer temperatures associated with urban areas. These can alter the atmospheric conditions for a small localized area when compared to the prevailing meteorological conditions. A higher dispersion coefficient results in a closer maximum ground-level concentrations as demonstrated in Figure 4.

TABLE 3: Constants  $g$ ,  $h$ , and  $i$  in McMullen's Equation (6) for rural dispersion coefficients [37]

Pasquill Stability Class	To obtain $\sigma_z$			To obtain $\sigma_y$		
	$g$	$h$	$i$	$g$	$h$	$i$
A	6.035	2.1097	0.2770	5.357	0.8828	-0.0076
B	4.694	1.0629	0.0136	5.058	0.9024	-0.0096
C	4.110	0.9201	-0.0020	4.651	0.9181	-0.0076
D	3.414	0.7371	-0.0316	4.230	0.9222	-0.0087
E	3.057	0.6794	-0.0450	3.922	0.9222	-0.0064
F	2.621	0.6564	-0.0540	3.533	0.9191	-0.0070

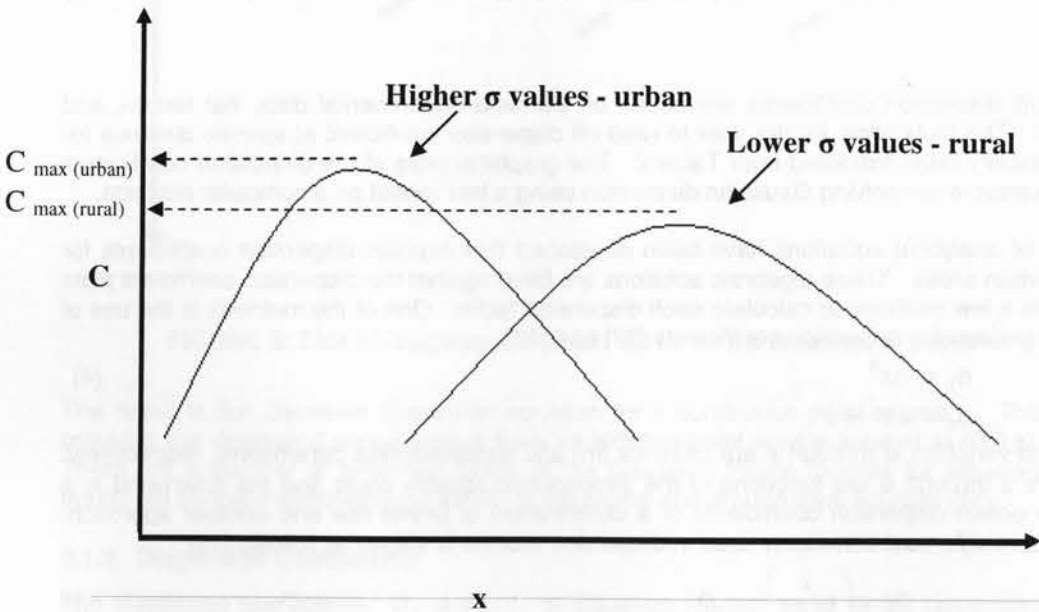


FIGURE 4: Effect of urban and rural dispersion coefficients. For urban areas a higher maximum ground level concentration, i.e.  $C_{\max(\text{urban})}$ , is observed and closer to the source. For rural areas a lower maximum ground level concentration, i.e.  $C_{\max(\text{rural})}$ , is observed and it occurs further from the source

For a plume passing through an urban area, the maximum ground-level concentration not only occurs closer to the source but also appears at a higher concentration than if modeled in rural area. In addition, further away from the urban area, a plume results in a lower ground level concentration than that if modeled in rural area. Initial mixing induced by the turbulence in a city

results in a better dispersion. For urban areas, the dispersion coefficients can be expressed by previously mentioned power law, with corrected constants, as shown in the following equation:

$$\sigma = jx(1 + kx)^l \tag{7}$$

Constants  $j$  through  $l$  are dimensionless parameters are provided in Table 4. There seems to not be a single better solution, therefore, when selecting a method, one should evaluate the various approaches [44].

TABLE 4: Constants  $j$ ,  $k$ , and  $l$  for estimation of Briggs urban dispersion coefficients in Equation (7) [37]

Pasquill Stability Class	To Obtain $\sigma_z$			To Obtain $\sigma_y$		
	$j$	$k$	$l$	$j$	$k$	$l$
A-B	240	1.00	0.50	320	0.40	-0.50
C	200	0.00	0.00	220	0.40	-0.50
D	140	0.30	-0.50	160	0.40	-0.50
E-F	80	1.50	-0.50	110	0.40	-0.50

2.1.3. Characterization of Various Emission Sources in Gaussian Dispersion Model

The Gaussian Plume model originally developed for point sources (i.e. tall stacks) can be also applied to other types of emission sources. These emission sources are most commonly described as volume, line, and area sources. The box dispersion models are also capable of handling sources below grade and flares. These sources (e.g. quarries or flares) are not typical of Toronto city and therefore, will not be discussed. Toronto is mainly characterized by sky scrapers and highways, which can translate to volume sources and line (or area) sources.

Volume Source

A building structure is characterized in an air dispersion model as a volume source. The solution proposed under the Gaussian Plume model is to model the volume source as a point source at a distance with matching dispersion coefficients to the dimensions of the virtual source [40], as shown in Figure 5. The initial lateral and vertical dimensions are modified dimensions of source width and height, as shown in Table 5.

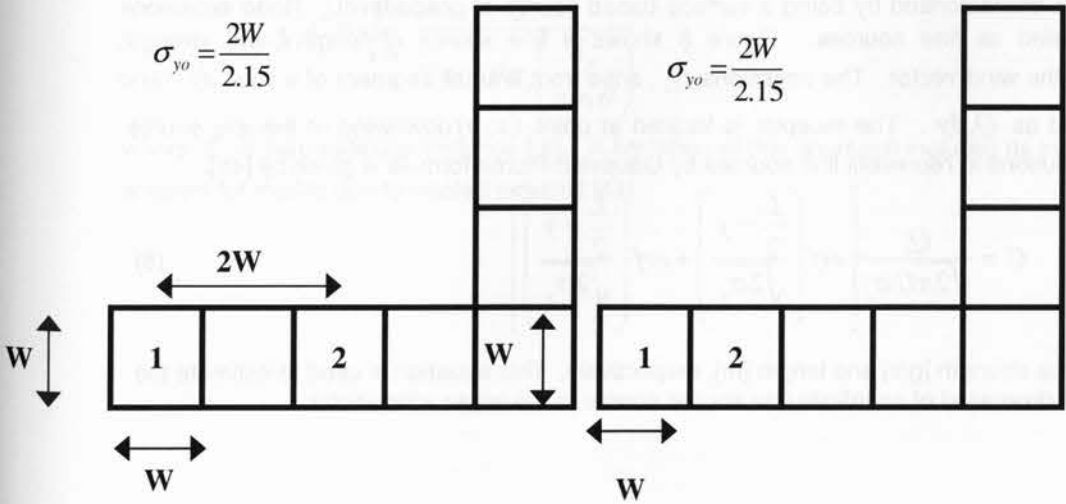


FIGURE 5: (Upper) Line source represented by adjacent volume source. (Lower) Line source represented by separated volume source

TABLE 5: Initial dimensions for a virtual source [40]

Type of Source	Procedure for Obtaining Initial Dimension
Initial Lateral Dimension ( $\sigma_{yo}$ )	
Single Volume Source	$\sigma_{yo} = \frac{L}{4.3}$
Line Source Represented by Adjacent Volume Source (Figure 5)	$\sigma_{yo} = \frac{L}{2.15}$
Line Source Represented by Separate Volume Source (Figure 5)	$\sigma_{yo} = \frac{A}{2.15}$ [A – centre to centre distance]
Initial Vertical Dimension ( $\sigma_{zo}$ )	
Surface-Based Source (H=0)	$\sigma_{zo} = \frac{B}{2.15}$ [B – vertical dimension]
Elevated Source (H > 0) on or Adjacent to Building	$\sigma_{zo} = \frac{C}{2.15}$ [C – building height]
Elevated Source (H > 0) not on or Adjacent to a Building	$\sigma_{zo} = \frac{A}{4.3}$

Line Source

Line source is characterized by being a surface based source at grade-level. Road emissions can be modeled as line sources. Figure 6 shows a line source of length  $L$  and strength  $Q_l$  normal to the wind vector. The emissions,  $Q_l$ , arise from a small segment of a line,  $dy'$ , and are expressed as  $Q_l dy'$ . The receptor is located at point  $(x, y)$  downwind of the line source. One of the solutions to represent line sources by Gaussian Plume formula is given by [45].

$$C = \frac{Q_l}{\sqrt{2\pi}U\sigma_z} \left[ \operatorname{erf} \left( \frac{\frac{L}{2} - y}{\sqrt{2}\sigma_y} \right) + \operatorname{erf} \left( \frac{\frac{L}{2} + y}{\sqrt{2}\sigma_y} \right) \right] \tag{8}$$

and are source strength [g/s] and length [m], respectively. This equation is used to estimate the concentration downwind of an infinite line source normal to the mean wind vector.

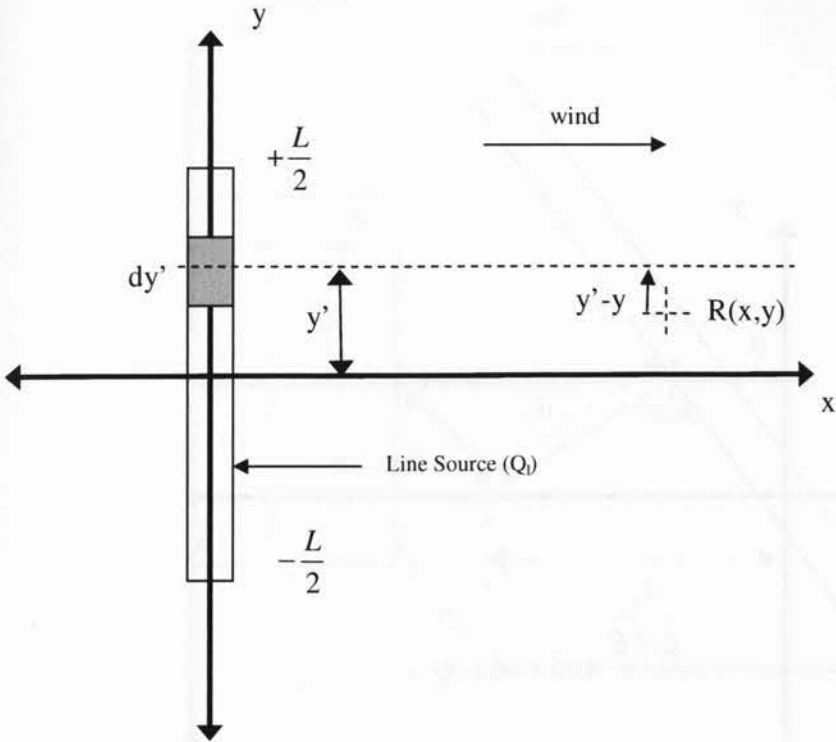


FIGURE 6: A line source of length  $L$  and strength  $Q_l$

The governing equation of a line source oriented at an oblique angle, as shown in Figure 7, to the mean wind vector was developed by Calder [43]. The perpendicular distance,  $d_p$ , is the distance between the receptor and the line source. Angle  $\theta$  is the angle between its normal and the wind vector and applies to angles as large as  $75^\circ$  [46].

This solution is shown in Equation (9) [45]:

$$C = \sqrt{\frac{2}{\pi}} \frac{Q_l}{U \cos \theta \sigma_z} \left( \frac{d_p}{\cos \theta} \right) \tag{9}$$

where  $d_p$  is perpendicular distance [m]. A limitation of this approach includes its inability to account for mixing due to heated exhaust [47].



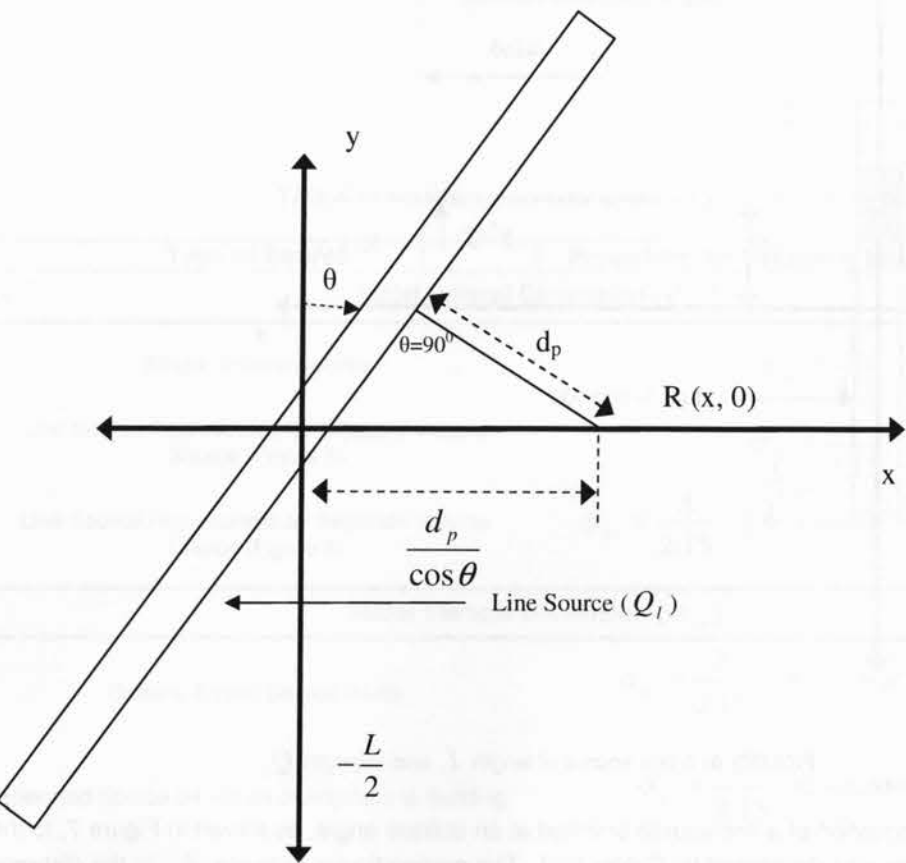


FIGURE 7: Infinite line source with strength  $Q_l$  at an oblique angle ( $\theta$ ) to the wind

Area Source

An alternative method that can be used to model emissions from a road is by describing the road as area source. Open fields from which wind erosion occurs is another example of an area source. In essence, a line source with width  $x_1$  normal to the wind direction can be used to represent an area source as shown in Figure 8. The area source (considered to be long enough to be infinite) is a sum of smaller line sources, each of strength  $Q_a dx'$  per unit length, where emission rate is  $Q_a$ . There are two descriptions of area sources that follow the Gaussian Plume model.

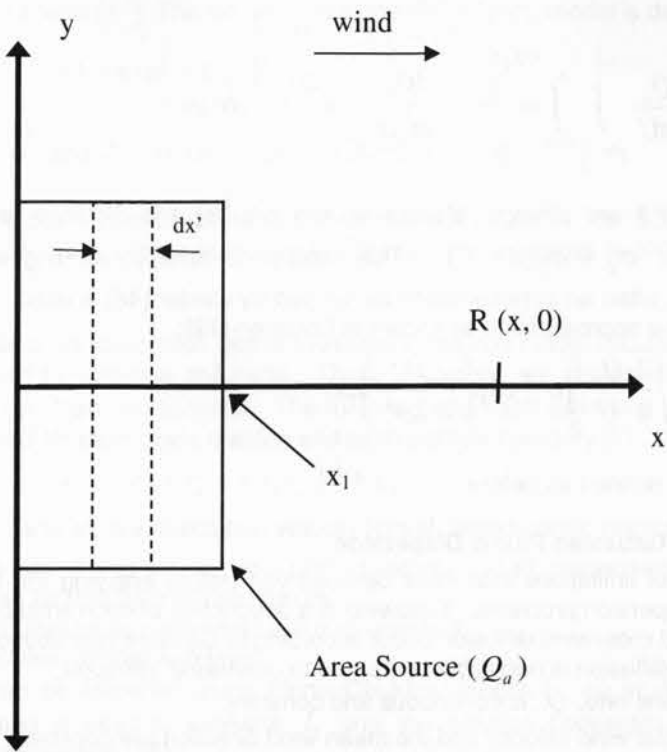


FIGURE 8: An area source with strength  $Q_a$  and width  $x_1$

In the case of area sources, dispersion coefficients are evaluated using power law as shown in Equation (10). The dispersion coefficient in the z-direction is to be evaluated for a distance of  $x - x'$  (concentration at a receptor) and thus, it is expressed in a power law form [45]:

$$\sigma_z = m(x - x')^n \tag{10}$$

where  $(x - x')$ ,  $m$ , and  $n$  are distance [m] and two dimensionless parameters, respectively. Dimensionless parameters are a function of atmospheric stability and selected from Table 6.

TABLE 6: Power law constants used to calculate the dispersion coefficients in Equation (10) [45]

Dispersion Class	$\sigma_{ya}$		$\sigma_z$ (0.5 – 5 km)		$\sigma_z$ (5 – 50 km)	
	a	b	m	n	m	n
A	0.3658	0.9031	$2.5 \times 10^{-4}$	2.1250	-	-
B	0.2751	0.9031	$1.9 \times 10^{-3}$	1.6021	-	-
C	0.2089	0.9031	0.20	0.8543	0.5742	0.7160
D	0.1474	0.9031	0.30	0.6532	0.9605	0.5409
E	0.1046	0.9031	0.40	0.6021	2.1250	0.3979
F	0.0722	0.9031	0.20	0.6020	2.1820	0.3310

<sup>a</sup> Use power law mentioned previously to evaluate horizontal dispersion.

The following equation [45] is used to determine concentrations at receptor from a downwind edge. The source height,  $H$ , allows one to utilize this approach to road sources where emissions are released at the above ground at the height of the truck.

$$C = \frac{Q_a}{\pi U} \int_{y'=-\frac{L}{2}}^{\frac{L}{2}} \int_{x'=0}^{x_1} \frac{\exp\left[-\frac{(y-y')^2}{2\sigma_y^2} - \frac{H^2}{2\sigma_z^2}\right]}{\sigma_y \sigma_z} dx' dy' \quad (11)$$

where  $Q_a$  and  $(y-y')$  are strength of area source [g/m<sup>2</sup>/s] and distance [m], respectively,  $\sigma_y = \sigma_y(x-x')$  and  $\sigma_z = \sigma_z(x-x')$ . This solution is time consuming when evaluated numerically, therefore, often an approximation developed by Calder [48] is used. This solution is called the narrow plume approximation as shown in Equation (12):

$$C = \sqrt{\frac{2}{\pi}} \frac{Q_a}{U} \int_0^{x_1} \sigma_z^{-1} \exp\left(-\frac{H^2}{2\sigma_z^2}\right) dx' \quad (12)$$

where parameters are defined as before.

### 2.1.4. Limitations of Gaussian Plume Dispersion

There are a number of limitations that must be observed before applying the basic Gaussian Plume model to air dispersion problems. Following is a description of each limitation [37]:

- vertical and crosswind diffusion occur according to Gaussian distribution;
- downwind diffusion is negligible compared to downwind transport;
- the emissions rate,  $Q$ , is continuous and constant;
- the horizontal wind velocity and the mean wind direction are constant;
- there is no deposition, washout, chemical conversion or absorption of emissions, and any emissions diffusing to the ground are reflected back into the plume (i.e. all emissions are totally conserved within the plume);
- there is no upper barrier to vertical diffusion and there is no crosswind diffusion barrier;
- emissions reflected upward from the ground are distributed vertically as if released from an imaginary plume beneath the ground and are additive to the actual plume distribution; and
- the use of  $\sigma_y$  and  $\sigma_z$  as constants at a given downwind distance and the assumption of an expanding conical plume require homogeneous turbulence throughout the  $x$ ,  $y$  and  $z$ -directions of the plume.

It is important to note that many of these limitations have been resolved by studies conducted in the application of Gaussian Plume dispersion model to urban areas. Additional limitations can arise in following situations, identified by this study, such as decision over election of source type (i.e. line, area or volume) adequate to be assigned to an emission source e.g. road sources. Another limitation of the model is its under performance during cooler months of the year. This can be potentially resolved through the modification of dispersion coefficients.

### 2.1.5. Chemistry in Gaussian Plume Dispersion

One of the most commonly used Gaussian Plume model is ISC-PRIME. [49][31][32][36] This box model handles NO<sub>x</sub> and SO<sub>x</sub> in following ways:

- decay term;
- dry deposition; and
- wet deposition.

The use of decay term  $D$  [s<sup>-1</sup>] is one way of including the removal of a pollutant in the Gaussian Plume model as follows [40]:

$$C(x, y, z) = \frac{Q_p D}{2\pi U \sigma_y \sigma_z} \exp\left(-\frac{y^2}{2\sigma_y^2}\right) \left\{ \exp\left[-\frac{(z-H)^2}{2\sigma_z^2}\right] + \exp\left[-\frac{(z+H)^2}{2\sigma_z^2}\right] \right\} \quad (13)$$

where  $D$  is decay term [s<sup>-1</sup>]. The decay term in the ISC-PRIME model is defined as follow:

$$D = \exp\left(-\psi \frac{x}{U}\right) \quad (14)$$

where  $\psi = \frac{0.693}{T_{1/2}}$  and  $T_{1/2}$  is the pollutant half life (s<sup>-1</sup>) [50].

Furthermore, the box model utilizes a decay term of  $4.81 \times 10^{-5} \text{ s}^{-1}$  for SO<sub>2</sub> concentrations when modeled in urban area. There is no similar decay term assigned to NO<sub>x</sub> pollutant in this box model [40].

There also exists a dry deposition option available in the box model ISC-PRIME. It is applied to particulate formed by gaseous pollutants. These emissions are characterized by a high fraction of particulate over 2 μm in diameter. The following approach estimates deposition velocity and must be evaluated for each mass fraction and each particle category [51].

$$v_d = (r_a + r_d + r_a r_d v_g)^{-1} + v_g \quad (15)$$

where  $v_d$ ,  $r_a$ ,  $r_d$ , and  $v_g$  are deposition velocity [cm/s], aerodynamic resistance [s/cm], deposition layer resistance [s/cm], and gravitational settling velocity [cm/s], respectively. The distance closer to the ground can be divided into two phases:

- fully turbulent region with vertical fluxes constant;
- a thick quasi-laminar sub-layer.

Both regions can be identified using Monin-Obukhov length,  $L$ , an implicit function of friction velocity. Iteration is used to evaluate  $L$  until the solution converges [51]. The iteration is completed using Equation (16):

$$u_* = \frac{k u_{ref}}{\ln\left(\frac{z_{ref}}{z_0}\right) - \Psi_m\left(\frac{z_{ref}}{L}\right) + \Psi_m\left(\frac{z_0}{L}\right)} \quad (16)$$

where:

$$\Psi_m\left(\frac{z_{ref}}{L}\right) = 2 \ln\left(\frac{1+\mu}{2}\right) + \ln\left(\frac{1+\mu^2}{2}\right) - 2 \tan^{-1} \mu + \frac{\pi}{2}$$

$$\mu = \left(1 - 16 \frac{z_{ref}}{L}\right)^{\frac{1}{4}}$$

$$\Psi_m\left(\frac{z_0}{L}\right) = 2 \ln\left(\frac{1+\mu_0}{2}\right) + \ln\left(\frac{1+\mu_0^2}{2}\right) - 2 \tan^{-1} \mu_0 + \frac{\pi}{2}$$

$$\mu = \left(1 - 16 \frac{z_0}{L}\right)^{\frac{1}{4}}$$

$$L = -\frac{\rho c_p T_{ref} u_*^3}{kgH}$$

In the above equations,  $u_*$ ,  $z_{ref}$ ,  $z_0$ ,  $k$ ,  $u_{ref}$ ,  $L$ , and  $\Psi_m$  are surface friction velocity [cm/s], reference elevation [m], elevation [m], surface roughness length [m], unit-less von Karman constant [0.40], wind speed at reference elevation [m/s], Monin-Obukhov length [m], and decay coefficient [s<sup>-1</sup>], respectively. Also,  $\mu$ ,  $\rho$ ,  $c_p$ ,  $T_{ref}$ , and  $g$  are absolute viscosity of air

$[1.81 \times 10^{-4} \text{ g/cm/s}]$ , particle density  $[\text{g/cm}^3]$ , specific heat of air at a constant pressure, reference temperature  $[\text{K}]$ , and acceleration due to gravity  $[\text{cm/s}^2]$ , respectively.

For the turbulent region, the dominant is the aerodynamic resistance. For the turbulent region following equation applies, where  $L$  is  $> 0$ :

$$r_a = \frac{1}{ku_*} \left[ \ln \left( \frac{z_d}{z_0} \right) + 4.7 \frac{z}{L} \right] \quad (17)$$

For  $L < 0$ , the following equation applies:

$$r_a = \frac{1}{ku_*} \ln \left[ \frac{\left( \sqrt{1+16 \left( \frac{z}{|L|} \right)} - 1 \right) \left( \sqrt{1+16 \left( \frac{z_0}{|L_0|} \right)} + 1 \right)}{\left( \sqrt{1+16 \left( \frac{z}{|L|} \right)} + 1 \right) \left( \sqrt{1+16 \left( \frac{z_0}{|L_0|} \right)} - 1 \right)} \right] \quad (18)$$

where  $u_*$ ,  $z_d$ , and  $L_0$  are surface friction velocity  $[\text{cm/s}]$ , surface roughness  $[\text{m}]$  and initial length  $[\text{m}]$ , respectively.

A minimum value of 1 m for Monin-Obukhov lengths is assumed for rural locations. The deposition layer resistance is expressed as:

$$r_d = \frac{1}{\left( Sc^{\frac{2}{3}} + 10^{\frac{3}{St}} \right) u_*} \quad (19)$$

where  $S_c$  and  $S_t$  are Schmidt and Stokes numbers, respectively.

The Schmidt number has an impact on the deposition rate of small particles, particles that follow Brownian motion. The parameter with the Stokes number is a measure of inertial impact, dominated by intermediate sized particles (2-20  $\mu\text{m}$ ). [51] The gravitational settling velocity is expressed as:

$$v_g = \frac{(\rho - \rho_{air}) g d_p^2 c_2}{18\mu} S_{CF} \quad (20)$$

where  $v_g$ ,  $\rho$ ,  $\rho_{air}$ ,  $d_p$ ,  $c_2$ , and  $S_{CF}$  are gravitational settling velocity  $[\text{cm/s}]$ , particle density  $[\text{g/cm}^3]$ , air density  $[1.2 \times 10^{-3} \text{ g/cm}^3]$ , particle diameter  $[\mu\text{m}]$ , air units conversion constant  $[1 \times 10^{-8} \text{ cm}^2/\mu\text{m}^2]$ , and dimensionless slip correction factor, respectively. Finally the slip factor can be estimated as follow:

$$S_{CF} = 1 + \frac{2x_2 \left( a_1 + a_2 \exp \left( -a_3 \frac{d_p}{x_2} \right) \right)}{10^{-4} d_p} \quad (21)$$

where  $x_2$ ,  $a_1$ ,  $a_2$ , and  $a_3$  are all dimensionless constants  $[6.5 \times 10^{-6}, 1.257, 0.4, \text{ and } 0.55 \times 10^{-4}]$ , respectively. A user of a box model who wishes to utilize acid rain can accomplish it by use of wet deposition syntax. The settling velocity and a product of the concentration as expressed in Equation (3) give dry deposition [40]:

$$C = v_d \frac{Q_p}{2\pi U \sigma_y \sigma_z} \exp \left( -\frac{y^2}{2\sigma_y^2} \right) \left\{ \exp \left[ -\frac{(z-H)^2}{2\sigma_z^2} \right] + \exp \left[ -\frac{(z+H)^2}{2\sigma_z^2} \right] \right\} \quad (22)$$

where  $v_d$  is deposition velocity  $[\text{cm/s}]$ . The wet deposition is estimated using scavenging ratio approach [52]. The ratio shown in Equation (23) is a function of scavenging coefficients and precipitation rate (cloud water droplets):

$$\Lambda = \lambda R \quad (23)$$

where  $\Lambda$ ,  $\lambda$ , and  $R$  are scavenging ratio  $[\text{s}^{-1}]$ , scavenging coefficient  $[\text{h/mm/s}]$ , and precipitation rate  $[\text{mm/h}]$ , respectively. The scavenging coefficients are influenced by pollutant characteristics such as solubility and reactivity for gases, size distribution for particles, and the nature of precipitation: liquid or frozen. Meteorological processors such as PCRAMMET use precipitation rate and precipitation type data to estimate scavenging ratio. Finally, this ratio is used in Equation (24), where  $t$  is the plume time traveled  $[\text{s}]$ , to estimate wet deposition:

$$C = C_0 \exp(-\Lambda t) \quad (24)$$

where  $C_0$  is initial average mass concentration  $[\mu\text{g/m}^3]$ .

#### 2.1.6. Treatment of Inversion Layers

Winter months not only give poor dispersion conditions but inversion layers can also trap pollutants. The Gaussian Plume model can be modified to include inversion layers. The approach is similar to that used in augmenting basic Gaussian Plume to include ground reflection.

A more rigorous approach in modeling inversion layers is shown in Equation (25) [53].

$$C = \frac{Q_p}{2\pi U \sigma_y \sigma_z} \exp \left( -\frac{y^2}{2\sigma_y^2} \right) \left\{ \exp \left[ -\frac{(z-H)^2}{2\sigma_z^2} \right] + \exp \left[ -\frac{(z+H)^2}{2\sigma_z^2} \right] + A \right\} \quad (25)$$

where:

$$A = \exp \left( \frac{-(z+2H_{bl}-H)^2}{2\sigma_z^2} \right) + \exp \left( \frac{-(z-2H_{bl}+H)^2}{2\sigma_z^2} \right) + \exp \left( \frac{-(z-2H_{bl}-H)^2}{2\sigma_z^2} \right)$$

is the height of the boundary layer  $[\text{m}]$ . A separate type of inversion layer fumigation is when the inversion layer is located above the effective stack height and acts as a barrier. This barrier prevents the plume from dispersing in the vertical direction and forces the emissions to the ground as shown in Figure 9. This is an extreme case of poor dispersion and often is a result of off-shore sea breeze. A ground based inversion, fumigation could also be expressed by modifying Gaussian Plume model. Fumigation as it can be handled by Gaussian Plume is shown in Equation (26) [40].

$$C(x, y, z) = \frac{Q_p}{(2\pi)^{\frac{1}{2}} U \sigma_y H} \exp \left( -\frac{1}{2} \frac{y^2}{\sigma_y^2} \right) \quad (26)$$



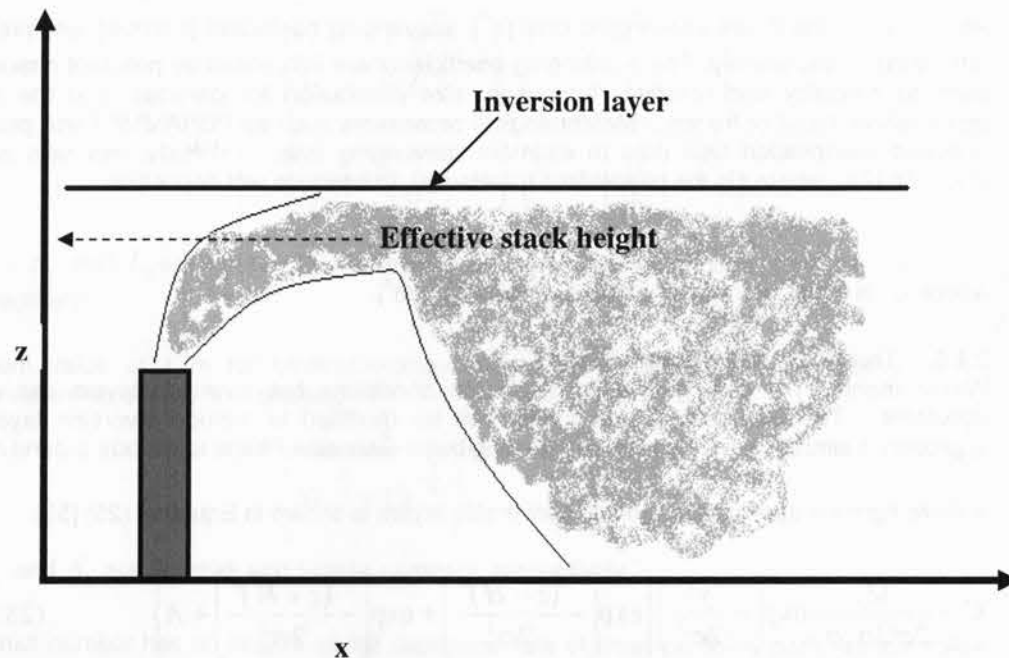


**FIGURE 9:** Fumigation induced by an inversion layer located above the effective stack height. The inversion layer acts similar to a mirror sealing and forces the plume to the group which result in poor dispersion and higher maximum ground level concentrations at the ground level

There are a number of other inversion layers and some assist the dispersion. Lofting is a reverse of fumigation as shown in Figure 9 [54]. The inversion layer is located below the top of the stack and therefore, forces the plume to disperse in the upward direction [50].

### 3. ATMOSPHERIC CHEMISTRY OF NO<sub>x</sub> AND SO<sub>x</sub>

In an urban area, the main sources of NO<sub>x</sub> and SO<sub>x</sub> emissions arise from the road traffic, emissions from fuel fired equipment which provides power/electricity, and fuel fired equipment which provides power/electricity, and industries. At the present time, the most complete databases (i.e. National Pollutant Release Inventory (NPRI)) available in Canada contain the emissions of NO<sub>x</sub> and SO<sub>x</sub> from industrial sources only. Most recent publication shows that transportation contributes to 40% of NO<sub>x</sub> (transportation) and 28% NO<sub>x</sub> (road vehicles) and 4% SO<sub>x</sub> (transportation) annually [55]. Emissions of NO<sub>x</sub> into the atmosphere due to combustion of fuel are driven by the nitrogen in the atmosphere. Approximately 90% of emissions due to combustion of fuel result in NO [53]. NO can potentially convert to NO<sub>2</sub>, therefore, it is often referred to as NO<sub>x</sub> and NO<sub>2</sub> when estimating emissions. In addition, for urban areas, diurnal variations in NO<sub>x</sub> are observed due to morning and afternoon traffics. Emissions of SO<sub>x</sub> into the

atmosphere due to combustion of fuel are strictly related to sulphur content in the fuel. Regulations are put in place to control the content of sulphur in fuel, result for the annual and diurnal cycles to be significantly reduced in comparison to that of NO<sub>x</sub> [56].

There are a number of deposition mechanisms that can be identified with NO<sub>x</sub> and SO<sub>2</sub> such as dry deposition, wet deposition, and cloud water deposition. These mechanisms are discussed in the following with means to further augment existing Gaussian Plume model.

#### 3.1. Dry Deposition

The surface concentration always tends towards the atmospheric concentration. This tendency can be disrupted by three processes which move the gasses down the gradient between the atmosphere and the surface. Turbulent diffusion moves the gas to the surface. Molecular diffusion transfers the gas across the laminar boundary layer next to the surface. Gas molecules dissolve or react with the surface itself. All three must be present for dry deposition to occur. Dry deposition is a function of deposition velocity and the transfer resistance. Formation of sulphuric acid and nitric acid are two dry reactions of importance to emissions from urban areas. Some measurements of dispersing plumes show a 4% per hour, on a sunny day for the conversion of SO<sub>2</sub> to H<sub>2</sub>SO<sub>4</sub> [53]. Production of nitric acid occurs at night as the radical is photolytically unstable.

##### Deposition Velocity

Given there is a flux due to a gradient between the atmospheric concentration at 1-2 m above the ground and zero concentration at the surface, the deposition velocity is given as [57]:

$$v_g = \frac{F_g}{C_z} \quad (27)$$

Where  $v_g$ ,  $F_g$ , and  $C_z$  are deposition velocity [m/s], flux to surface [kg/m<sup>2</sup>/s] and atmospheric concentration [kg/m<sup>3</sup>], respectively [53]. The concentration in Equation (27) is evaluated at known height,  $z$ .

##### Transfer Resistance

Transfer resistance is considered as a part of the concept of conductance to describe particulate deposition from atmosphere to surface. Deposition velocity is defined as conductance.

$$r_t = \frac{1}{v_g} \quad (28)$$

Where  $r_t$  is the total transfer resistance [s/m]. Total resistance is calculated using Equations (28) and (29), and incorporating ground level concentration:

$$r = \frac{C_z - C_s}{F_g} + \frac{C_s}{F_g} = r_{rain} + r_{surface} = r_a + r_s \quad (29)$$

Where  $r$ ,  $C_z$ ,  $C_s$ ,  $F_g$ ,  $r_a$ , and  $r_s$  are resistance [s/m], atmospheric concentration [kg/m<sup>3</sup>] at reference height, surface concentration [kg/m<sup>3</sup>], flux to surface [kg/m<sup>2</sup>/s], aerodynamic resistance [s/m], and surface resistance [m/s], respectively. The aerodynamic resistance,  $r_a$ , can be added as two resistors in series: turbulent resistance transfer and by eddies and molecular diffusion of the gas through the laminar boundary layer to the surface itself. For urban area, an area with high surface roughness and strong winds, the aerodynamic resistance becomes low. Table 7 summarizes typical aerodynamic values used for  $r_a$ . The surface resistance values have been widely studied and are readily available [57].

**TABLE 7:** Typical aerodynamic resistance values ( $r_a$ ) for various wind speeds and vegetation [53]

Aerodynamic Resistance ( $r_a$ )	Condition
[s/m]	
200	Wind speed < 1 m/s, vegetation 10 cm tall
20	Wind speeds > 4 m/s, over 1 m vegetation
20	Wind speeds of < 10 m/s, forest canopy

The resistances that related to stomata: deposition to dry leaf surface, deposition to liquid water on leaf surface and deposition to the soil, are additional paths that might be considered. Each path having its own resistance component adds to the equation. Suggested values of  $V_g$  are 10 mm/s during the day time and 5 mm/s at night for  $\text{NO}_2$  and  $\text{SO}_2$  [57].

Dry deposition, Equation (29), was expanded by Wesely [58] for  $\text{SO}_2$ . This equation is augmented to include a term which represents bulk surface resistance,  $r_c$ . The  $r_c$  includes not only vegetated surfaces but the range of surface conditions. Bulk surface resistance for seasonal categories and land use may be estimated using equation augmented in Equation 29. As the temperature drops (< -2 °C), the surface resistance increases. Therefore, Wesely [58] briefly discussed surface uptake of  $\text{HNO}_3$ ,  $\text{SO}_2$ , and  $\text{NO}_2$  by the following term for each substance.

$$\text{Surface Uptake} = 1000e^{-(T_s+4)} \quad (30)$$

where  $T_s$  is the surface temperature [K].

### 3.2. Wet Deposition

Sulphur and nitrogen are incorporated into cloud droplets, raindrops and snow flakes, which are deposited on ground. The reactions of sulphur and nitrogen in water form a complex set based on presence of gaseous  $\text{O}_3$  and  $\text{H}_2\text{O}_2$ , and catalysts Mn and Fe at surface of aerosol particles. These reactions last for days, thus deposition may occur thousand kilometers from the source [53].

### 3.3. Cloud Water Deposition

Scavenging below and in-cloud of gases is yet another transport phenomenon which should be accounted for in air dispersion models. The  $\text{SO}_2$  gas can dissolve in clouds as it is considered a moderately soluble gas [59].

One approach to estimate below-cloud scavenging is proposed by Asman [59]. The equations are limited to rain and do not include "snow" type of precipitation. Below cloud scavenging coefficient,  $\Lambda_b$ , is a function of rain fall,  $I$ , as described in Equation (31). Temperature,  $T_a(0)$ , and relative humidity,  $rh(0)$ , are measured at ground level.

$$\Lambda_b = aI_{mm}^{b_{av}} \quad (31)$$

where:

$$a = aa + bbD_g(1298.15)$$

$$aa = a_0 + a_1rh(0)$$

$$bb = b_0 + b_1rh(0)$$

$$b_{av} = b_{av0} + b_{av1}rh(0)$$

In these equations,  $\Lambda_b$ ,  $I_{mm}$ ,  $D_g$ ,  $rh(0)$ ,  $T_a(0)$ ,  $a$ ,  $b$ ,  $aa$ ,  $bb$ ,  $a_0$ ,  $b_0$ ,  $b_1$ ,  $b_{av0}$  and  $b_{av1}$  are cloud scavenging coefficient [ $\text{s}^{-1}$ ], rain fall [mm/h], relative humidity at ground level [%], temperature at ground level [K], and remaining are parameters with individual functions shown in Tables 8 and 9.

TABLE 8: Below-cloud scavenging constants [59]

Constant	Formula
$a_0$	$4.476 \times 10^{-5} - 1.347 \times 10^{-7} T_a(0)$
$a_1$	$-3.004 \times 10^{-7} + 1.498 \times 10^{-9} T_a(0)$
$b_0$	$8.717 - 2.787 \times 10^{-2} T_a(0)$
$b_1$	$-5.074 \times 10^{-2} + 2.894 \times 10^{-4} T_a(0)$
$b_{av0}$	$9.016 \times 10^{-2} + 2.315 \times 10^{-3} T_a(0)$
$b_{av1}$	$4.458 \times 10^{-3} - 2.115 \times 10^{-5} T_a(0)$

TABLE 9: Scavenging coefficients for temperature of 10 °C [59]

Gas	a	$b_{av}$
$\text{NH}_3$	$9.85 \times 10^{-5}$	0.616
$\text{HNO}_3$	$7.70 \times 10^{-5}$	0.616
$\text{N}_2\text{O}_5$	$5.23 \times 10^{-5}$	0.616

A second approach to calculate below-cloud scavenging was developed by Chang [60]. A simpler approach which utilizes one equation and applies to rain and snow fall is as follows:

$$\Lambda_b = 0.33 \times 10^{-4} I_{mm}^{0.42} + 1.0 \times 10^{-4} I_{mm}^{0.58} \quad (32)$$

Furthermore, the following equation was also proposed to be used for in-cloud removal of  $\text{HNO}_3$ :

$$\Lambda_c = 4.6 \times 10^{-4} I^{0.86} \quad (33)$$

where  $\Lambda_c$  is in-cloud removal [ $\text{s}^{-1}$ ]. Snow scavenging can be expressed in a similar manner as shown in Equation (34):

$$\Lambda_s = 0.88 \times 10^{-4} I_{mm}^{0.33} + 0.6 \times 10^{-4} I_{mm}^{0.76} \quad (34)$$

where  $\Lambda_s$  is snow scavenging [ $\text{s}^{-1}$ ]. Chang [60] poses a question for  $\text{NO}_2$  scavenging by liquid cloud.  $\text{NO}_2$  is considered to be slow due to low  $\text{NO}_2$  solubility in water. The study points out that in snow  $\text{NO}_2$  dissolves well.



#### 4. APPLICATIONS OF GAUSSIAN PLUME MODEL TO URBAN AREAS

The evaluation of emissions for an urban area depends on emission summary, meteorological data, and surroundings. This information can be embedded into a dispersion model to estimate concentrations of various chemicals across the area of interest. The predicted concentrations can further be compared to the monitored data of the area. There are a number of approaches applied to dispersion of pollutants around a city which include the study of street canyons, forecasting type of modeling, and applications of statistical distribution to describe behaviour of a plume. This section evaluates the applications of Gaussian dispersion to five cities around the world and provides a critique of different applications of Gaussian dispersion for urban areas. Two studies have been completed on predicting ground level concentrations of various pollutants for the City of Toronto, one using land use regression and second a Gaussian dispersion model. The final subsection contains a description of a small scale study conducted for the city of Toronto, Ontario, Canada, and emissions due to traffic specifically emissions of  $\text{NO}_2$ . The ground level concentrations were predicted using ISC-PRIME model and compared to the monitored data. The dispersion modeling was conducted for the first few days of February 2005, days leading to the earliest smog season recorded in Toronto [12].

##### 4.1. Dispersion Modeling of the City of Kanto, Japan

Kitabayashi et al. [4] studied  $\text{NO}_x$  emissions for a mega city, Kanto, Japan. The main sources included mobile sources (trucks), an electric power plant, and ventilation towers that service automotive tunnels. In that study, the Gaussian plume model was augmented with a chemical reaction module and incorporated concentrations for background gases. The integrated model was tested against a typical stack gas (point source). Results were stated as reliable with no analysis provided. This would quantify the relationship of data that led to a conclusion of the model's reliability. Proposed investigations for the future include inclusion of more data (i.e. monitoring stations) for the area of interest and comparison of observed concentrations to the predicted by the integrated Gaussian plume model.

The above model lacks statistical analysis in the form of comparing percentiles of modeled concentrations to monitored data for different time frames. The study overcomes one of the Gaussian dispersion limitations: the equation of continuity assumes dispersion of a chemically stable material that did not deposit to the ground [53]. The model could be augmented by the addition of dry and wet deposition for the  $\text{NO}_x$  and  $\text{SO}_x$  species using methods described in the open literature [61], [62], [63] and [64]; thus, improving the overall mass balance.

##### 4.2. Dispersion Modeling of the City of London, UK

Two dispersion models were studied for the city of London, UK.

###### First Model

Owen et al. [5] utilized an existing air dispersion model which incorporated skewed – Gaussian distribution, ADMS-URBAN, along with meteorological data from one meteorological station, background concentrations of pollutants of interest for the 1995, year and emissions inventory from 1997 for the city of London. The model covered a domain of approximately 40 km by 40 km in the city of London and estimated ground level concentrations of  $\text{NO}_x$  and  $\text{NO}_2$ . The main sources of emissions (75 wt%) were roads characterized as line sources and industrial sources characterized as point sources.

The modeled concentrations were compared to the monitored data for the summer and winter of 1995. Concentrations of  $\text{NO}_x$  and  $\text{NO}_2$  were predicted utilizing the empirical function derived by Derwent and Middleton [65]. The modeled concentrations showed an under-prediction for winter months with a conclusion that the overall model's performance was reasonable when compared to the monitored data.

For the predicted occurrences of the highest concentrations, the meteorological data during the winter season was reviewed and reasons for possible under predictions were provided. The under prediction in the cooler season was due to (cold stable conditions) the poor dispersion. In addition, the average daily traffic flow was used while the remaining information was set in the model on an hourly basis. The cold stable conditions may be described by using the approach of Milliez and Carissimo [66] and Owen et al. [5] commented on missed smaller sources (i.e. winter emissions due to combustion related to heating of homes). Perhaps if hourly data of traffic were available, the correlation would have been improved.

The study did include review of modeled concentrations for the top percentiles against the observed data. The statistical analysis included the calculation of mean, standard deviation, correlation, and fraction of data within a factor of two.

A description of the model setup and grid density, chemistry, building effect and dry and wet deposition was not discussed in the above model. The chemistry may be approached using methods of Asman, Chang, Wesely and Cana-Cascallar [59], [60], [58] and [67]. The building effect on the dispersion and modification to the dispersion code can be set as per any of the proposed solutions by Milliez and Carissimo, Xie et al., Baker et al., Baik et al. [66], [68], [69] and [70]. Treatment of slow winds may be approached by the method used by Goyal et al. [71]. All these approaches would have been refined the algorithm and possibly lead to a better correlation. The study did not also comment on the use of various years for input into the model. Obtaining input data and meteorological information for the same year as the observed ambient concentrations would yield refined correlations.

###### Second Model

Seika et al. [6] transformed the German dispersion model IMMAUS designed for the former city of west-Berlin into a computer platform formulated for the city of London, UK. The emission inventory included traffic, non traffic point, and area sources. Concentrations were evaluated on a grid of various densities from 1 to 10 km spatial separation. The model included hourly meteorological data and background concentrations. The Gaussian plume included total reflection. The dispersion model handled dry and wet deposition for area sources only. The modeled concentrations showed a good agreement to the monitored data observed for the year 1993.

The study also provided an in depth review of the physics behind the assumed dispersion, meteorology, and emissions inventory. An observed limitation was the need to improve how the Gaussian plume diffusion applied to wind speeds below 1 m/s, varying wind speeds and need a module which calculated mid-day boundary layer depths. The dry deposition for area sources was simulated using Chamberlain's source depletion formulation. The study did not provide statistical analysis of the comparison for the modeled concentrations and observed values.

##### 4.3. Dispersion Modeling of the City of Helsinki, Finland

The  $\text{NO}_x$  emissions, dispersion, and chemical transformation for Helsinki metropolitan area was also modeled by Karppinen et al. [7] and [8]. Its objective was to study traffic-originated  $\text{NO}_x$  and to compare the results to four local monitoring stations for the year 1993. The domain of the city of Helsinki is approximately 30 by 30 km. Concentrations were modeled on a receptor grid with a network having dense grid (50 by 50 m) in the vicinity of the major roads and largest grid interval of 500 by 500 m around the perimeter of the city. Results were plotted as iso-concentration curves.

The hourly traffic emissions were based on EEME/2 transportation planning system (INRO 1994) and new emission factors that related to Helsinki city traffic. Pollutant concentrations were computed using the road network dispersion model CAR-FMI and urban dispersion modeling system UDM-FMI. Road sources were modeled as line source and remaining sources were



assigned characteristics of point sources. The meteorological data was obtained from two YTV meteorological stations and the mixing height of the atmospheric boundary layer was evaluated from a sounding station 90 km North-West of the city.

The 1998 study compared predicted annual average concentration to the observed data, showing a good agreement. There was a good agreement between the modeled data and three of the 4 YTV stations, however, there was a poor agreement with the 4th station. Road emissions contributed less than 50% of total emissions. Their analysis showed traffic sources have greater effect than industrial sources on the ground-level concentrations. In another study [8], the evaluation of seasonal and monthly concentrations was included. The results still contain severe under prediction of the modeled  $\text{NO}_x$  for the same 4th monitoring station as identified in the 1998 study. Furthermore, within the later study, the under prediction has been recognized for the winter months [8].

That study, comments on the variation between the modeled and observed concentrations. The statistical analysis included root mean squared error, index of agreement, correlation coefficient, normalized mean square error, and fractional bias. These parameters were applied to predicted and observed data sets as suggested by Willmott [38].

Both studies did not provide a review of all data provided by external bodies (meteorology, traffic, and ambient concentrations) utilized. The review of meteorology (i.e. wind roses, wind speeds, and stability classes) could provide an insight into variables that drive dispersion. Review of the calms and the treatment of calm conditions were not addressed. The study did not discuss traffic data to assess its limitations in the analysis. The review of ambient concentrations can give an insight of sampling methods and their limitations. Finally, the study did not address review data that did not pass quality control and thus, was not included in the modeling.

Furthermore, Karppinen et al. [8] proceeded to compare modeled hourly average concentrations to the observed data. A discussion was not given on the shortcomings of the data. The hourly average concentrations did not have a good agreement with the monitored data. A preferred approach can include a review of more than 1 year of modeled, selecting a year that best represents the meteorological conditions. A further look at the hourly averages on a daily basis along with the review of the meteorological conditions for these hours and traffic data may have provided an insight into why certain hourly averages did not match the modeled values (e.g. reduced traffic due to shutdown of a street would have resulted in lower observed concentrations but was not seen by the model). The monitored data was obtained at 4 m for two stations and 6 m for the fourth station. The study did not specify at what heights the concentrations were predicted and if those heights relate to the monitored data.

The study commented on road emissions being below 50% of the total emission and having a great impact on the final concentrations. It did not provide an explanation for this observation and it can be explained by source characteristics. Roads modeled as area sources are ground based and therefore, do not disperse as well as tall sources which have thermal and momentum rise (i.e. industrial sources). Tall sources, even though made more than 50% of the total emissions, disperse better than sources which behave as ground based sources. [40], [53], [37] and [45]. In addition, road sources could have also been modeled as smaller virtual sources (i.e. width/length) as proposed in US EPA [51]. This approach is time consuming but addresses the dispersion associated with the traffic.

The lack of agreement between the modeled concentrations and the observed data at the 4th monitoring station may be explained by building downwash effect. The severe under prediction could be explained by a possible plume trap (i.e. busy intersection with tall buildings) around the area thus, resulting in higher observed concentrations. By reviewing the traffic data and locations of the monitoring stations, adjustments could have been made to correct the study to account for a better representation of the dispersion around the 4th monitoring station.

#### 4.4. Dispersion Modeling of the City of Prague, Czech Republic

Brechler [9] developed a Gaussian dispersion model for the city of Prague. Sources were characterized as point (stacks of thermal power plants), line (traffic sources), and area sources (cross roads, petrol stations, parking sites, railway, and bust stations). Emissions due to furnaces which heat homes were included. Brigg's formula was used to define plume rise [72]. A complex network of monitors maintained by Czech Hydrometeorological Institute and hygienic service of the Prague city includes 27 monitors. The model was used to estimate concentrations of various pollutants for years 1994, 1996, and 1998.

The study did not explain the selection of non-consecutive years for which concentrations were evaluated. The model did resolve a limitation of a Gaussian dispersion model, inability to resolve flow field due to complex terrain. This was resolved by dividing the domain into smaller segments with individual meteorological conditions computed by a mesoscale model. Gaussian dispersion was selected primarily due to time limitations and simplicity of the model. An alternative approach to describing stability of the atmosphere was done by utilizing Bubnik – Koldovsky classification and not Pasquill [73]. This approach uses a classification based on the value of vertical gradient of temperature and splits all possible conditions of vertical temperature stability into 5 categories for each vertical segment. Pasquill-Gifford approach utilized solar insulation and wind speed [37]. The study did not discuss statistical analysis of the predicted values and monitored data.

#### 4.5. Historical Work Completed on the Simulation of Pollution Type of Studies Completed for the City of Toronto, Canada

Remarkably, little work has been published on simulating ground level concentrations of various pollutants for the City of Toronto [74], [75] and [76]. All three studies look at the emissions from the city using various tools and on various domain sizes.

##### First Study

The 1996 publication by Lin et al. was a study of a single poor air quality episode observed on April 6, 1992, at some distance away from the City of Toronto. This publication was a result of a program entitled Southern Ontario Oxidants Study (SONTOS 92). The objective of the SONTOS 92 program was to study the impact of emissions from the City of Toronto on the ozone levels in two areas: the first one located 140 km North-East of the City of Toronto in the city of Hastings and the second one 80 km South-West of Toronto in the city of Binbrook. Lin et al. [74] applied a one dimensional photochemical transport model along with Lagrangian calculations to model the emission of pollutants from the city. The City of Toronto was assumed to be a box of 20 by 30 km. The model predicted concentrations of various contaminants in Hastings and compared them to the observed data on April 6, 1992. The study concludes that the City of Toronto has an impact on the ozone levels downwind and further studies on regional scale were to be completed. No results were published for the city of Binbrook. It is important to note that no other results or analysis of data collected under SONTOS 92 have been published.

##### Second Study

Yang et al. [75] conducted a smaller in domain exercise by looking at pollution around a specific intersection located in the core of the City of Toronto at Bay Street and King Street. The study concentrated on the street canyon effect, similar to CFD type of exercises. This study was designed with a dense grid and included an area with very tall buildings (i.e. 330 m above grade). A non-steady state dispersion model (CALPUFF) was used to predict concentrations at the ground level and at various heights above grade. The meteorological data was predicted using MM5-a prognostic model. This publication did not study any particular air quality event that occurred in the city and did not compare results to measured data. The study concluded that CALPUFF is a potentially adequate tool which can simulate flow fields.



Third Study

Unlike the two previous mentioned studies by which dispersion models were utilized, the study conducted by Jerrett et al. considered traffic pollution in the City of Toronto and utilized a land use regression (LUR) approach to predict ground level concentrations of NO<sub>2</sub>. The study was conducted in 2002 for a period of 2 weeks with numerous air samplers deployed across the City of Toronto. A regression of 0.69 was determined with the intention to include other sources and meteorological data to improve the results. In addition, the authors propose to generate more data to encompass a full year.

4.6. Preliminary Dispersion Modeling of the City of Toronto, Canada

In our own study, the Gaussian dispersion model along with local meteorological data was applied to road network with the objective to predict 1-h ground level concentrations of NO<sub>2</sub>. Furthermore, the objective of this study was to compare the predicted concentrations to those recorded by a local monitoring station.

Description of the Event and Modeling Domain

The timing of study was selected to be the first few days of February 2005, coinciding with the beginning of the earliest episode of smog recorded in Toronto. The area of study was selected to be two blocks of major streets surrounding a monitoring station located at Finch Avenue and Yonge Street, station I.D. 34020 [77], an approximate area of 36 km<sup>2</sup>. The monitoring station did not capture full data for the entire smog episode. The 1-h concentrations of SO<sub>2</sub>, NO<sub>2</sub>, NO<sub>x</sub>, PM<sub>2.5</sub> and O<sub>3</sub> observed at the monitoring station could be obtained from the historical depository [77]. The hourly meteorological data were obtained from a meteorological station at Toronto's Lester B. Pearson International Airport [78], approximately 30 km away from the selected area of study shown in Figure 10. The meteorological data was collected 10 m above the ground. For the time under consideration, there were two predominant wind directions, with the winds occurring at 2 m/s from south-south-east and at 5.7 m/s from north-north-west, shown in Figure 11. Morning and afternoon peak-traffic times were modeled to occur from 7 am to 9 am and from 4 pm to 6 pm, respectively. Traffic data from 2001 [79] and the Environment Canada's emission factors [80] for various vehicles were used to estimate emission rates of NO<sub>2</sub>.

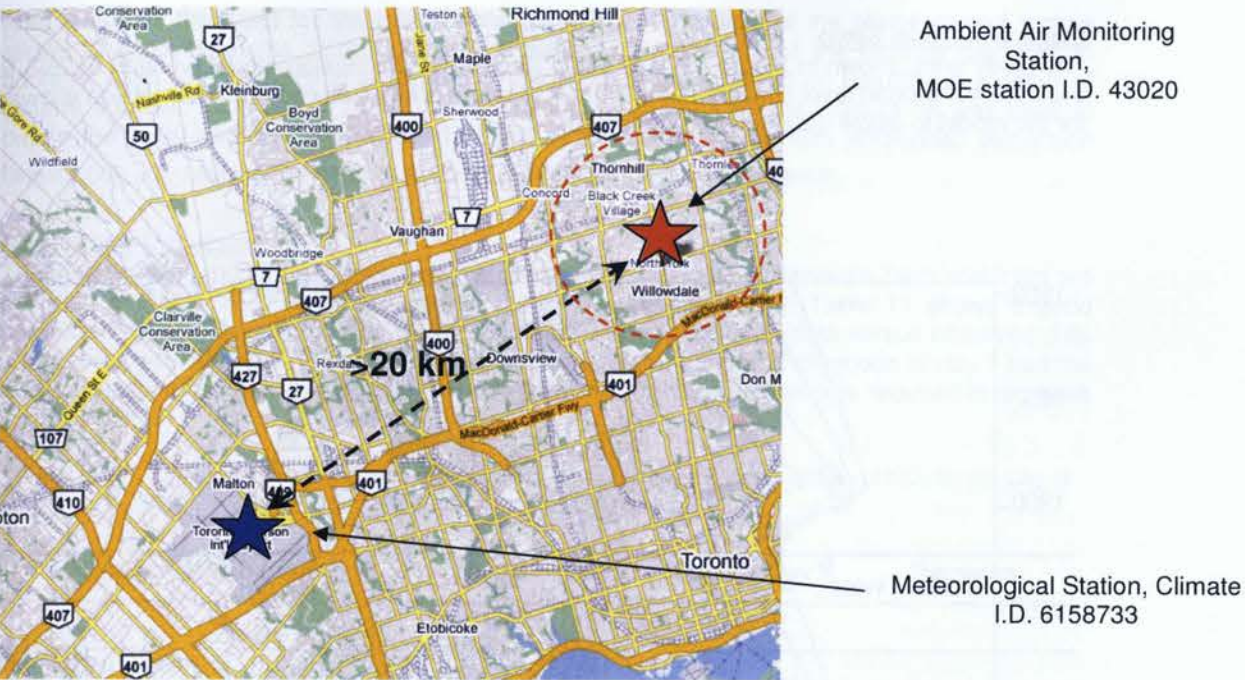


FIGURE 10: The preliminary study was conducted by simulating emissions from a 3 block sector around Yonge Street and Finch Avenue intersection located more than 20 km from the nearest source of meteorological data (Toronto Pearson International Airport)

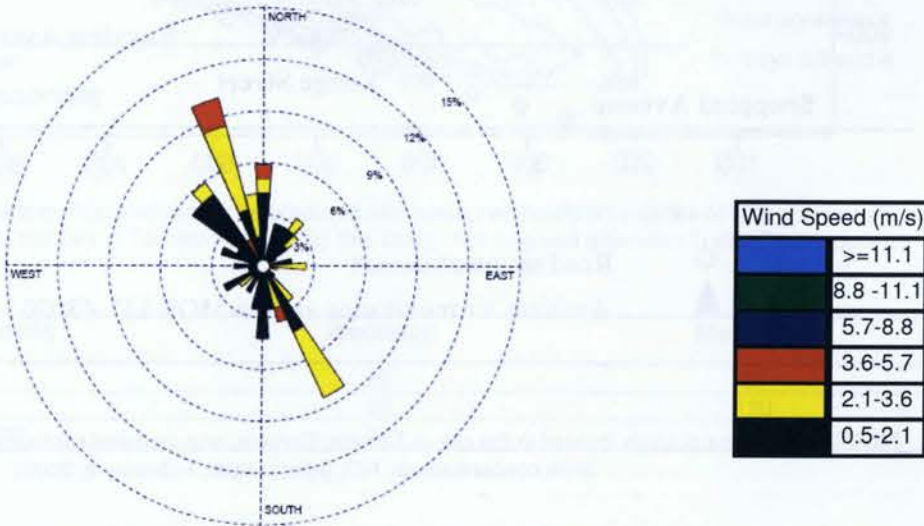


FIGURE 11: February 1 to 5, 2005 - wind rose from Toronto Lester B. Pearson International Airport (WMO Identifier 6158733) for the period associated with the study of emissions from a road network located in the city of Toronto, Ontario, Canada. Wind direction is to be read FROM



Dispersion Model Setup

The study area, shown in Figure 12, was set in ISC-PRIME dispersion model (version 04269) to evaluate 1-h ground level concentrations of NO<sub>x</sub> in urban area. Selection of urban option allowed for the model to utilize urban dispersion factors.

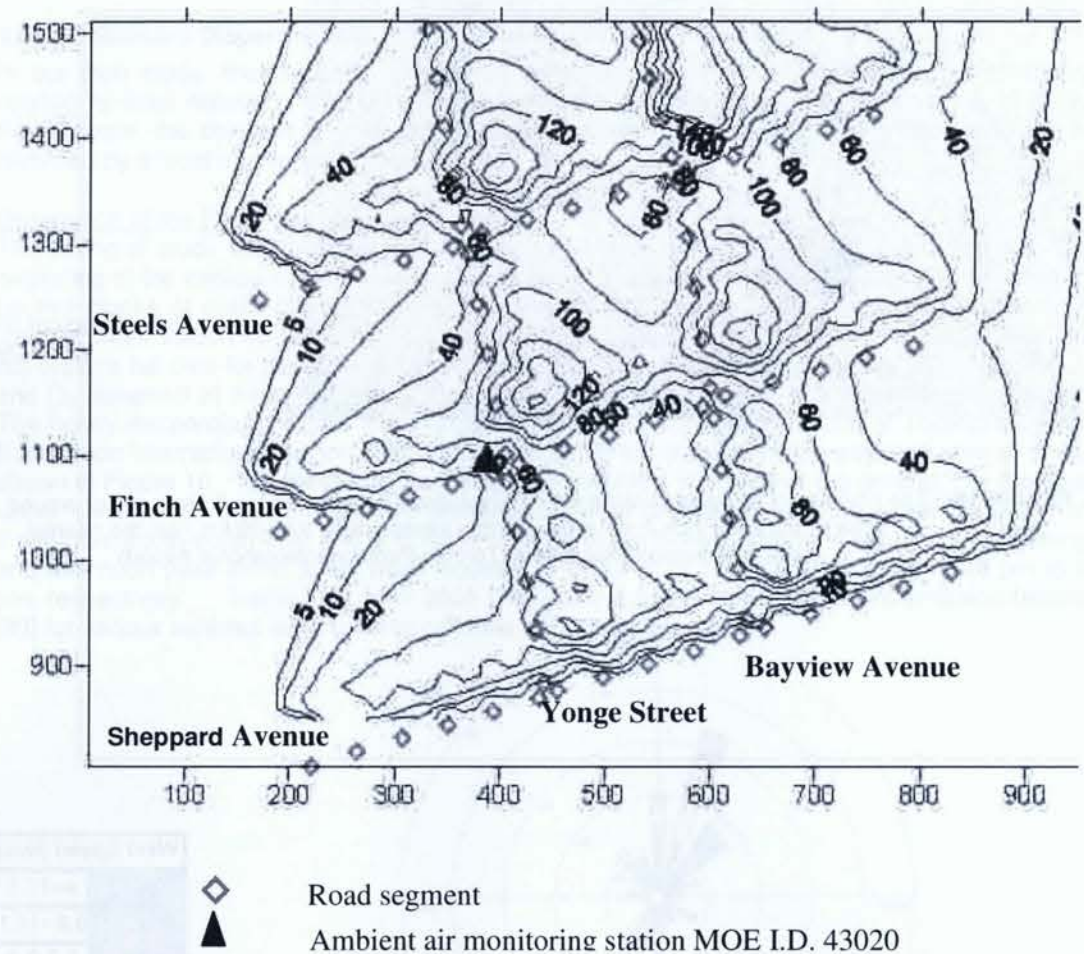


FIGURE 12: Area of study located in the city of Toronto, Canada, and modeled contour plots of ground level concentrations, NO<sub>x</sub> µg/m<sup>3</sup> (4 pm, February 4, 2005)

The characterization of road within the dispersion model was based on three options: as line been studied as potential methods to characterize road emissions within the Gaussian dispersion model. The limitation of a line source as mentioned earlier arises when winds approach at angles greater than 75°. The area source has a limit on the length to width ratio 10:1. Furthermore, the use of line or area sources yields an over prediction of the ground level concentrations [81] therefore, it was not evaluated in this study. A third option of setting up a road in a Gaussian dispersion model is to use numerous volume sources along the stretch of the path that follows road [51]. Sometimes this method is referred to as "equivalent line" source where the width of the

road becomes the basis for the initial lateral dimension. Inclusion of the plume spread factors allows to account for the mixing due to the elevated temperature of the exhaust gas [82]. In addition, each virtual source is separated by the width of the road (25 m) resulting in a series of volume sources. The height of the mobile equipment present on the road (3 m) was used to define the initial vertical dimension. The use of a volume source with embedded dispersion factors ( $\sigma_y, \sigma_z$ ) allows the code to account for vehicle induced turbulence.

Results and Discussion

The modeled and monitored concentrations for the peak traffic times between 7 am and 9 am are provided in Table 10. Preliminary statistical analysis summarized in Table 11 shows a good agreement between predicted and measured data. Plot of monitored data versus observed data yields a regression of 0.5. It was observed that both the morning and afternoon of day 1 had the least correlation. Note, the sample size is relatively small and further work is required to increase it.

TABLE 10: Summary of morning and afternoon peak time average concentrations of NO<sub>2</sub> for the City of Toronto obtained in this study

Concentration (µg/m <sup>3</sup> )	Day 1	Day 2	Day 3	Day 4	Remarks
Morning					
Monitoring Station I.D. 43020	79	88	81	120	Good agreement for days 2, 3 and 4
Results from the Simulation in ISC-PRIME	55	87	56	88	
Afternoon					
Monitoring Station I.D. 43020	41	90	111	100	Good agreement for days 2,3 and 4
Results from the Simulation in ISC-PRIME	106	105	173	114	

TABLE 11: The statistical analysis of the predicted and measured hourly time series of NO<sub>2</sub> concentrations for the City of Toronto modeled by this study. Morning and afternoon Traffic Peak Hours for February 1-4, 2005

Statistic	Predicted	Measured
Mean	55	84
Maximum	88	120
Standard Deviation	22	15



Two additional observations with regards to the relationships between the modeled concentrations and road traffic emissions could be made from the results. For the morning traffic, the model under-predicted the ground level concentrations. This can be explained by the presence of calm meteorological conditions that have limited mixing [5]. The afternoon traffic model over-predicted the ground level concentrations. This over-prediction could be a result of the presence of fog/clouds in the afternoon hours however, further study is necessary.

To further refine calculations, one can add emissions from local industrial sources as well as the nearby 400 series highways in addition to updating the traffic information with a 2005 traffic count. The meteorological conditions, specifically the presence of fog and clouds, could be accounted via the inclusion of the wet deposition. The analysis of hourly and 24 hour averages would be of interest and allow one to further refine the results. As indicated in the previous sections, the Gaussian dispersion model did not perform accurately when simulating during the winter period.

## 5. CONCLUSIONS

The air quality in Ontario is on a decline and causes the province additional cost in health care as well as limits enjoyment of the outdoors. The provincial governing bodies introduced regulations to reduce air emissions; and communication tools in the form of AQI however, this communication tool has its own limitations. One major limitation of the AQI is that for many cities, the local air quality, often over 50 km in radius, is evaluated by a single monitoring station. This lack of resolution results in large areas being declared with "poor" air quality when in fact the situation may be highly localized. Another limitation is that the air quality is based on unprocessed data from the monitoring stations. Without some appreciation of the quality of the data, and an understanding of the data in context with the region, it is difficult to fully trust that predictions of air quality are accurate. Finally, the program is costly in maintenance. With governments at all levels experiencing budgetary limits, a costly environmental system is much more difficult to run and manage when the return is rarely visible.

An improved set of methods to determine the AQI should include canyon effects, land regression modeling, and dispersion modeling. Canyon effects and land regression modeling have their own limitations since they only cover a small geographical area of study and require extensive pre-processing and manipulation of large data sets. Dispersion modeling is not a new approach and has been carried out in major cities across the world and showed a good agreement with monitored data for the area of interest.

In the preliminary study shown in this paper, a small scale dispersion model for the city of Toronto, Ontario, Canada, was carried out. The results showed a reasonable agreement with the monitoring data with respect to predicting localized contaminant concentrations. Furthermore, by super-imposing the hourly concentrations over the modeled area, the results showed locations of localized hot spots (i.e. poor air quality).

The readily available tools and data combined with a dispersion model provide a more accurate representation of the air quality at a lower cost than the existing systems in place. A dispersion model applied to the city of Toronto removes the assumption of uniform air quality within the vicinity of a monitoring station. This clearly addresses one of the key limitations of the AQI. The preliminary results are encouraging to apply existing air dispersion model, available emissions data for assessing air quality in the city of Toronto.

## REFERENCES

1. Ontario Medical Association, "The Illness Costs of Air Pollution, 2005-2006 Health and Economic Damage Estimates", June 2005
2. Toronto Public Health, "Air Pollution Burden of Illness from Traffic in Toronto, Problems and Solutions", November 2007
3. M. Jerrett, A. Arain, P. Kanaroglou, B. Beckerman, D. Potoglou, T. Sahsuvaroglu, J. Morrison and C. Giovis, "A review and evaluation of intraurban air pollution exposure models", Journal of Exposure Analysis and Environmental Epidemiology, 15, 185-204, 2005
4. K. Kitabayashi, S. Konishi and A. Katatani, "A  $\text{NO}_x$  Plume Dispersion Mode with Chemical Reaction in Polluted Environment", JSME International Journal, 49, 1, 2006
5. B. Owen, H.A. Edmunds, D.J. Carruthers and R. J. Singles, "Prediction of Total Oxides of Nitrogen and Nitrogen Dioxide Concentrations in a Large Urban Area Using a New Generation Urban Scale Dispersion Model with Integral Chemistry Model", Atmospheric Environment, 34, 397-406, 2000
6. M. Seika, R.M. Harrison and N. Metz, "Ambient Background Model (ABM): Development of an Urban Gaussian Dispersion Model and Its Application to London", Atmospheric Environment, 32 (11), 1881-1891, 1998
7. A. Karppinen, J. Kukkonen, M. Kontinen, J. Härkönen, E. Rantakrans, E. Volkonen, T. Koskentalo and T. Elolähde, "The emissions, dispersion and chemical transformation of traffic-originated nitrogen oxides in the Helsinki metropolitan area", International Journal Vehicle Design, 20, 1-4, 1998
8. A. Karppinen, J. Kukkonen, T. Elolähde, M. Kontinen and T. Koskentalo, "A modeling system for predicting urban air pollution: comparison of model predictions with the data of an urban measurement network in Helsinki", Atmospheric Environment, 34, 3735-3743, 2000
9. J. Brechler, "Model Assessment of Air-Pollution in Prague, Environmental Monitoring and Assessment", 65, 269-276, 2000
10. S. R. Hayes and G.E. Moore, "Air Quality Model Performance: a Comparative Analysis of 15 Model Evaluations Studies", Atmospheric Environment, 1986
11. S. Cheng, J. Li, B. Feng, Y. Jin and R. Hao, "A Gaussian-box modeling approach for urban air quality management in a northern Chinese city – I. model development", Water Air Soil Pollution, 178: 37-57, 2006
12. Ontario Ministry of the Environment, "Air Quality in Ontario 2005 Report", PIBs6041, 2006
13. Ontario Ministry of the Environment, "Air Quality in Ontario 2002 Report", 2003
14. Ontario Ministry of the Environment, "Air Quality in Ontario 2003 Report", 2004
15. Ontario Ministry of the Environment, "Air Quality in Ontario 2004 Report", 2005
16. Ontario Ministry of the Environment, "Air Quality in Ontario 1999 Report", 2000
17. Ontario Ministry of the Environment, "Air Quality in Ontario 2000 Report", 2001



18. Ontario Ministry of the Environment, "Air Quality in Ontario 2001 Report", 2002
19. Ontario Ministry of the Environment, "Green Facts – Ontario's Air Quality Index", May 2005
20. Environment Canada Air Quality Services, [http://www.msc-smc.ec.gc.ca/eq\\_smog/on/on\\_e.cfm](http://www.msc-smc.ec.gc.ca/eq_smog/on/on_e.cfm) - 2008
21. The Association of Municipalities of Ontario: <http://www.yourlocalgovernment.com/ylg/muniont.html> - total number of municipalities in Ontario, February 2009
22. Ontario Ministry of the Environment, "Industrial Pollution Team", July 30 2004
23. Ontario Ministry of the Environment: <http://www.ene.gov.on.ca/envision/scb/> - SCB results, February 2009
24. Ontario Ministry of the Environment, <http://www.ene.gov.on.ca/envision/general/leadership/index.htm> – Environmental Leaders, 2009
25. Ontario Ministry of the Environment, "Procedure for Preparing an Emission Summary and Dispersion Modeling Report", Version 2.0, PIBs # 3614e02, July 2005
26. Ontario Ministry of the Environment, "Step by Step Guide for Emission Calculation, Record Keeping and Reporting for Airborne Contaminant Discharge", 2001
27. Ontario Ministry of the Environment, <http://www.oetr.on.ca/oetr/index.jsp> - O.Reg. 194/05 Industrial Emissions – Nitrogen Oxides and Sulphur Dioxide, 2005
28. Environment Canada- [http://www.qc.ec.gc.ca/dpe/Anglais/dpe\\_main\\_en.asp?air\\_inrp](http://www.qc.ec.gc.ca/dpe/Anglais/dpe_main_en.asp?air_inrp) National Pollutant Release Inventory, February 2009
29. Environment Canada, General Guidance Document, "Notice with Respect to Reporting of Information on Air Pollutants, Greenhouse Gases and Other Substances for the 2006 Calendar Year, Canada Gazette Part I under section 71 of the Canadian Environmental Protection Act 1999", December 8, 2007
30. Environment Canada, "Greenhouse Gas Emissions Reporting Technical Guidance on Reporting Greenhouse Gas Emissions", 2006
31. British Columbia Ministry of Environment, "Guidelines for Air Quality Dispersion Modeling in British Columbia", October 2006
32. Alberta Environment, "Air Quality Model Guide", March 2003
33. Ontario Ministry of the Environment, <http://www.ene.gov.on.ca/en/air/aqo/index.php> - 2009
34. Environmental Commissioner of Ontario, "2007/08 Annual Report – Getting to K(No)w", pg. 57, 2008
35. US EPA, [http://www.epa.gov/scram001/dispersion\\_prefrec.htm](http://www.epa.gov/scram001/dispersion_prefrec.htm) - US EPA, Preferred / Recommended Models, 2007
36. Ministry of the Environment New Zealand, "Good Practice Guide for Atmospheric Modeling", June 2004

37. M. R. Beychok, "Fundamentals of Stack Gas Dispersion", Third Edition, 1994
38. C. J. Willmott, "On the validation of models, Physical Geography", 1981
39. H.O. Perkins, "Air Pollution", 1974
40. D. Cooper and F.C. Alley, "Air Pollution Control A Design Approach", 3rd edition, 2002
41. R. W. McMullen, "The change of concentration standard deviations with distance", JAPCA, 30 (7), 773, 1980
42. Y.S. Shum, W.D. Loveland and E. W. Hewson, "The use of artificial Activable trace Elements to Monitor Pollutants Source Strengths and Dispersal Patterns", JAPCA, November 1976
43. K.L. Calder, "On Estimating Air Pollution Concentrations from a Highway in an Oblique Wind", Atmosphere Environment, 7, 863-868, 1973
44. M.D. Carrascal, M. Puigcerver and P. Puig, "Sensitivity of Gaussian Plume Model to Dispersion Specifications", Theoretical and Applied Climatology, 48, 147-157, 1993
45. R. A. Dobbins, "Atmospheric Motion and Air Pollution", 1979
46. A. Venkatram A. and T.W. Horst, "Approximating dispersion from a finite line source. Atmospheric Environment", 40, 2401-2408, 2006
47. S. M. S. Nagendra and M. Khare, "Review Line Source Emission Modeling, Atmospheric Environment", 36, 2083-2098, 2002
48. K. L. Calder, "Multiple-Source Plume Models of Urban Air Pollution – The General Structure", Atmospheric Environment, 11, 403 – 414, 1977
49. Ontario Ministry of the Environment, "Air Dispersion Modeling Guideline for Ontario", July, 2005
50. H. F. Hemond and E. J. Fechner-Levy, "Chemical Fate and Transport in the Environment", Second Edition, 2000
51. US EPA, "User's Guide for the Industrial Source Complex (ISC3) Dispersion Models", EPA-454/B-95-003b, 1995
52. J.S. Scire, D. G. Strimaitis and R. J. Yamartino, "Model formulation and user's guide for the CALPUFF dispersion model", Sigma Research Corp., 1990
53. J. Colls, "Air Pollution an Introduction", E&FN Spon, an imprint of Chapman & Hall, 70, 1997
54. Y. Ogawa, P.G. Diosey, K. Uehara and H. Ueda, "Plume behaviour in stratified flows", Atmospheric Environment, 16 (6), 1419-1433, 1982
55. Ontario Ministry of the Environment, "Air Quality in Ontario 2007 Report", 2008
56. Canada Gazette, "Regulations Amending the Sulphur in Diesel Fuel Regulations", 138, 40, October 2, 2004
57. T. McMahon and P.J. Denison, "Review Paper Empirical Atmospheric Deposition Parameters –A Survey", Atmospheric Environment, 13, 571-585, 1979



58. M. L. Wesely, "Parameterization of Surface Resistances to Gaseous Dry Deposition in Regional-Scale Numerical Models", *Atmospheric Environment*, 23 (6), 1293-1304, 1989
59. W. Asman, "Parameterization of Below-Cloud Scavenging Of Highly Soluble Gases Under Convective Conditions", *Atmospheric Environment*, 29 (12), 1359-1368, 1995
60. T. Y. Chang, "Rain and Snow Scavenging and  $\text{HNO}_3$  vapor in the atmosphere", *Atmospheric Environment*, 18 (1), 191 – 197, 1984
61. D. Quelo, V. Mallet and B. Sportisse, "Inverse Modeling of  $\text{NO}_x$  Emissions at Regional Scale Over Northern France. Preliminary Investigation of the Second-Order Sensitivity", *Journal of Geophysical Research*, DOI:10.1029. 2005
62. D. Jacob, "Heterogeneous Chemistry and Tropospheric  $\text{O}_3$ ", *Atmospheric Environment* 34, 2131-2159, 2000
63. Vila-Guerau de Arellano, A. Dosio, J.F. Vinuesa, A.A. M. Holtslang and S. Galmarini, "The dispersion of chemically reactive species in the atmospheric boundary layer", *Meteorology and Atmospheric Physics*, Austria, 87, 23-38, 2004
64. R. F. Adamowicz, "A model for the reversible washout of sulfur dioxide, ammonia and carbon dioxide from a polluted atmosphere and production of sulfates in raindrops", *Atmospheric Environment*, 13, 105-121, 1979
65. R.G. Derwent and D.R. Middleton, "An Empirical Function for the Ratio  $\text{NO}_2:\text{NO}_x$ , Clean Air", *The National Society for Clean Air*, Brighton, 26, 3/4, 57-59, 1996
66. M. Milliez and B. Carissimo, "Numerical simulations of pollutant dispersion in an idealized urban area for different meteorological conditions", *Boundary-Layer Meteorology*, 122: 321-342, 2007
67. L.C. Cana-Cascallar, "On the Relationship Between Acid Rain and Cloud Type", *Air and Waste Management Association*, 52, 334-338, 2002
68. X. Xie, Z. Huang and J. Wang, "Impact of building configuration on air quality in street canyon", *Atmospheric Environment*, 39, 4519-4530, 2005
69. J. Baker, H.L. Walker and X. Cai, "A study of dispersion and transport of reactive pollutants in and above street canyons – a large eddy simulation", *Atmospheric Environment* 38, 6883-6892, 2004
70. J. Baik, Y. Kang and J. Kim, "Modeling reactive pollutant dispersion in an urban street canyon", *Atmospheric Environment*, 41, 934-949, 2007
71. P. Goyal, M. P. Singh and T.K. Bandyopadhyay, "Environmental Studies of  $\text{SO}_2$ , SPM and  $\text{NO}_x$  over Agra, with various methods of treating calms", *Atmospheric Environment*, 28, 19, 3113-3123, 1994
72. R. W. Boubel, D. L. Fox, D. B. Turner D.B. and A. C. Stern, "Fundamentals of Air Pollution", Academic Press, London, 1994
73. J. H. Seinfeld, "Atmospheric Chemistry and Physics of Air Pollution", A Willey Interscience Publications, New York, 1986

74. X. Lin, P.B. Roussel, S. Laszlo, R. Taylor, O. Melo, P. B. Shepson, D. R. Hastie and H. Niki, "Impact of Toronto Urban Emissions on Ozone Levels Downtown", *Atmospheric Environment*, 30, 12, 2177-2193, 1996
75. R. Yang, A. Ciccone and C. Morgen, "Modeling Air Pollution Dispersion in Urban Canyons of Downtown Toronto", *Air and Waste Management Association*, 2007
76. M. Jerrett, M. A. Arain, P. Kanaroglou, B. Beckerman, D. Crouse, N. L. Gilbert, J. R. Brook, N. Finkelstein and M. M. Finklestein, "Modeling the Intraurban Variability of Ambient Traffic Pollution in Toronto, Canada", *Journal of Toxicology and Environmental Health, Part A*, 70, 200-212, 2007
77. Ontario Ministry of the Environment, [http://www.airqualityontario.com/reports/historical\\_data.cfm](http://www.airqualityontario.com/reports/historical_data.cfm) - MOE Air Quality Index, Historical Data, 2007
78. Environment Canada Weather Network, [http://climate.weatheroffice.ec.gc.ca/climateData/canada\\_e.html](http://climate.weatheroffice.ec.gc.ca/climateData/canada_e.html) - 2007
79. University of Toronto, "Greater Toronto Area Gordon Count Summary", 2002
80. Transport Canada, <http://www.tc.gc.ca/programs/environment/UTEC/CacEmissionFactors.aspx> - 2007
81. S. M. S. Nagendra and M. Khare, "Review Line Source Emission Modeling", *Atmospheric Environment*, 36, 2083-2098, 2002
82. M. Bady, S. Kato, R. Ooka, H. Huang H. and T. Jiang, "Comparative study of concentrations and distributions of CO and NO in an urban area: Gaussian plume model and CFD analysis", *Air Pollution*, 86, 2006



## CHAPTER 2

# DEVELOPMENT OF THE ARSUS MODEL

### 2.1 *The ARSUS Computer Model*

An Air dispersion model for the Road Sources in Urban areaS (ARSUS) based on the Gaussian air dispersion principles was developed and written in MATLAB (version 7.0.0.19920 (R14)). The ARSUS model was developed to simulate dispersion of tailpipe emissions in an urban area such as the City of Toronto. The modelling runs were executed on a standard PC platform equipped with Pentium(R) M processor 1.4 GHz and 586 MHz of RAM and Windows XP based environment. MATLAB was selected for the following reasons:

- a) the ability to handle data in a matrix and array structures (i.e. input and output data);
- b) the majority of the code was written in function format, therefore, reducing the redundancy of the code (i.e. "IF-ELSE" and "FOR-END" loops), and allowing for "one point" of correcting or updating the code;
- c) the ability to run batch files without the user watching over the ARSUS model;
- d) the ability to plot the results (isopleths) which normally would have to be completed using a secondary software and required processing of data (i.e. geographical interface software such as SURFER);
- e) the possibility to edit equations and approaches to solving plume dispersion equations (i.e. change of plume dispersion parameters and or plume rise solutions);
- f) a new code allows the user to expand beyond current limitations of existing US EPA dispersion models (i.e. ISC3) where it is able to use: and
  - i.) capable to include more than 300 sources; and
  - ii.) capable of handling more than 3,000 receptors.
- g) it is readily available.



The ARSUS model is based on selected equations, Equations (3) and (7), which estimate ground level concentrations based on meteorological data and emissions data following the standard Gaussian air dispersion solutions.

## 2.2 Limitations of the ARSUS Model

Following are some of the identified limitations of the ARSUS model:

- The ARSUS model currently mimics the US EPA's ISC3 air dispersion model<sup>1</sup>. The original purpose for this initial setup was to validate the ARSUS model against ISC3.
- The executing time is a function of both the number of emission sources and grid density.
- As with any modelling exercises, there exists an important aspect of quality of data fed into the ARSUS model. At the present time, the meteorological data can be easily obtained but the traffic data required a number of assumptions to be made and can be further refined.

## 2.3 Pseudo-Code for the ARSUS Model

The pseudo-code of the ARSUS model is provided in Figures 2-1a to 2-1d. The main code is written in a MATLAB m-file entitled Concentration.m (Figure 2-1a). The file reads two EXCEL input data files:

- Source data file – containing the source details; and
- Meteorological data file – containing the hourly meteorological details.

The domain is sub-divided into a grid of points. The program evaluates concentration from each source to each grid point and sums the calculated concentrations for every hour. The final matrix of concentrations is written to an EXCEL file. The program evaluates the hourly concentrations and can be set to run for a continuous series of meteorological hours.

<sup>1</sup> Note that the US EPA's ISC3 model is limited in the number of sources and receptors; the ARSUS code does not suffer the same limitation.

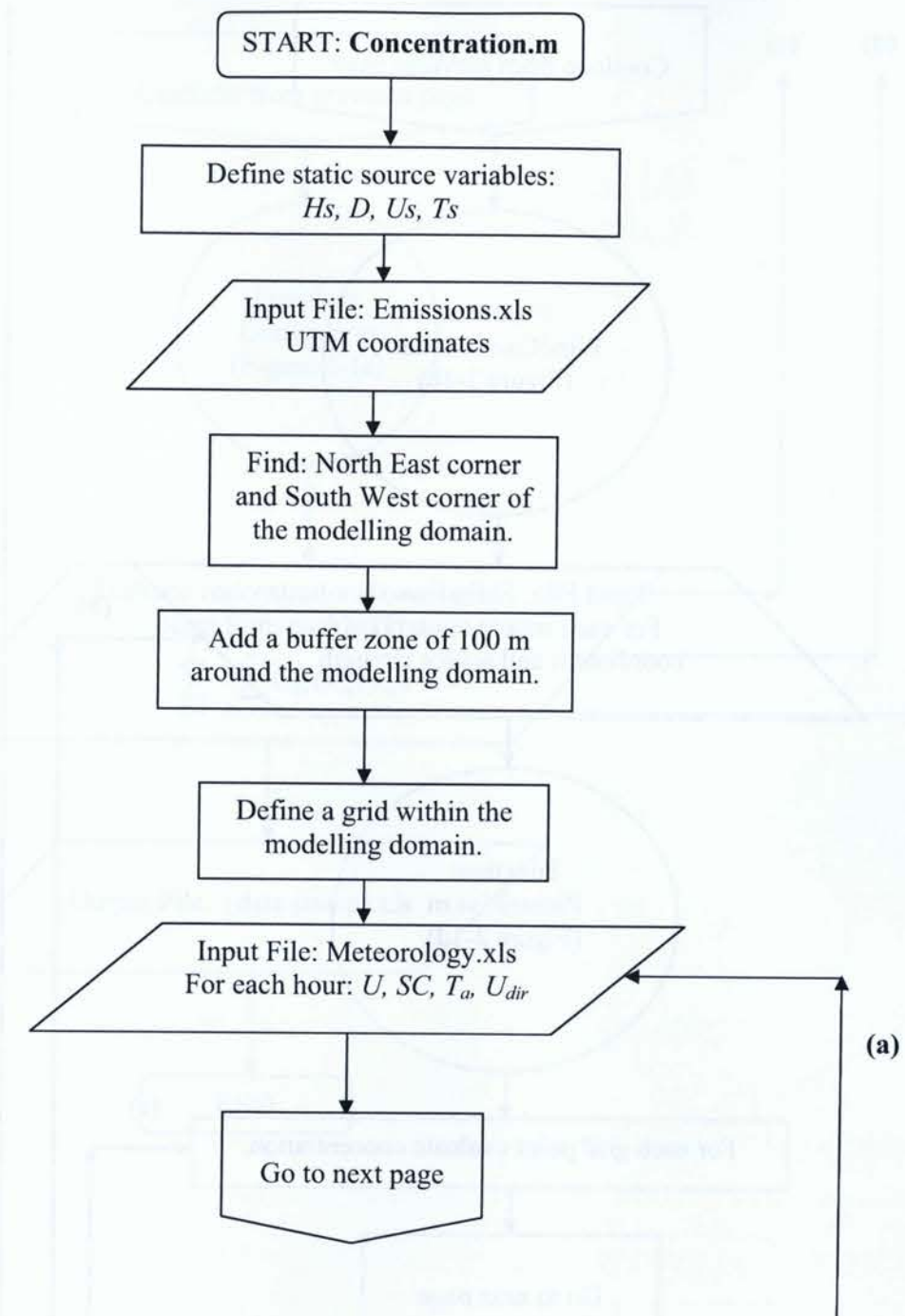


Figure 2-1a. Flow diagram of FUNCTION: Concentration.m. This is the main program which reads input file and meteorological file, utilizes WindCorrection.m and Gaussian.m functions to estimate concentrations and write them into an EXCEL file.

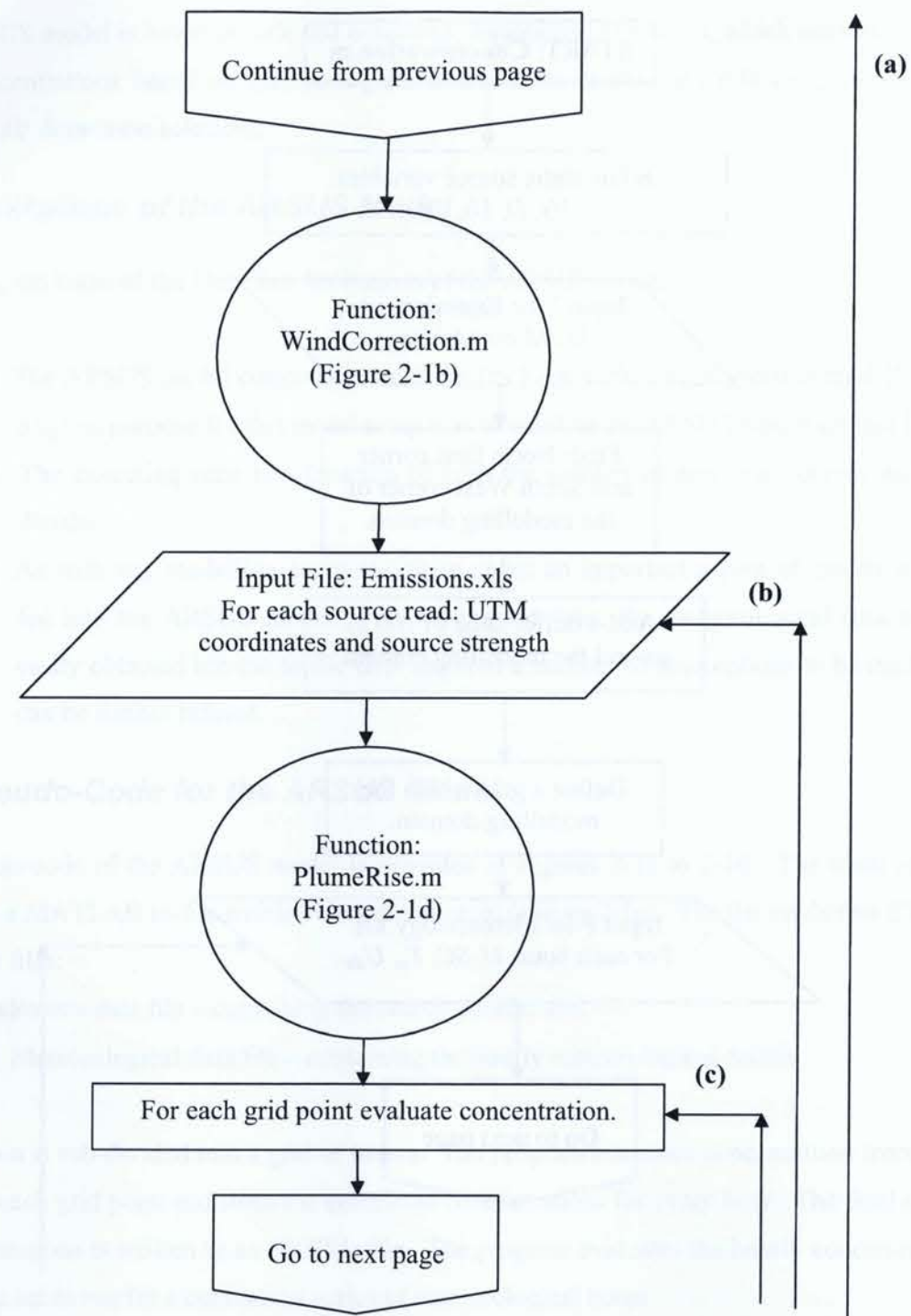


Figure 2-1a. Continuation of the: Flow diagram of FUNCTION: Concentration.m.

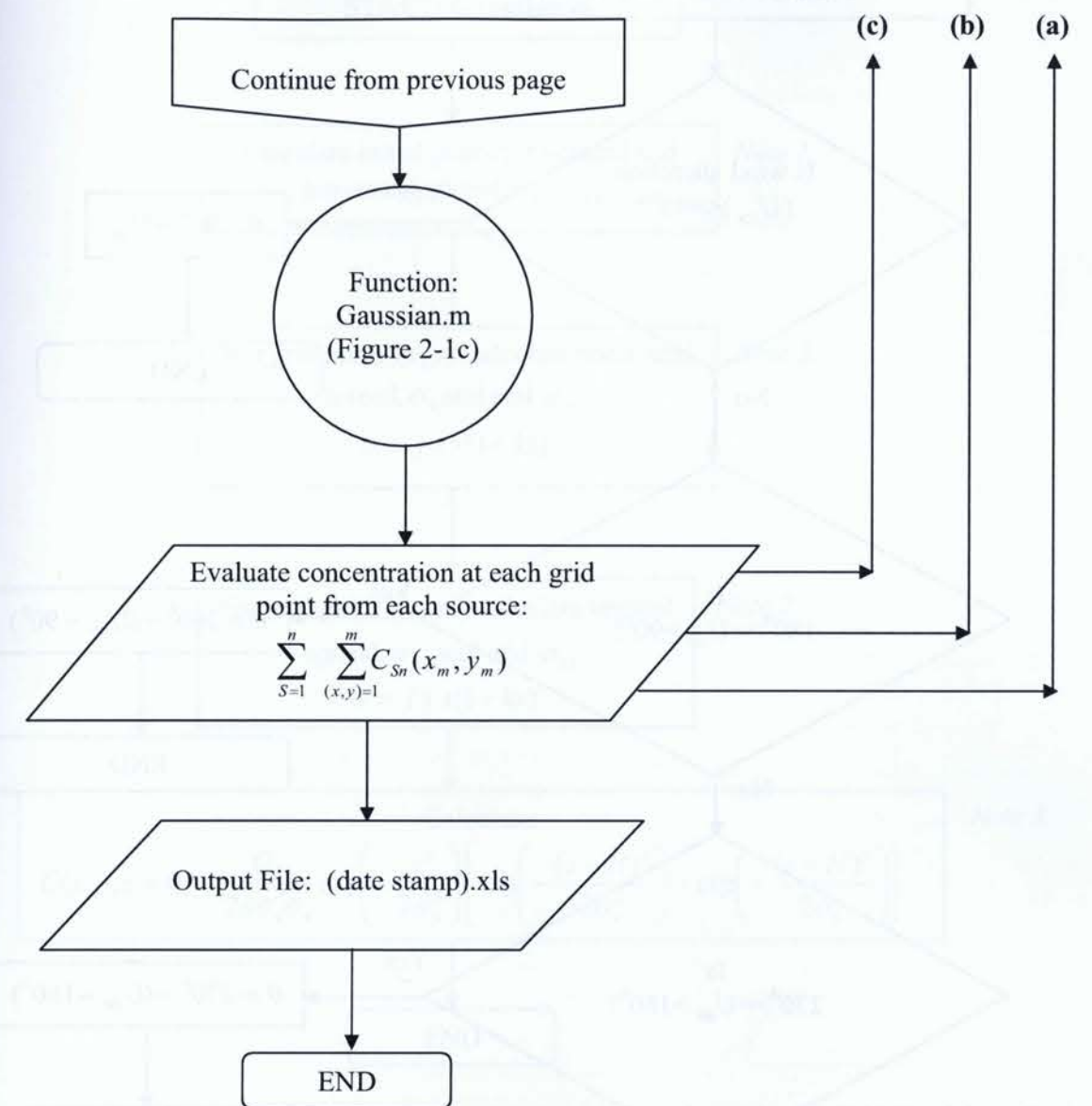


Figure 2-1a. Continuation of the: Flow diagram of FUNCTION: Concentration.m.



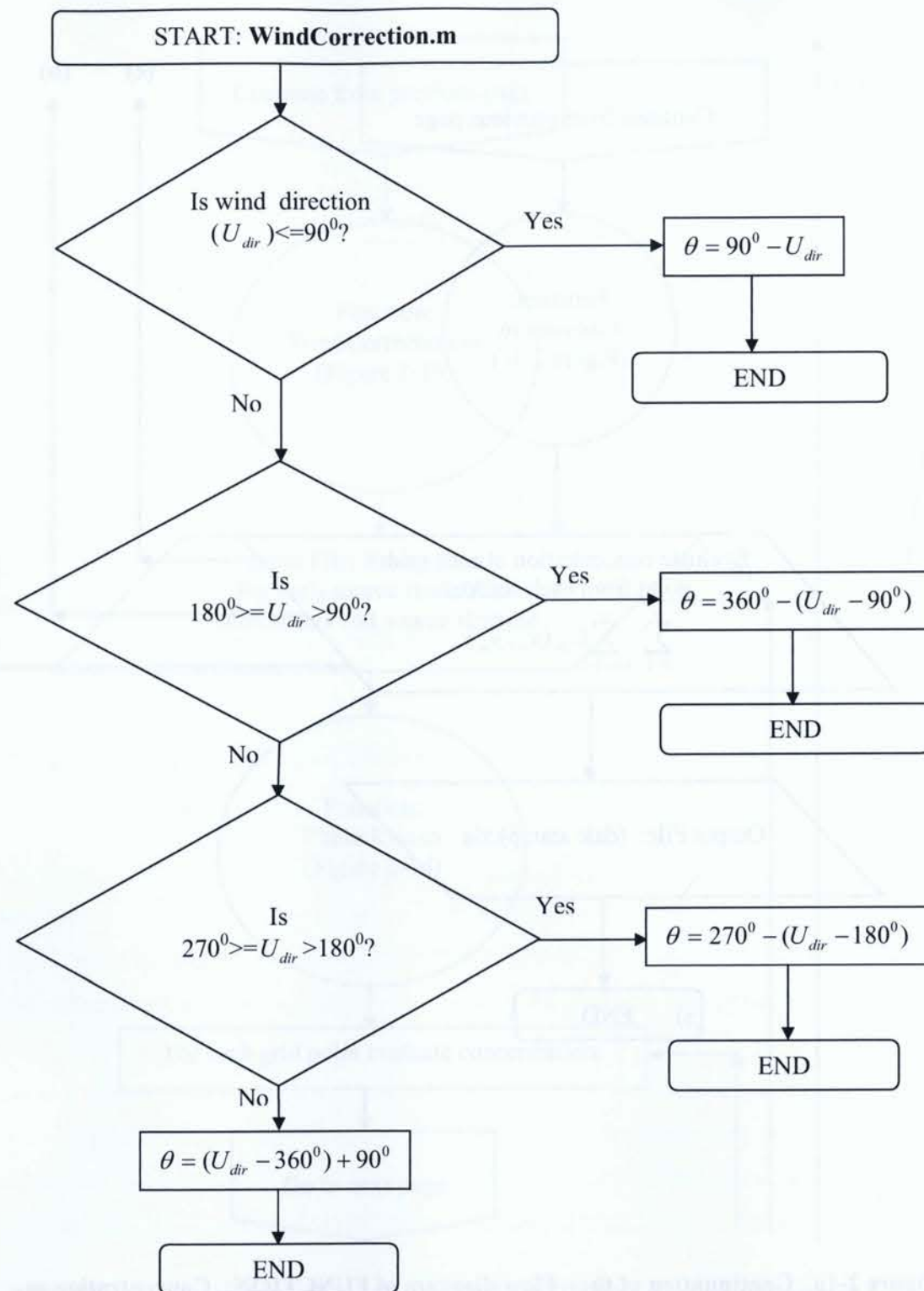
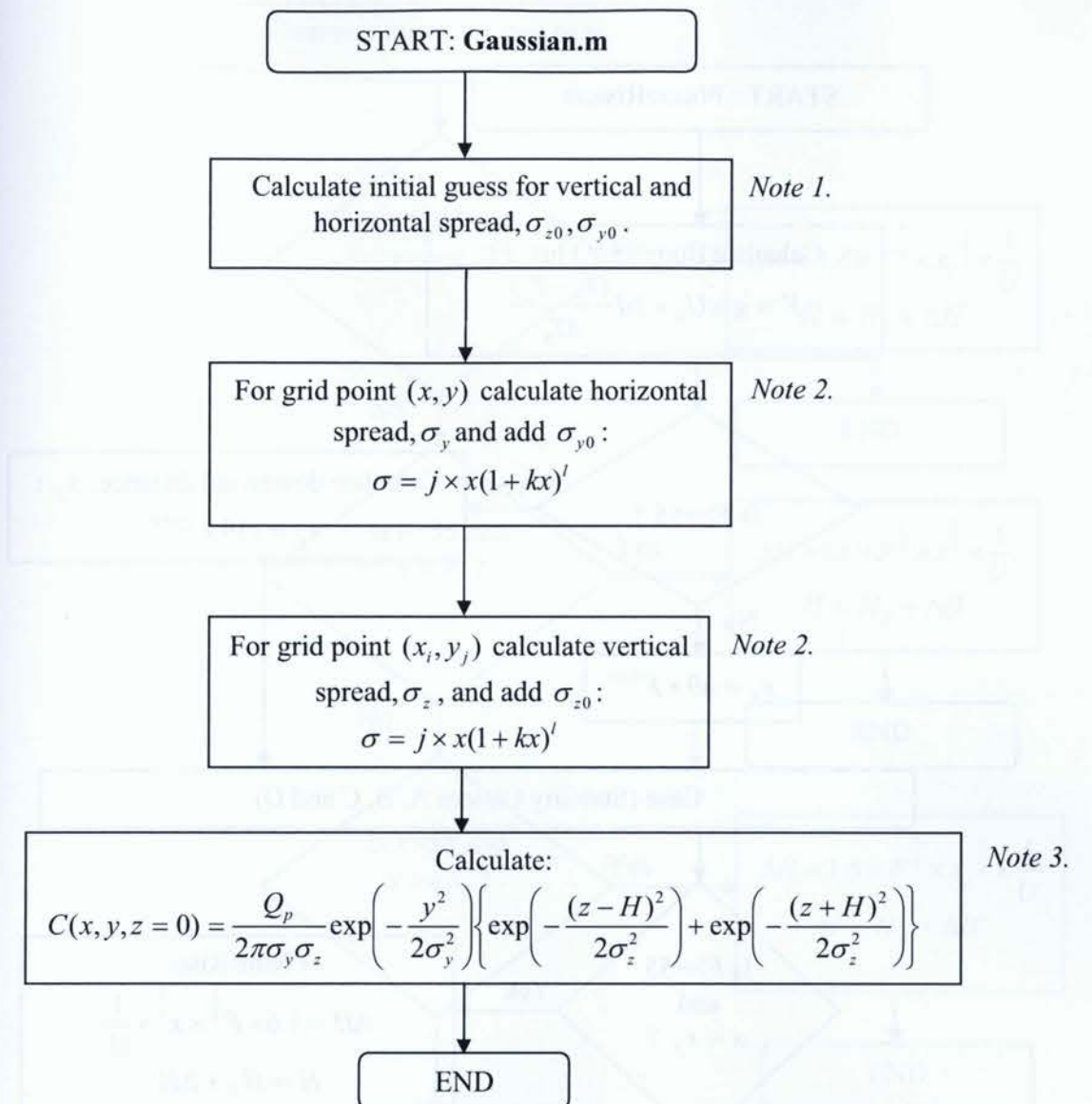


Figure 2-1b. Flow diagram of FUNCTION: WindCorrection.m. This function converts the wind angle from North = 0° to North = 90° and returns the corrected value to the main program (Concentration.m).



Note 1. Initial vertical and horizontal spreads were calculated using method outlined in Table 5 and shown in Figure 5.

Note 2. Vertical and horizontal spreads are calculated using Equation (7). Variables  $j$ ,  $k$  and  $l$  are provided in Table 4.

Note 3. The Gaussian dispersion as shown in Equation (3) and effective stack height is calculated using Brigg's equations see Figure 2-1d.

Figure 2-1c. Flow diagram of FUNCTION: Gaussian.m. This function calculates dispersion parameters using Equation (7) which as subsequently used to calculate ground level concentration using Equation (3). The calculated concentration for point  $(x, y)$  is returned to the main program: Concentration.m (Figure 2-1a).

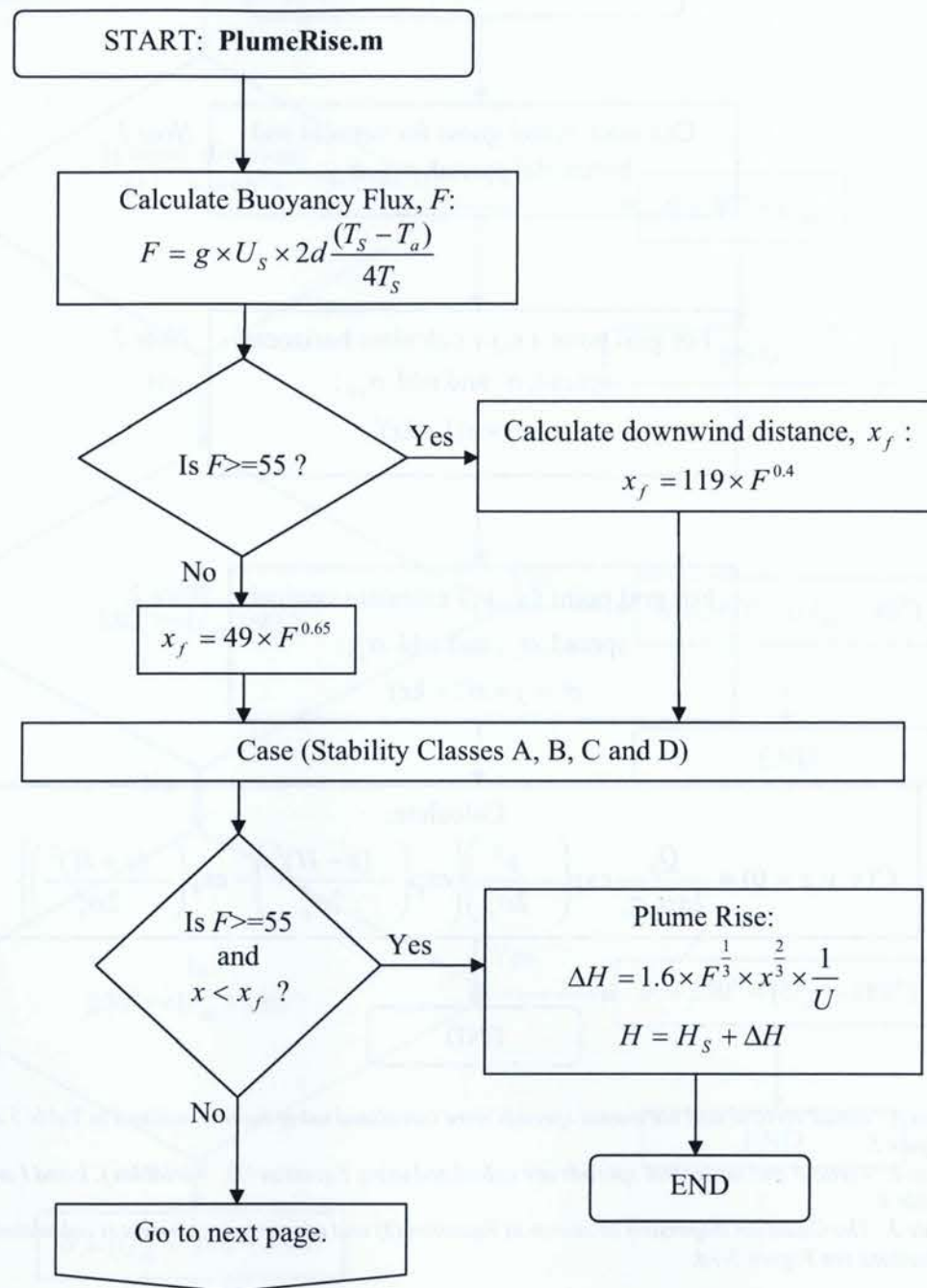


Figure 2-1d. Flow diagram of FUNCTION: PlumeRise.m. This function calculates effective stack height due to momentum rise and thermal rise as shown in Figures 1 and 2. The solutions were adopted from the Brigg's approach to estimating effective stack height as a function of atmospheric stability class and downwind distance from the source (Beychok, 1994), (US EPA, 1995).

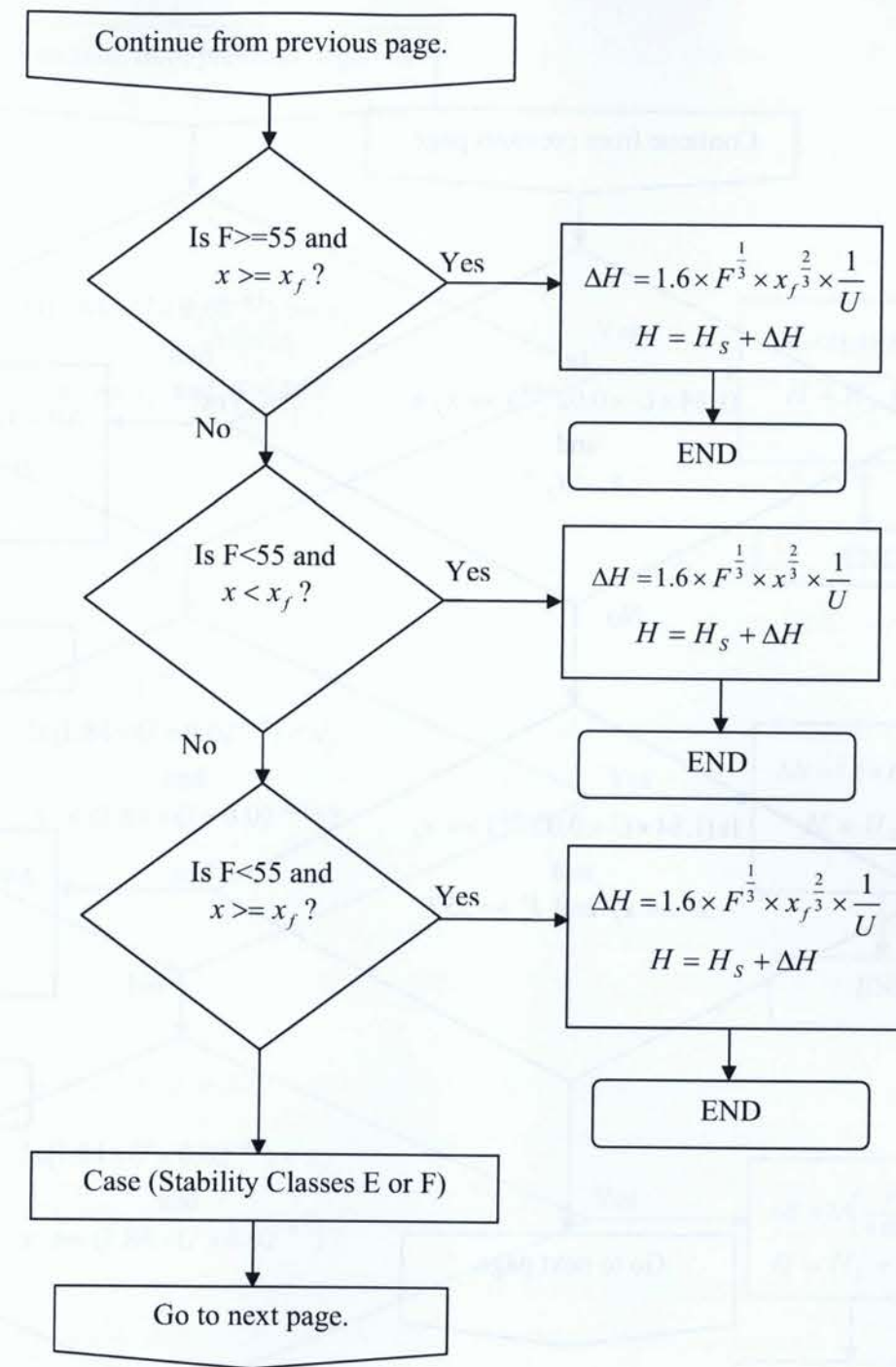


Figure 2-1d. Continuation of the: Flow diagram of FUNCTION: PlumeRise.m.



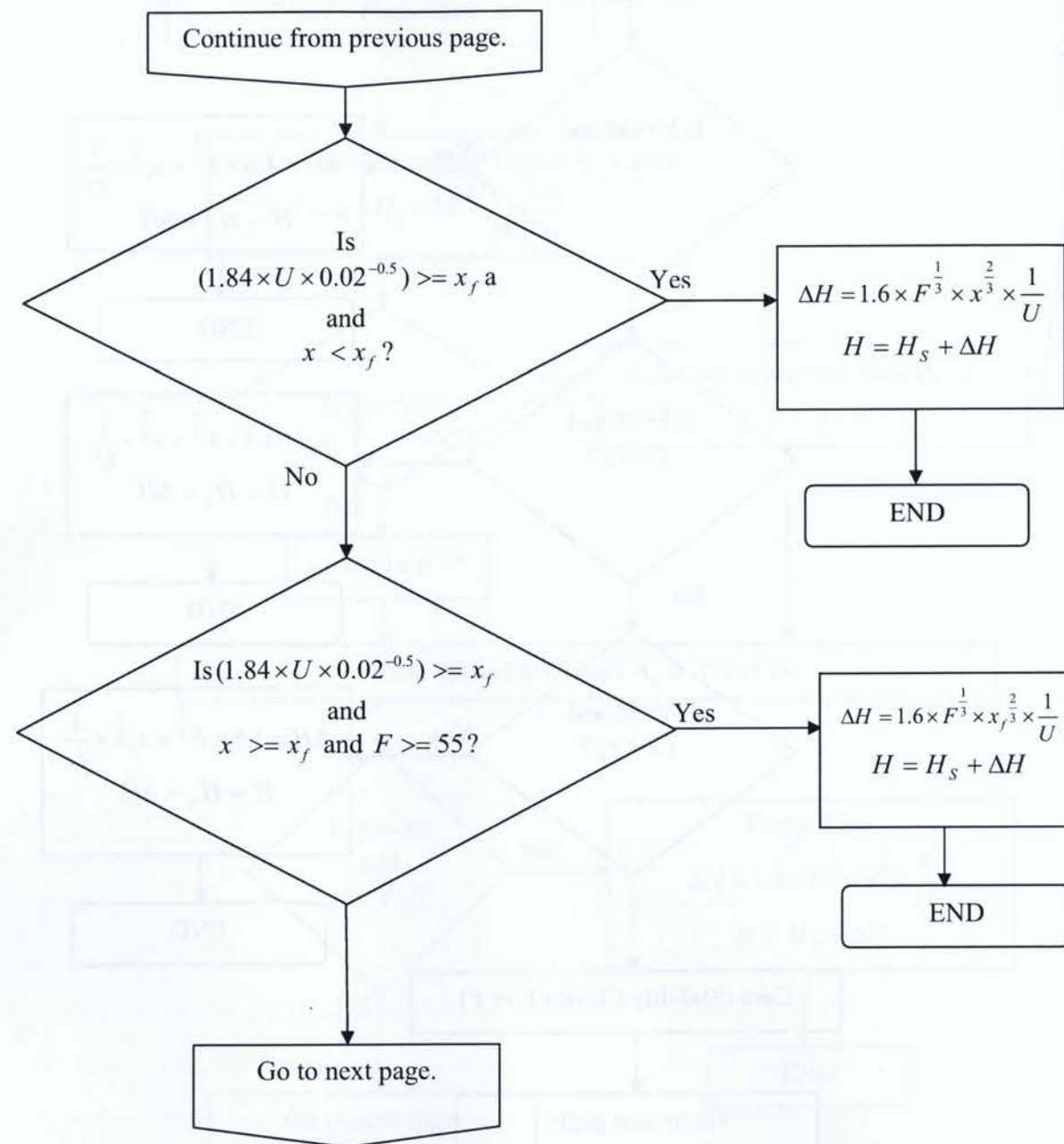


Figure 2-1d. Continuation of the: Flow diagram of FUNCTION: PlumeRise.m.

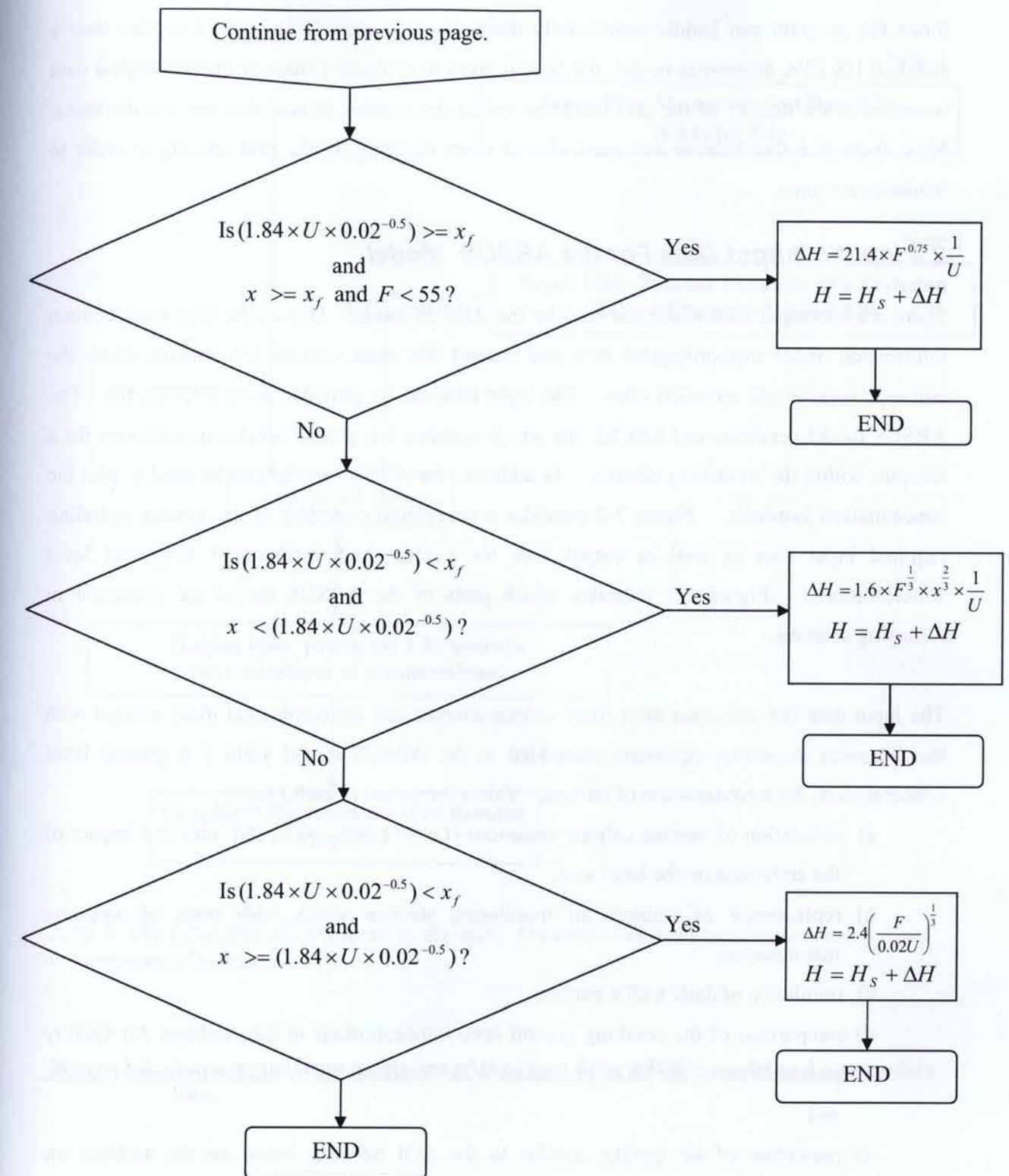


Figure 2-1d. Continuation of the: Flow diagram of FUNCTION: PlumeRise.m.



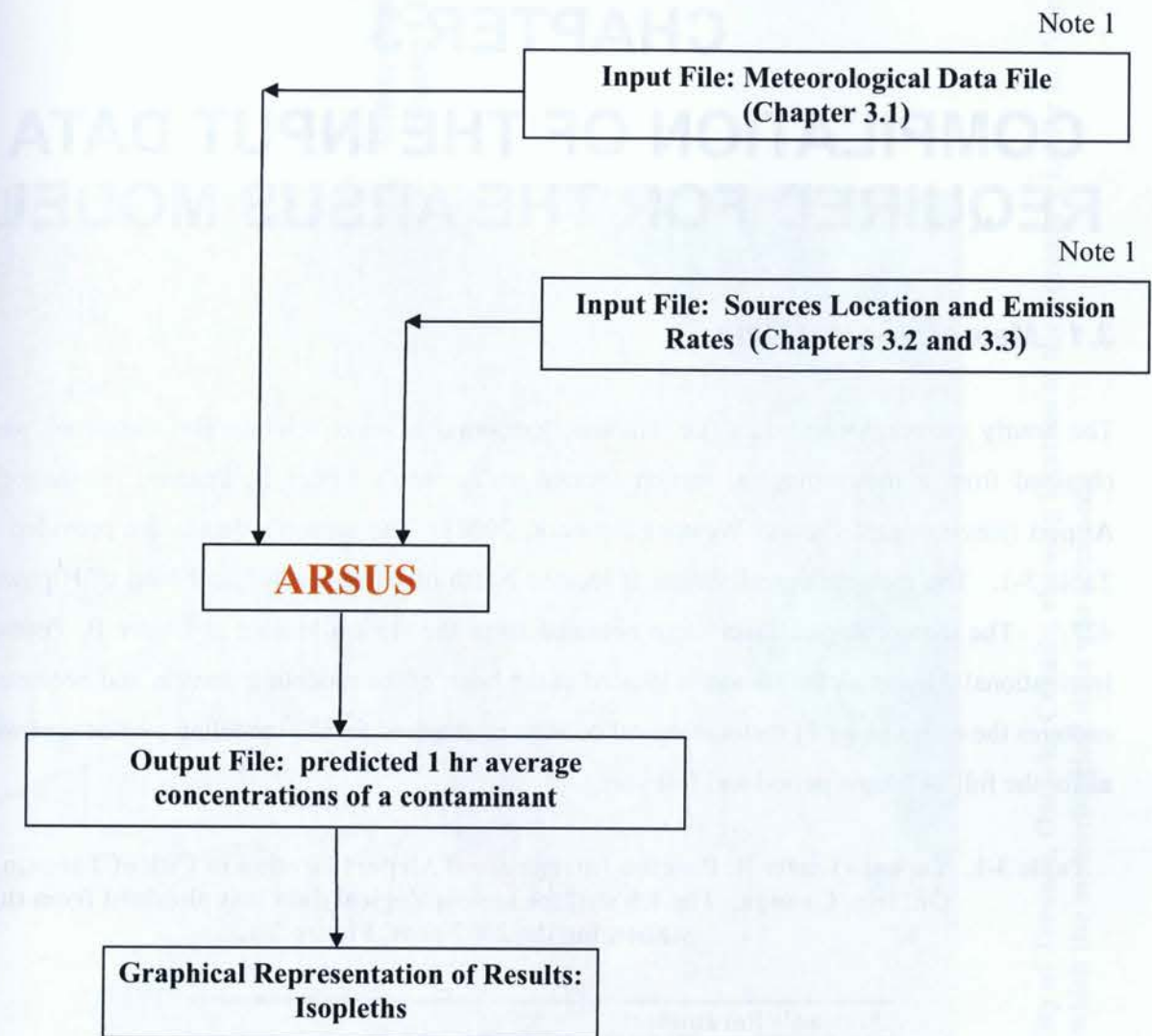
Since the program can handle significantly more emission sources and grid receptors than a standard US EPA dispersion model, the time it takes to evaluate 1 hour of meteorological data increases as the density of the grid increases and/or the number of emission sources increases. Note, there is a fine balance one must choose when deciding on the grid spacing in order to minimize run time.

## 2.4 Input / Output Data For the ARSUS Model

There are two input files which are read by the ARSUS model. One of the files must contain information about meteorological data and second file must contain information about the emission sources and emission rates. The input files can be provided as an EXCEL file. The ARSUS model generates an EXCEL file which contains 1 h ground level concentrations for a receptor within the modelling domain. In addition, the ARSUS model can be used to plot the concentration isopleths. Figure 2-2 provides a conceptual overview of the system including required input data as well as output files for a run which estimates 1 h ground level concentrations. Figure 2-2 indicates which parts of the ARSUS model are discussed in following sections.

The input data (i.e. emission rates from various sources and meteorological data) utilized with the Gaussian dispersion equations embedded in the ARSUS model yield 1 h ground level concentrations for a contaminant of interest. This information is useful for:

- simulation of various tailpipe emissions (i.e. CO, SO<sub>x</sub>, NO<sub>x</sub>, PM, etc) and impact of the emissions on the local area;
- replacement of ambient air monitoring stations which adds costs of on-going maintenance;
- simulation of daily traffic patterns;
- comparison of the resulting ground level concentrations to the Ambient Air Quality standards set by the MOE or Canada Wide Standards set by the Environment Canada; and
- prediction of air quality, similar to the AQI network based on the ambient air monitoring stations, to communicate the findings to the public.



*Note 1. The input files are prepared by the user. The emissions rates can be estimated for any contaminant of interest.*

**Figure 2-2. A conceptual representation of the input data, ARSUS model and output data files.**



## CHAPTER 3

### 3.1 Meteorological Data

The hourly meteorological data (i.e. ambient temperature, wind velocity and direction) were obtained from a meteorological station located at Toronto's Lester B. Pearson International Airport (Environment Canada Weather Network, 2008). The station's details are provided in Table 3-1. The meteorological station is located North of Highway 401 and west of Highway 427. The meteorological data were obtained from the station located at Lester B. Pearson International Airport as the station is located in the heart of the modeling domain and because it captures the entire range of meteorological conditions required for the modeling purposes as well as for the full 24 h time period and full year.

**Table 3-1. Toronto Lester B. Pearson International Airport location in City of Toronto, Ontario, Canada. The 1 h surface meteorological data was obtained from this station for the 2007 year, Figure 3-1.**

Station's Parameter:	
Latitude	43 <sup>0</sup> 40.800' N
Longitude	79 <sup>0</sup> 37.800' W
Elevation	173.4 m
Climate ID.	6158733
World Meteorological Organization (WMO) ID.	71624

### Post processing of the Raw Meteorological Data

The stability classes, as defined in Table 2, are a measure of atmosphere's mixing and are not measured at the meteorological stations; they must be predicted. One such processing program is a widely used tool called CALMET; a sub-program that accompanies the CALPUFF dispersion

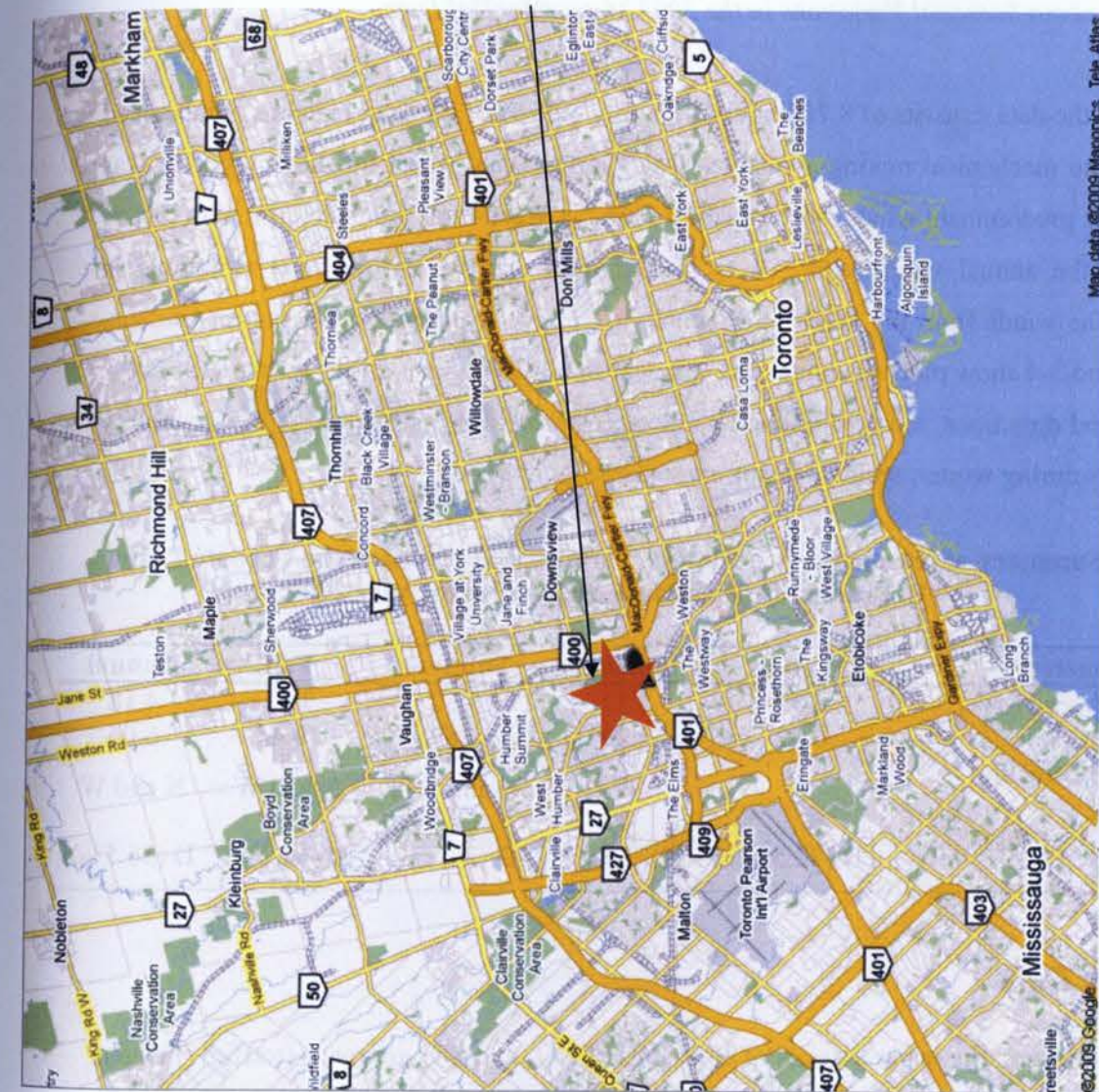


**Figure 3-1** Modelling domain for the City of Toronto, Ontario, Canada, showing location of the Toronto's Lester B. Pearson International Airport from which the meteorological data was obtained.



model suite. For the purpose of this modeling exercise, the CALMET processor was used to process the raw data and predict the stability classes for each hour in the months April to May, 2007. The processed meteorological data are provided in Table 1 of Appendix 1.

*Observations about Seasonal Variations in the 2007 Meteorological Data*

A full year of the data consists of 8,760 hours with only 6.06 % of the total in calms, wind speed at 0 m/s and no mechanical mixing available. The average wind speed for the entire year was 4.18 m/s. The predominant winds were traveling from the West and from the North, with Figure 3-2 showing the annual wind rose. It is important to observe the seasonal variations in Table 3-2. The winds from the Western direction do not dominate during the summer season. Figures 3-3 and 3-4 show plots of annual and seasonal stability class variations for the year 2007. Similar to wind directions, the predominant wind speeds range from 2.1 to 5.6 m/s and stability class D occurs during winter, spring and autumn seasons.

**Table 3-2. Summary of seasonal meteorological variations observed at the Toronto Lester B. Pearson International Airport for the year 2007.**

Parameter	Winter	Spring	Summer	Fall	Annual
Average Wind Speed (m/s)	4.39	5.32	3.52	3.51	4.18
Percent of Calms (%)	6.52	2.29	4.89	10.44	6.06
Dominant Wind Direction (FROM)	W	W	N and SSE	N and W	N and W
Dominant Stability Class (Percent)	D (72.5%)	D (71.8%)	D (26.9%)	D (45.2%)	D (56.5%)

**3.2 Traffic Data**

For most urban areas, the major sources of emissions of NO<sub>x</sub> and SO<sub>2</sub> are roads (traffic) (Fenger, 1999; 2009; Mage et al., 1996; Yang et al., 2007) and such applies to the City of Toronto as well (Siemiatycki, 2007; Toronto Public Health, 2007; Jerrett et al., 2007). The City of Toronto's unique structure contains few small scale businesses, a network of roads and highways but no major non-industries, unlike the city of Sault St. Marie located in Ontario. The Sault St. Marie city is well known for its local pulp and paper and steel industries and their impact on local

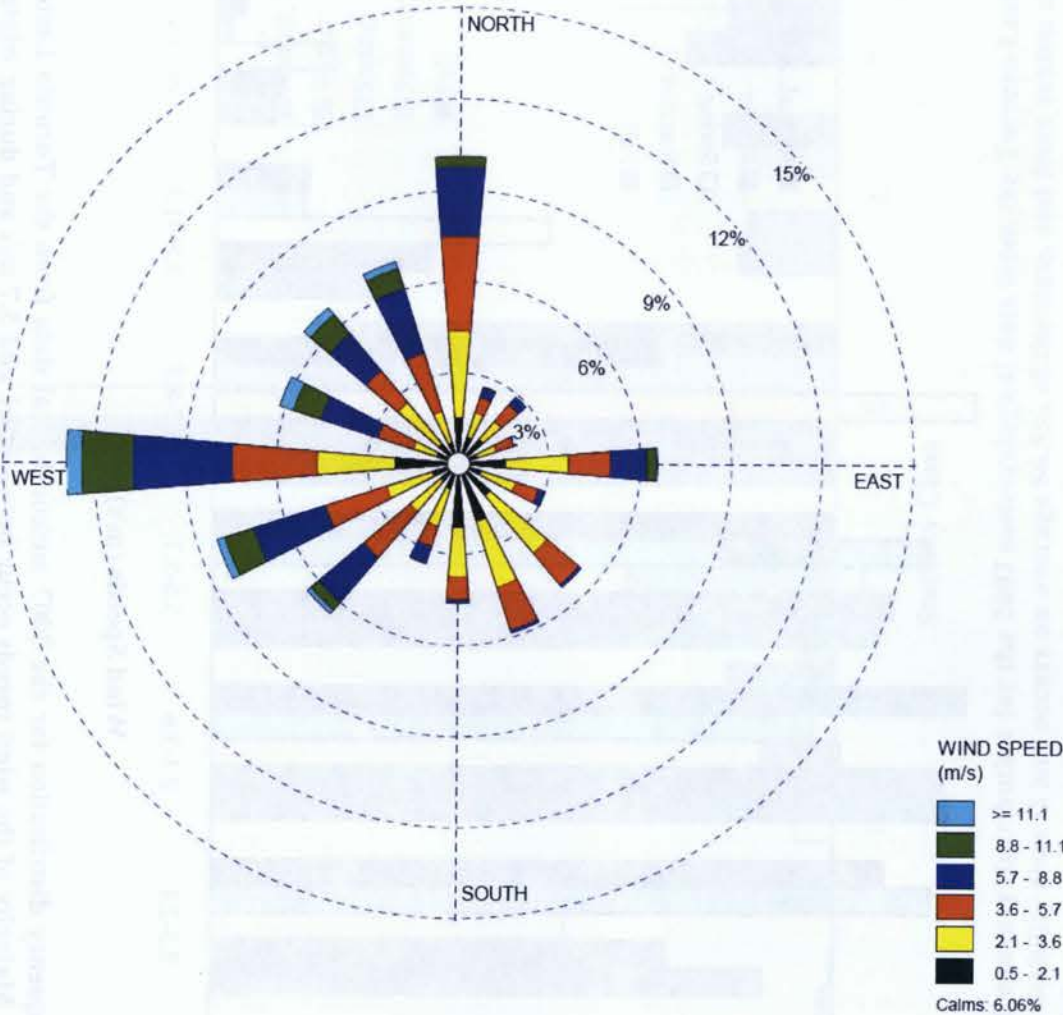


**Figure 3-2. Wind rose for the year 2007 showing wind speeds and dominant wind direction. The meteorological data were obtained from the Meteorological Station, Climate I.D. 6158733.**



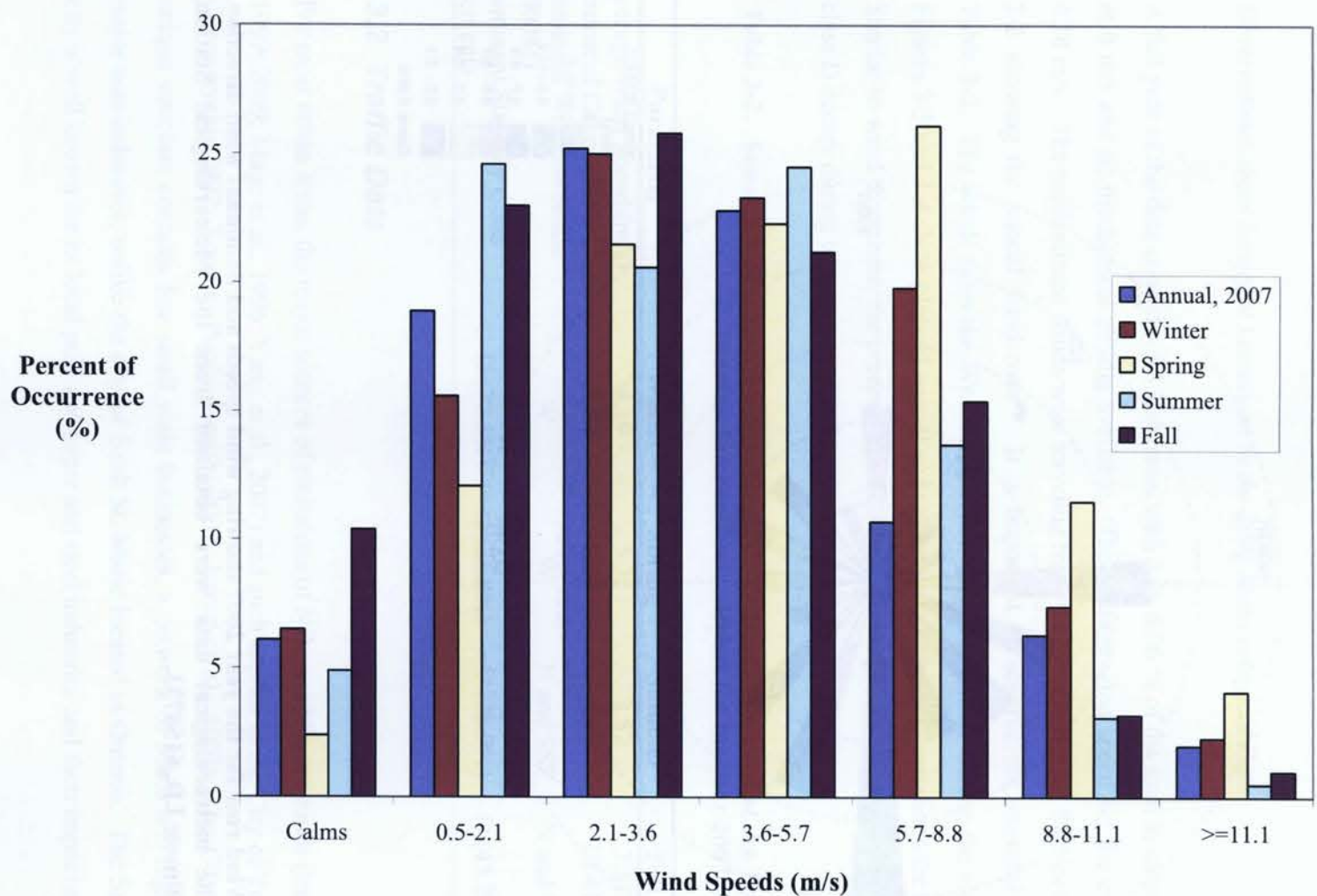


Figure 3-3. Annual wind class frequency distribution for the 2007 meteorological data from the Toronto Lester B. Pearson International Airport. Majority of the wind speeds occur between 2.1 and 5.7 m/s and during winter, spring and fall seasons.

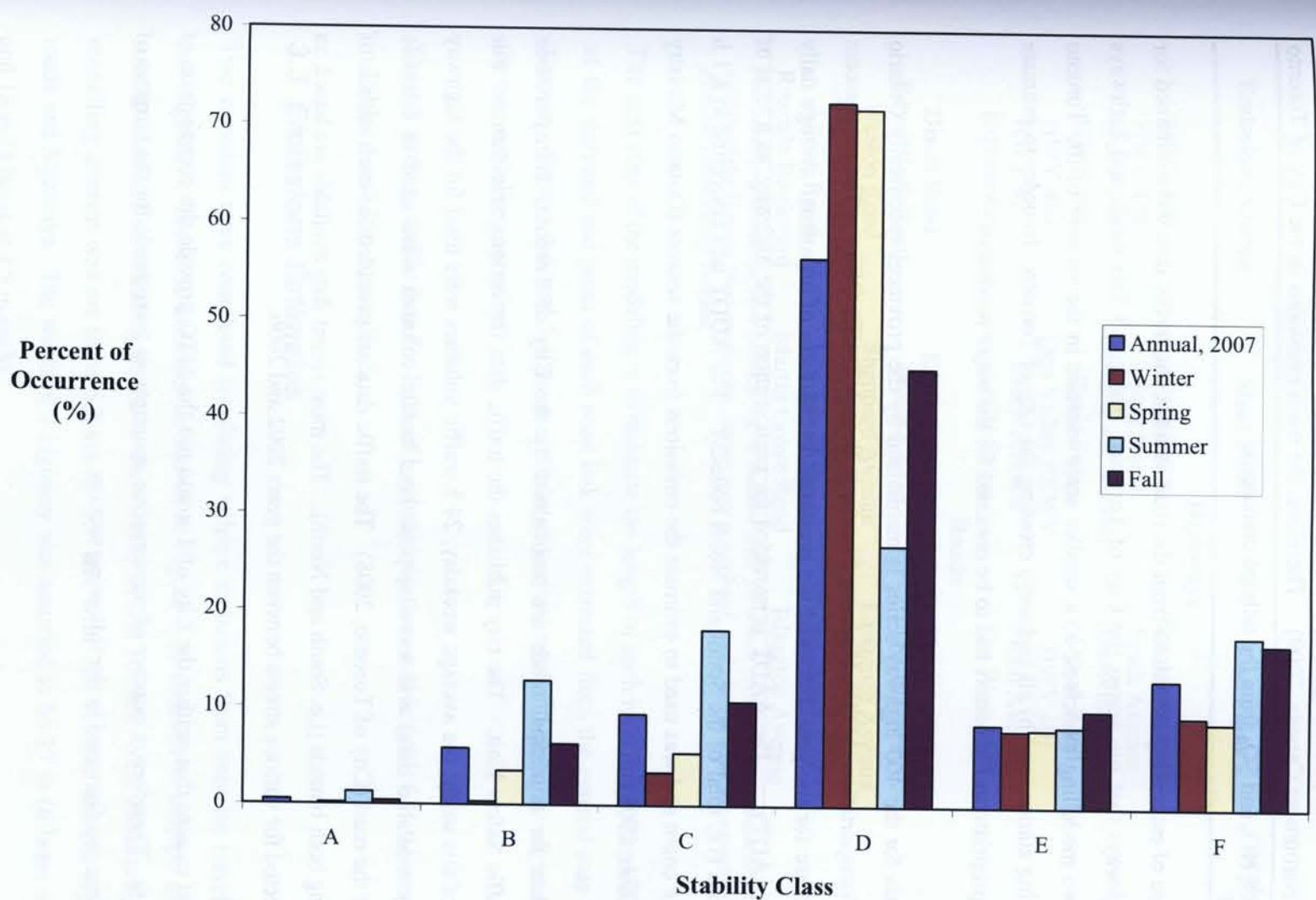


Figure 3-4. Annual stability class frequency distribution for the 2007 meteorological data from the Toronto Lester B. Pearson International Airport. Stability class D occurs on average 56.5% of the time, and from season analysis occurs in winter, spring and fall seasons.



air quality (Environment Canada, 2009). Therefore, the main emissions in the City of Toronto are those of CO, NO<sub>x</sub> and SO<sub>2</sub> from the tailpipe emissions.

For the purpose of estimating emissions from the road sources, the traffic data were obtained for the major highways that run across the City of Toronto. Table 3-3 lists roads and highways included in two modelling exercises; a) a smaller scale exercise in the vicinity of the Toronto West monitoring station, and b) all highways crossing the city of Toronto. In order to estimate emissions, appropriate traffic counts had to be obtained for the major roadways.

The traffic data for the 400 highway series is maintained by the province, specifically Ontario Ministry of Transportation (MTO), Highway Standards Branch Traffic Office. The most recent data available are for the year 2005 and are presented in the form of an annual average daily traffic count (AADT). The AADT is provided for each section of the highway, as a total of both the bounds (i.e. total of the South and North bounds). The ADDT was converted to a 1 h average traffic count and was used to estimate the emissions from the sources (Ontario Ministry of Transportation, 2008).

The traffic data for municipal roads are maintained by the City of Toronto, Transportation Services, Traffic Safety Unit. The city publishes the traffic data for various time frames. For the purpose of this study, the average weekday, 24 h traffic volumes were used for the highway sources (only available data) and morning peak hour traffic volumes were used to estimate emissions for the road (City of Toronto, 2008). The traffic data are provided for each section of the road listing both bounds (i.e. South and North). The most recent data available are based on the data collected for various streets between the years 2002 and 2006.

It is important to note that neither the City of Toronto nor the MTO provide the composition of the traffic data. Therefore, a number of conservative assumptions were made for the purpose of this study; these are discussed in the following section.

**Table 3-3. Summary of Major Highways From which Emissions were Estimated, City of Toronto, Ontario, Canada.**

Emissions Source	Start Point	End Point	Scale of Modelling Exercise: <sup>1</sup>
<b>Highways</b>			
HWY 400	Jane Street	Steeles Avenue	Large
HWY 400	Jane Street	Finch Avenue	Small
HWY 401	Morningside Avenue	Renforth Drive	Large
HWY 401	Keele Street	Dixon Road	Small
HWY 404	Don Valley PKWY	HWY 401	Large
HWY 427	Evans Avenue	Finch Avenue	Large
Expressway	Leslie Street	The West Mall	Large
<b>Roads</b>			
Dixon Road	Kipling Avenue	The Westway	Small
Royal York Road	Weston Road	The Westway	Small
Weston Road	Sheppard Avenue	Lawrence Avenue	Small
Islington Avenue	Albion Road	The Westway	Small
Albion Road	Islington Avenue	The Westway	Small
Rexdale Boulevard	Martin Grove Road	Islington Avenue	Small

<sup>1</sup> Two modelling scenarios were considered; a) smaller scale for which emissions from roads and highways in the vicinity of the Toronto West monitoring station were considered; and b) larger scale for emissions from highways from the entire city of Toronto.

The next step of the modeling is to estimate the length of each road link. The UTM coordinates of the start and end point of each road link were extracted from the general map of the City of Toronto. Figures 3-5 and 3-6 show all links of various road and highway segments included in the two modelling exercises.

The 1 h average traffic data for links of highways sections and length of the section are provided in Tables 1 and 2 in Appendix 2.

### 3.3 Emissions Estimates

Two exercises were completed simulating tailpipe emissions from vehicles travelling on roads and highways. The first exercise, as shown in Figure 3-5, considered tailpipe emissions for a smaller area and surrounding traffic in the vicinity of the Toronto West monitoring station. The modelling domain was set to be 8.2 km by 5.9 km, with 723 volume sources representing the roads and highways. The width of a highway was assumed to be 27 m (6 lanes at 4.5 m each) and 18 m (4 lanes at 4.5 m each).



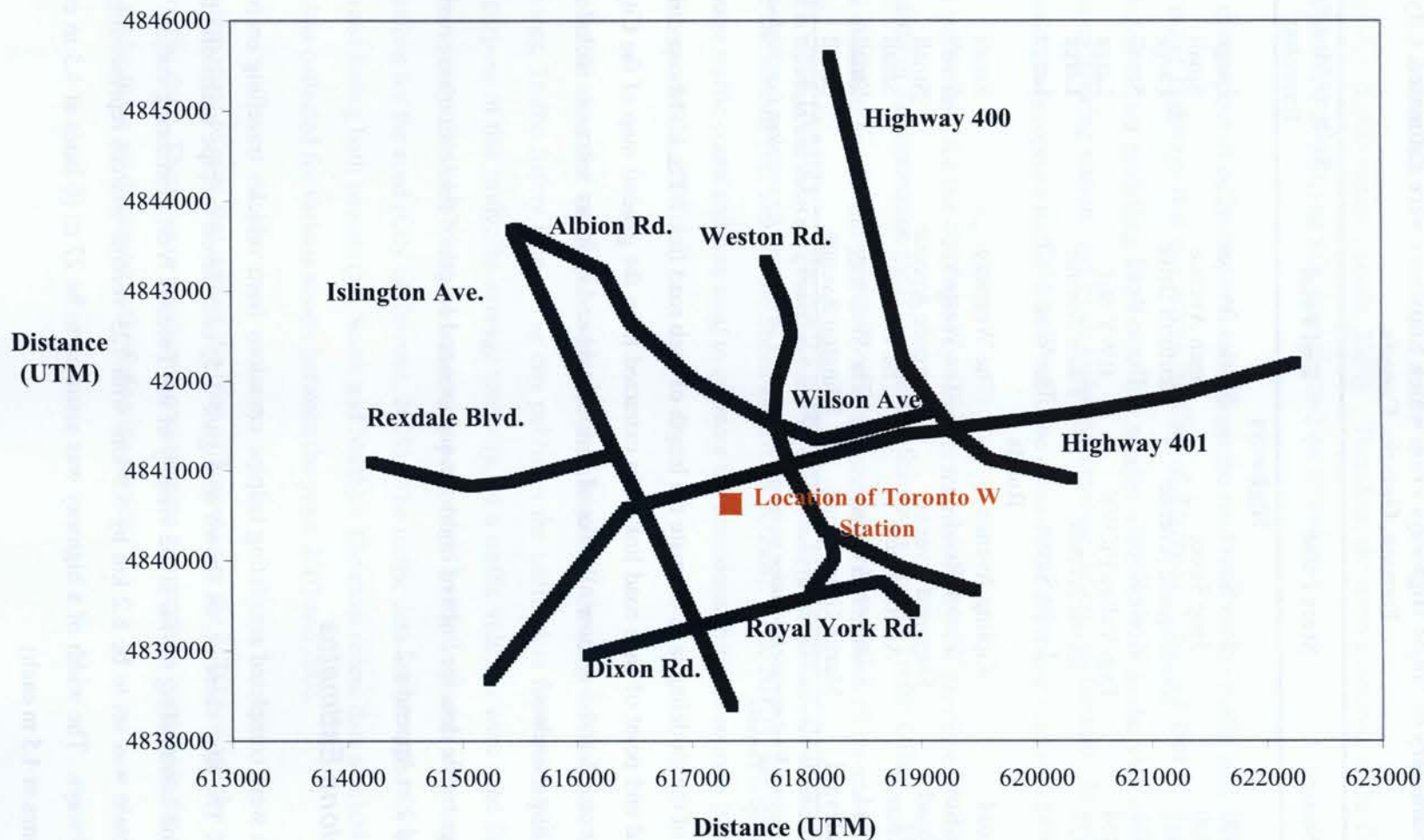


Figure 3-5. Summary of road and highway links used to complete the dispersion modelling exercise for the smaller scale exercise. Emissions from the roads and highways in the vicinity of the Toronto West monitoring station were considered in this modelling exercise.

60

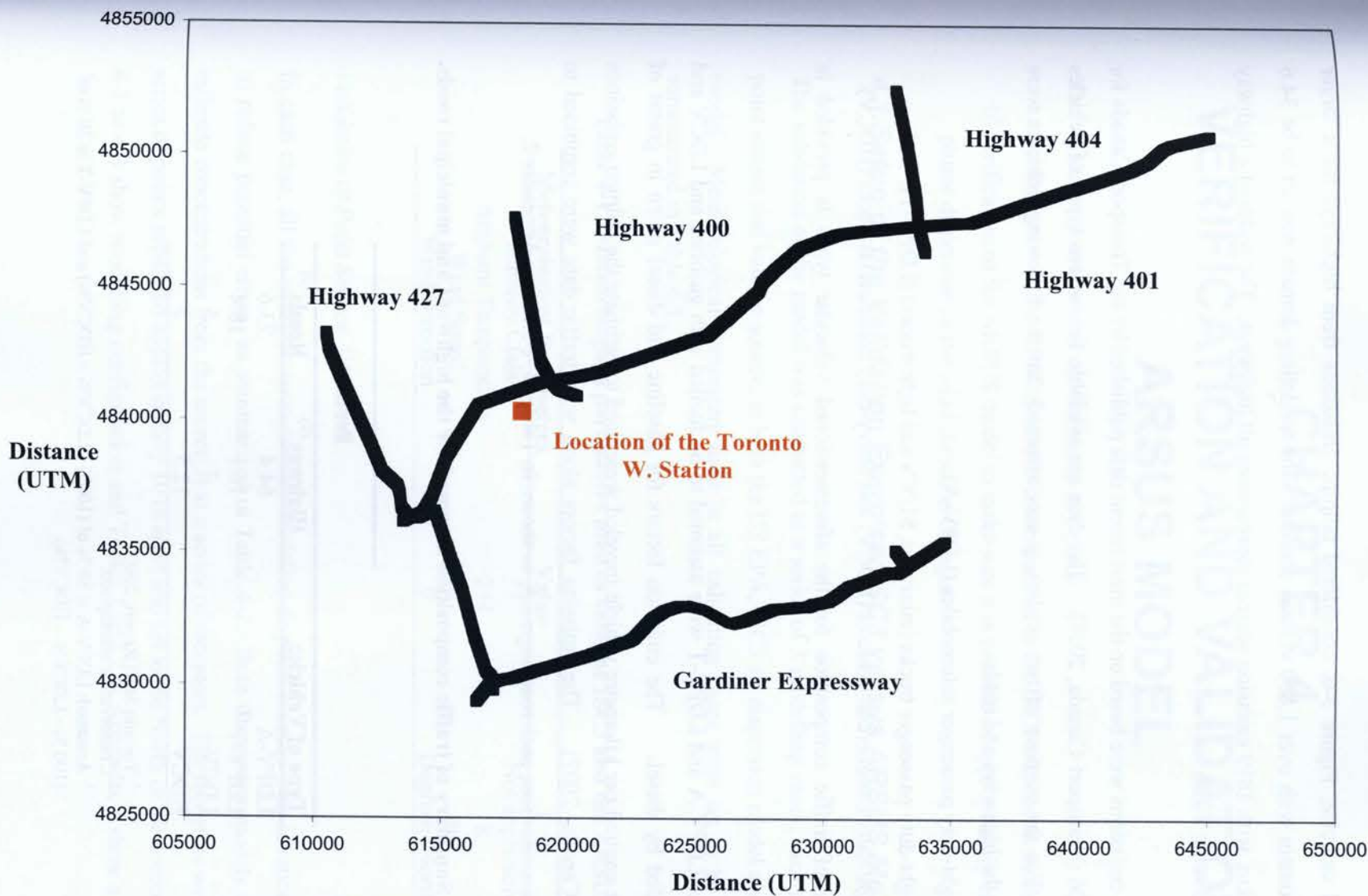


Figure 3-6. Summary of road and highway links used to complete the dispersion modelling exercise for the larger scale exercise. Emissions from the highways passing through the city of Toronto were considered in this modelling exercise.

61



The second exercise, Figure 3-6, considered tailpipe emissions from highways for a larger modelling domain with over 1,800 volume sources. The modelling domain was set to be 34.6 km by 23.2 km, with 1819 emission sources representing all highways. The width of a highway was assumed to be 27 m.

The tailpipe emissions were based on the most recent data published by the Transport Canada for the year 2006 (Transport Canada, 2008). The data are available for various types of vehicles and fuels. For the purpose of two studies, it was assumed that the following vehicles were traveling on the highways and roads:

- a) light-duty passenger automobiles (LDPV-A),
- b) light-duty passenger trucks (minivans, SUV's and light trucks) (LDPV-T), and
- c) light-duty commercial vehicles (LDCV) and heavy-duty commercial trucks (HDCV).

A summary of traffic composition for the aforementioned vehicular types is provided in Table 3-4.

Furthermore, LDPV-A and LDPV-T were assumed to be fuelled with gasoline and LDCV and HDCV fuelled by diesel. The emission factors for gasoline and diesel given in grams of contaminant emitted per kilometre vehicle traveled were used to estimate the tailpipe emissions (Transport Canada, 2007). The emission factors along with traffic data were combined to estimate emissions from each road segment, as shown in Tables 1, 2 and 3 in Appendix 2.

**Table 3-4. Summary of traffic composition assumed for the highways and municipal roads.**

Type of Vehicle:	Percent	
	Highway <sup>(1)</sup>	Roads <sup>(2)</sup>
LDPV-A	64.4	73.6
LDPV-T <sup>(3)</sup>	16.1	18.4
LDCV	7	5
HDCV	12.5	3

<sup>1</sup> Toronto Staff Report, 2007.

<sup>2</sup> Conservative assumption.

<sup>3</sup> Assumed: LDPV-A is 80 % of (100% - LDCV% - HDCV%) and LDPV-T is 20 % of (100 % - LDCV% - HDCV%).

## CHAPTER 4

# VERIFICATION AND VALIDATION OF ARSUS MODEL

The validation exercise was carried out in two parts:

- a) performance of the ARSUS model in comparison to the ISC3 dispersion model; and
- b) verification of the ARSUS model to make sure it is capable of appropriately estimating plume dispersion as the wind direction changes.

### 4.1 Setup of the Validation Exercise: ISC3 versus ARSUS Model

The validation of the model was conducted in a series of 3 modelling cases, each repeated for a point source and volume source, in both the US EPA, ISC3 air dispersion model and the ARSUS model. Meteorological parameters used in all validation cases were set to be the same as summarized in Table 4-1.

**Table 4-1. Meteorological parameters used to validate ISC3 and the ARSUS model.**

Meteorological Parameters	Value	Unit
Stability Class	3	Not applicable
Ambient Temperature	294	K
Wind Speed	3	m/s
Wind Direction	0	Degrees (North)

#### Validation of Point Source Algorithm

In each case, all the emission sources were modelled as point sources with identical parameters to reduce potential errors, as summarized in Table 4-2. Both dispersion models were used to estimate concentrations from the source(s) at a series of receptors. The receptors were set to be a series of points separated approximately 10 m apart and set to the North of the source(s). Figures 4-1 to 4-3 show modelling configuration and Tables 1 and 2 in Appendix 3 show a summary of



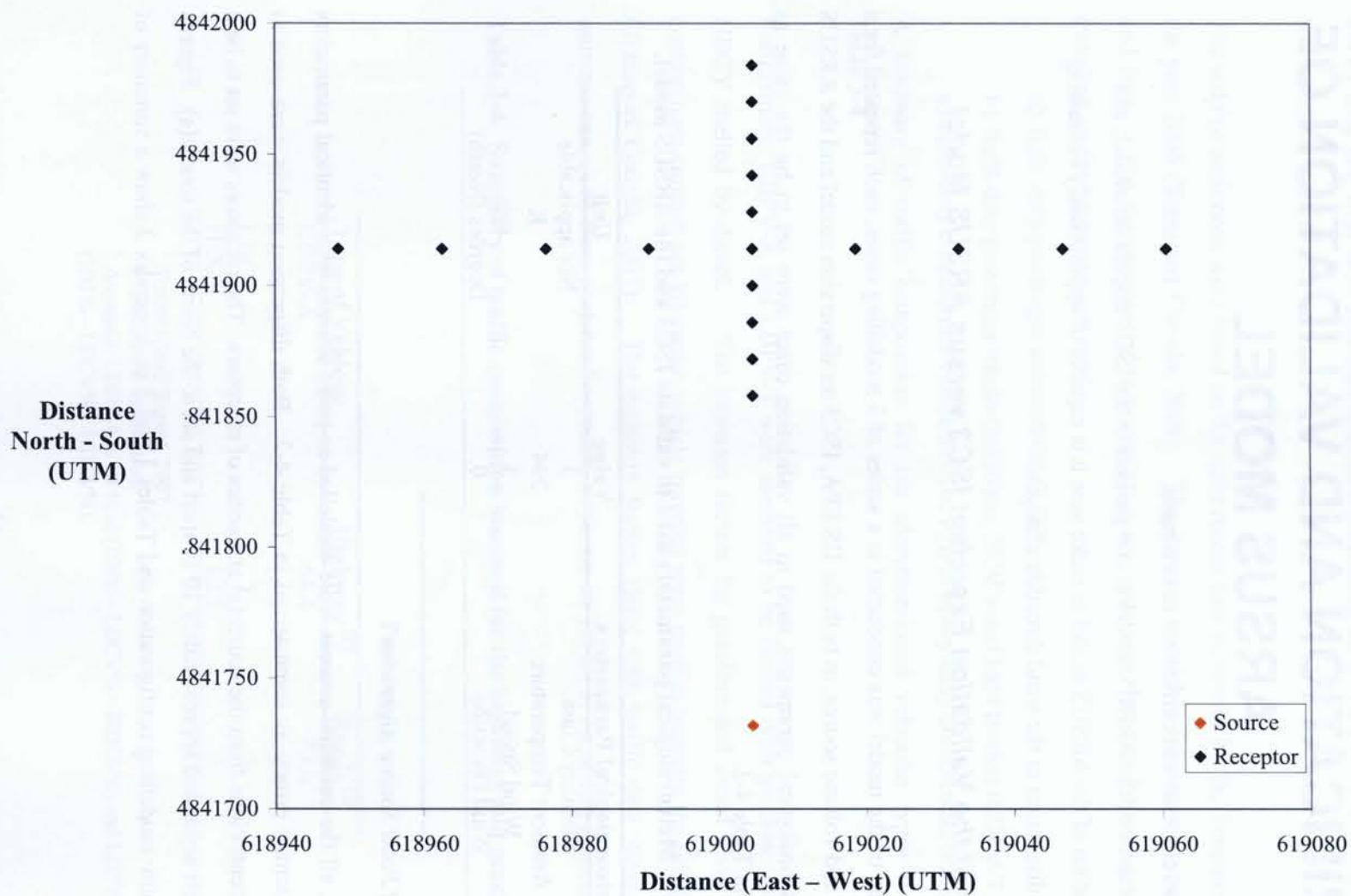


Figure 4-1. CASE 1 - Simple setup with a single source emitting at 1 g/s and location of selected receptors at which concentrations were modelled.

64

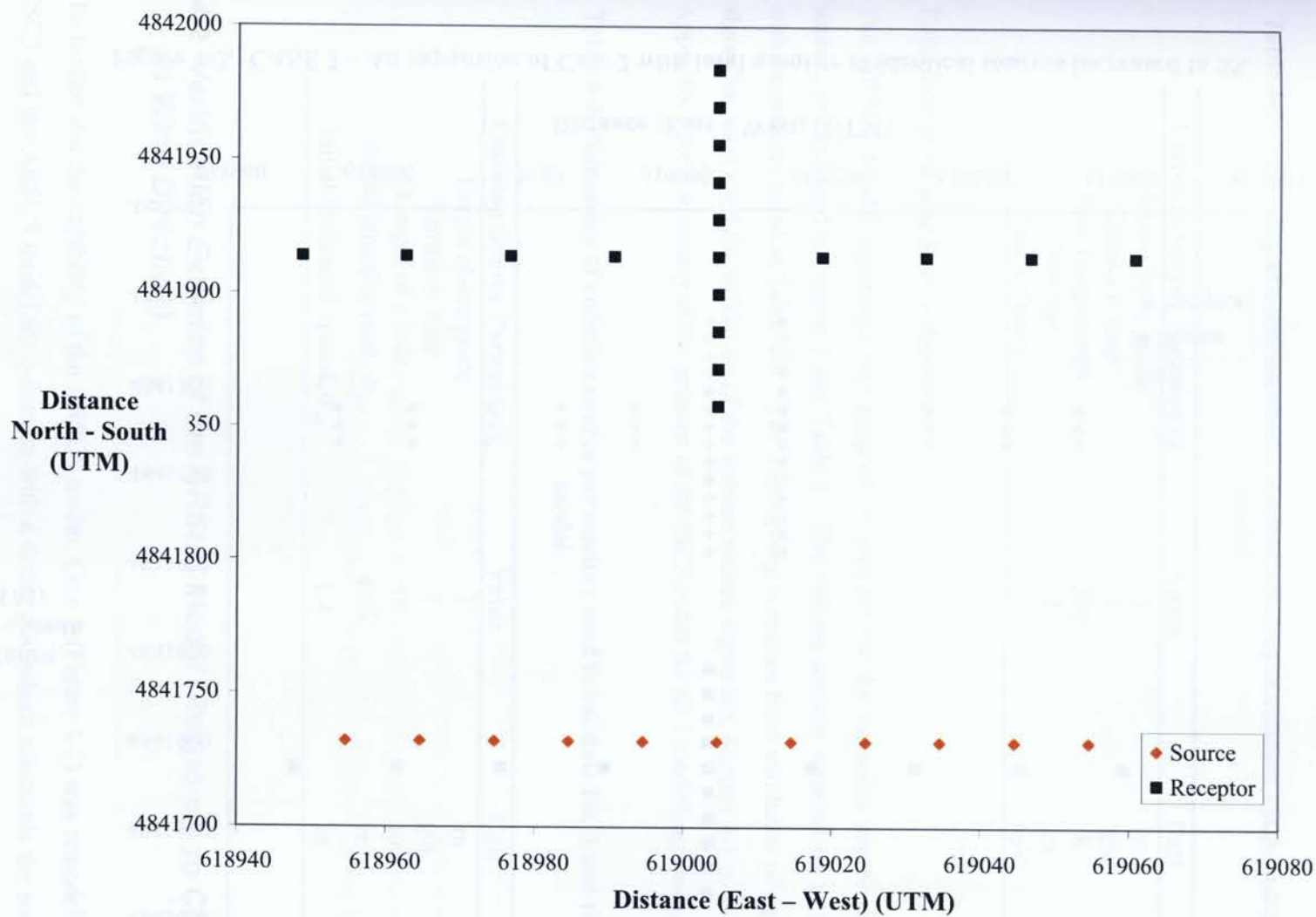


Figure 4-2. CASE 2 - An expansion of CASE 1 with identical sources increased to a total of 11.

65

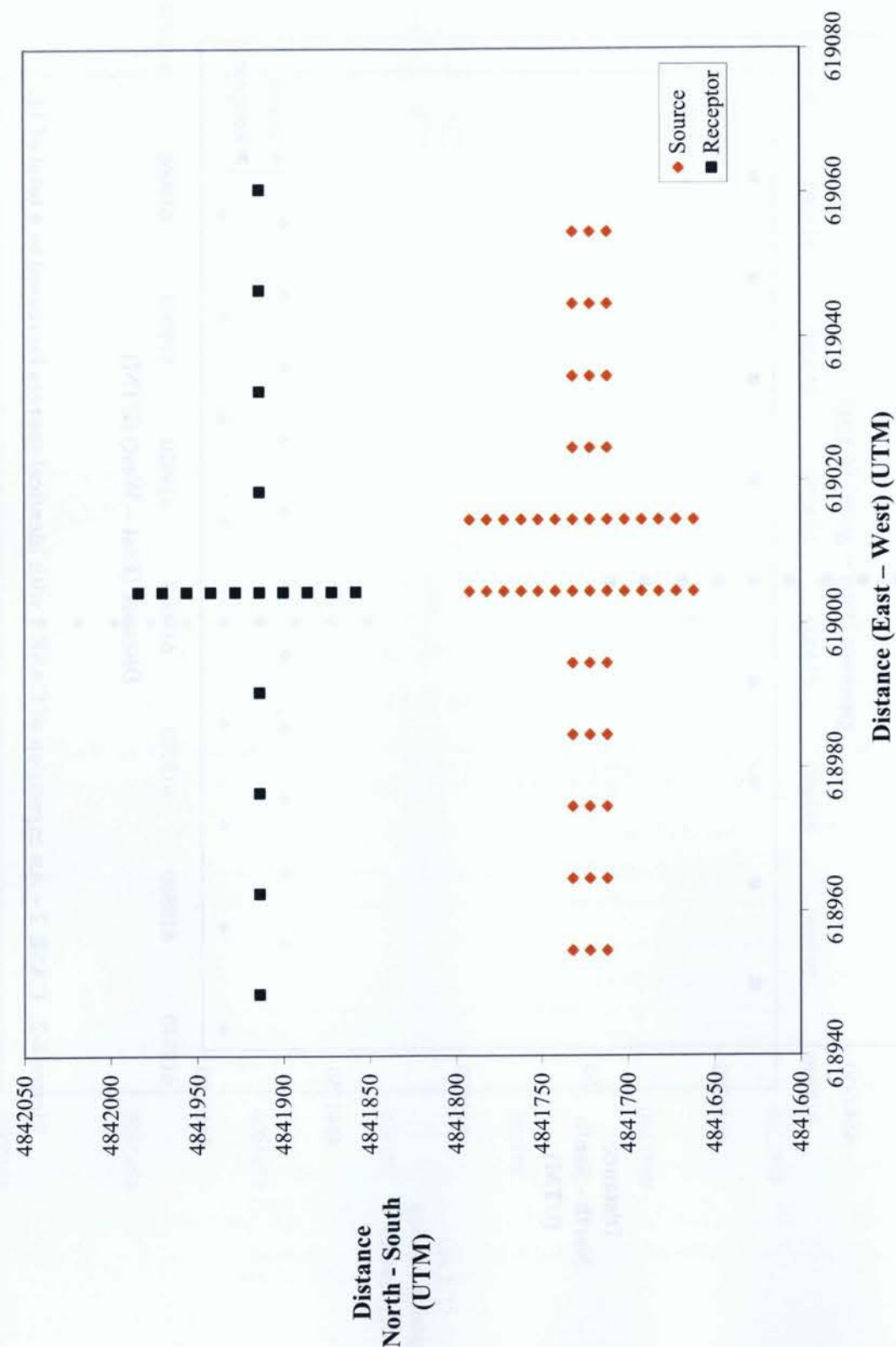


Figure 4-3. CASE 3 – An expansion of Case 2 with total number of identical sources increased to 55.

the UTM coordinates for all sources and receptors. A sample of the ISC3 code for Case 1 is provided in Appendix 4.

Table 4-2. Summary of emission source parameters used to validate ISC3 and the ARSUS model.

Emission Source Parameters	Value	Unit
Height above grade	3	m
Emission Rate	1	g/s
Exit Temperature	294	K
Diameter	2	m
Exit Velocity	1	m/s

#### Validation of Volume Source Algorithm

The ARSUS Model algorithm was updated to account for the emission source as a volume source, as explained in Figure 5 and Table 5. The volume sources were all set to be identical with parameters listed in Table 4-3. The 3 modelling scenarios from validation of a point source algorithm were used for validation of the volume source algorithm, Figures 4-1 to 4-3. Refer to Appendix 5 for a summary of the printout of the ISC3 codes for all 3 modelling cases.

Table 4-3. Summary of emission source parameters used to validate ISC3 and the ARSUS model.

Emission Source Parameters	Value	Unit
Height above grade	3	m
Emission Rate	1	g/s
Length of a Side	10	m
Initial lateral spread, $\sigma_{y0}$	4.65	m
Initial horizontal spread, $\sigma_{z0}$	1.4	m

#### 4.2 Verification Exercise of the ARSUS Model (Response to Change in Wind Direction)

To further test the capability of the ARSUS model, Case 1 (Figure 4-1) was remodelled in both ISC3 and the ARSUS model for a domain with a dense grid which surrounds the source. This



exercise was conducted to test if the ARSUS model reads meteorological data properly and accounts for changes in wind direction. Winds from North ( $0^0$ ), East ( $90^0$ ), South ( $180^0$ ) and West ( $270^0$ ) were considered. Similar tests were performed for the  $45^0$  angles in each quadrant and  $10^0$  angle. This test was of importance to verify if the trigonometry used to evaluate concentrations at various points as the wind changes work well. The modelled concentrations were then plotted in SURFER (geographical interface software, Version 8.05) to overlap the isopleths from both modelling runs.

### 4.3 Results of the Validation Exercise

The modelled concentrations from the test cases, both the validation of point and volume source algorithms, Cases 1-3, were plotted against each other. The plots of predicted concentrations by the ARSUS model versus ISC3 were generated. Two statistics were derived from each plot:

- a) Regression ( $r^2$ ) value: how well the ARSUS model results compare to ISC3 model results; and
- b) Slope of line (m): is an indicator whether the ARSUS model over predicts or under-predicts.

A plot of residuals was prepared for each exercise.

#### Validation of the Point Source Algorithm

The  $r^2$  values and slopes are summarized in Table 4-4 and plots are in Figures 4-4 to 4-6. These statistics show that even as the number of sources increases, the ARSUS model handles the addition of the concentrations from the numerous sources very well; Case 3 with the slope, m, is 0.9966.

**Table 4-4. Summary of the linear regression conducted on the plots for Cases 1-3, validation of point source algorithm, on Figures 4-4 to 4-6.**

Case	m	$r^2$
1	0.9976	1
2	0.9977	1
3	0.9966	1

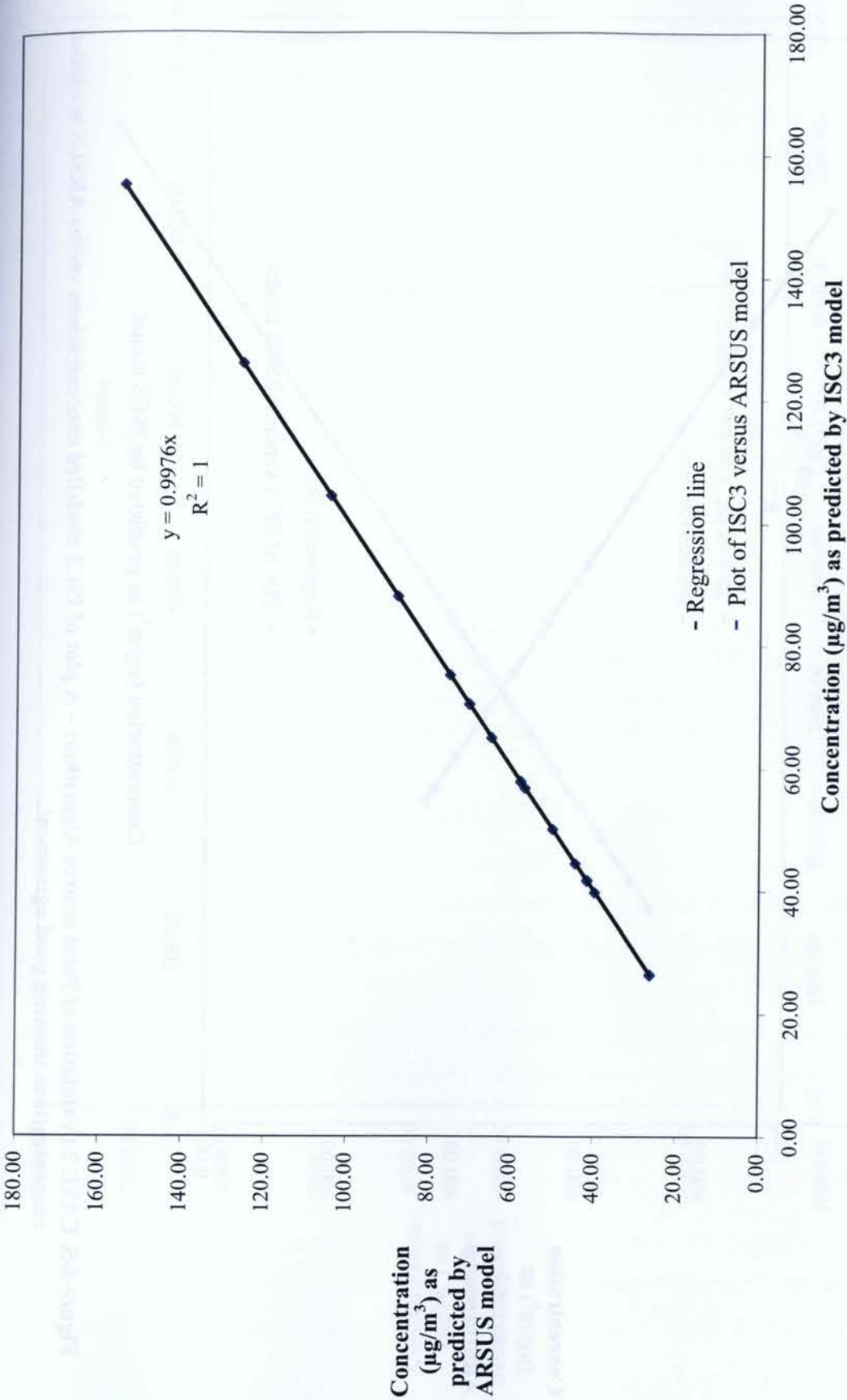


**Figure 4-4. CASE 1 (Validation of Point Source Algorithm) – A plot of ISC3 modelled concentrations versus ARSUS modelled concentrations showing good agreement.**

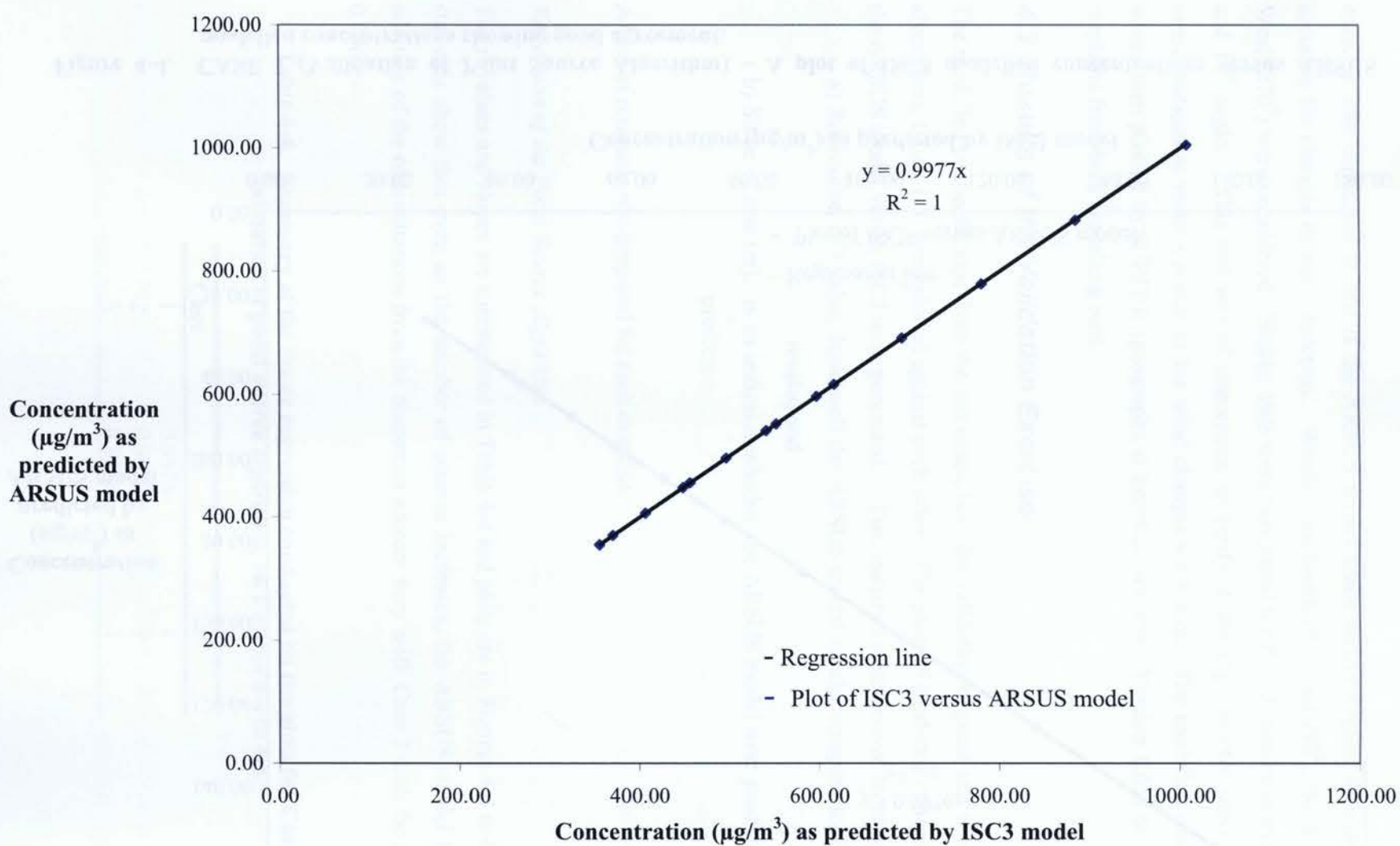


Figure 4-5. CASE 2 (Validation of Point Source Algorithm) – A plot of ISC3 modelled concentrations versus ARSUS modelled concentrations showing good agreement.

70

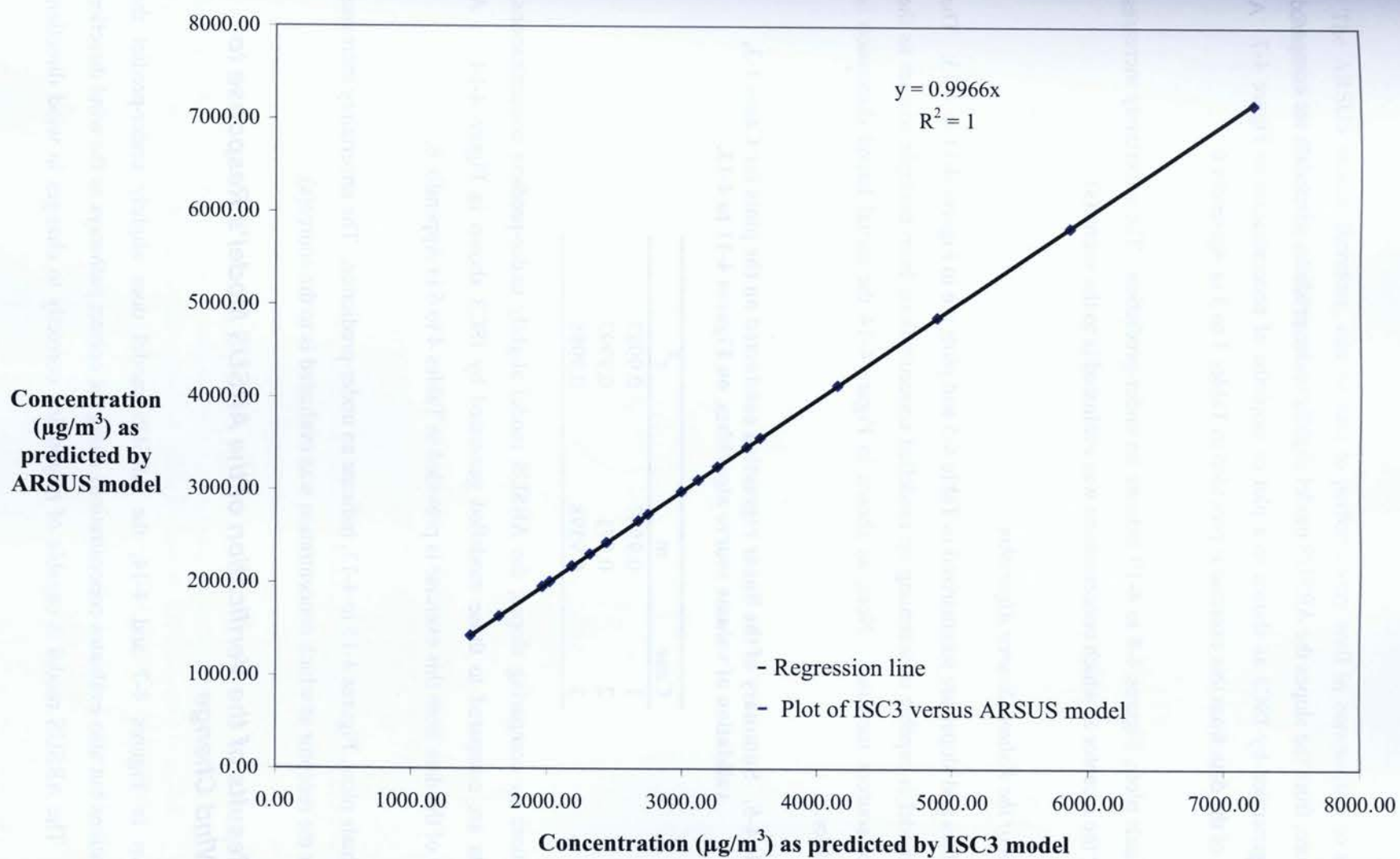


Figure 4-6. CASE 3 (Validation of Point Source Algorithm) – A plot of ISC3 modelled concentrations versus ARSUS modelled concentrations showing good agreement.

71



Furthermore, from the slopes the ARSUS model slightly under-predicts, when data are compared to those generated by ISC3 as shown in a plot of isopleths of concentration in Figure 4-7. A summary of the data from this exercise is provided in Tables 1 to 3 in Appendix 6.

The residuals plots, Figures 4-8 to 4-10 indicate an under-prediction. The uncertainty increases the closer the receptor at which concentration was evaluated is to the source(s).

#### *Validation of the Volume Source Algorithm*

The  $r^2$  values and slopes are summarized in Table 4-5 and plots are in Figures 4-11 to 4-13. The ARSUS model is capable of summing up modelled concentrations from multiple sources as the number of sources increases. Note, as shown in Figure 4-14 the initial lateral dimension is accounted for.

**Table 4-5. Summary of the linear regression conducted on the plots for Cases 1-3, validation of volume source algorithm, on Figures 4-11 to 4-13.**

Case	m	$r^2$
1	0.9567	0.9987
2	0.971	0.9997
3	0.9598	0.9986

Further more by comparing slopes, the ARSUS model slightly under-predicts concentrations, when data are compared to those modelled generated by ISC3 shown in Figure 4-14. A summary of the data from this exercise is provided in Tables 4 to 6 in Appendix 6.

The residuals plots, Figures 4-15 to 4-17, indicate an under-prediction. The uncertainty increases the closer the receptor at which concentration was evaluated is to the source(s).

#### **4.4 Results of the Verification of the ARSUS Model's Response to Wind Change**

As shown in Figures 4-7 and 4-14, the ARSUS model does slightly under-predict the concentrations but also evaluates concentrations along the correct pathways as the wind direction changes. The ARSUS model is capable of responding correctly to changes in wind direction.

The ARSUS model, therefore, can be said to perform very well in comparison to an existing Gaussian air dispersion model such as ISC3.



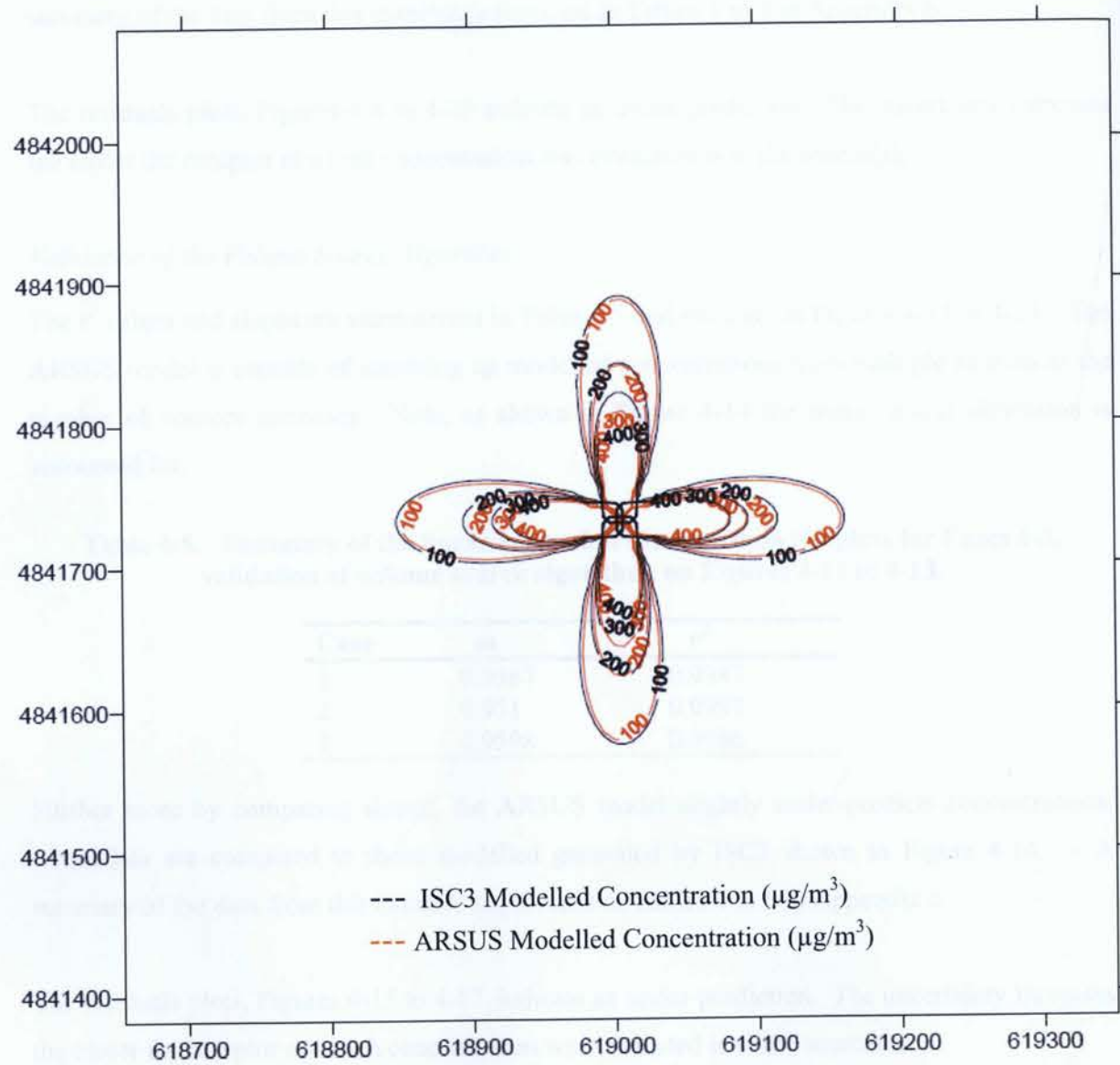


Figure 4-7. A plot of concentration isopleths, concentration generated by the ARSUS and ISC3. The ARSUS model slightly under-predicts and does respond well to changes in wind direction.

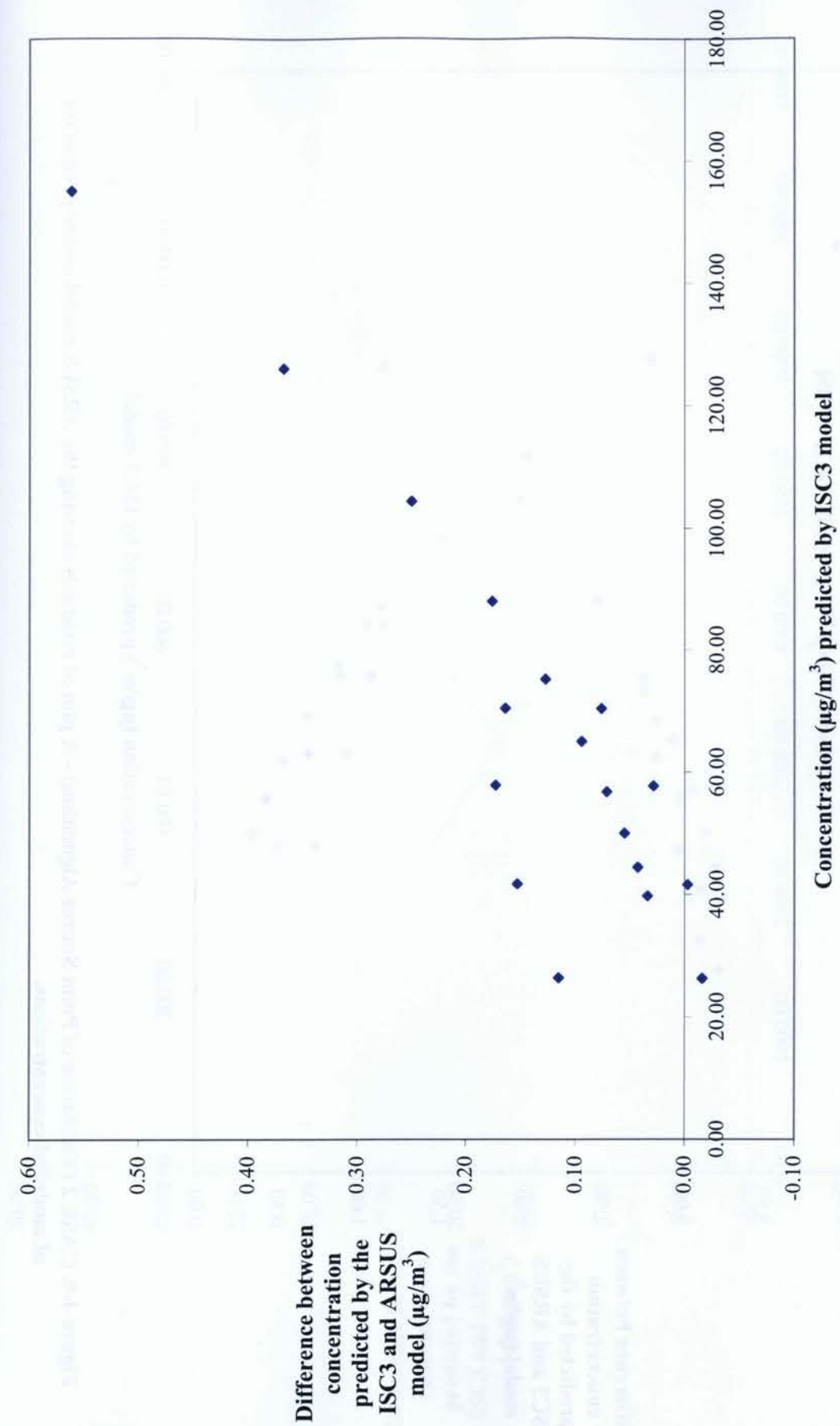
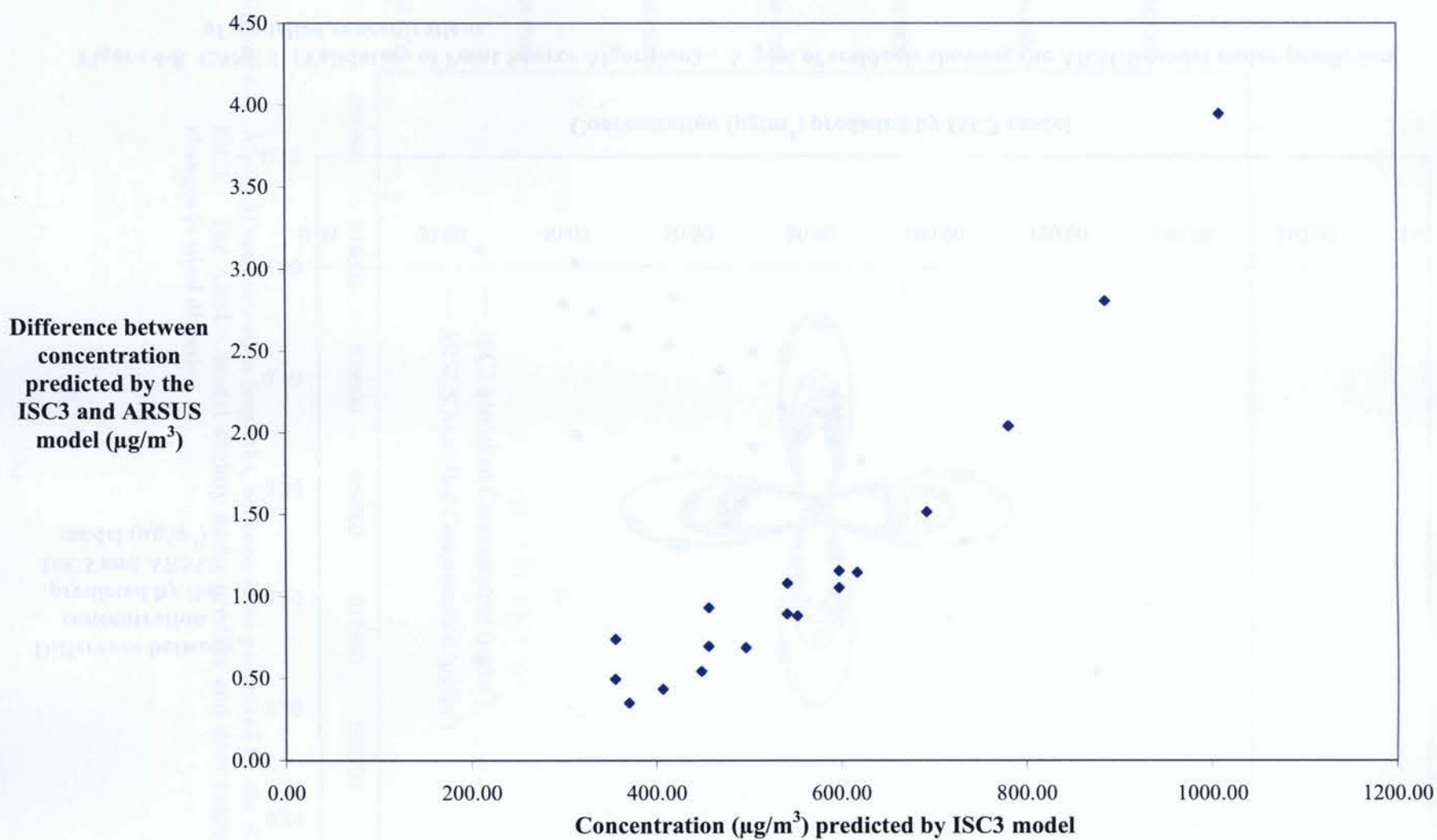
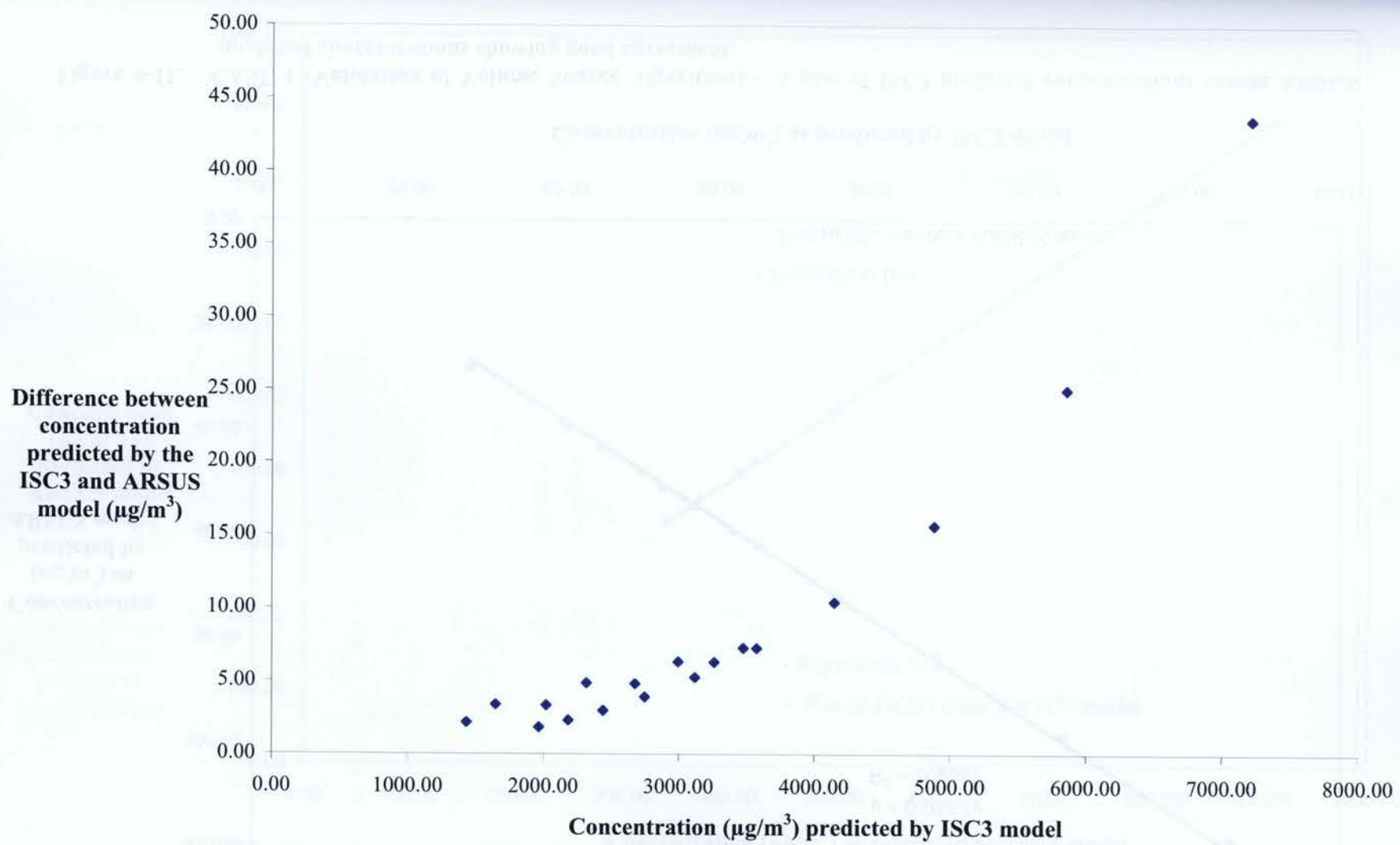


Figure 4-8. CASE 1 (Validation of Point Source Algorithm) – A plot of residuals showing the ARSUS model under-prediction of modelled concentrations.





**Figure 4-9. CASE 2 (Validation of Point Source Algorithm) - A plot of residuals showing the ARSUS model under-prediction of modelled concentrations.**



**Figure 4-10. CASE 3 (Validation of Point Source Algorithm) – A plot of residuals showing the ARSUS model under-prediction of modelled concentrations.**

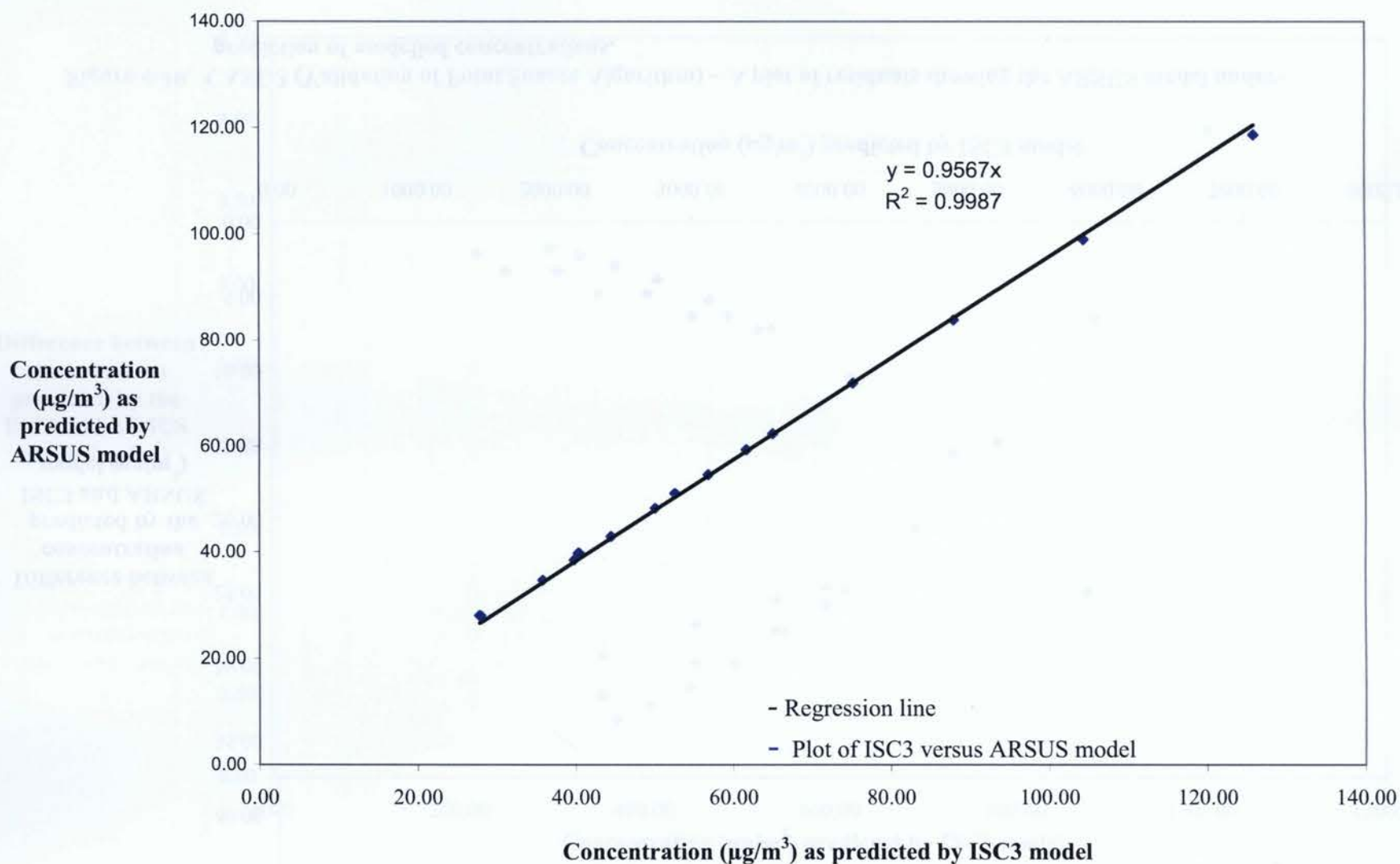


Figure 4-11. CASE 1 (Validation of Volume Source Algorithm) – A plot of ISC3 modelled concentrations versus ARSUS modelled concentrations showing good agreement.

78

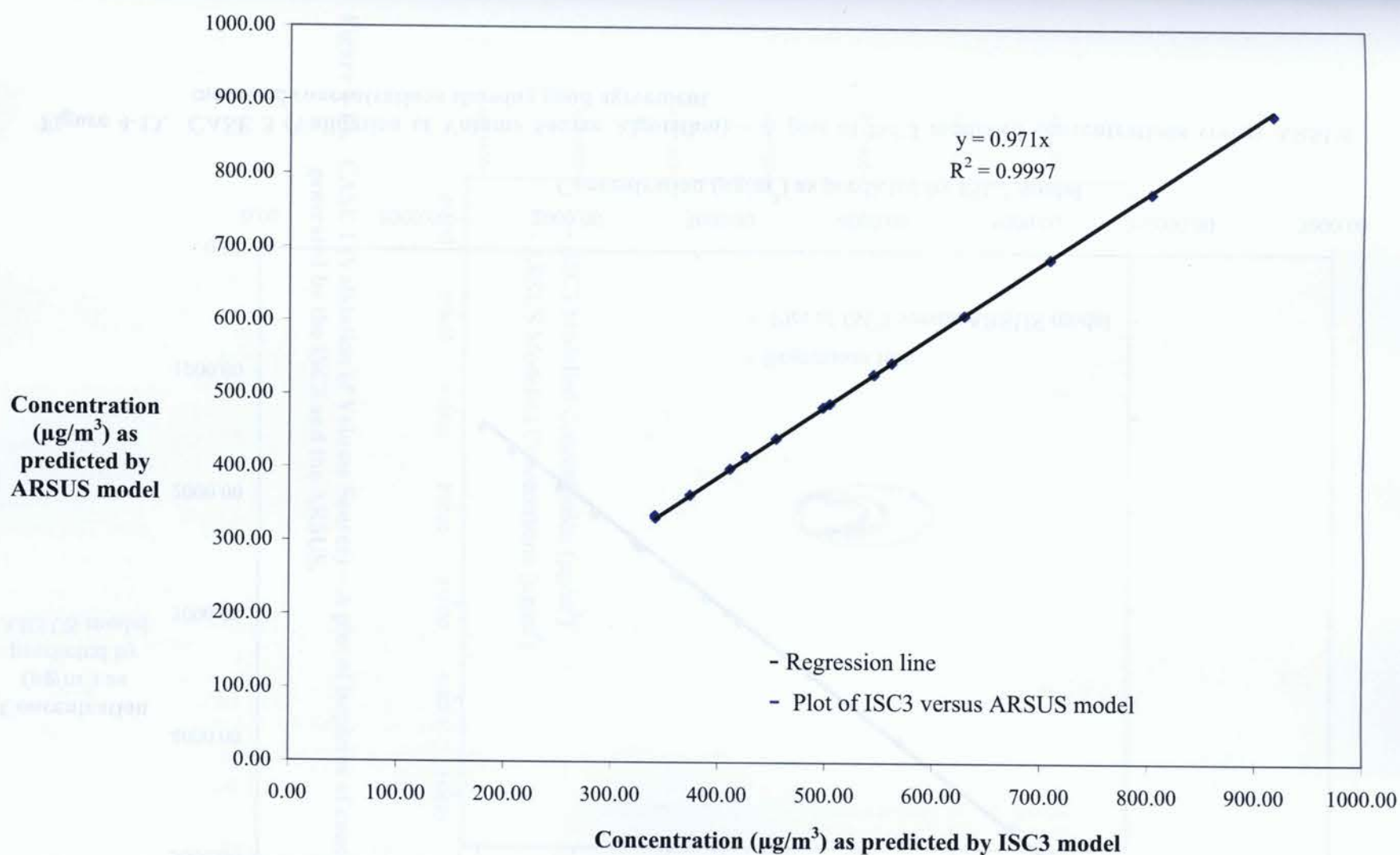


Figure 4-12. CASE 2 (Validation of Volume Source Algorithm) – A plot of ISC3 modelled concentrations versus ARSUS modelled concentrations showing good agreement.

79



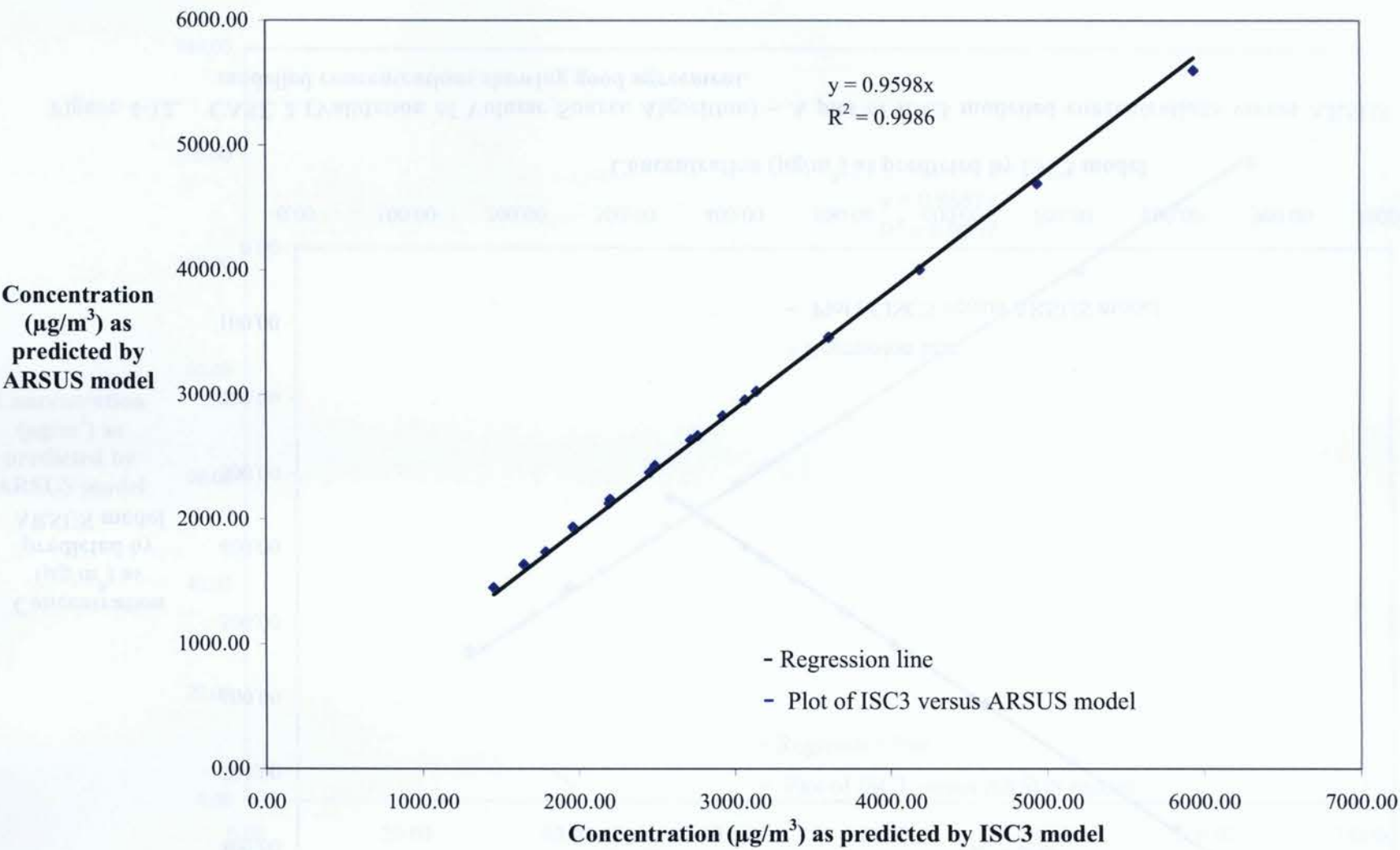
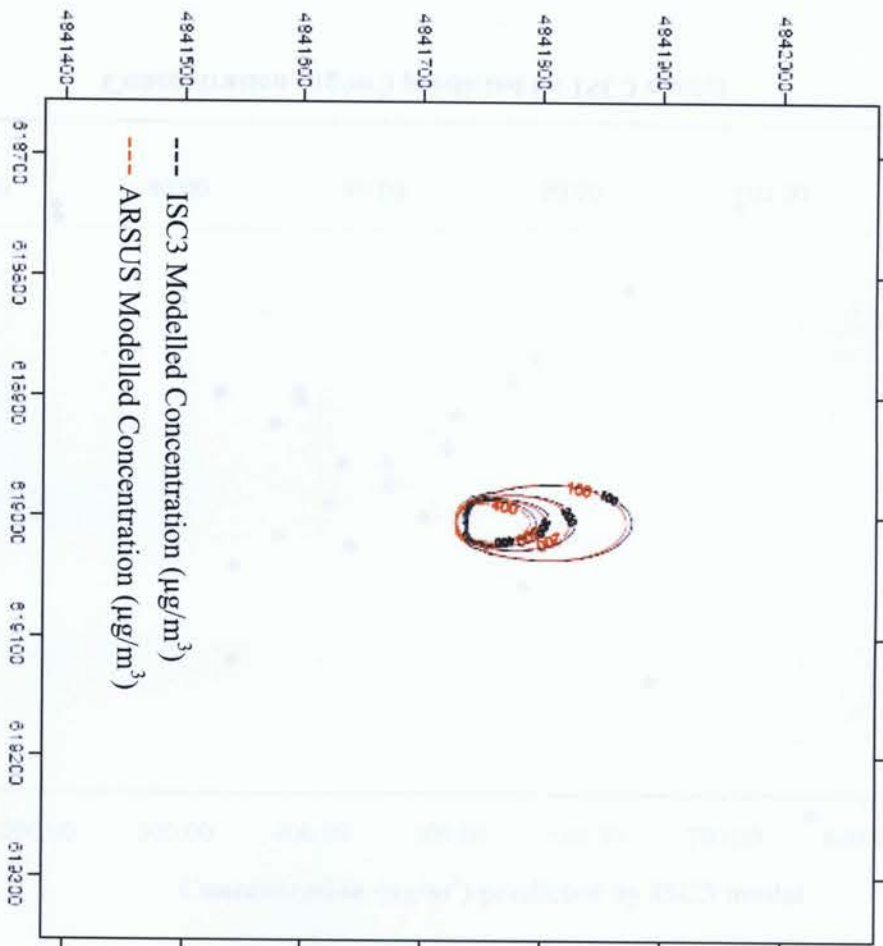


Figure 4-13. CASE 3 (Validation of Volume Source Algorithm) – A plot of ISC3 modelled concentrations versus ARSUS modelled concentrations showing good agreement.

Figure 4-14. CASE 1 (Validation of Volume Source) – A plot of isopleths of concentrations generated by the ISC3 and the ARSUS.



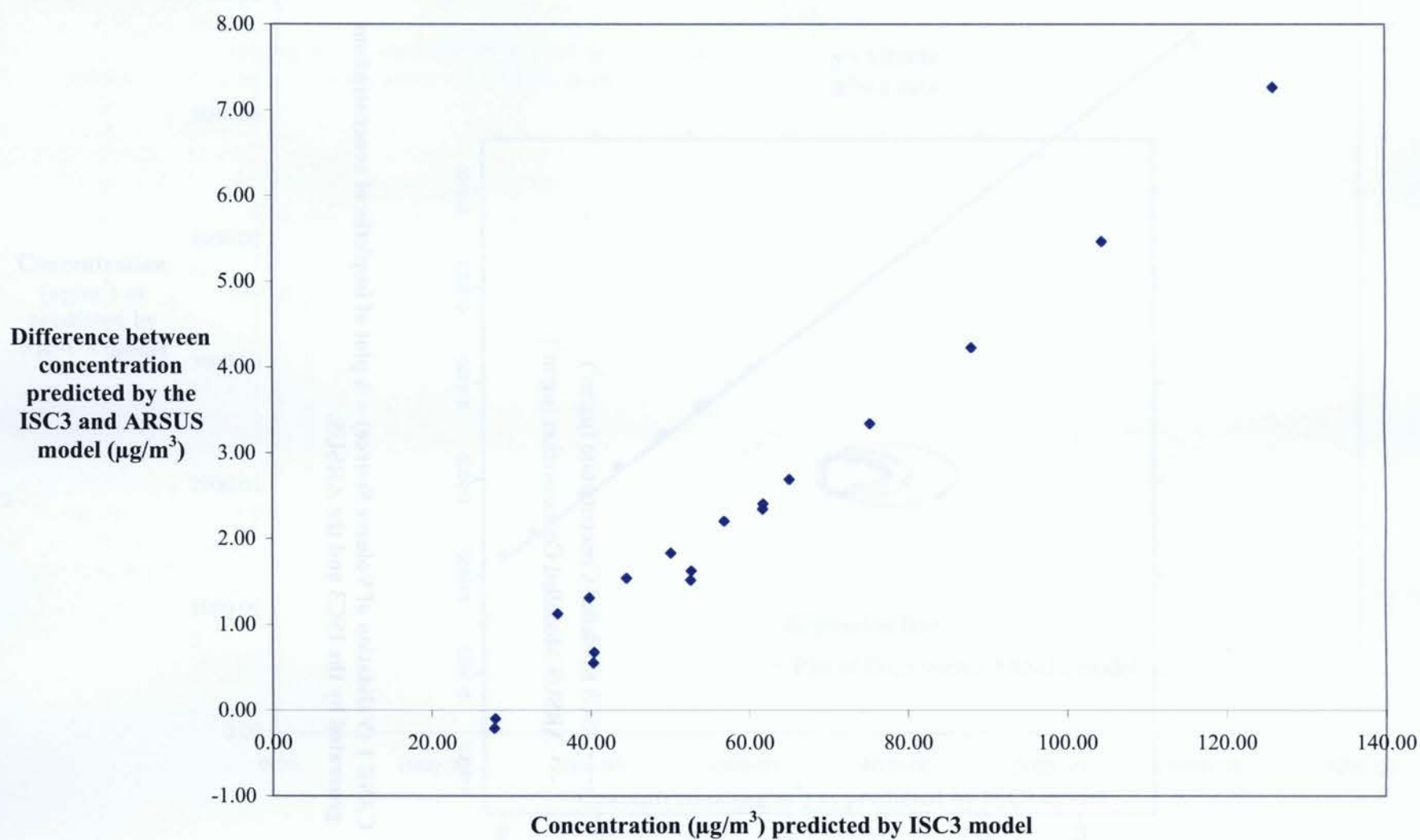


Figure 4-15. CASE 1 (Validation of Volume Source Algorithm) - A plot of residuals showing the ARSUS model under-prediction of modelled concentrations.

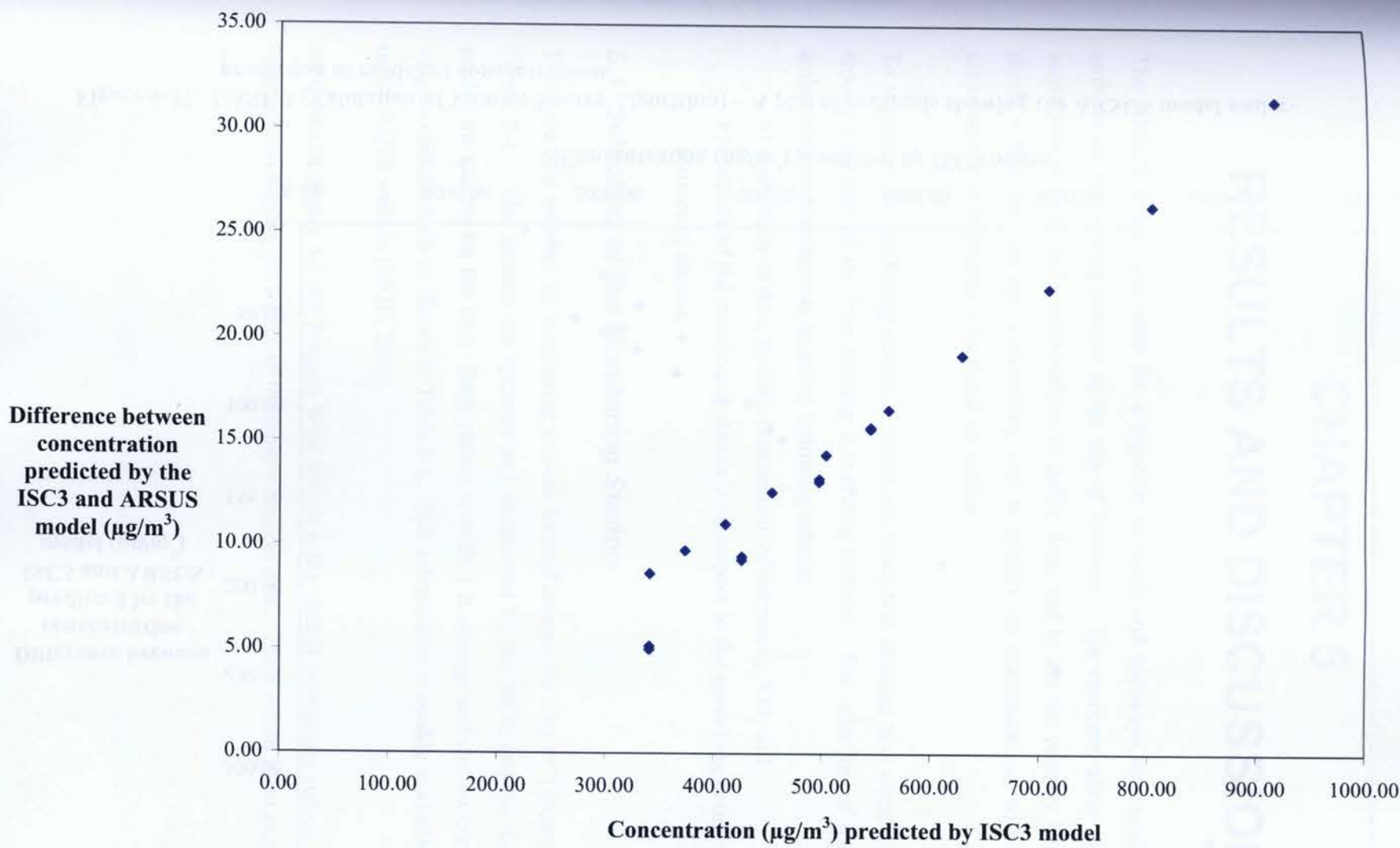


Figure 4-16. CASE 2 (Validation of Volume Source Algorithm) - A plot of residuals showing the ARSUS model under-prediction of modelled concentrations.



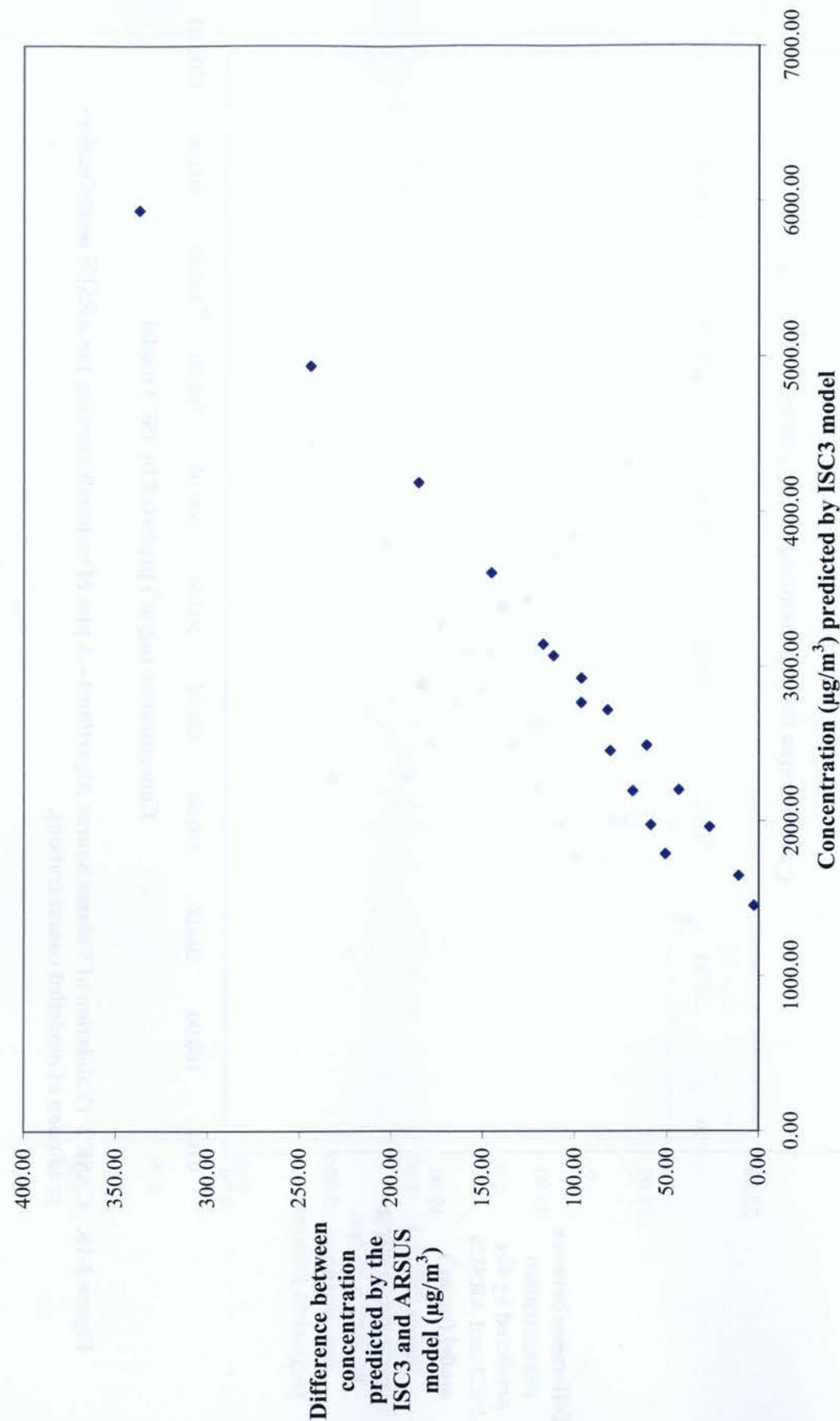


Figure 4-17. CASE 3 (Validation of Volume Source Algorithm) – A plot of residuals showing the ARSUS model under-prediction of modelled concentrations.

## CHAPTER 5

# RESULTS AND DISCUSSION

The ARSUS model was used for a segment of roads and highways surrounding one of the ambient air monitoring stations in the city of Toronto. The exercises allow one to study the sensitivity of modelled concentrations to traffic data, and to test the primary hypothesis of the thesis – that one can use a modelling tool to predict the concentrations within an air shed, allowing one to determine a localized air quality.

To minimize the modelling domain (reduce run time) this exercise was completed for an area around only one of the four existing monitoring stations. The selection of most appropriate ambient air monitoring was based on following criteria:

- a) availability of data, specific contaminant of interest i.e. CO; and
- b) location of the monitoring station with respect to the modelling domain and emission sources of interest.

### 5.1 Selection of the Monitoring Station

There are four ambient air monitoring stations located around the City of Toronto, as shown on Figure 5-1. The stations are operated and maintained by the MOE and the data are used to predict air quality for the city. Each station records 1 h average ambient air concentrations of various contaminants as shown in Table 5-1. This information is readily available to the public on the AQI's website (MOE, 2007).

As shown in Figure 5-1 the Toronto West station is the closest monitoring station to the Pearson International airport, the source of the meteorological data. The Toronto West station monitors







networks within the domain. The modelling was completed for the months of April and May, 2007. Only weekdays between the hours of 6 am and 11 am were modelled to capture morning rush hour traffic emissions. The monitoring station has many blank periods lasting up to days when no data are available. April and May represented the most complete data for the station. For the month of April and May, 2007, the Toronto West monitoring station data are presented in Table 1 in Appendix 7.

Figure 5-2 is a plot of isopleths for the modelling domain for April 6<sup>th</sup> at 6 am 2007. This sample plot demonstrates the impact of tailpipe emissions from road and highway sources on the air quality in the vicinity of each source. The plot clearly shows the emissions from the roads and highway do not disperse very well. It is observed that higher concentrations occur closer to the sources, which reduce slowly as the distance from the roads increases.

Statistical analysis was carried out on the 136 h of results and a plot of the residuals is shown in Figure 5-3, and Figure 5-4 shows a plot of the ARSUS modelled emissions as a percentage of the observed concentrations at the monitoring station. Tabulated results are provided in Table 1 in Appendix 8. The ARSUS model consistently under-predicts the concentrations to those measured from the monitoring station. As shown in Figure 5-3, when the monitoring station's recorded concentrations fall within 200 to 300  $\mu\text{g}/\text{m}^3$ , the modelled results are closer to the monitoring station's. As the recorded concentrations measured by the monitoring station increase (400 to 600  $\mu\text{g}/\text{m}^3$ ), the accuracy of the ARSUS model decreases, under-predicting to a larger magnitude. However, when looking at the modelled emissions as a percentage of the observed concentrations in Figure 5-4, the results are consistent between 10% and 80%, regardless of the magnitude of the observed concentrations.

### 5.2.2 Large Scale Study of Tailpipe Emissions for the City of Toronto

For the large scale study, only highways situated throughout the City were used to estimate emissions. The modelling domain was set to be 34.6 km by 23.2 km, with 1,819 volume sources representing all highways. The width of a highway was assumed to be 27 m. While this study was conducted on a large domain, it only included the highway networks. The modelling

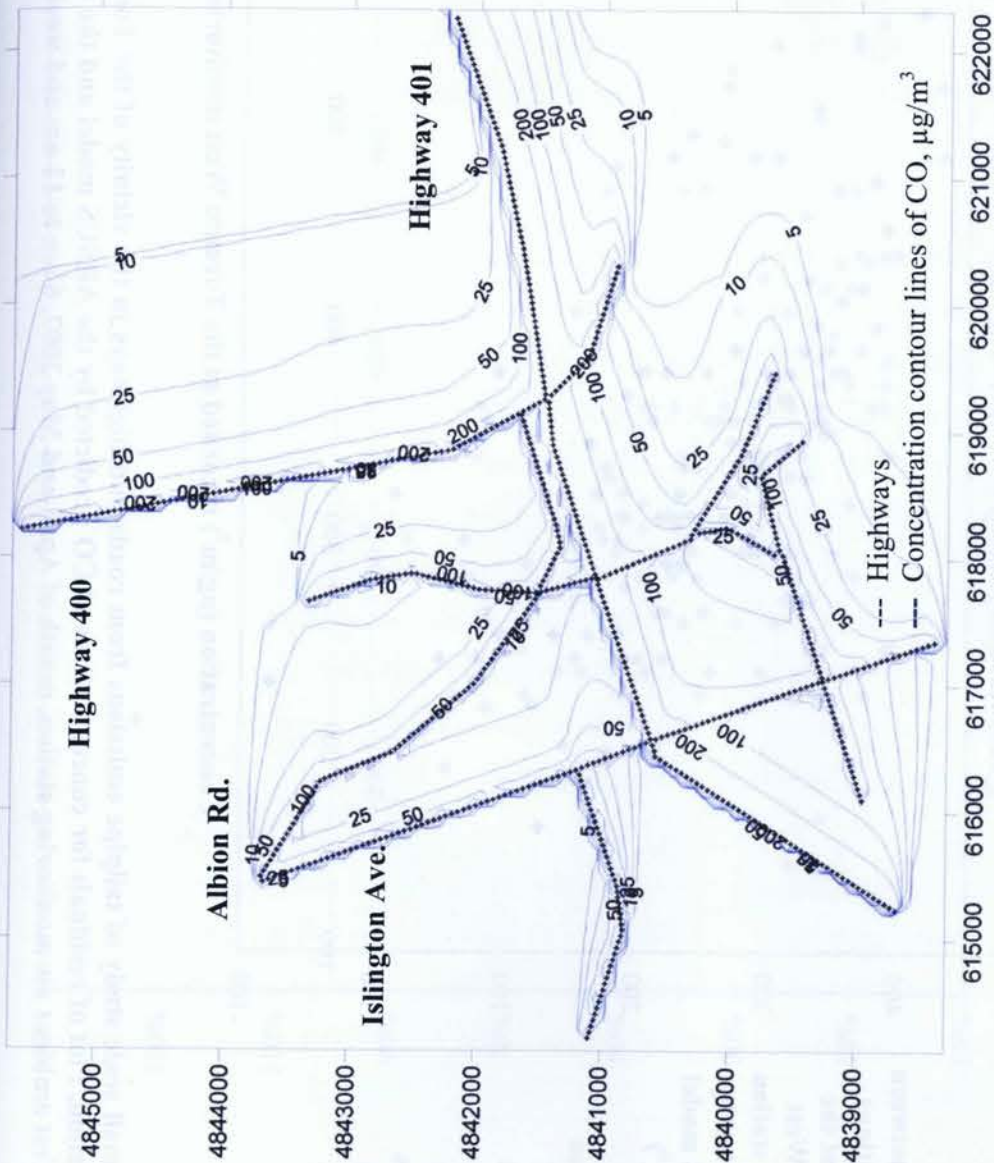


Figure 5-2. Sample of an isopleths plot for 1 h, CO concentration predicted by the ARSUS model, April 6 at 6 am 2007. Contribution of CO to the ground level concentrations from the local roads and highways, in the vicinity of the Toronto West monitoring station.



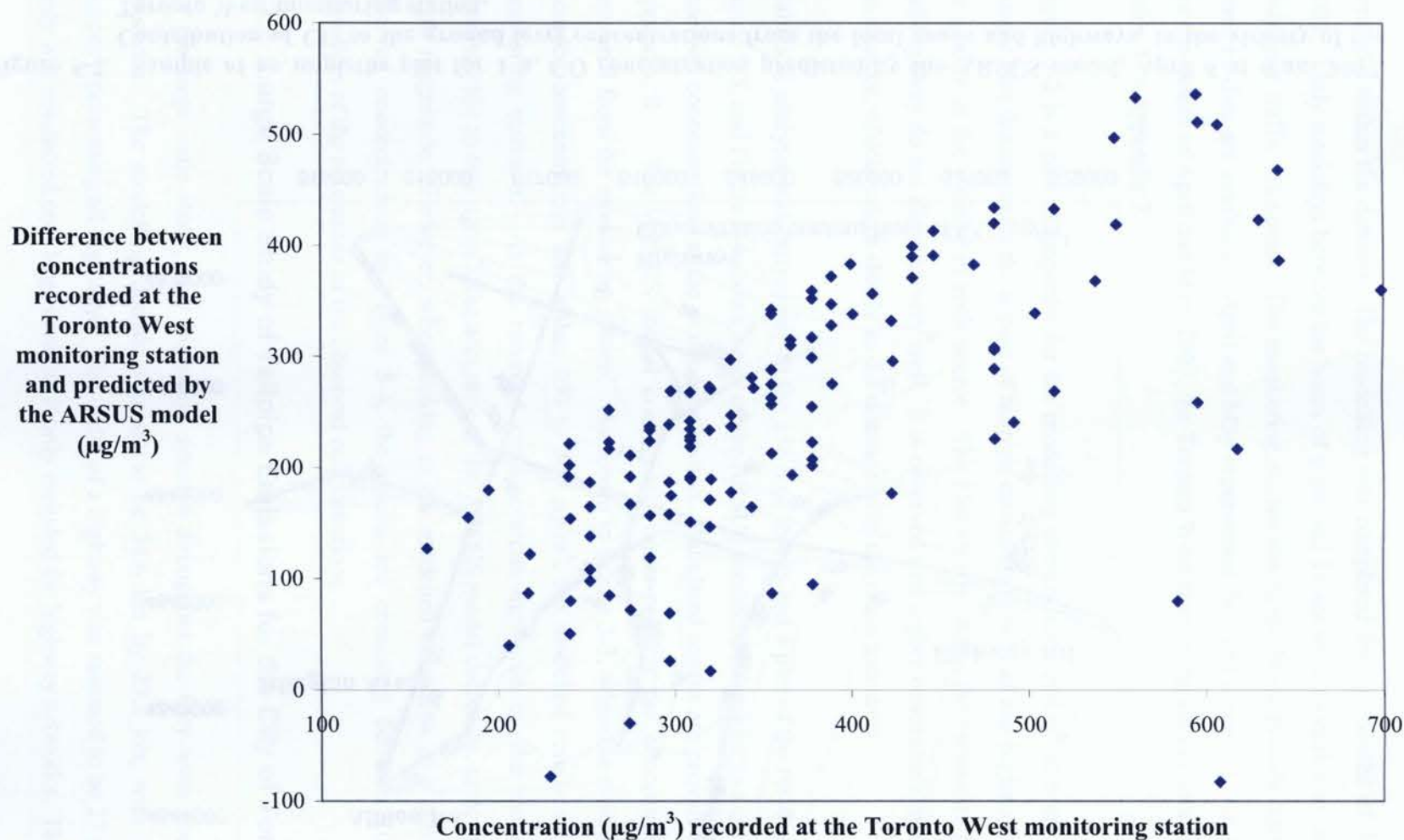


Figure 5-3. Small scale study of tailpipe emissions from roads and highways in the vicinity of the Toronto West monitoring station. Plot of residuals for concentrations of CO predicted by the ARSUS model and the data from the Toronto West ambient air monitoring station, month of April and May 2007, 6 am to 11 am and weekdays.

90

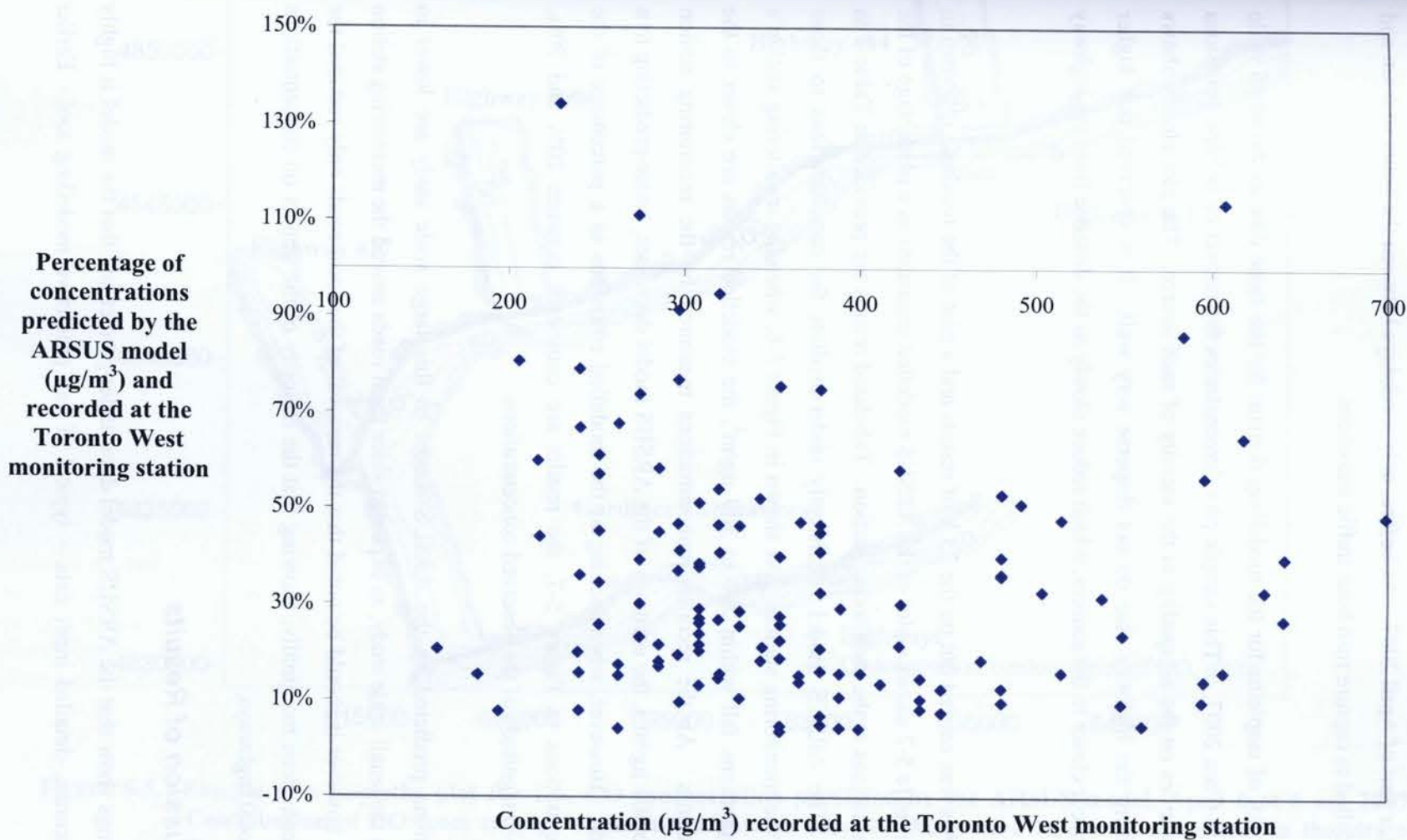


Figure 5-4. Small scale study of tailpipe emissions from roads and highways in the city of Toronto. Plot of percentage for concentrations of CO predicted by the ARSUS model and the data from the Toronto West ambient air monitoring station, month of April 2007 and May, 6 am to 11 am and weekdays.



was completed for part of April 2007. As before, only weekdays between the hours of 6 am and 11 am were modelled to capture rush hour traffic emissions.

Figure 5-5 is a plot of isopleths for the modelling domain for the same date as the small scale study, April 6<sup>th</sup> at 6 am 2007. This sample plot demonstrates the impact of tailpipe emissions from highway sources on the air quality in the vicinity of each source. The plot clearly shows the emissions from the highway also do not disperse very well. It is observed that higher concentrations occur closer to the sources, which reduce slowly as the distance from the highway increases.

Statistical analysis was carried out on the 73 h of results and a plot of the residuals is shown in Figure 5-6 and Figure 5-7 shows a plot of the ARSUS modelled emissions as a percentage of the observed concentrations at the monitoring station. Tabulated results are provided in Table 2 in Appendix 8. The ARSUS model consistently under-predicts the concentrations to those measured from the monitoring station. As shown in Figure 5-6, when the monitoring station's recorded concentrations fall within 200 to 300  $\mu\text{g}/\text{m}^3$ , the modelled results are closer to the monitoring station's. As the recorded concentrations measured by the monitoring station increase (400 to 500  $\mu\text{g}/\text{m}^3$ ), the accuracy of the ARSUS model decreases, under-predicting to a larger magnitude. However, when looking at the modelled emissions as a percentage of the observed concentrations in Figure 5-7, the results are consistent between 20% and 70%, regardless of the magnitude of the observed concentrations.

The concentrations predicted by the ARSUS model in this large scale study are lower in magnitude than the small scale study, as expected since local roads around the monitoring station were removed, however it should be noted that the removal of the local roads only reduced the predicted concentrations marginally, showing that the majority of the impact on concentrations are due to the local highways.

### 5.3 Discussion of Results

The main findings show that the ARSUS model does under-predict and that the model is highly sensitive to accurate, detailed input data – typical of any predictive modelling tool. Earlier

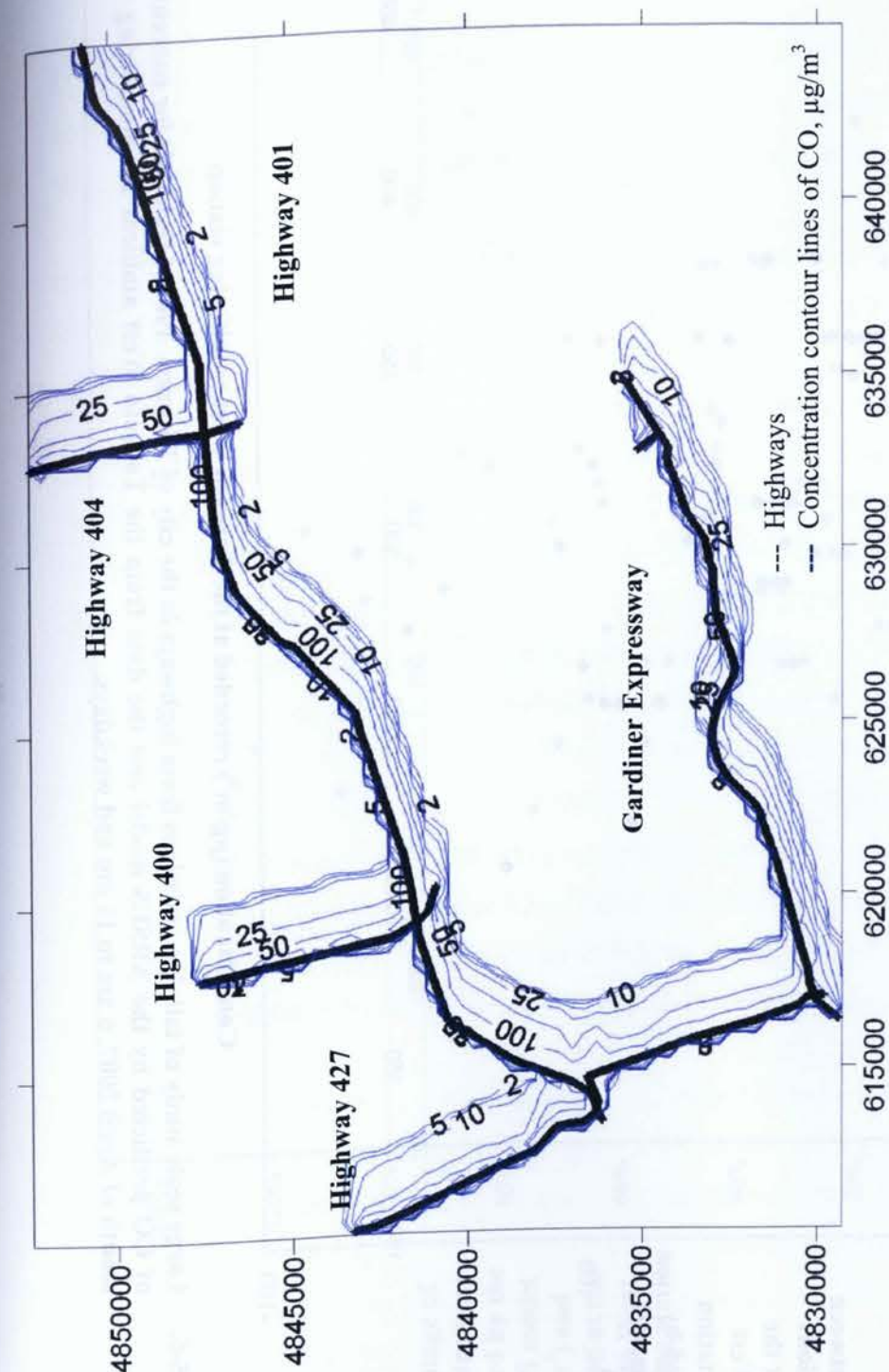


Figure 5-5. Sample of a isopleths plot for 1 h, CO concentration predicted by the ARSUS model, April 6 at 6 am 2007. Contribution of CO from tailpipe emissions (highways only) to the ground level concentrations, in the city of Toronto.



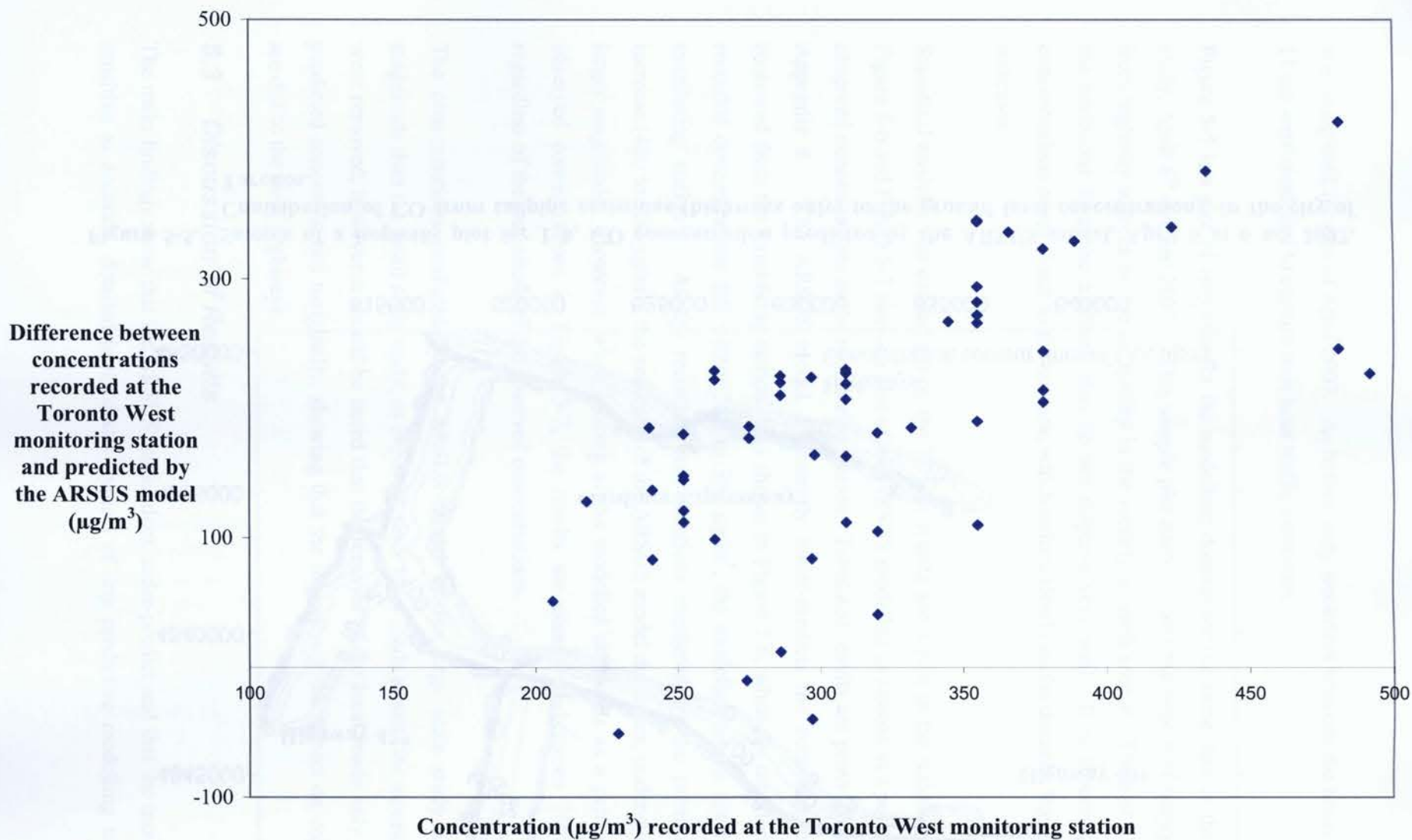


Figure 5-6. Large scale study of tailpipe emissions from highways in the city of Toronto. Plot of residuals for concentrations of CO predicted by the ARSUS model and the data from the Toronto West ambient air monitoring station, month of April 2007, 6 am to 11 am and weekdays.

94

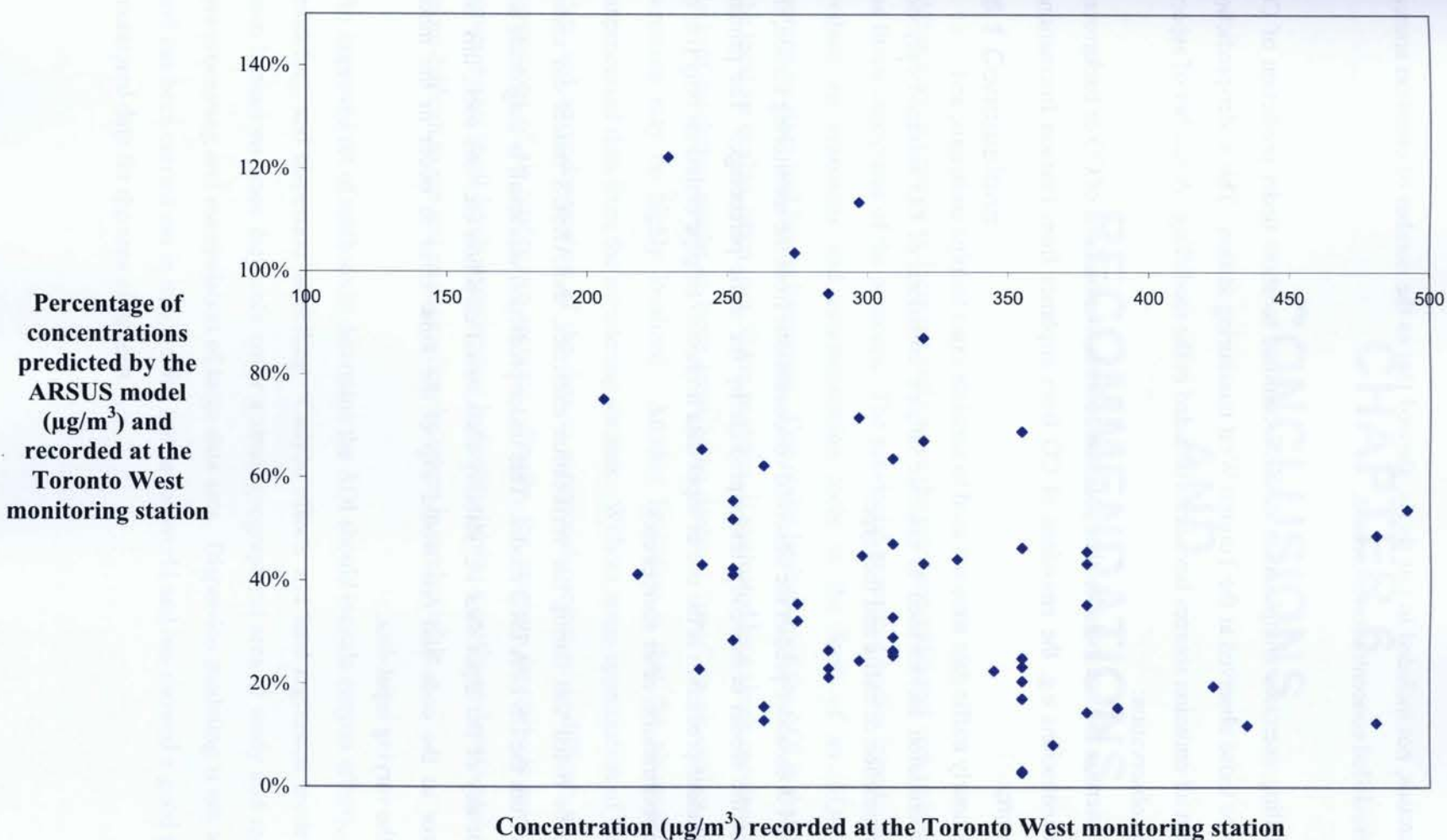


Figure 5-7. Large scale study of tailpipe emissions from highways in the city of Toronto. Plot of percentage for concentrations of CO predicted by the ARSUS model and the data from the Toronto West ambient air monitoring station, month of April 2007, 6 am to 11 am and weekdays.



modelling exercises, not included in this thesis, showed that as the number of emission sources increased the modelled concentration increased.

The two modelling exercises completed in ARSUS continue to show under-prediction of CO concentrations to those observed at the Toronto West monitoring station. This under-prediction is a sign that not all emission sources have been included in the modelling. A number of aspects account for this observation:

- a) the exercise did not include other potential sources of emissions of CO or background concentrations e.g. the emissions of CO from airplanes from Pearson International airport;
- b) the hourly traffic data were not used to simulate exact tailpipe emissions; and
- c) the emission factors used to estimate tailpipe emissions of CO assumed only one composition of traffic and fuel type.

While the model does under-predict the observed concentrations from the monitoring station, the data show that the model consistently under-predicts by the same percentage. The primary reason for this under-prediction is the use of input data limited to tailpipe emissions only (i.e. no background concentrations, other sources etc).

It should also be noted that during the verification exercises, the ARSUS model did under-predict results from the US EPA ISC3 model. This under-prediction was small in magnitude and independent of any of the input data i.e. stability class, wind direction etc. As such, this is a systematic error in the code and one would expect the same error to occur in the model regardless of the varying input data.

## **CHAPTER 6**

# **CONCLUSIONS AND RECOMMENDATIONS**

### **6.1 Conclusions**

Air quality in Ontario is declining and causes the province additional cost in health care as well as limits enjoyment of the outdoors. The provincial governing bodies introduced regulations to reduce air emissions and communication tools in the form of an AQI; however, this communication tool has its limitations. One major limitation of the AQI is that for many cities, the local air quality, often over 50 km in radius, is evaluated by a single monitoring station. This lack of resolution results in large areas being declared "poor" in air quality when in fact the situation may be highly localized. Another limitation is that the air quality is based on unprocessed data from the monitoring stations. Without some appreciation of the quality of the data and an understanding of the data in a regional context, it is difficult to fully trust that predictions of air quality are accurate. Finally, the program is costly in maintenance. With governments at all levels experiencing budgetary limits, a costly environmental system is much more difficult to run and manage when the return is rarely visible.

An improved set of methods to determine the AQI should include canyon effects, land regression modeling, and dispersion modelling. Canyon effects and land regression modeling have their own limitations since they only cover a small geographical area of study and require extensive pre-processing and manipulation of large data sets. Dispersion modeling is not a new approach and has been carried out in major cities across the world and has showed a good agreement with monitored data for the area of interest.



The readily available tools and data combined with a dispersion model provide a more detailed representation of the air quality at a lower cost than the existing systems in place. A dispersion model applied to the City of Toronto removes the assumption of uniform air quality within the vicinity of a monitoring station. This clearly addresses one of the key limitations of the AQI.

#### *Results of the Validation Exercises*

The ARSUS model underwent a number of validation exercises which resulted in following conclusions:

- a) it is possible to successfully develop an air dispersion model in MATLAB;
- b) the ARSUS model consistently but slightly under-predicts modelled concentrations for both point and volume type of emission sources when compared to US EPA ISC3 dispersion model;
- c) the under-prediction is consistent and does not amplify as the distance from the emission source(s) increases or number of emission sources increases;
- c) the ARSUS model has the ability to respond to wind direction changes and changes in stability classes; and
- d) the ARSUS model is capable of handling over 300 volume sources and 3,000 receptors which are current limitations of US EPA air dispersion models.

Therefore, the ARSUS model in its current state can successfully simulate emissions from both point and volume type sources using Gaussian dispersion to calculate ground level concentrations of a non-reactive contaminant of interest.

#### *Results from the Modelling of Tailpipe Emissions Exercises*

The working ARSUS model was further used to simulate tailpipe emissions of CO from local roads and highways in the vicinity of Toronto West ambient air monitoring station. The exercise was conducted to simulate weekday morning rush hour traffic. The findings include:

- a) the residuals plot of the results of a comparison between the ARSUS model-predicted concentrations and those observed at the Toronto West monitoring station show constant under-prediction of the ARSUS model. This under-prediction is mainly due to the fact that only tailpipe emissions were considered;
- b) the emissions of CO from the morning rush hour have the highest impact closest to the road / highway source and drop off significantly away from the source. This reinforces understood dispersion knowledge of low sources such as tailpipe emissions which lack momentum or thermal rise; and
- c) the impact of tailpipe emissions on areas immediately adjacent to the sources (i.e. roads and highways) is high.

Finally, the ARSUS model was used to simulate tailpipe emissions of CO for a larger modelling domain for only highway sources that cross the City of Toronto. The results from the ARSUS model continued to under-predict concentrations of CO. The ARSUS model demonstrated that emissions from the highways rather than roads have a greater impact on the local concentration of CO.

## **6.2 Recommendations**

It has been shown that a computerized air dispersion model can be used to generate data used in the AQI predictions. The ARSUS model could be modified to account for the following factors:

- a) additional algorithms to calculate plume spread;
- b) additional sources other than roads i.e. industrial emissions, airport;
- c) cumulative 24 h or annual average concentrations;
- d) wet and dry deposition including in-cloud, below cloud deposition; and
- f) hourly traffic emissions.

#### *a) Additional algorithms to calculate plume spread*

As summarised in previous sections, there are a number of algorithms published which allow a person to estimate urban plume spread ( $\sigma_y$  and  $\sigma_z$ ). New findings by Yuan and Venkatram (2005) and Venkatram et al. (2005) can be used to update the plume spread approach. The method used in the ARSUS model was developed by Briggs in the late 70's and is the preferred



approach used in the US EPA Gaussian air dispersion models. A further development of the model can account the effect of land on the dispersion also known as Golder's approach (1972).

*b) Account for additional sources other than roads*

The City of Toronto's structure is mainly dominated by a network of roads and highways. The model can be used to study emissions of substances other than those that contribute to smog i.e. mercury. Other sources of emissions can include:

- i) commercial industries/office buildings;
- ii) small size non-commercial industries such as ready-mix concrete plants and hot mix asphalt plants;
- iii) one international airport and one smaller airport (i.e. Toronto Island airport);
- iv) ship yard/marina at the South edge of the city; and
- v) on-going construction activities that occur through out the city.

Inclusion of these sources would allow the study of contribution of emissions from each source which subsequently can impact city's environmental policy and environmental management development.

*c) Cumulative 24 h or annual average concentrations*

The ambient air quality standards for the smog-causing air pollutants are normally based on 1 h and 24 h average. The ARSUS model does estimate the 1 h average concentrations of a pollutant and can be converted to estimate the 24 h averages, well within the constraints of a steady state Gaussian air dispersion assumptions.

*d) Wet and dry deposition*

The geographical location of the city of Toronto means changes in season as well as precipitation (i.e. snow and rain). The effect of precipitation can be studied in the form of expanding the ARSUS model to allow for wet deposition and its variations (i.e. in-cloud, below cloud, snow, rain) (Asman, 1995; Chang 1984).

*e) Hourly traffic emissions*

As indicated in the review, in the studies by Kitabayashi et al. (2006), Owen et al. (2000), Seika et al. (1998), Karppinen et al. (1998, 2000) and Brechler (2000), the common element to all was the importance of input data specifically the emission rates from the traffic. A further expansion of the existing ARSUS model would be to develop an input file containing emissions from the traffic on an hourly basis.

The ARSUS model can further be used to study emissions from the city of Toronto to assist the city with the development of environmental policies and environmental management systems.

Some may include:

- a) a study of various fuel compositions and their impact on the air quality;
- b) the impact of the proposed feet change by the City of Toronto on air quality;
- c) analyzing hourly concentrations to determine road closure or restrictions on transportation;
- d) analyzing traffic around most impacted areas (hot spots of high concentration with poor dispersion) to provide solutions to poor air quality;
- e) developing a forecasting tool;
- f) a study of source contributions of pollution from future expansions of industry, development, construction, and highways in order to evaluate impacts on air quality.

## APPENDICES

## APPENDIX 1: SAMPLE OF PROCESSED METEOROLOGICAL DATA

Year	Month	Day	Hour	Temp (°C)	Humidity (%)	Wind Speed (km/h)	Wind Dir (°)	Pressure (hPa)	Clouds (%)	Visib (km)	Station
2010	1	1	0	-1.2	95	15	135	1013.2	100	10	101
2010	1	1	1	-1.5	95	15	135	1013.2	100	10	101
2010	1	1	2	-1.8	95	15	135	1013.2	100	10	101
2010	1	1	3	-2.1	95	15	135	1013.2	100	10	101
2010	1	1	4	-2.4	95	15	135	1013.2	100	10	101
2010	1	1	5	-2.7	95	15	135	1013.2	100	10	101
2010	1	1	6	-3.0	95	15	135	1013.2	100	10	101
2010	1	1	7	-3.3	95	15	135	1013.2	100	10	101
2010	1	1	8	-3.6	95	15	135	1013.2	100	10	101
2010	1	1	9	-3.9	95	15	135	1013.2	100	10	101
2010	1	1	10	-4.2	95	15	135	1013.2	100	10	101
2010	1	1	11	-4.5	95	15	135	1013.2	100	10	101
2010	1	1	12	-4.8	95	15	135	1013.2	100	10	101
2010	1	1	13	-5.1	95	15	135	1013.2	100	10	101
2010	1	1	14	-5.4	95	15	135	1013.2	100	10	101
2010	1	1	15	-5.7	95	15	135	1013.2	100	10	101
2010	1	1	16	-6.0	95	15	135	1013.2	100	10	101
2010	1	1	17	-6.3	95	15	135	1013.2	100	10	101
2010	1	1	18	-6.6	95	15	135	1013.2	100	10	101
2010	1	1	19	-6.9	95	15	135	1013.2	100	10	101
2010	1	1	20	-7.2	95	15	135	1013.2	100	10	101
2010	1	1	21	-7.5	95	15	135	1013.2	100	10	101
2010	1	1	22	-7.8	95	15	135	1013.2	100	10	101
2010	1	1	23	-8.1	95	15	135	1013.2	100	10	101
2010	1	1	24	-8.4	95	15	135	1013.2	100	10	101
2010	1	1	25	-8.7	95	15	135	1013.2	100	10	101
2010	1	1	26	-9.0	95	15	135	1013.2	100	10	101
2010	1	1	27	-9.3	95	15	135	1013.2	100	10	101
2010	1	1	28	-9.6	95	15	135	1013.2	100	10	101
2010	1	1	29	-9.9	95	15	135	1013.2	100	10	101
2010	1	1	30	-10.2	95	15	135	1013.2	100	10	101
2010	1	1	31	-10.5	95	15	135	1013.2	100	10	101
2010	2	1	0	-10.8	95	15	135	1013.2	100	10	101
2010	2	1	1	-11.1	95	15	135	1013.2	100	10	101
2010	2	1	2	-11.4	95	15	135	1013.2	100	10	101
2010	2	1	3	-11.7	95	15	135	1013.2	100	10	101
2010	2	1	4	-12.0	95	15	135	1013.2	100	10	101
2010	2	1	5	-12.3	95	15	135	1013.2	100	10	101
2010	2	1	6	-12.6	95	15	135	1013.2	100	10	101
2010	2	1	7	-12.9	95	15	135	1013.2	100	10	101
2010	2	1	8	-13.2	95	15	135	1013.2	100	10	101
2010	2	1	9	-13.5	95	15	135	1013.2	100	10	101
2010	2	1	10	-13.8	95	15	135	1013.2	100	10	101
2010	2	1	11	-14.1	95	15	135	1013.2	100	10	101
2010	2	1	12	-14.4	95	15	135	1013.2	100	10	101
2010	2	1	13	-14.7	95	15	135	1013.2	100	10	101
2010	2	1	14	-15.0	95	15	135	1013.2	100	10	101
2010	2	1	15	-15.3	95	15	135	1013.2	100	10	101
2010	2	1	16	-15.6	95	15	135	1013.2	100	10	101
2010	2	1	17	-15.9	95	15	135	1013.2	100	10	101
2010	2	1	18	-16.2	95	15	135	1013.2	100	10	101
2010	2	1	19	-16.5	95	15	135	1013.2	100	10	101
2010	2	1	20	-16.8	95	15	135	1013.2	100	10	101
2010	2	1	21	-17.1	95	15	135	1013.2	100	10	101
2010	2	1	22	-17.4	95	15	135	1013.2	100	10	101
2010	2	1	23	-17.7	95	15	135	1013.2	100	10	101
2010	2	1	24	-18.0	95	15	135	1013.2	100	10	101
2010	2	1	25	-18.3	95	15	135	1013.2	100	10	101
2010	2	1	26	-18.6	95	15	135	1013.2	100	10	101
2010	2	1	27	-18.9	95	15	135	1013.2	100	10	101
2010	2	1	28	-19.2	95	15	135	1013.2	100	10	101
2010	2	1	29	-19.5	95	15	135	1013.2	100	10	101
2010	2	1	30	-19.8	95	15	135	1013.2	100	10	101
2010	2	1	31	-20.1	95	15	135	1013.2	100	10	101



**APPENDIX 1: SAMPLE OF PROCESSED METEOROLOGICAL DATA**

Table 1 below provides a summary of 1 h of processed meteorological data for the year 2007 for month of April and May. The 1 h values were obtained from the Toronto’s Lester B. Pearson International airport. The data are maintained and published on the Environment Canada’s website under Climate Normals. The first 3 columns are used by the ARSUS model to name the output file and they contain: hour of the day, month, day of the month. The simulation was conducted for a morning rush hour period 6 am to 11 am, Monday to Friday due to following:

- a) traffic data were readily available for morning rush hour;
- b) morning and afternoon rush hour has a significant impact on air quality due to high volume of traffic;
- c) to minimize required run time.

Table 1. 2007 Processed Meteorological Data for the Months of April and May.

Hour of the Day	Month	Day	Day of the Week	Wind Direction (TO) in Degrees	Wind Speed (m/s)	Ambient Temperature (K)	Stability Class
6	4	2	Monday	80.0355	6.6907	281.5	4
7	4	2	Monday	79.9839	7.2005	282	4
8	4	2	Monday	79.9904	9.7727	282	4
9	4	2	Monday	69.9811	9.7724	283.2	4
10	4	2	Monday	79.988	14.4019	284.3	4
11	4	2	Monday	69.9839	12.3454	284.3	4
6	4	3	Tuesday	100.0627	0.5148	276.5	3
7	4	3	Tuesday	315.2405	0.0025	278.1	2
8	4	3	Tuesday	190.2848	0.5124	280.9	2
9	4	3	Tuesday	310.0105	3.0911	282	3
10	4	3	Tuesday	349.9667	2.5744	280.9	4
11	4	3	Tuesday	349.9711	3.0895	280.4	4
6	4	4	Wednesday	136.4403	0.0009	278.7	4
7	4	4	Wednesday	79.8704	0.5131	279.3	4
8	4	4	Wednesday	89.9923	9.7724	280.9	4

Hour of the Day	Month	Day	Day of the Week	Wind Direction (TO) in Degrees	Wind Speed (m/s)	Ambient Temperature (K)	Stability Class
9	4	4	Wednesday	79.9893	10.2875	282	4
10	4	4	Wednesday	79.9879	9.7724	280.4	4
11	4	4	Wednesday	89.9864	11.3151	279.3	4
6	4	5	Thursday	80.0397	7.2045	267	4
7	4	5	Thursday	79.9914	8.2292	267	4
8	4	5	Thursday	79.9933	10.8009	268.1	4
9	4	5	Thursday	79.9785	6.6855	277.6	4
10	4	5	Thursday	109.9944	10.2868	270.4	4
11	4	5	Thursday	109.9951	12.3447	269.3	4
6	4	6	Friday	90.0421	5.6629	266.5	4
7	4	6	Friday	89.9944	9.7729	268.1	4
8	4	6	Friday	140.0023	6.171	267	4
9	4	6	Friday	109.989	7.7137	268.1	4
10	4	6	Friday	109.994	9.7718	269.3	4
11	4	6	Friday	109.9915	7.1997	269.3	4
6	4	9	Monday	100.0387	3.6042	272	4
7	4	9	Monday	109.9918	4.1146	272	4
8	4	9	Monday	129.9991	6.6859	273.1	4
9	4	9	Monday	119.993	7.1985	273.1	4
10	4	9	Monday	89.9623	4.1133	274.3	4
11	4	9	Monday	99.9791	6.1698	275.4	4
6	4	10	Tuesday	119.992	2.0569	272	4
7	4	10	Tuesday	109.967	2.0555	274.3	3
8	4	10	Tuesday	315.2374	0.0035	274.3	2
9	4	10	Tuesday	140.0033	5.6554	275.9	4
10	4	10	Tuesday	109.9742	3.5975	275.9	4
11	4	10	Tuesday	89.948	3.0842	275.9	4
6	4	11	Wednesday	240.0221	3.0873	272.6	4
7	4	11	Wednesday	260.0156	4.6309	275.4	4
8	4	11	Wednesday	290.0076	6.6898	275.9	4
9	4	11	Wednesday	270.0116	8.2326	275.9	4
10	4	11	Wednesday	260.0144	8.2324	275.9	4
11	4	11	Wednesday	260.0126	9.7755	275.9	4
6	4	12	Thursday	269.9608	4.627	277	4
7	4	12	Thursday	270.0177	3.6021	277	4
8	4	12	Thursday	260.0236	4.1172	277	4
9	4	12	Thursday	280.0302	2.5739	278.1	4
10	4	12	Thursday	319.9769	0.5165	278.1	4
11	4	12	Thursday	300.0192	2.0605	279.3	4



Hour of the Day	Month	Day	Day of the Week	Wind Direction (TO) in Degrees	Wind Speed (m/s)	Ambient Temperature (K)	Stability Class
6	4	13	Friday	70.0361	7.7191	274.8	4
7	4	13	Friday	89.9868	8.229	275.9	4
8	4	13	Friday	99.9897	10.2863	275.9	4
9	4	13	Friday	99.9923	9.7721	277	4
10	4	13	Friday	119.9972	12.3446	277	4
11	4	13	Friday	119.9962	9.7715	278.2	4
6	4	16	Monday	149.994	12.3525	276.5	4
7	4	16	Monday	160.0039	10.8015	277	4
8	4	16	Monday	150.0026	13.373	277	4
9	4	16	Monday	150.0026	14.9167	277	4
10	4	16	Monday	160.005	12.8587	277	4
11	4	16	Monday	150.0027	15.9455	277	4
6	4	17	Tuesday	159.9769	4.1199	278.1	4
7	4	17	Tuesday	190.0188	4.115	278.1	4
8	4	17	Tuesday	190.0148	6.6868	278.1	4
9	4	17	Tuesday	180.0157	6.1713	279.3	4
10	4	17	Tuesday	160.0142	6.6845	280.9	4
11	4	17	Tuesday	160.0146	6.6844	280.4	4
12	4	17	Tuesday	150.0071	5.6564	280.4	4
6	4	18	Wednesday	239.9538	5.6579	279.3	4
7	4	18	Wednesday	240.0151	6.1734	279.3	4
8	4	18	Wednesday	240.0327	3.6015	279.3	4
9	4	18	Wednesday	250.0303	4.117	280.4	4
10	4	18	Wednesday	270.0337	3.0888	280.4	4
11	4	18	Wednesday	290.021	3.0894	280.9	4
6	4	19	Thursday	180.0296	2.5707	279.3	4
7	4	19	Thursday	250.0336	4.6313	282	3
8	4	19	Thursday	260.0545	3.089	283.2	3
9	4	19	Thursday	220.0625	3.6006	284.3	2
10	4	19	Thursday	250.0603	3.6027	285.9	2
11	4	19	Thursday	339.9717	3.6049	285.9	2
6	4	20	Friday	180.0304	2.5706	279.3	4
7	4	20	Friday	250.0338	4.6313	282	3
8	4	20	Friday	260.0547	3.089	283.1	3

Hour of the Day	Month	Day	Day of the Week	Wind Direction (TO) in Degrees	Wind Speed (m/s)	Ambient Temperature (K)	Stability Class
9	4	20	Friday	220.0626	3.6006	284.3	2
10	4	20	Friday	250.0604	3.6028	285.9	2
11	4	20	Friday	339.9717	3.6049	285.9	2
6	4	23	Monday	29.9813	6.1736	289.8	4
7	4	23	Monday	39.9789	7.7173	290.9	4
8	4	23	Monday	39.9753	7.7173	293.1	4
9	4	23	Monday	39.9746	8.2313	295.9	4
10	4	23	Monday	39.9786	10.2894	295.4	4
11	4	23	Monday	39.979	10.8034	293.1	4
6	4	24	Tuesday	140.0034	3.085	280.4	4
7	4	24	Tuesday	160.0253	3.0842	280.9	3
8	4	24	Tuesday	150.0175	3.0837	283.2	3
9	4	24	Tuesday	315.2354	0.0037	283.1	1
10	4	24	Tuesday	315.2351	0.0039	284.3	1
11	4	24	Tuesday	160.0244	4.1123	285.9	3
6	4	25	Wednesday	140.0061	3.0849	280.4	4
7	4	25	Wednesday	160.025	3.0844	280.9	3
8	4	25	Wednesday	150.0182	3.0838	283.1	3
9	4	25	Wednesday	315.2354	0.0037	283.1	1
10	4	25	Wednesday	315.2351	0.0039	284.3	1
11	4	25	Wednesday	160.0245	4.1124	285.9	3
6	4	26	Thursday	260.0094	4.1162	280.9	4
7	4	26	Thursday	260.0135	6.1738	280.9	4
8	4	26	Thursday	270.0146	6.6894	280.9	4
9	4	26	Thursday	260.0158	7.2031	280.9	4
10	4	26	Thursday	270.017	6.6897	283.1	4
11	4	26	Thursday	260.0128	9.7753	282	4
6	4	27	Friday	280.0208	2.0587	282.6	4
7	4	27	Friday	320.0016	2.5742	284.3	4
8	4	27	Friday	310.0106	2.5745	284.3	4
9	4	27	Friday	329.9893	2.5748	284.3	4
10	4	27	Friday	339.9805	3.0898	285.9	4
11	4	27	Friday	329.9852	2.0608	285.9	4
6	4	30	Monday	150.0034	9.772	282.6	4
7	4	30	Monday	160.0085	9.2571	283.2	4



Hour of the Day	Month	Day	Day of the Week	Wind Direction (TO) in Degrees	Wind Speed (m/s)	Ambient Temperature (K)	Stability Class
8	4	30	Monday	160.0096	9.7706	284.3	4
9	4	30	Monday	160.0141	7.1983	285.4	4
10	4	30	Monday	109.9837	6.1691	287	4
11	4	30	Monday	180.0494	3.5979	288.2	2
6	5	1	Tuesday	220.1283	1.0288	281.5	3
7	5	1	Tuesday	270.0244	3.0883	282	4
8	5	1	Tuesday	300.0112	3.0891	283.1	4
9	5	1	Tuesday	300.0106	3.6034	283.1	4
10	5	1	Tuesday	250.0379	3.6021	283.2	4
11	5	1	Tuesday	290.0184	3.6034	282	4
6	5	2	Wednesday	160.0185	3.0849	280.9	4
7	5	2	Wednesday	180.036	3.5987	283.1	3
8	5	2	Wednesday	180.0325	4.6274	284.3	3
9	5	2	Wednesday	210.087	2.5709	285.9	2
10	5	2	Wednesday	260.0649	3.0894	287	2
11	5	2	Wednesday	79.7998	1.0265	288.1	2
6	5	3	Thursday	220.0499	2.5718	281.5	4
7	5	3	Thursday	250.0522	3.0882	285.4	3
8	5	3	Thursday	250.0406	4.6314	285.4	3
9	5	3	Thursday	280.0447	3.0902	285.9	2
10	5	3	Thursday	319.9965	4.1204	285.9	3
11	5	3	Thursday	319.9963	4.1205	285.9	3
6	5	4	Friday	190.0996	1.0279	282	3
7	5	4	Friday	259.0914	0.5124	285.4	2
8	5	4	Friday	250.083	2.0593	287	2
9	5	4	Friday	310.0147	2.5769	289.3	2
10	5	4	Friday	300.0129	6.1772	289.3	4
11	5	4	Friday	319.9979	5.6639	289.3	3
6	5	7	Monday	339.9442	1.0312	280.4	3
7	5	7	Monday	310.0331	0.5172	283.1	2
8	5	7	Monday	180.2959	0.5113	285.4	1
9	5	7	Monday	349.9486	2.5753	288.1	2
10	5	7	Monday	319.9935	3.0913	289.3	2
11	5	7	Monday	310.006	3.6051	289.3	2
6	5	8	Tuesday	29.9621	3.6017	287	4
7	5	8	Tuesday	39.9743	7.2023	290.4	4
8	5	8	Tuesday	39.9624	5.6593	292	3
9	5	8	Tuesday	29.9493	4.117	294.3	3
10	5	8	Tuesday	29.9673	6.689	295.9	4

Hour of the Day	Month	Day	Day of the Week	Wind Direction (TO) in Degrees	Wind Speed (m/s)	Ambient Temperature (K)	Stability Class
11	5	8	Tuesday	19.9686	6.6897	298.1	3
6	5	9	Wednesday	339.9324	0.5153	291.5	3
7	5	9	Wednesday	315.2357	0.0031	293.1	2
8	5	9	Wednesday	349.9557	2.5749	295.4	2
9	5	9	Wednesday	49.895	2.0577	294.3	2
10	5	9	Wednesday	19.9322	2.0592	298.1	3
11	5	9	Wednesday	310.0048	3.0897	295.4	2
6	5	10	Thursday	329.9285	0.5164	290.9	3
7	5	10	Thursday	69.9483	3.0857	292	4
8	5	10	Thursday	39.903	2.0583	293.2	3
9	5	10	Thursday	319.9925	2.0618	293.1	4
10	5	10	Thursday	49.9106	2.5716	293.1	4
11	5	10	Thursday	89.9684	5.6558	294.3	3
6	5	11	Friday	99.9594	2.0559	289.3	3
7	5	11	Friday	160.0311	2.569	292	3
8	5	11	Friday	180.0229	6.6853	294.3	4
9	5	11	Friday	170.0147	9.2566	293.1	4
10	5	11	Friday	180.026	6.685	292	4
11	5	11	Friday	180.0289	6.1699	293.1	3
6	5	14	Monday	315.2394	0.0024	283.1	3
7	5	14	Monday	359.9612	2.0594	285.9	4
8	5	14	Monday	9.97	3.6023	288.2	4
9	5	14	Monday	329.9824	3.0907	287	3
10	5	14	Monday	300.0133	3.0895	285.9	4
11	5	14	Monday	319.9956	4.1201	287	3
6	5	15	Tuesday	359.9517	2.0598	290.4	4
7	5	15	Tuesday	69.9759	6.6867	294.3	4
8	5	15	Tuesday	99.984	7.1991	295.9	4
9	5	15	Tuesday	89.9848	10.8001	298.1	4
10	5	15	Tuesday	79.981	9.7717	299.3	4
11	5	15	Tuesday	89.9823	9.2571	300.9	4
6	5	16	Wednesday	140.0013	6.6865	286.5	4
7	5	16	Wednesday	129.9988	7.2	287	4
8	5	16	Wednesday	170.0167	4.6281	285.9	4
9	5	16	Wednesday	180.0333	3.0852	285.9	4
10	5	16	Wednesday	190.2438	0.5125	285.4	4
11	5	16	Wednesday	290.0262	2.5744	284.3	4
6	5	17	Thursday	190.0451	2.5706	280.9	4



Hour of the Day	Month	Day	Day of the Week	Wind Direction (TO) in Degrees	Wind Speed (m/s)	Ambient Temperature (K)	Stability Class
7	5	17	Thursday	180.0411	3.0848	282	4
8	5	17	Thursday	230.0986	2.0583	283.1	4
9	5	17	Thursday	190.0582	3.0848	285.4	4
10	5	17	Thursday	310.0069	3.091	285.4	4
11	5	17	Thursday	329.9855	4.12	285.9	3
6	5	18	Friday	315.2396	0.0026	280.9	2
7	5	18	Friday	359.7308	0.5164	283.1	2
8	5	18	Friday	359.8521	1.0317	284.3	2
9	5	18	Friday	140.0195	1.0249	285.4	2
10	5	18	Friday	339.9601	2.5759	287	2
11	5	18	Friday	339.8973	1.033	288.2	1
6	5	21	Monday	160.0313	2.0556	280.9	3
7	5	21	Monday	200.0681	2.5706	283.1	3
8	5	21	Monday	190.3505	0.5118	284.3	1
9	5	21	Monday	99.9336	2.0546	285.9	2
10	5	21	Monday	315.2352	0.0043	287	1
11	5	21	Monday	109.965	3.083	288.2	2
6	5	22	Tuesday	270.0994	1.0307	284.8	3
7	5	22	Tuesday	240.1701	1.0298	287	2
8	5	22	Tuesday	260.0816	2.06	289.3	2
9	5	22	Tuesday	339.9703	3.0905	290.4	2
10	5	22	Tuesday	310.0069	3.091	290.9	2
11	5	22	Tuesday	319.9954	4.1201	290.9	2
6	5	23	Wednesday	280.1723	0.5162	287.6	2
7	5	23	Wednesday	315.2366	0.0034	289.3	2
8	5	23	Wednesday	315.2363	0.0038	292	1
9	5	23	Wednesday	300.0302	2.062	293.1	2
10	5	23	Wednesday	329.9797	3.0912	295.4	2
11	5	23	Wednesday	310.0057	4.1204	294.3	2
6	5	24	Thursday	339.9686	2.0605	290.9	3
7	5	24	Thursday	339.9213	1.0321	294.3	2
8	5	24	Thursday	39.9294	3.0874	298.2	2
9	5	24	Thursday	39.9244	3.0874	300.4	2
10	5	24	Thursday	89.9152	2.055	302	2
11	5	24	Thursday	89.9131	2.0549	302	1
6	5	25	Friday	59.9581	3.6003	294.8	3
7	5	25	Friday	59.9544	4.1151	297	3
8	5	25	Friday	69.965	5.6574	299.3	3

Hour of the Day	Month	Day	Day of the Week	Wind Direction (TO) in Degrees	Wind Speed (m/s)	Ambient Temperature (K)	Stability Class
9	5	25	Friday	99.9812	6.6849	300.4	4
10	5	25	Friday	89.9758	6.6852	300.4	4
11	5	25	Friday	69.9771	9.2583	300.4	3
6	5	28	Monday	69.9643	4.1147	287	3
7	5	28	Monday	69.9494	3.5994	289.3	3
8	5	28	Monday	89.9753	6.1701	290.9	4
9	5	28	Monday	99.9832	7.1987	292	4
10	5	28	Monday	99.9861	9.7703	293.1	4
11	5	28	Monday	99.9812	7.7134	293.1	3
6	5	29	Tuesday	315.2382	0.0027	287.6	2
7	5	29	Tuesday	359.9556	3.0894	289.3	3
8	5	29	Tuesday	310.0068	3.0908	290.4	2
9	5	29	Tuesday	310.0073	3.0911	290.9	2
10	5	29	Tuesday	329.9758	2.5762	290.9	2
11	5	29	Tuesday	310.0117	2.0624	292	1
6	5	30	Wednesday	315.2415	0.0027	290.9	2
7	5	30	Wednesday	359.8685	1.0314	293.1	2
8	5	30	Wednesday	339.9649	2.5755	295.4	2
9	5	30	Wednesday	319.9928	2.5761	295.9	2
10	5	30	Wednesday	329.9799	3.0912	297	2
11	5	30	Wednesday	319.9936	3.0914	300.4	2
6	5	31	Thursday	315.2369	0.0028	295.9	2
7	5	31	Thursday	315.235	0.0032	297	3
8	5	31	Thursday	39.6014	0.5143	299.3	1
9	5	31	Thursday	59.5833	0.513	300.9	1
10	5	31	Thursday	339.9688	3.0907	299.3	3
11	5	31	Thursday	359.9802	5.661	297	4



## APPENDIX 2: TRAFFIC AND EMISSIONS DATA

## APPENDIX 2: TRAFFIC AND EMISSIONS DATA

Tables 1 and 2 contain a summary of road source information as well as tailpipe emission factors used to estimate emissions of CO. Table 1 is the summary of the tailpipe emissions broken by type of mobile equipment used for the small scale modelling exercise. Table 2 is a summary of the tailpipe emissions broken by the type of mobile equipment used for the large scale modelling exercise. Sample calculations and assumptions presented below are for:

- one section of Highway 400 using average daily traffic count; and
- for a section of Dixon Road using morning peak hour traffic count.

The traffic count for the highway sources is given as 24 h traffic count where the traffic for municipal roads is available in peak hour counts.

### Sample Calculations:

- Following sample calculation is for the emissions associated with traffic from the road link modelling I.D. 4001 using average 24 h traffic count.

Given:

Length of the road =  $1.2\text{km}$

Daily average traffic count =  $91,900 \frac{\text{passes}}{\text{day}}$

Emission rate of CO, from LDPV-A =  $10.9 \frac{\text{g(CO)}}{\text{km}}$

Assumed: 64.4 % of traffic is composed of LDPV-A

Emissions of CO from the 4001 segment =

$$= 1.2\text{km} * 91,900 \frac{\text{passes}}{\text{day}} * 10.9 \frac{\text{g(CO)}}{\text{km}} * \frac{\text{day}}{24\text{hr}} * \frac{\text{hr}}{3,600\text{s}} * 64.4\% = 8.96 \frac{\text{g}}{\text{s}}$$

- Following sample calculation is for the emissions associated with traffic from the road link modelling I.D. DXRD1 using morning peak hour traffic count.

Given:

Length of the road =  $1.01\text{km}$



Daily average traffic count =  $2,281 \frac{\text{Passes}}{\text{hour}}$

Emission rate of CO, from LDPV-A =  $10.9 \frac{\text{g(CO)}}{\text{km}}$

Assumed: 73.6 % of traffic is composed of LDPV-A

Emissions of CO from the 4001 segment =  $1.01 \text{ km} * 2,281 \frac{\text{Passes}}{\text{day}} * 10.9 \frac{\text{g(CO)}}{\text{km}} * \frac{\text{hr}}{3,600 \text{ s}} * 73.6\% = 5.13 \frac{\text{g}}{\text{s}}$

NOTE, this emission rate is for the entire length of the road segment i.e. 1.01 km long. The ARSUS model utilizes either point or volume sources to represent the road link. Therefore, the estimated emission rate was then divided by the total number of volume sources assigned to the road link and each fraction of emission rate was assigned to the volume source.

Table 1. A summary of road emissions, traffic count and tailpipe emissions for the morning rush hour estimated for the smaller scale exercise (i.e. roads and highways in the vicinity of the Toronto West monitoring station).

Type of Vehicle:	Highway <sup>(1)</sup>	Roads <sup>(2)</sup>
LDPV-A	64.4	73.6
LDPV-T <sup>(3)</sup>	16.1	18.4
LDCV	7	5
HDCV	12.5	3

<sup>1</sup> Toronto Staff Report, 2007  
<sup>2</sup> Assumed  
<sup>3</sup> Assumed: LDPV-A is 80 % of LDPV-A and T.

					CO			
HWY	Streets from to	Modelling ID	Distance (km)	AADT <sup>(4)</sup>	LDPV-A	LDPV-T	LDCV	HDCV
					G	G	D	D
					EF (g/km)			
					10.9	12.8	0.636	1.49
					1 h average - Emission Rate (g/s)			
400	Jane St to HWY 401	4001	1.2	91900	8.96	2.63	0.06	0.24
	HWY 401 to Finch Ave	4002	4.4	180100	64.38	18.90	0.41	1.71
401	Keele St. to HWY 400	40117	3.1	377000	94.95	27.88	0.60	2.52
	HWY 400 to Weston Rd.	40118	1.5	426400	51.96	15.26	0.33	1.38
	Weston Rd. to Islington Ave.	40119	1.4	403800	45.93	13.48	0.29	1.22
	Islington Ave. to Dixon Rd.	40120	2.5	376700	76.51	22.46	0.49	2.03
Dixon Road	From Kipling Avenue to Islington Avenue	DXRD1	1.01	2281	5.13	1.51	0.02	0.03
	From Islington Avenue to Weston Road	DXRD2	1.1	2257	5.53	1.62	0.02	0.03
	From Weston Road to The Westway	DXRD3	1.04	1963	4.55	1.34	0.02	0.03



					CO			
HWY	Streets from to	Modelling ID	Distance (km)	AADT <sup>(4)</sup>	LDPV-A	LDPV-T	LDCV	HDCV
					G	G	D	D
					EF (g/km)			
					10.9	12.8	0.636	1.49
					1 h average - Emission Rate (g/s)			
Royal York Road	From Weston Road to The Westway	RYRD1	0.79	2038	3.59	1.05	0.01	0.02
Weston Road	From Sheppard Avenue to 401	WSTRD1	2.3	2630	13.48	3.96	0.05	0.08
	From 401 to Royal York Road	WSTRD2	0.81	2707	4.89	1.43	0.02	0.03
	From Royal York Road to Lawrence Avenue	WSTRD3	1.45	1158	3.74	1.10	0.01	0.02
Islington Avenue	From Albion Road to Rexdale Blvd	ISLAVE1	2.68	1854	11.07	3.25	0.04	0.06
	From Rexdale Blvd to 401	ISLAVE2	0.59	2372	3.12	0.92	0.01	0.02
	From 401 to Dixon Rd	ISLAVE3	1.4	2495	7.78	2.29	0.03	0.04
	From Dixon Rd to The Westway	ISLAVE4	0.94	2115	4.43	1.30	0.02	0.02
Albion Road	From Islington Avenue to Weston Road	ALBRD1	3.3	1696	12.47	3.66	0.05	0.07
	From Weston Road to 400	ALBRD2	1.49	2031	6.74	1.98	0.03	0.04
Rexdale Boulevard	From Martin Grove Road to Kipling Avenue	RXBLV1	1.23	1575	4.32	1.27	0.02	0.02
	From Kipling Avenue to Islington Avenue	RXBLV2	0.9	1306	2.62	0.77	0.01	0.01

<sup>4</sup> The traffic count for the highways was extracted from: <http://www.raqs.b.mto.gov.on.ca/techpubs/TrafficVolumes.nsf/tvweb?OpenForm&Seq=1>  
The data are collected and maintained by the province of Ontario and only available as 24 h traffic counts. Traffic count for the municipal roads was provided by the City of Toronto. The data for the municipal roads are available as morning peak hour counts and were utilized to simulate morning rush hour.

Table 2. A summary of road emissions, traffic count and tailpipe emissions for the morning rush hour estimated for the large scale exercise (i.e. highways in the vicinity of the Toronto West monitoring station).

Type of Vehicle:	Highway <sup>(1)</sup>	Roads <sup>(2)</sup>
LDPV-A	74.4	73.6
LDPV-T (3)	18.6	18.4
LDCV	7	5
HDCV	0	3

Assumed: No HDCV during day hours.  
1. Toronto Staff Report, 2007.  
2. Assumed  
3. Assumed: LDPV-A is 80% of LDPV-A and T.

HWY	Streets from to	Modelling ID	Distance (km)	AADT	CO		
					LDPV-A	LDPV-T	LDCV
					Light -duty passenger automobiles	Light-duty passenger trucks (minivans, SUV's, light trucks)	Light-duty commercial vehicles
					EF (g/km)		
					G	G	D
					10.9	12.8	1.49
					24 h average - Emission Rate (g/s)		
400	Jane St to HWY 401	4001	1.2	91900	10.35	3.04	0.13
	HWY 401 to Finch Ave	4002	4.4	180100	74.38	21.84	0.96
	Finch Ave to Steeles Ave	4003	2.1	189200	37.29	10.95	0.48



HWY	Streets from to	Modelling ID	Distance (km)	AADT	CO		
					LDPV-A	LDPV-T	LDCV
					Light -duty passenger automobiles	Light-duty passenger trucks (minivans, SUV's, light trucks)	Light-duty commercial vehicles
					EF (g/km)		
					G	G	D
					10.9	12.8	1.49
					24 h average – Emission Rate (g/s)		
401	Morningside Ave to Neilson Rd	4011	1.5	244800	34.47	10.12	0.44
	Neilson Rd to HWY 48/Markham Rd	4012	1.8	274100	46.31	13.60	0.60
	HWY 48/Markham Rd to McCowan Rd	4013	1.6	274000	41.15	12.08	0.53
	McCowan Rd to Brimley Rd.	4014	0.8	309100	23.21	6.81	0.30
	Brimley Rd. to Kennedy Rd.	4015	1.6	281700	42.31	12.42	0.54
	Kennedy Rd. tp Warden Ave.	4016	1.6	346300	52.01	15.27	0.67
	Warden Ave. to Victoria Park Ave.	4017	1.3	339300	41.40	12.15	0.53
	Victoria Park Ave. to Hwy 404/Don V. PKWY	4018	1.4	330300	43.40	12.74	0.56
	HWY 404/Don V. PKWY to Leslie St.	4019	2	344000	64.58	18.96	0.83
	Leslie St. to Bayview Ave.	40110	1.9	354300	63.18	18.55	0.81

					CO		
HWY	Streets from to	Modelling ID	Distance (km)	AADT	LDPV-A	LDPV-T	LDCV
					Light -duty passenger automobiles	Light-duty passenger trucks (minivans, SUV's, light trucks)	Light-duty commercial vehicles
					EF (g/km)		
					G	G	D
					10.9	12.8	1.49
					24 h average – Emission Rate (g/s)		
401	Bayview Ave. to HWY 11/Yonge St.	40111	2	369400	69.34	20.36	0.89
	HWY 11/Yonge St. to Avenue Rd.	40112	1.7	369600	58.97	17.31	0.76
	Avenue Rd. to Bathurst St.	40113	1.1	364900	37.67	11.06	0.48
	Bathurst St. to Allen Rd.	40114	1.4	360100	47.32	13.89	0.61
	Allen Rd. to Duferin St.	40115	0.8	370300	27.81	8.16	0.36
	Dufferin St. to Keele St.	40116	2	354300	66.51	19.53	0.86
	Keele St. to HWY 400	40117	3.1	377000	109.70	32.20	1.41
	HWY 400 to Weston Rd.	40118	1.5	426400	60.03	17.62	0.77
	Weston Rd. to Islington Ave.	40119	1.4	403800	53.06	15.58	0.68
	Islington Ave. to Dixon Rd.	40120	2.5	376700	88.39	25.95	1.14
	Dixon Rd. to HWY 427	40121	2.4	319400	71.95	21.12	0.93
	HWY 427 to Renforth Dr.	40122	0.8	325600	24.45	7.18	0.31
	404	End of Don Valley PKWY to HWY 401	4041	0.5	261700	12.28	3.61
HWY 401 to Sheppard Ave.		4042	0.9	273900	23.14	6.79	0.30



HWY	Streets from to	Modelling ID	Distance (km)	AADT	CO		
					LDPV-A	LDPV-T	LDCV
					Light -duty passenger automobiles	Light-duty passenger trucks (minivans, SUV's, light trucks)	Light-duty commercial vehicles
					EF (g/km)		
					G	G	D
					10.9	12.8	1.49
					24 h average – Emission Rate (g/s)		
404	Sheppard Ave. to Finch Ave.	4043	2.1	235500	46.42	13.63	0.60
	Finch Ave. to Steels Ave	4044	2.2	221600	45.76	13.43	0.59
427	Evans Ave. to QEW	4271	0.3	52000	1.46	0.43	0.02
	QEW to HWY 5/Dundas St.	4272	1.7	309800	49.43	14.51	0.64
	HWY 5/Dundas St. to Burnhamthorpe Rd.	4273	1.9	326000	58.14	17.07	0.75
	Burnhamthorpe Rd. to Rathburn Rd.	4274	1	335200	31.46	9.24	0.40
	Rathburn Rd to HWY 401	4275	2.6	307000	74.92	21.99	0.96
	HWY 401 to Dixon Rd.	4276	2.5	181700	42.64	12.52	0.55
	Dixon Rd. to HWY 409	4277	1.3	105500	12.87	3.78	0.17
	HWY 409 to Rexdale Blvd.	4278	2.6	130700	31.90	9.36	0.41
	Rexdale Blvd. to Finch Ave.	4279	1.8	110600	18.69	5.49	0.24
Gardiner	Leslie St. to DVP	G1	1.74	44021	7.19	2.11	0.09
	DVP to Cherry St.	G2	1.6	70724	10.62	3.12	0.14
	Cherry St. to Parliament St.	G3	0.45	111838	4.72	1.39	0.06

HWY	Streets from to	Modelling ID	Distance (km)	AADT	CO		
					LDPV-A	LDPV-T	LDCV
					Light -duty passenger automobiles	Light-duty passenger trucks (minivans, SUV's, light trucks)	Light-duty commercial vehicles
					EF (g/km)		
					G	G	D
					10.9	12.8	1.49
					24 h average – Emission Rate (g/s)		
Gardiner	Parliament St. to Sherbourline St.	G4	0.416	116607	4.55	1.34	0.06
	Sherbourline St. to Jarvis St.	G5	0.314	92728	2.73	0.80	0.04
	Jarvis St. to Yonge St.	G6	0.524	84071	4.13	1.21	0.05
	Yonge St. to York St.	G7	0.483	103089	4.67	1.37	0.06
	York St. to Rees St.	G8	0.335	100981	3.18	0.93	0.04
	Rees St. to Spadina Ave.	G9	0.6	150024	8.45	2.48	0.11
	Spadina Ave. to Bathurst St.	G10	0.662	121982	7.58	2.23	0.10
	Bathurst St. to Dufferin St.	G11	2.1	160010	31.54	9.26	0.41
	Dufferin St. to Dunn Ave.	G12	0.429	166565	6.71	1.97	0.09
	Dunn Ave. to Parkside Dr.	G13	1.2	155739	17.54	5.15	0.23
	Parkside Dr. to South Kingsway	G14	1.6	178963	26.88	7.89	0.35
	South Kingsway to Royal York Dr.	G15	2.77	211854	55.08	16.17	0.71
	Royal York Dr. to Kipling Ave.	G16	2.096	218530	42.99	12.62	0.55
	Kipling Ave. to The East Mall	G17	1.55	233521	33.97	9.97	0.44
	The East Mall to The West Mall	G18	1.3	200906	24.51	7.20	0.32



Table 3 is a sample of an input file prepared in EXCEL containing location of each source, emission rate in g/s i.e. CO, and width in m of the source used for initial guess of lateral spread. This sample of input file is for the large scale ARSUS modelling exercise. There are over 1800 emission sources associated with this exercise, for simplicity only first 20 are shown below.

**Table 3. A sample of an input file listing location in UTM for each virtual source, corresponding emission rate of CO in g/s and width in m.**

X (UTM)	Y (UTM)	CO (g/s)	Width (m)
617306.7	4830176	0.94196	27
617270.1	4830166	0.94196	27
617233.6	4830156	0.94196	27
617197.1	4830146	0.94196	27
617160.5	4830136	0.94196	27
617124	4830126	0.94196	27
617087.5	4830115	0.94196	27
617050.9	4830105	0.94196	27
617014.4	4830095	0.94196	27
616977.9	4830085	0.94196	27
616941.3	4830075	0.94196	27
616913.4	4830050	0.94196	27
616888.8	4830019	0.94196	27
616864.2	4829989	0.94196	27
616839.5	4829959	0.94196	27
616814.9	4829929	0.94196	27
616790.3	4829899	0.94196	27
616765.7	4829868	0.94196	27
616741.1	4829838	0.94196	27
616716.5	4829808	0.94196	27

**APPENDIX 3: SUMMARY OF UTM COORDINATES FOR BOTH SOURCES AND RECEPTORS USED IN THE VALIDATION EXERCISE**

Source	Receptor	UTM X	UTM Y
1	1	617306.7	4830176
2	2	617270.1	4830166
3	3	617233.6	4830156
4	4	617197.1	4830146
5	5	617160.5	4830136
6	6	617124	4830126
7	7	617087.5	4830115
8	8	617050.9	4830105
9	9	617014.4	4830095
10	10	616977.9	4830085
11	11	616941.3	4830075
12	12	616913.4	4830050
13	13	616888.8	4830019
14	14	616864.2	4829989
15	15	616839.5	4829959
16	16	616814.9	4829929
17	17	616790.3	4829899
18	18	616765.7	4829868
19	19	616741.1	4829838
20	20	616716.5	4829808



### APPENDIX 3: SUMMARY OF UTM COORDINATES FOR BOTH SOURCES AND RECEPTORS USED IN THE VALIDATION EXERCISE

Table 1 lists coordinates of all sources as they were modelled for Case 1, Case 2 and Case

3. Table 2 lists coordinates of all receptors.

**Table 1. List of sources as modelled in Case 1, Case 2 and Case 3.**

X (UTM)	Y (UTM)	Source
619005	4841732	S1
618995	4841732	S2
618985	4841732	S3
618975	4841732	S4
618965	4841732	S5
618955	4841732	S6
619015	4841732	S7
619025	4841732	S8
619035	4841732	S9
619045	4841732	S10
619055	4841732	S11
619005	4841712	S12
618995	4841712	S13
618985	4841712	S14
618975	4841712	S15
618965	4841712	S16
618955	4841712	S17
619015	4841712	S18
619025	4841712	S19
619035	4841712	S20
619045	4841712	S21
619055	4841712	S22
619005	4841722	S23
618995	4841722	S24
618985	4841722	S25
618975	4841722	S26
618965	4841722	S27
618955	4841722	S28

X (UTM)	Y (UTM)	Source
619014.59	4841721.95	S29
619024.59	4841721.95	S30
619034.59	4841721.95	S31
619044.59	4841721.95	S32
619054.59	4841721.95	S33
619004.59	4841741.95	S34
619004.59	4841751.95	S35
619004.59	4841761.95	S36
619004.59	4841771.95	S37
619004.59	4841781.95	S38
619004.59	4841791.95	S39
619004.59	4841701.95	S40
619004.59	4841691.95	S41
619004.59	4841681.95	S42
619004.59	4841671.95	S43
619004.59	4841661.95	S44
619014.59	4841741.95	S45
619014.59	4841751.95	S46
619014.59	4841761.95	S47
619014.59	4841771.95	S48
619014.59	4841781.95	S49
619014.59	4841791.95	S50
619014.59	4841701.95	S51
619014.59	4841691.95	S52
619014.59	4841681.95	S53
619014.59	4841671.95	S54
619014.59	4841661.95	S55
618754.594	4841481.949	*
619254.594	4841981.949	*

\* For the purpose of the ARSUS model two points were used to determine lower and upper boundaries of the modelling domain. No emissions were set from these two points.



**Table 2. List of coordinates of the receptors at which the concentrations were modelled.**

X(UTM)	Y(UTM)	Receptor
619004.59	4841858	R1
619004.59	4841872	R2
619004.59	4841886	R3
619004.59	4841900	R4
618948.59	4841914	R5
618962.59	4841914	R6
618976.59	4841914	R7
618990.59	4841914	R8
619004.59	4841914	R9
619018.59	4841914	R10
619032.59	4841914	R11
619046.59	4841914	R12
619060.59	4841914	R13
619004.59	4841928	R14
619004.59	4841942	R15
619004.59	4841956	R16
619004.59	4841970	R17
619004.59	4841984	R18

#### APPENDIX 4: SAMPLE OF THE ISC3 INPUT FILE FOR VALIDATION OF POINT SOURCE ALGORITHM EXERCISE



## APPENDIX 4: SAMPLE OF THE ISC3 INPUT FILE FOR VALIDATION OF POINT SOURCE ALGORITHM EXERCISE

Note, following is an input file which was created according to the US EPA, ISC3 (version 02035) air dispersion model guideline. The input file is set to model a single point source emitting at 1 g/s. The ISC3 estimates maximum ground level concentration to be evaluated at set receptors. To run this model place the input file, meteorological file and ISC3 executable file in single folder and run from DOS.

### Sample of the ISC3 input file for one point source:

```
CO STARTING
  MODELOPT DFAULT CONC NOCMPL URBAN
  AVERTIME 1 PERIOD
  POLLUTID TSP
  TERRHGTS FLAT
  RUNORNOT RUN
CO FINISHED
**
*****
** ISCST3 Source Pathway
*****
**
**
SO STARTING
** Source Location **
** Source ID - Type - X Coord. - Y Coord. **
  LOCATION STCK1 POINT 619004.594 4841731.949
** Source Parameters **
  SRCPARAM STCK1 1 3.000 294.000 1.00000 2.000
  SRCGROUP ALL
SO FINISHED
**
*****
** ISCST3 Receptor Pathway
*****
**
**
RE STARTING
** DESCRREC "" ""
  DISCCART 619004.59 4841857.95
  DISCCART 619004.59 4841871.95
  DISCCART 619004.59 4841885.95
  DISCCART 619004.59 4841899.95
  DISCCART 618948.59 4841913.95
  DISCCART 618962.59 4841913.95
```

```
DISCCART 618976.59 4841913.95
DISCCART 618990.59 4841913.95
DISCCART 619004.59 4841913.95
DISCCART 619018.59 4841913.95
DISCCART 619032.59 4841913.95
DISCCART 619046.59 4841913.95
DISCCART 619060.59 4841913.95
DISCCART 619004.59 4841927.95
DISCCART 619004.59 4841941.95
DISCCART 619004.59 4841955.95
DISCCART 619004.59 4841969.95
DISCCART 619004.59 4841983.95
** BEGIN OF NESTED GRID RECEPTORS
** END OF NESTED GRID RECEPTORS
RE FINISHED
**
*****
** ISCST3 Meteorology Pathway
*****
**
**
ME STARTING
  INPUTFIL To_ISC.met
  ANEMHGHT 10 METERS
  SURFDATA 58733 2007
  UAIRDATA 72528 2007
  STARTEND 2007 1 1 6 2007 1 1 6
ME FINISHED
**
*****
** ISCST3 Output Pathway
*****
**
**
OU STARTING
  PLOTFILE 1 ALL 1ST TEST.IS\16am.PLT
OU FINISHED
```



## APPENDIX 5: SAMPLE OF THE ISC3 INPUT FILE FOR VALIDATION OF VOLUME SOURCE ALGORITHM EXERCISE

## APPENDIX 5: SAMPLE OF THE ISC3 INPUT FILE FOR VALIDATION OF VOLUME SOURCE ALGORITHM EXERCISE

Following are copies of the US EPA, ISC3 input files used to validate volume sources. An exercise completed for 3 cases.

- A) Case 1: US EPA, ISC3 input file for validation of 1 volume source;
- B) Case 2: US EPA, ISC3 input file for validation of more than 10 identical, volume sources; and
- C) Case 3: US EPA, ISC3 input file for validation of more than 50 identical, volume sources.

The entire summary of the input/compilation/output file for Case 1 only has been included. This format is automatically generated by ISC3 summarizing compilation of the input file, analysis, modelling results as well as errors/warning messages.

The input files were setup using a modelling interface and version 02035 of ISC3. The meteorological data was set for wind blowing towards North ( $0^0$ ), at 3 m/s, stability class C and ambient temperature of 294 K. The model was set to calculate 1 h maximum ground level concentrations at specified receptors.

Since, validation of the ARSUS model's performance of point source algorithm showed response of the model to wind direction changes; this exercise was not repeated again.



A) Case 1: US EPA, ISC3 input file for validation of 1 volume source.

```
**
*****
**
** ISCST3 Input Produced by:
** ISC-AERMOD View Ver. 5.7.0
** Lakes Environmental Software Inc.
** Date: 3/12/2009
** File: C:\Lakes\ISC-AERMODView\SCHOOL\Validation March 8 2009 - volume source\Case 1 - 1 volume
source\1vol.INP
**
*****
**
**
*****
** ISCST3 Control Pathway
*****
**
**
CO STARTING
  TITLEONE C:\Lakes\ISC-AERMODView\SCHOOL\Validation March 8 2009 - volume sour
  MODELOPT DFAULT CONC NOCMPL  URBAN
  AVERTIME 1 PERIOD
  POLLUTID TSP
  TERRHGTS FLAT
  RUNORNOT RUN
CO FINISHED
**
*****
** ISCST3 Source Pathway
*****
**
**
SO STARTING
** Source Location **
```

```
** Source ID - Type - X Coord. - Y Coord. **
  LOCATION STCK1 VOLUME 619004.594 4841731.949
** Source Parameters **
  SRCPARAM STCK1 1 3.000 4.650 1.395
  SRCGROUP ALL
SO FINISHED
**
*****
** ISCST3 Receptor Pathway
*****
**
**
RE STARTING
** DESCRREC "" ""
  DISCCART 619004.59 4841857.95
  DISCCART 619004.59 4841871.95
  DISCCART 619004.59 4841885.95
  DISCCART 619004.59 4841899.95
  DISCCART 618948.59 4841913.95
  DISCCART 618962.59 4841913.95
  DISCCART 618976.59 4841913.95
  DISCCART 618990.59 4841913.95
  DISCCART 619004.59 4841913.95
  DISCCART 619018.59 4841913.95
  DISCCART 619032.59 4841913.95
  DISCCART 619046.59 4841913.95
  DISCCART 619060.59 4841913.95
  DISCCART 619004.59 4841927.95
  DISCCART 619004.59 4841941.95
  DISCCART 619004.59 4841955.95
  DISCCART 619004.59 4841969.95
  DISCCART 619004.59 4841983.95
** BEGIN OF NESTED GRID RECEPTORS
** END OF NESTED GRID RECEPTORS
RE FINISHED
**
*****
** ISCST3 Meteorology Pathway
```



```

*****
**
**
ME STARTING
  INPUTFIL Valid.met
  ANEMHGHT 10 METERS
  SURFDATA 58733 2007
  UAIRDATA 72528 2007
  STARTEND 2007 1 1 1 2007 1 1 1
ME FINISHED
**
*****
** ISCST3 Output Pathway
*****
**
**
OU STARTING
  RECTABLE 1 1ST
  PLOTFILE 1 ALL 1ST 1VOL.IS\1src.PLT
OU FINISHED

*****
*** SETUP Finishes Successfully ***
*****
*** ISCST3 - VERSION 02035 ***      *** C:\Lakes\ISC-AERMODView\SCHOOL\Validation March 8 2009 - volume sour
***      03/12/09                  ***

***      21:37:28
**MODELOPTs:
PAGE      1
CONC              URBAN FLAT          DFAULT
NOCMPL

***      MODEL SETUP OPTIONS SUMMARY      ***
-----
**Simple Terrain Model is Selected

**Model Is Setup For Calculation of Average CONCentration Values.

```

134

```

-- SCAVENGING/DEPOSITION LOGIC --
**Model Uses NO DRY DEPLETION.  DDPLETE = F
**Model Uses NO WET DEPLETION.  WDPLETE = F
**NO WET SCAVENGING Data Provided.
**NO GAS DRY DEPOSITION Data Provided.
**Model Does NOT Use GRIDDED TERRAIN Data for Depletion Calculations

**Model Uses URBAN Dispersion.

**Model Uses Regulatory DEFAULT Options:
  1. Final Plume Rise.
  2. Stack-tip Downwash.
  3. Buoyancy-induced Dispersion.
  4. Use Calms Processing Routine.
  5. Not Use Missing Data Processing Routine.
  6. Default Wind Profile Exponents.
  7. Default Vertical Potential Temperature Gradients.
  8. "Upper Bound" Values for Supersquat Buildings.
  9. No Exponential Decay for URBAN/Non-SO2

**Model Assumes Receptors on FLAT Terrain.

**Model Assumes No FLAGPOLE Receptor Heights.

**Model Calculates 1 Short Term Average(s) of: 1-HR
  and Calculates PERIOD Averages

**This Run Includes:      1 Source(s);      1 Source Group(s); and      18 Receptor(s)

**The Model Assumes A Pollutant Type of: TSP

**Model Set To Continue RUNning After the Setup Testing.

**Output Options Selected:
  Model Outputs Tables of PERIOD Averages by Receptor
  Model Outputs Tables of Highest Short Term Values by Receptor (RECTABLE Keyword)
  Model Outputs External File(s) of High Values for Plotting (PLOTFILE Keyword)

```

135



137







\*\*\* ISCST3 - VERSION 02035 \*\*\* \*\*\* C:\Lakes\ISC-AERMODView\SCHOOL\Validation March 8 2009 - volume sour  
\*\*\* 03/12/09 \*\*\*  
\*\*\* 21:37:28 \*\*\*  
\*\*MODELOPTs:  
PAGE 7  
CONC URBAN FLAT DFAULT  
NOCMPL

\*\*\* THE PERIOD ( 1 HRS) AVERAGE CONCENTRATION VALUES FOR SOURCE GROUP: ALL \*\*\*  
INCLUDING SOURCE(S): STCK1 ,  
\*\*\* DISCRETE CARTESIAN RECEPTOR POINTS \*\*\*  
\*\* CONC OF TSP IN MICROGRAMS/M\*\*3 \*\*  
X-COORD (M) Y-COORD (M) CONC X-COORD (M) Y-COORD (M) CONC  
619004.56 4841858.00 125.94573 619004.56 4841872.00 104.44946  
619004.56 4841886.00 88.05287 619004.56 4841900.00 75.26046  
618948.56 4841914.00 27.81735 618962.56 4841914.00 40.33458  
618976.56 4841914.00 52.60110 618990.56 4841914.00 61.69747  
619004.56 4841914.00 65.08716 619018.56 4841914.00 61.75592  
619032.56 4841914.00 52.70080 619046.56 4841914.00 40.44932  
619060.56 4841914.00 27.92290 619004.56 4841928.00 56.86283  
619004.56 4841942.00 50.11879 619004.56 4841956.00 44.51924  
619004.56 4841970.00 39.81853 619004.56 4841984.00 35.83359

\*\*\* ISCST3 - VERSION 02035 \*\*\* \*\*\* C:\Lakes\ISC-AERMODView\SCHOOL\Validation March 8 2009 - volume sour  
\*\*\* 03/12/09 \*\*\*  
\*\*\* 21:37:28 \*\*\*  
\*\*MODELOPTs:  
PAGE 8  
CONC URBAN FLAT DFAULT  
NOCMPL

\*\*\* THE 1ST HIGHEST 1-HR AVERAGE CONCENTRATION VALUES FOR SOURCE GROUP: ALL \*\*\*  
INCLUDING SOURCE(S): STCK1 ,  
\*\*\* DISCRETE CARTESIAN RECEPTOR POINTS \*\*\*  
\*\* CONC OF TSP IN MICROGRAMS/M\*\*3 \*\*  
X-COORD (M) Y-COORD (M) CONC (YYMMDDHH) X-COORD (M) Y-COORD (M) CONC (YYMMDDHH)  
619004.56 4841858.00 125.94573 (07010101) 619004.56 4841872.00 104.44946 (07010101)  
619004.56 4841886.00 88.05287 (07010101) 619004.56 4841900.00 75.26046 (07010101)  
618948.56 4841914.00 27.81735 (07010101) 618962.56 4841914.00 40.33458 (07010101)

140

618976.56 4841914.00 52.60110 (07010101) 618990.56 4841914.00 61.69747 (07010101)  
619004.56 4841914.00 65.08716 (07010101) 619018.56 4841914.00 61.75592 (07010101)  
619032.56 4841914.00 52.70080 (07010101) 619046.56 4841914.00 40.44932 (07010101)  
619060.56 4841914.00 27.92290 (07010101) 619004.56 4841928.00 56.86283 (07010101)  
619004.56 4841942.00 50.11879 (07010101) 619004.56 4841956.00 44.51924 (07010101)  
619004.56 4841970.00 39.81853 (07010101) 619004.56 4841984.00 35.83359 (07010101)  
\*\*\* ISCST3 - VERSION 02035 \*\*\* \*\*\* C:\Lakes\ISC-AERMODView\SCHOOL\Validation March 8 2009 - volume sour  
\*\*\* 03/12/09 \*\*\*  
\*\*\* 21:37:28 \*\*\*  
\*\*MODELOPTs:  
PAGE 9  
CONC URBAN FLAT DFAULT  
NOCMPL

\*\*\* THE SUMMARY OF MAXIMUM PERIOD ( 1 HRS) RESULTS \*\*\*  
\*\* CONC OF TSP IN MICROGRAMS/M\*\*3 \*\*  
NETWORK  
GROUP ID AVERAGE CONC RECEPTOR (XR, YR, ZELEV, ZFLAG) OF TYPE GRID-  
ID  
ALL 1ST HIGHEST VALUE IS 125.94573 AT ( 619004.56, 4841858.00, 0.00, 0.00) DC NA  
2ND HIGHEST VALUE IS 104.44946 AT ( 619004.56, 4841872.00, 0.00, 0.00) DC NA  
3RD HIGHEST VALUE IS 88.05287 AT ( 619004.56, 4841886.00, 0.00, 0.00) DC NA  
4TH HIGHEST VALUE IS 75.26046 AT ( 619004.56, 4841900.00, 0.00, 0.00) DC NA  
5TH HIGHEST VALUE IS 65.08716 AT ( 619004.56, 4841914.00, 0.00, 0.00) DC NA  
6TH HIGHEST VALUE IS 61.75592 AT ( 619018.56, 4841914.00, 0.00, 0.00) DC NA  
7TH HIGHEST VALUE IS 61.69747 AT ( 618990.56, 4841914.00, 0.00, 0.00) DC NA  
8TH HIGHEST VALUE IS 56.86283 AT ( 619004.56, 4841928.00, 0.00, 0.00) DC NA  
9TH HIGHEST VALUE IS 52.70080 AT ( 619032.56, 4841914.00, 0.00, 0.00) DC NA  
10TH HIGHEST VALUE IS 52.60110 AT ( 618976.56, 4841914.00, 0.00, 0.00) DC NA  
\*\*\* RECEPTOR TYPES: GC = GRIDCART  
GP = GRIDPOLR  
DC = DISCCART  
DP = DISCPOLR  
BD = BOUNDARY

\*\*\* ISCST3 - VERSION 02035 \*\*\* \*\*\* C:\Lakes\ISC-AERMODView\SCHOOL\Validation March 8 2009 - volume sour  
\*\*\* 03/12/09 \*\*\*  
\*\*\* 21:37:28 \*\*\*



\*\*MODELOPTs:

PAGE 10

CONC

NOCMPL

URBAN FLAT      DEFAULT

\*\*\* THE SUMMARY OF HIGHEST 1-HR RESULTS \*\*\*  
\*\* CONC OF TSP      IN MICROGRAMS/M\*\*3

\*\*

NETWORK

DATE

GROUP ID      GRID-ID  
OF TYPE      AVERAGE CONC      (YYMMDDHH)

RECEPTOR      (XR, YR, ZELEV, ZFLAG)

ALL HIGH 1ST HIGH VALUE IS 125.94573 ON 07010101: AT ( 619004.56, 4841858.00, 0.00, 0.00) DC      NA

\*\*\* RECEPTOR TYPES:

GC = GRIDCART

GP = GRIDPOLR

DC = DISCCART

DP = DISCPOLR

BD = BOUNDARY

\*\*\*

\*\*\* ISCST3 - VERSION 02035 \*\*\*      \*\*\* C:\Lakes\ISC-AERMODView\SCHOOL\Validation March 8 2009 - volume sour

03/12/09

\*\*\*

21:37:28

\*\*MODELOPTs:

PAGE 11

CONC

NOCMPL

URBAN FLAT      DEFAULT

\*\*\* Message Summary : ISCST3 Model Execution \*\*\*

----- Summary of Total Messages -----

A Total of

A Total of

A Total of

0 Fatal Error Message(s)

0 Warning Message(s)

0 Informational Message(s)

\*\*\*\*\* FATAL ERROR MESSAGES \*\*\*\*\*

\*\*\* NONE \*\*\*

\*\*\*\*\* WARNING MESSAGES \*\*\*\*\*

\*\*\* NONE \*\*\*

\*\*\*\*\* ISCST3 Finishes Successfully \*\*\*\*\*

\*\*\*\*\*

## B) Case 2: US EPA, ISC3 input file for validation of over 10 identical volume sources.

\*\*

\*\*\*\*\*

\*\*

\*\* ISCST3 Input Produced by:

\*\* ISC-AERMOD View Ver. 5.7.0

\*\* Lakes Environmental Software Inc.

\*\* Date: 3/14/2009

\*\* File: C:\Lakes\ISC-AERMODView\SCHOOL\Validation March 8 2009 - volume  
source\Case 2 - over 10 volume sources\l0src.INP

\*\*

\*\*\*\*\*

\*\*

\*\*

\*\*\*\*\*

\*\* ISCST3 Control Pathway

\*\*\*\*\*

\*\*

\*\*

CO STARTING

TITLEONE C:\Lakes\ISC-AERMODView\SCHOOL\Validation March 8 2009 - volume  
sour

MODELOPT DFAULT CONC NOCMPL URBAN

AVERTIME 1 PERIOD

POLLUTID TSP

TERRHGTS FLAT

RUNORNOT RUN

CO FINISHED

\*\*

\*\*\*\*\*

\*\* ISCST3 Source Pathway

\*\*\*\*\*

\*\*

\*\*

SO STARTING

\*\* Source Location \*\*

\*\* Source ID - Type - X Coord. - Y Coord. \*\*

LOCATION STCK1 VOLUME 619004.594 4841731.949

LOCATION VOL1 VOLUME 618994.590 4841731.949

LOCATION VOL2 VOLUME 618984.590 4841731.949

LOCATION VOL3 VOLUME 618974.590 4841731.949

LOCATION VOL4 VOLUME 618964.590 4841731.949

LOCATION VOL5 VOLUME 618954.590 4841731.949

LOCATION VOL6 VOLUME 619014.590 4841731.949

LOCATION VOL7 VOLUME 619024.590 4841731.949

LOCATION VOL8 VOLUME 619034.590 4841731.949

LOCATION VOL9 VOLUME 619044.590 4841731.949

LOCATION VOL10 VOLUME 619054.590 4841731.949

\*\* Source Parameters \*\*

SRCPARAM STCK1 1 3.000 4.650 1.395

SRCPARAM VOL1 1 3.000 4.650 1.395

SRCPARAM VOL2 1 3.000 4.650 1.395

SRCPARAM VOL3 1 3.000 4.650 1.395

SRCPARAM VOL4 1 3.000 4.650 1.395



```
SRCPARAM VOL5 1 3.000 4.650 1.395
SRCPARAM VOL6 1 3.000 4.650 1.395
SRCPARAM VOL7 1 3.000 4.650 1.395
SRCPARAM VOL8 1 3.000 4.650 1.395
SRCPARAM VOL9 1 3.000 4.650 1.395
SRCPARAM VOL10 1 3.000 4.650 1.395
SRCGROUP ALL
```

SO FINISHED

\*\*

\*\*\*\*\*

\*\* ISCST3 Receptor Pathway

\*\*\*\*\*

\*\*

\*\*

RE STARTING

\*\* DESCRREC "" ""

DISCCART	619004.59	4841857.95
DISCCART	619004.59	4841871.95
DISCCART	619004.59	4841885.95
DISCCART	619004.59	4841899.95
DISCCART	618948.59	4841913.95
DISCCART	618962.59	4841913.95
DISCCART	618976.59	4841913.95
DISCCART	618990.59	4841913.95
DISCCART	619004.59	4841913.95
DISCCART	619018.59	4841913.95
DISCCART	619032.59	4841913.95
DISCCART	619046.59	4841913.95
DISCCART	619060.59	4841913.95
DISCCART	619004.59	4841927.95
DISCCART	619004.59	4841941.95
DISCCART	619004.59	4841955.95
DISCCART	619004.59	4841969.95
DISCCART	619004.59	4841983.95

\*\* BEGIN OF NESTED GRID RECEPTORS

\*\* END OF NESTED GRID RECEPTORS

RE FINISHED

\*\*

\*\*\*\*\*

\*\* ISCST3 Meteorology Pathway

\*\*\*\*\*

\*\*

\*\*

ME STARTING

INPUTFIL Valid.met

ANEMHGHT 10 METERS

SURFDATA 58733 2007

UAIRDATA 72528 2007

STARTEND 2007 1 1 1 2007 1 1 1

ME FINISHED

\*\*

\*\*\*\*\*

\*\* ISCST3 Output Pathway

\*\*\*\*\*

\*\*

\*\*

OU STARTING

RECTABLE 1 1ST

PLOTFILE 1 ALL 1ST 10SRC.IS\10src.PLT

OU FINISHED

\*\*\*\*\*

\*\*\* SETUP Finishes Successfully \*\*\*

\*\*\*\*\*



**C) Case 3: US EPA, ISC3 input file for validation of over 50 identical volume source.**

```

**
*****
**
** ISCST3 Input Produced by:
** ISC-AERMOD View Ver. 5.7.0
** Lakes Environmental Software Inc.
** Date: 3/14/2009
** File: C:\Lakes\ISC-AERMODView\SCHOOL\Validation March 8 2009 - volume
source\Case 3 - over 50 volume sources\50vol.INP
**
*****
**
**
*****
** ISCST3 Control Pathway
*****
**
**
CO STARTING
  TITLEONE C:\Lakes\ISC-AERMODView\SCHOOL\Validation March 8 2009 - volume
sour
  MODELOPT DFAULT CONC NOCMPL URBAN
  AVERTIME 1 PERIOD
  POLLUTID TSP
  TERRHGTS FLAT
  RUNORNOT RUN
CO FINISHED
**
*****
** ISCST3 Source Pathway
*****
**
**
SO STARTING
** Source Location **
** Source ID - Type - X Coord. - Y Coord. **
LOCATION 1 VOLUME 619004.590 4841731.950
LOCATION 2 VOLUME 618994.590 4841731.950
LOCATION 3 VOLUME 618984.590 4841731.950
LOCATION 4 VOLUME 618974.590 4841731.950
LOCATION 5 VOLUME 618964.590 4841731.950
LOCATION 6 VOLUME 618954.590 4841731.950
LOCATION 7 VOLUME 619014.590 4841731.950
LOCATION 8 VOLUME 619024.590 4841731.950
LOCATION 9 VOLUME 619034.590 4841731.950
LOCATION 10 VOLUME 619044.590 4841731.950
LOCATION 11 VOLUME 619054.590 4841731.950
LOCATION 12 VOLUME 619004.594 4841711.950
LOCATION 13 VOLUME 618994.590 4841711.950
LOCATION 14 VOLUME 618984.590 4841711.950
LOCATION 15 VOLUME 618974.590 4841711.950
LOCATION 16 VOLUME 618964.590 4841711.950
LOCATION 17 VOLUME 618954.590 4841711.950

```

```

LOCATION 18 VOLUME 619014.590 4841711.950
LOCATION 19 VOLUME 619024.590 4841711.950
LOCATION 20 VOLUME 619034.590 4841711.950
LOCATION 21 VOLUME 619044.590 4841711.950
LOCATION 22 VOLUME 619054.590 4841711.950
LOCATION 23 VOLUME 619004.594 4841721.950
LOCATION 24 VOLUME 618994.590 4841721.950
LOCATION 25 VOLUME 618984.590 4841721.950
LOCATION 26 VOLUME 618974.590 4841721.950
LOCATION 27 VOLUME 618964.590 4841721.950
LOCATION 28 VOLUME 618954.590 4841721.950
LOCATION 29 VOLUME 619014.590 4841721.950
LOCATION 30 VOLUME 619024.590 4841721.950
LOCATION 31 VOLUME 619034.590 4841721.950
LOCATION 32 VOLUME 619044.590 4841721.950
LOCATION 33 VOLUME 619054.590 4841721.950
LOCATION 34 VOLUME 619004.590 4841741.950
LOCATION 35 VOLUME 619004.590 4841751.950
LOCATION 36 VOLUME 619004.590 4841761.950
LOCATION 37 VOLUME 619004.590 4841771.950
LOCATION 38 VOLUME 619004.590 4841781.950
LOCATION 39 VOLUME 619004.590 4841791.950
LOCATION 40 VOLUME 619004.590 4841701.950
LOCATION 41 VOLUME 619004.590 4841691.950
LOCATION 42 VOLUME 619004.590 4841681.950
LOCATION 43 VOLUME 619004.590 4841671.950
LOCATION 44 VOLUME 619004.590 4841661.950
LOCATION 45 VOLUME 619014.590 4841741.950
LOCATION 46 VOLUME 619014.590 4841751.950
LOCATION 47 VOLUME 619014.590 4841761.950
LOCATION 48 VOLUME 619014.590 4841771.950
LOCATION 49 VOLUME 619014.590 4841781.950
LOCATION 50 VOLUME 619014.590 4841791.950
LOCATION 51 VOLUME 619014.590 4841701.950
LOCATION 52 VOLUME 619014.590 4841691.950
LOCATION 53 VOLUME 619014.590 4841681.950
LOCATION 54 VOLUME 619014.590 4841671.950
LOCATION 55 VOLUME 619014.590 4841661.950
** Source Parameters **
SRCPARAM 1 1 3.000 4.650 1.400
SRCPARAM 2 1 3.000 4.650 1.400
SRCPARAM 3 1 3.000 4.650 1.400
SRCPARAM 4 1 3.000 4.650 1.400
SRCPARAM 5 1 3.000 4.650 1.400
SRCPARAM 6 1 3.000 4.650 1.400
SRCPARAM 7 1 3.000 4.650 1.400
SRCPARAM 8 1 3.000 4.650 1.400
SRCPARAM 9 1 3.000 4.650 1.400
SRCPARAM 10 1 3.000 4.650 1.400
SRCPARAM 11 1 3.000 4.650 1.400
SRCPARAM 12 1 3.000 4.650 1.400
SRCPARAM 13 1 3.000 4.650 1.400
SRCPARAM 14 1 3.000 4.650 1.400
SRCPARAM 15 1 3.000 4.650 1.400
SRCPARAM 16 1 3.000 4.650 1.400
SRCPARAM 17 1 3.000 4.650 1.400
SRCPARAM 18 1 3.000 4.650 1.400

```



```

SRCPARAM 19 1 3.000 4.650 1.400
SRCPARAM 20 1 3.000 4.650 1.400
SRCPARAM 21 1 3.000 4.650 1.400
SRCPARAM 22 1 3.000 4.650 1.400
SRCPARAM 23 1 3.000 4.650 1.400
SRCPARAM 24 1 3.000 4.650 1.400
SRCPARAM 25 1 3.000 4.650 1.400
SRCPARAM 26 1 3.000 4.650 1.400
SRCPARAM 27 1 3.000 4.650 1.400
SRCPARAM 28 1 3.000 4.650 1.400
SRCPARAM 29 1 3.000 4.650 1.400
SRCPARAM 30 1 3.000 4.650 1.400
SRCPARAM 31 1 3.000 4.650 1.400
SRCPARAM 32 1 3.000 4.650 1.400
SRCPARAM 33 1 3.000 4.650 1.400
SRCPARAM 34 1 3.000 4.650 1.400
SRCPARAM 35 1 3.000 4.650 1.400
SRCPARAM 36 1 3.000 4.650 1.400
SRCPARAM 37 1 3.000 4.650 1.400
SRCPARAM 38 1 3.000 4.650 1.400
SRCPARAM 39 1 3.000 4.650 1.400
SRCPARAM 40 1 3.000 4.650 1.400
SRCPARAM 41 1 3.000 4.650 1.400
SRCPARAM 42 1 3.000 4.650 1.400
SRCPARAM 43 1 3.000 4.650 1.400
SRCPARAM 44 1 3.000 4.650 1.400
SRCPARAM 45 1 3.000 4.650 1.400
SRCPARAM 46 1 3.000 4.650 1.400
SRCPARAM 47 1 3.000 4.650 1.400
SRCPARAM 48 1 3.000 4.650 1.400
SRCPARAM 49 1 3.000 4.650 1.400
SRCPARAM 50 1 3.000 4.650 1.400
SRCPARAM 51 1 3.000 4.650 1.400
SRCPARAM 52 1 3.000 4.650 1.400
SRCPARAM 53 1 3.000 4.650 1.400
SRCPARAM 54 1 3.000 4.650 1.400
SRCPARAM 55 1 3.000 4.650 1.400
SRCGROUP ALL
SO FINISHED
**
*****
** ISCST3 Receptor Pathway
*****
**
**
RE STARTING
** DESCRREC "" ""
DISCCART 619004.59 4841857.95
DISCCART 619004.59 4841871.95
DISCCART 619004.59 4841885.95
DISCCART 619004.59 4841899.95
DISCCART 618948.59 4841913.95
DISCCART 618962.59 4841913.95
DISCCART 618976.59 4841913.95
DISCCART 618990.59 4841913.95
DISCCART 619004.59 4841913.95
DISCCART 619018.59 4841913.95

```

```

DISCCART 619032.59 4841913.95
DISCCART 619046.59 4841913.95
DISCCART 619060.59 4841913.95
DISCCART 619004.59 4841927.95
DISCCART 619004.59 4841941.95
DISCCART 619004.59 4841955.95
DISCCART 619004.59 4841969.95
DISCCART 619004.59 4841983.95
** BEGIN OF NESTED GRID RECEPTORS
** END OF NESTED GRID RECEPTORS
RE FINISHED
**
*****
** ISCST3 Meteorology Pathway
*****
**
**
ME STARTING
INPUTFIL Valid.met
ANEMHGHT 10 METERS
SURFDATA 58733 2007
UAIRDATA 72528 2007
STARTEND 2007 1 1 1 2007 1 1 1
ME FINISHED
**
*****
** ISCST3 Output Pathway
*****
**
**
OU STARTING
RECTABLE 1 1ST
PLOTFILE 1 ALL 1ST 50VOL.IS\55src.PLT
OU FINISHED

*****
*** SETUP Finishes Successfully ***
*****

```



APPENDIX 6: TABULATED DATA FROM THE  
VALIDATION EXERCISES OF POINT AND VOLUME SOURCE  
ALGORITHHEMS

APPENDIX 6: TABULATED DATA FROM THE VALIDATION  
EXERCISES OF POINT AND VOLUME  
SOURCE ALGORITHHEMS

Tables 1-3 are summaries of Cases 1-3, respectively, for the validation exercise of point source algorithm. Tables 4 -6 are summaries of Case 1-3, respectively, for the validation exercises of volume source algorithm. All emission sources were set to be identical and emitting at 1 g/s, unit emission rate (UER).

Table 1. Case 1, validation of the point source algorithm, ISC3 versus ARSUS model  
estimated concentrations at given receptors.

		Case 1	
		1 Source at UER (g/s)	
X	Y	ISC3 (µg/m³)	ARSUS (µg/m³)
619004.6	4841858	155.14	154.58
619004.6	4841872	126.08	125.71
619004.6	4841886	104.52	104.27
619004.6	4841900	88.09	87.91
618948.6	4841914	26.30	26.32
618962.6	4841914	41.65	41.65
618976.6	4841914	57.84	57.81
618990.6	4841914	70.46	70.38
619004.6	4841914	75.28	75.15
619018.6	4841914	70.54	70.38
619032.6	4841914	57.98	57.81
619046.6	4841914	41.80	41.64
619060.6	4841914	26.43	26.31
619004.6	4841928	65.09	65.00
619004.6	4841942	56.86	56.79
619004.6	4841956	50.11	50.05
619004.6	4841970	44.51	44.46
619004.6	4841984	39.80	39.77



**Table 2. Case 2, validation of the point source algorithm, ISC3 versus ARSUS model estimated concentrations at given receptors.**

Case 2			
10 Sources each at UER (g/s)			
X	Y	ISC3 ( $\mu\text{g}/\text{m}^3$ )	ARSUS ( $\mu\text{g}/\text{m}^3$ )
619004.563	4841858	1009.11	1005.16
619004.563	4841872	885.62	882.82
619004.563	4841886	781.44	779.39
619004.563	4841900	692.96	691.44
618948.563	4841914	355.64	355.14
618962.563	4841914	456.64	455.95
618976.563	4841914	541.60	540.71
618990.563	4841914	597.82	596.77
619004.563	4841914	617.45	616.30
619018.563	4841914	597.90	596.74
619032.563	4841914	541.75	540.66
619046.563	4841914	456.82	455.89
619060.563	4841914	355.82	355.08
619004.563	4841928	552.73	551.85
619004.563	4841942	497.03	496.34
619004.563	4841956	448.86	448.32
619004.563	4841970	407.04	406.60
619004.563	4841984	370.56	370.21

**Table 3. Case 3, validation of the point source algorithm, ISC3 versus ARSUS model estimated concentrations at given receptors.**

Case 3			
55 Sources each at UER (g/s)			
X	Y	ISC3 ( $\mu\text{g}/\text{m}^3$ )	ARSUS ( $\mu\text{g}/\text{m}^3$ )
619004.563	4841858	7211.02	7167.46
619004.563	4841872	5858.85	5833.84
619004.563	4841886	4883.01	4867.34
619004.563	4841900	4147.78	4137.34
618948.563	4841914	1434.45	1432.29
618962.563	4841914	2021.60	2018.27
618976.563	4841914	2676.09	2671.26
618990.563	4841914	3261.18	3254.86
619004.563	4841914	3575.68	3568.40
619018.563	4841914	3476.15	3468.85
619032.563	4841914	2995.54	2989.19

Case 3			
55 Sources each at UER (g/s)			
X	Y	ISC3 ( $\mu\text{g}/\text{m}^3$ )	ARSUS ( $\mu\text{g}/\text{m}^3$ )
619046.563	4841914	2319.35	2314.48
619060.563	4841914	1647.30	1643.91
619004.563	4841928	3119.37	3114.10
619004.563	4841942	2748.22	2744.30
619004.563	4841956	2441.52	2438.53
619004.563	4841970	2184.71	2182.39
619004.563	4841984	1967.27	1965.44

**Table 4. Case 1, validation of the volume source algorithm, ISC3 versus ARSUS model estimated concentrations at given receptors.**

Case 1			
1 Source at UER (g/s)			
X	Y	ISC3 ( $\mu\text{g}/\text{m}^3$ )	ARSUS ( $\mu\text{g}/\text{m}^3$ )
619004.6	4841858	125.95	118.68
619004.6	4841872	104.45	98.99
619004.6	4841886	88.05	83.83
619004.6	4841900	75.26	71.92
618948.6	4841914	27.82	28.03
618962.6	4841914	40.33	39.78
618976.6	4841914	52.60	51.08
618990.6	4841914	61.70	59.35
619004.6	4841914	65.09	62.40
619018.6	4841914	61.76	59.35
619032.6	4841914	52.70	51.08
619046.6	4841914	40.45	39.77
619060.6	4841914	27.92	28.02
619004.6	4841928	56.86	54.66
619004.6	4841942	50.12	48.29
619004.6	4841956	44.52	42.98
619004.6	4841970	39.82	38.51
619004.6	4841984	35.83	34.71

**Table 5. Case 2, validation of the volume source algorithm, ISC3 versus ARSUS model estimated concentrations at given receptors.**

Case 2			
10 Sources each at UER (g/s)			
X	Y	ISC3 ( $\mu\text{g}/\text{m}^3$ )	ARSUS ( $\mu\text{g}/\text{m}^3$ )
619004.563	4841858	914.90	883.49
619004.563	4841872	802.53	776.21



X	Y	Case 2	
		10 Sources each at UER (g/s)	
		ISC3 ( $\mu\text{g}/\text{m}^3$ )	ARSUS ( $\mu\text{g}/\text{m}^3$ )
619004.563	4841886	708.36	686.03
619004.563	4841900	628.87	609.73
618948.563	4841914	340.77	335.77
618962.563	4841914	425.88	416.57
618976.563	4841914	497.26	484.19
618990.563	4841914	544.69	529.09
619004.563	4841914	561.31	544.80
619018.563	4841914	544.75	529.07
619032.563	4841914	497.36	484.16
619046.563	4841914	425.99	416.53
619060.563	4841914	340.88	335.72
619004.563	4841928	503.57	489.22
619004.563	4841942	453.92	441.38
619004.563	4841956	411.00	399.98
619004.563	4841970	373.70	363.96
619004.563	4841984	341.11	332.47

Table 6. Case 3, validation of the volume source algorithm, ISC3 versus ARSUS model estimated concentrations at given receptors.

X	Y	Case 3	
		55 Sources each at UER (g/s)	
		ISC3 ( $\mu\text{g}/\text{m}^3$ )	ARSUS ( $\mu\text{g}/\text{m}^3$ )
619004.563	4841858	5939.79	5602.60
619004.563	4841872	4939.85	4696.03
619004.563	4841886	4188.87	4003.87
619004.563	4841900	3606.09	3460.73
618948.563	4841914	1452.30	1449.65
618962.563	4841914	1963.94	1937.18
618976.563	4841914	2490.39	2429.32
618990.563	4841914	2924.38	2827.89
619004.563	4841914	3142.31	3025.06
619018.563	4841914	3067.39	2955.72
619032.563	4841914	2718.88	2636.67
619046.563	4841914	2201.90	2158.32
619060.563	4841914	1646.71	1635.82
619004.563	4841928	2765.84	2669.30
619004.563	4841942	2455.26	2374.47
619004.563	4841956	2195.60	2127.05
619004.563	4841970	1976.01	1917.20
619004.563	4841984	1788.48	1737.53

## APPENDIX 7: AMBIENT AIR MONITORING DATA 2007



APPENDIX 7: AMBIENT AIR MONITORING DATA 2007

Table 1 summarizes CO concentrations recorded at the Toronto West monitoring station for the months of April and May of 2007. The station records 1 h averages for CO. A yellow cell indicates the monitoring station was off-line and data was not available for the time period.

The Toronto West monitoring data are in given in ppm, below is a sample calculation for conversion of ppm to µg/m³.

Sample Calculations:

Conversion factor for CO from ppm to µg/m³.

Molecular weight of CO = 28.01  
Volume at standard T and P = 24.45

1 ppm =  $\frac{28.01}{24.45} \times 1,000 = 1,145.6 \frac{\mu g}{m^3}$

Table 1. Summary of CO concentrations recorded at the Toronto West monitoring station for the months of April and May 2007, 6 am to 11 am.

Date	H06 ppm	µg/m³	H07 ppm	µg/m³	H08 ppm	µg/m³	H09 ppm	µg/m³	H10 ppm	µg/m³	H11 ppm	µg/m³
4/1/2007	0.2	229.1207	0.22	252.0327	0.22	252.0327	0.24	274.9448	0.33	378.0491	0.37	423.8732
4/2/2007	0.53	607.1697	0.37	423.8732	0.38	435.3292	0.32	366.593	0.23	263.4888	0.23	263.4888
4/3/2007	0.52	595.7137	0.66	756.0982	0.82	939.3947			0.31	355.137	0.31	355.137
4/4/2007	0.35	400.9611	0.44	504.0654	0.71	813.3783	0.72	824.8344	0.31	355.137	0.3	343.681
4/5/2007	0.31	355.137	0.31	355.137	0.33	378.0491	0.31	355.137	0.24	274.9448	0.27	309.3129
4/6/2007	0.18	206.2086	0.19	217.6646	0.21	240.5767	0.22	252.0327	0.22	252.0327	0.22	252.0327
4/7/2007	0.23	263.4888	0.25	286.4008	0.24	274.9448	0.22	252.0327	0.24	274.9448	0.24	274.9448
4/8/2007	0.23	263.4888	0.24	274.9448	0.19	217.6646	0.19	217.6646	0.16	183.2965	0.16	183.2965
4/9/2007	0.28	320.7689	0.31	355.137	0.29	332.2249	0.28	320.7689	0.26	297.8569	0.23	263.4888
4/10/2007	0.51	584.2577	0.78	893.5706	0.6	687.362	0.33	378.0491	0.2	229.1207	0.24	274.9448
4/11/2007	0.54	618.6258	0.52	595.7137	0.35	400.9611	0.23	263.4888	0.14	160.3845	0.16	183.2965
4/12/2007	0.26	297.8569	0.29	332.2249	0.35	400.9611	0.38	435.3292	0.42	481.1534	0.45	515.5215
4/13/2007	0.21	240.5767	0.22	252.0327	0.24	274.9448	0.21	240.5767	0.27	309.3129	0.27	309.3129
4/14/2007	0.28	320.7689	0.32	366.593	0.33	378.0491	0.26	297.8569	0.28	320.7689	0.26	297.8569
4/15/2007	0.25	286.4008	0.26	297.8569	0.25	286.4008	0.27	309.3129	0.23	263.4888	0.23	263.4888
4/16/2007	0.27	309.3129	0.27	309.3129	0.26	297.8569	0.25	286.4008	0.25	286.4008	0.25	286.4008
4/17/2007	0.42	481.1534	0.43	492.6094	0.33	378.0491	0.31	355.137	0.27	309.3129	0.27	309.3129
4/18/2007	0.28	320.7689	0.27	309.3129	0.26	297.8569	0.25	286.4008	0.27	309.3129	0.28	320.7689
4/19/2007	0.61	698.818	0.65	744.6421	0.34	389.5051	0.26	297.8569	0.22	252.0327	0.2	229.1207
4/20/2007	0.52	595.7137	0.52	595.7137	0.42	481.1534	0.33	378.0491	0.24	274.9448	0.24	274.9448
4/21/2007	0.27	309.3129	0.33	378.0491	0.26	297.8569	0.24	274.9448	0.23	263.4888	0.2	229.1207
4/22/2007	0.63	721.7301	0.62	710.274	0.43	492.6094	0.37	423.8732	0.36	412.4172	0.31	355.137
4/23/2007	0.39	446.7853	0.4	458.2413	0.36	412.4172	0.48	549.8896	0.29	332.2249	0.28	320.7689
4/24/2007	0.37	423.8732	0.42	481.1534	0.33	378.0491	0.26	297.8569	0.2	229.1207	0.19	217.6646
4/25/2007	0.45	515.5215	0.56	641.5378	0.47	538.4335	0.45	515.5215	0.28	320.7689	0.25	286.4008



Date	H06 ppm	µg/m <sup>3</sup>	H07 ppm	µg/m <sup>3</sup>	H08 ppm	µg/m <sup>3</sup>	H09 ppm	µg/m <sup>3</sup>	H10 ppm	µg/m <sup>3</sup>	H11 ppm	µg/m <sup>3</sup>
4/26/2007	0.3	343.681	0.34	389.5051					0.33	378.0491	0.33	378.0491
4/27/2007	0.32	366.593	0.38	435.3292	0.48	549.8896	0.49	561.3456	0.34	389.5051	0.39	446.7853
4/28/2007	0.28	320.7689	0.31	355.137	0.31	355.137	0.3	343.681	0.33	378.0491	0.33	378.0491
4/29/2007	0.69	790.4663	0.63	721.7301	0.37	423.8732	0.25	286.4008	0.21	240.5767	0.22	252.0327
4/30/2007	0.33	378.0491	0.28	320.7689	0.27	309.3129	0.26	297.8569	0.26	297.8569	0.27	309.3129
5/1/2007	0.53	607.1697	0.65	744.6421	0.78	893.5706	0.42	481.1534	0.21	240.5767	0.21	240.5767
5/2/2007	0.42	481.1534	0.44	504.0654	0.37	423.8732	0.3	343.681	0.28	320.7689	0.24	274.9448
5/3/2007	0.64	733.1861	0.68	779.0102	0.29	332.2249	0.21	240.5767	0.17	194.7526	0.17	194.7526
5/4/2007	0.4	458.2413	0.85	973.7628	0.47	538.4335	0.34	389.5051	0.23	263.4888	0.15	171.8405
5/5/2007	0.4	458.2413	0.42	481.1534	0.3	343.681	0.22	252.0327	0.26	297.8569	0.22	252.0327
5/6/2007	0.11	126.0164	0.12	137.4724	0.11	126.0164	0.1	114.5603	0.15	171.8405	0.15	171.8405
5/7/2007	0.63	721.7301	0.75	859.2025	0.34	389.5051	0.21	240.5767	0.24	274.9448	0.22	252.0327
5/8/2007	0.34	389.5051	0.31	355.137	0.25	286.4008	0.26	297.8569	0.24	274.9448	0.24	274.9448
5/9/2007	0.35	400.9611	0.47	538.4335	0.45	515.5215	0.38	435.3292	0.28	320.7689	0.3	343.681
5/10/2007	0.5	572.8016	0.56	641.5378	0.59	675.9059	0.42	481.1534	0.39	446.7853	0.33	378.0491
5/11/2007	0.56	641.5378	0.55	630.0818	0.48	549.8896	0.41	469.6973	0.28	320.7689	0.29	332.2249
5/12/2007	0.18	206.2086	0.18	206.2086	0.16	183.2965	0.17	194.7526	0.24	274.9448	0.24	274.9448
5/13/2007	0.22	252.0327	0.21	240.5767	0.22	252.0327	0.17	194.7526	0.13	148.9284	0.14	160.3845
5/14/2007	0.83	950.8507	0.72	824.8344	0.7	801.9223	0.53	607.1697	0.32	366.593	0.32	366.593
5/15/2007	0.29	332.2249	0.3	343.681	0.4	458.2413	0.33	378.0491	0.37	423.8732	0.37	423.8732
5/16/2007	0.34	389.5051	0.36	412.4172	0.32	366.593	0.33	378.0491	0.35	400.9611	0.39	446.7853
5/17/2007	0.37	423.8732	0.41	469.6973	0.32	366.593	0.25	286.4008	0.23	263.4888	0.23	263.4888
5/18/2007	0.68	779.0102	0.58	664.4499	0.34	389.5051	0.3	343.681	0.33	378.0491	0.32	366.593
5/19/2007	0.58	664.4499	0.68	779.0102	0.39	446.7853	0.28	320.7689	0.22	252.0327	0.17	194.7526
5/20/2007	0.25	286.4008	0.24	274.9448	0.24	274.9448	0.23	263.4888	0.25	286.4008	0.25	286.4008
5/21/2007	0.24	274.9448	0.23	263.4888	0.21	240.5767	0.2	229.1207	0.15	171.8405	0.15	171.8405
5/22/2007	0.49	561.3456	0.44	504.0654	0.37	423.8732	0.3	343.681	0.25	286.4008	0.2	229.1207
5/23/2007	0.61	698.818	0.55	630.0818	0.38	435.3292	0.42	481.1534	0.35	400.9611	0.3	343.681
5/24/2007	0.64	733.1861	0.73	836.2904	0.7	801.9223	0.65	744.6421	0.35	400.9611	0.36	412.4172

Date	H06 ppm	µg/m <sup>3</sup>	H07 ppm	µg/m <sup>3</sup>	H08 ppm	µg/m <sup>3</sup>	H09 ppm	µg/m <sup>3</sup>	H10 ppm	µg/m <sup>3</sup>	H11 ppm	µg/m <sup>3</sup>
5/25/2007	0.44	504.0654	0.56	641.5378	0.5	572.8016	0.39	446.7853	0.35	400.9611	0.31	355.137
5/26/2007	0.24	274.9448	0.26	297.8569	0.26	297.8569	0.24	274.9448	0.18	206.2086	0.2	229.1207
5/27/2007	0.14	160.3845	0.15	171.8405	0.14	160.3845	0.16	183.2965	0.27	309.3129	0.29	332.2249
5/28/2007	0.37	423.8732	0.37	423.8732			0.25	286.4008	0.23	263.4888	0.22	252.0327
5/29/2007	0.59	675.9059	0.7	801.9223	0.4	458.2413	0.25	286.4008	0.2	229.1207	0.18	206.2086
5/30/2007	0.77	882.1145	0.68	779.0102	0.64	733.1861	0.59	675.9059	0.43	492.6094	0.38	435.3292
5/31/2007	0.69	790.4663	0.82	939.3947	1.04	1191.427	0.75	859.2025	0.52	595.7137	0.49	561.3456



## APPENDIX 8: TABULATED DATA FROM THE SMALL AND LARGE SCALE MODELLING EXERCISE

## APPENDIX 8: TABULATED DATA FROM THE SMALL AND LARGE SCALE MODELLING EXERCISE

Table 1 is a summary of data from the small scale study, tailpipe emissions from the roads and highways in the vicinity of the Toronto West monitoring station. Where CO concentrations recorded at the station,  $C_{i,obs}$ , and ARSUS model generated data for the same hour is  $C_{i,model}$ . This data were used to plot the residual plot.

Table 2 is a summary of the data from the large scale study, tailpipe emissions from highways in the city of Toronto. Where CO concentrations recorded at the Toronto West monitoring station,  $C_{i,obs}$ , and ARSUS model generated data for the same hour is  $C_{i,model}$ . This data were used to plot the residual plot.



**Table 1. Data from the small scale exercise used to plot residuals based on the CO concentrations recorded for the months April to May, 6 am to 11 am, weekdays in 2007 along with those concentrations generated by the ARSUS model.**

C <sub>i,obs</sub>	C <sub>i,model</sub>	C <sub>i,obs</sub> -C <sub>i,model</sub>
607	98	509
423	91	332
435	64	371
366	51	315
263	46	217
263	40	223
939	939	0
355	17	338
355	13	342
813	96	717
824	75	749
355	67	288
345	73	272
355	92	263
355	80	275
378	61	317
355	98	257
275	108	167
309	90	219
206	166	40
218	96	122
241	161	80
252	144	108
252	114	138
252	154	98
320	303	17

C <sub>i,obs</sub>	C <sub>i,model</sub>	C <sub>i,obs</sub> -C <sub>i,model</sub>
355	268	87
332	154	178
320	149	171
297	228	69
263	178	85
584	504	80
893	351	542
687	0	687
378	176	202
229	307	-78
274	304	-30
618	401	217
595	59	536
400	17	383
263	11	252
160	33	127
183	28	155
298	29	269
332	35	297
401	63	338
435	45	390
481	175	306
515	82	433
240	48	192
252	87	165
275	83	192
241	87	154
309	67	242
309	84	225
309	63	225
309	74	235
297	58	239
286	52	234
286	62	224
286	49	237
481	192	289
492	251	241
378	155	223
355	142	213
309	119	190



$C_{i,obs}$	$C_{i,model}$	$C_{i,obs}-C_{i,model}$
309	119	190
320	173	147
309	158	151
297	271	26
286	167	119
309	41	268
320	47	273
699	339	360
745	85	660
389	61	328
298	123	175
252	65	187
596	337	259
596	85	511
481	61	420
378	123	255
275	64	211
423	246	177
481	173	308
378	170	208
217	130	87
515	246	269
641	173	468
538	170	368
286	129	157
344	63	281
389	42	347
378	19	359
378	26	352
366	56	310
435	36	399
549	52	497
561	28	533
389	17	372
447	34	413
378	79	299
320	86	234
309	81	228
297	110	187
297	139	158
309	117	192

$C_{i,obs}$	$C_{i,model}$	$C_{i,obs}-C_{i,model}$
607	690	-83
745	41	704
894	51	843
481	47	434
241	190	51
241	38	203
481	255	226
504	165	339
424	128	296
344	179	165
321	50	271
275	203	72
733	445	288
779	128	651
332	85	247
241	19	222
195	15	180
195	15	180
642	255	387
630	207	423
550	131	419
470	87	383
321	131	190
332	95	237
390	114	276
412	56	356
367	173	194
378	283	95
447	56	391



**Table 2. Data from the small scale exercise used to plot residuals based on the CO concentrations recorded for the part April, 6 am to 11 am, weekdays in 2007 along with those concentrations generated by the ARSUS model.**

C <sub>i,obs</sub>	C <sub>i,model</sub>	C <sub>i,obs</sub> -C <sub>i,model</sub>
607	89	518
423	83	340
435	52	383
366	30	336
263	41	222
263	34	229
595	1152	-557
756	924	-168
355	11	344
355	10	345
504	1101	-597
813	90	723
824	58	766
355	61	294
345	78	267
355	83	272
355	73	282
378	55	323
355	89	266
275	89	186
309	82	227
206	155	51
218	90	128
241	158	83
252	131	121
252	104	148
252	140	112
320	279	41
355	245	110
332	147	185
320	139	181
297	213	84
263	164	99
584	471	113
893	322	571
687	466	221

C <sub>i,obs</sub>	C <sub>i,model</sub>	C <sub>i,obs</sub> -C <sub>i,model</sub>
378	173	205
229	280	-51
274	284	-10
618	393	225
595	54	541
240	55	185
252	107	145
275	98	177
241	104	137
309	81	228
309	102	207
309	79	230
309	90	219
297	73	224
286	66	220
286	76	210
286	61	225
481	235	246
492	265	227
378	164	214
355	165	190
309	146	163
309	146	163
320	215	105
309	197	112
297	337	-40
286	274	12
699	390	309
745	114	631
389	60	329
298	134	164
252	72	180
596	389	207
596	114	482
481	60	421
378	134	244



## APPENDIX 9: ARSUS CODE

## APPENDIX 9: ARSUS CODE

Main Function: **Concentration.m** which is used as the main code.

function concentration

clear all

tic

```
%%%%%%%%%%
%%%%%%%%%
%
```

% DEFINE VARIABLES

```
%%%%%%%%%%
%%%%%%%%%
%
```

stepsize=250; %This defines the resolution of the grid

Hs=3; % stack height m

D=2; % diameter of the exhaust m

Us=1; % exit velocity m/s

Ts=300; % temperature of the exhaust in K

```
%%%%%%%%%%
%%%%%%%%%
%
```

% READING IN THE SOURCE CHARACTERIZATION DATA & DETERMINATION OF THE

% MODELLING DOMAIN

```
%%%%%%%%%%
%%%%%%%%%
%
```

Source=xlsread('Emissions-CO1vsource.xls','A2:D5');

mins=min(Source);xmin=mins(1)-100;ymin=mins(2)-100; % determine the lower end of the domain based on what sources lie in it

maxs=max(Source);xmax=maxs(1)+100;ymax=maxs(2)+100; % determine the upper end of the domain based on what sources lie in it

xrange=xmax-xmin;yrange=ymax-ymin; % extending the domain by 500 m beyond the minimum and maximum locations of sources

clear mins maxs;

x=[xmin:xrange/stepsize:xmax];y=[ymin:yrange/stepsize:ymax]'; %grid size: start point: increment : total distance.

```
%%%%%%%%%%
%%%%%%%%%
%
```



# % READING METEOROLOGICAL FILE

```
%%%%%%%%%%
%%%%%%%%%
%%%%%%%%%
%
```

```
Wind=xlsread('metfilevalidation.xls','A1:H5'); % do not modify, range should be of the entire
file it includes: year, month,day,hour,wind dir,wind spd,amb temp, stab. class
for hour=1:1 % specify range is needed, start reading hour to end hour of met file
    h = waitbar(0,'Please wait...');
```

```
Filename=Wind(hour,1:3);
U=Wind(hour,6);
SC=Wind(hour,8);
Ta=Wind(hour,7);
Udir=Wind(hour,5);
```

```
%%%%%%%%%%
%%%%%%%%%
%%%%%%%%%
%
% Calculate Wind Correction
%%%%%%%%%
%%%%%%%%%
%
```

```
[theta]=WindCorrection(Udir);
```

```
C=zeros(length(x),length(y)); %creates a blank matrix for Concentration grid
for Iter=1:length(Source)
```

```
    Q=Source(Iter,3);
    xpos=Source(Iter,1);
    ypos=Source(Iter,2);
    Width=Source(Iter,4);
    %%%%%%%%%%
    %%%%%%%%%%
    %
```

## % GAUSSIAN DISPERSION

```
% following code allows to check from which direction wind is coming so
% that the direction of the plume (quadrant in Cartesian coordinates) can
% be determined.
```

```
% NOTE 1: There are exact solutions to evaluating wind in direction 0, 90, 180 and
% 270 degrees. All grind points, away from (0,0)and on line intercepting the axis
% will be evaluated.
```

```
% NOTE 2: If wind is coming between e.g. 0 and 90 degrees, a line equation
% is determined (intercept and slope) to evaluate all grid points away from
% the (0,0) direction.
```

```
% Notes 1 and 2 are performed in the following set of FOR and IF statements.
```

```
%%%%%%%%%%
%%%%%%%%%
%%%%%%%%%
%
```

```
for Y=1:length(y)
    for X=1:length(x)
        %figure out wind direction and find 'side' of where C is calc'ed
        if theta==90 % RE: Note 1 from above. Solution for winds coming specifically from angles 0,
90, 180 and 270 degrees.
```

```
            xdist_t=y(Y,1)-ypos; ydist_t=x(1,X)-xpos;
            if xdist_t>0 && ydist_t<2000 && xdist_t<2000 % code after && compensates for the fact
that the dispersion factors
                [He]=PlumeRise(SC,Ta,Ts,Hs,Us,U,D,abs(xdist_t)); %Plume Rise
                C(X,Y)=C(X,Y)+Gaussian(abs(xdist_t),abs(ydist_t),He,U,Q,SC,Width);
            end
```

```
        elseif theta==270
            xdist_t=y(Y,1)-ypos; ydist_t=x(1,X)-xpos;
            if xdist_t<0 && ydist_t>-1000 && xdist_t>-1000
                [He]=PlumeRise(SC,Ta,Ts,Hs,Us,U,D,abs(xdist_t)); %Plume Rise
                C(X,Y)=C(X,Y)+Gaussian(abs(xdist_t),abs(ydist_t),He,U,Q,SC,Width);
            end
```

```
        elseif theta==180
            ydist_t=y(Y,1)-ypos; xdist_t=x(1,X)-xpos;
            if xdist_t<0 && ydist_t>-2000 && xdist_t>-1000
                [He]=PlumeRise(SC,Ta,Ts,Hs,Us,U,D,abs(xdist_t)); %Plume Rise
                C(X,Y)=C(X,Y)+Gaussian(abs(xdist_t),abs(ydist_t),He,U,Q,SC,Width);
            end
```

```
        elseif theta==0
            ydist_t=y(Y,1)-ypos; xdist_t=x(1,X)-xpos;
            if xdist_t>0 && ydist_t<2000 && xdist_t<2000
                [He]=PlumeRise(SC,Ta,Ts,Hs,Us,U,D,abs(xdist_t)); %Plume Rise
                C(X,Y)=C(X,Y)+Gaussian(abs(xdist_t),abs(ydist_t),He,U,Q,SC,Width);
            end
```

```
        elseif (theta>0 && theta<90) || (theta>90 && theta<180)
            % RE: Note 2 from above. Solution for wind direction between
            % 0, 90 and 180 degrees but not those specific angles.
            m=-1/(tan(theta/180*pi)); % slope of the line
            b=ypos-m*xpos; %calc equation of line
            Ylimit=m*x(1,X)+b;
            ydist_t=y(Y,1)-ypos; xdist_t=x(1,X)-xpos;
            % following ydist_t and xdist_t has been developed so that it only grid points that line in
the direction to which wind blows
```



```

% are used to estimate the concentrations for.
    chi=atan(ydist/xdist)*180/pi;    gamma=theta-chi;
    r=sqrt(xdist^2+ydist^2);
    xdist_t=r*cos(gamma/180*pi);
    ydist_t=r*sin(gamma/180*pi);

    if y(Y,1)>=Ylimit && ydist_t<2000 && xdist_t<2000
        [He]=PlumeRise(SC,Ta,Ts,Hs,Us,U,D,abs(xdist_t)); %Plume Rise
        C(X,Y)=C(X,Y)+Gaussian(abs(xdist_t),abs(ydist_t),He,U,Q,SC,Width);
    end

elseif (theta>180 && theta<270) || (theta>270 && theta<360)
    %bottom quadrant

    m=-1/(tan(theta/180*pi)); % slope of the line
    b=ypos-m*xpos; %calc equation of line
    Ylimit=m*x(1,X)+b;
    ydist=y(Y,1)-ypos; xdist=x(1,X)-xpos;
    % following ydist_t and xdist_t has been developed so that it only grid points that line in
the direction to which wind blows
    % are used to estimate the concentrations for.
    chi=atan(ydist/xdist)*180/pi;    gamma=theta-chi;
    r=sqrt(xdist^2+ydist^2);
    xdist_t=r*cos(gamma/180*pi);
    ydist_t=r*sin(gamma/180*pi);

    if y(Y,1)<=Ylimit && ydist_t<2000 && xdist_t<2000
        [He]=PlumeRise(SC,Ta,Ts,Hs,Us,U,D,abs(xdist_t)); %Plume Rise
        C(X,Y)=C(X,Y)+Gaussian(abs(xdist_t),abs(ydist_t),He,U,Q,SC,Width);
    end
end
end
end

waitbar(Iter/length(Source),h,num2str(hour))
end
close(h)
xlswrite(num2str(Filename),x,'B1:IQ1');
xlswrite(num2str(Filename),y,'A2:A251');
xlswrite(num2str(Filename),C,'B2:IQ251');
end

```

```

%%%%%%%%%%%%%%%%%%%%%%%%%%%%%%%%%%%%%%%%%%%%%%%%%%%%%%%%%%%%%%%%%%%%%%%%
%%%%%%%%%%%%%%%%%%%%%%%%%%%%%%%%%%%%%%%%%%%%%%%%%%%%%%%%%%%%%%%%%%%%%%%%
%
% PLOT OF RESULTS
%%%%%%%%%%%%%%%%%%%%%%%%%%%%%%%%%%%%%%%%%%%%%%%%%%%%%%%%%%%%%%%%%%%%%%%%
%%%%%%%%%%%%%%%%%%%%%%%%%%%%%%%%%%%%%%%%%%%%%%%%%%%%%%%%%%%%%%%%%%%%%%%%
%

v=[100:200:1000]; % definition of first contour to be plotted; step;last contour to be plotted
[cs,h]=contour(x,y,C',v); % allows to plot isopleths with defined contour lines
clabel(cs,h); % displays labels for each contour line

hold off

toc
end

```



# Sub-function: **WindCorrection.m**

```
function [theta]=WindCorrection(Udir)
%Calculates theta based on the wind direction: the meteorological file contains winds
% with convention of North being 0 degrees. For the purpose of this
% program angle theta has to be rotated where North (Y-axis) is 90
% degrees. Following, reads the angle of wind direction given in the
% meteorological file and then converts it to theta.
```

```
if Udir<=90
    theta=90-Udir;
elseif Udir>90 && Udir<=180
    theta=360-(Udir-90);
elseif Udir>180 && Udir<=270
    theta=270-(Udir-180);
else
    theta=abs(Udir-360)+90;
end
end
```

# Sub-function: **PlumeRise.m**

```
function [He]=PlumeRise(SC,Ta,Ts,Hs,Us,U,D,xdist_t)
```

```
%Calculates Plume Rise as a function of
% Stability Class (Sc), Ambient Temperature (Ta), Stack Temperature (Ts);
% Stack Exit velocity (Us) & Stack Diameter (D)
```

```
F=9.81*Us*D^2*(Ts-Ta)/(4*Ts); %Briggs Buoyancy Flux
if F>=55
```

```
    xf=119*F^0.4;
    else
    xf=49*F^0.625;
    end
```

```
switch SC
```

```
    case {1,2,3,4}
```

```
        if F>=55 && xdist_t<xf
```

```
            dh=(1.6*F^(1/3)*xdist_t^(2/3))/U;
```

```
            elseif F>=55 && xdist_t>=xf
```

```
            dh=(1.6*F^(1/3)*xf^(2/3))/U;
```

```
        elseif F<55 && xdist_t<xf
```

```
            dh=(1.6*F^(1/3)*xdist_t^(2/3))/U;
```

```
        elseif F<55 && xdist_t>=xf
```

```
            dh=(1.6*F^(1/3)*xf^(2/3))/U;
```

```
    end
```

```
    case {5,6}
```

```
        if (1.84*U*(0.02)^(-1/2))>=xf && xdist_t<xf
```

```
            dh=(1.6*F^(1/3)*xdist_t^(2/3))/U;
```

```
        elseif (1.84*U*(0.02)^(-1/2))>=xf && xdist_t>=xf && F>=55
```

```
            dh=(1.6*F^(1/3)*xf^(2/3))/U;
```

```
        elseif (1.84*U*(0.02)^(-1/2))>=xf && xdist_t>=xf && F<55
```

```
            dh=(21.4*F^(0.75))/U;
```

```
        elseif 1.84*U*(0.02)^(-1/2)<xf && xdist_t<1.84*U*0.02^(-1/2)
```

```
            dh=(1.6*F^(1/3)*xdist_t^(2/3))/U;
```

```
        elseif 1.84*U*(0.02)^(-1/2)<xf && xdist_t>=1.84*U*0.02^(-1/2)
```

```
            dh=2.4*(F/(U*0.02))^(1/3);
```

```
    end
```

```
end
```

```
% if SC<=4 &&
```



```

% Fm=Us^2*D^2*Ta/(4*Ts); % to match ISC
% He=Hs+1.5*(Fm/(Us))^1.3; % to match ISC
% % U=U*(Hs/10)^0.25;
% elseif SC>=5
% U=U*(Hs/10)^0.5
% else
% U=((U*(Hs/10)^0.25)+(U*(Hs/10)^0.5))/2;
% end
%
% He=Hs;
% if Ts>(Ta+25) && Us>1.5*U
% F=9.81*U*(D/2)^2*(Ts-Ta)/Ta;
% %Hr=150*(F/U^3); % plume rise
% He=Hs+150*(F/U^3); % effective height of the stack
% end
He=Hs+dh;
end

```

#### Sub-function: Gaussian.m

```

function [POI]=Gaussian(xdist_t,ydist_t,He,U,Q,SC,Width);
% The Gaussian Dispersion function was written in 3 parts, just to keep
% the function more easily to work with. Part one contains info about the
% source, ambient wind and both sigmas, part 2 contains the horizontal
% spread EY and part 3 contains the vertical spread and accounts for
% ground reflection EY.

Fz0=3/2.15;

if SC==1 || SC==2
    constY=0.32;
    sigmaz=Fz0+0.24*(xdist_t+Fz0)*(1+0.001*(xdist_t+Fz0))^(1/2);
elseif SC==3
    constY=0.22;
    sigmaz=Fz0+0.2*(xdist_t+Fz0);
elseif SC==4
    constY=0.16;
    sigmaz=Fz0+0.14*(xdist_t+Fz0)*(1+0.0003*(xdist_t+Fz0))^(-1/2);
else
    constY=0.11;
    sigmaz=Fz0+0.08*(xdist_t+Fz0)*(1+0.0015*(xdist_t+Fz0))^(-1/2);
end

% sigmaz=0.220*xdist_t*(1+0.0004*xdist_t)^(-0.5);
sigmay=(Width/2.15)+constY*(xdist_t+Width/2.15)*(1+0.0004*(xdist_t+Width/2.15))^(-0.5);
EY=exp(-(ydist_t^2)/(2*sigmay^2)); % Part 1 of 3 (Gaussian Dispersion)
EZ=exp(-0.5*(0-He)^2/(sigmaz^2))+exp(-0.5*(0+He)^2/(sigmaz^2)); % Part 2 of 3 (Gaussian Dispersion)
POI=Q*1e6/(2*pi*sigmaz*sigmay*U)*EY*EZ; % Part 3 of 3 (Gaussian Dispersion)
end

```



## REFERENCES

1. Adamowicz R. F., A model for the reversible washout of sulfur dioxide, ammonia and carbon dioxide from a polluted atmosphere and production of sulfates in raindrops, *Atmospheric Environment*, 13, 105-121, 2000.
2. Alberta Environment, Air Quality Model Guide, March 2003.
3. Asman W., Parameterization of Below-Cloud Scavenging Of Highly Soluble Gases Under Convective Conditions, *Atmospheric Environment*, 29, 12, 1359-1368, 1995.
4. Bady M., Kato S., Ooka R., Huang H., Jiang T., Comparative study of concentrations and distributions of CO and NO in an urban area: Gaussian plume model and CFD analysis. *Air Pollution*, 86, 2006.
5. Baik, J., Kang Y., Kim J., Modelling reactive pollutant dispersion in an urban street canyon, *Atmospheric Environment*, 2007.
6. Baker, Helen L. Walker, Xiaoming Cai, A study of dispersion and transport of reactive pollutants in and above street canyons – a large eddy simulation, *Atmospheric Environment* 38, 6883-6892, 2004.
7. Beychok M. R., *Fundamentals of Stack Gas Dispersion*, Third Edition, 1994.
8. Boubel R.W., Fox D. L., Turner D.B., Stern A.C., *Fundamentals of Air Pollution*, Academic Press, London, 1994.
9. Brechler J., Model Assessment of Air-Pollution in Prague, *Environmental Monitoring and Assessment*, 2000.
10. British Columbia Ministry of Environment, Guidelines for Air Quality Dispersion Modelling in British Columbia, October 2006.
11. Calder K.L., On Estimating Air Pollution Concentrations from a Highway in an Oblique Wind, *Atmosphere Environment*, 7, 863-868, 1973.
12. Calder K.L., Multiple-Source Plume Models of Urban Air Pollution – The General Structure, *Atmospheric Environment*, 11, 403 – 414, 1977.
13. Cana-Cascallar L. C., On the Relationship Between Acid Rain and Cloud Type, Air and Waste Management Association, 2002.
14. Carrascal M.D., Puigcerver M., Puig P., Sensitivity of Gaussian Plume Model to Dispersion Specifications, *Theoretical and Applied Climatology*, 48, 147-157, 1993.
15. Canada Gazette, Regulations Amending the Sulphur in Diesel Fuel Regulations, 138, 40, October 2, 2004.
16. Chang T. Y., Rain and Snow Scavenging and HNO<sub>3</sub> vapor in the atmosphere, *Atmospheric Environment*, 18, 191 – 197, 1984.
17. Cheng S., Li J., Feng B., Jin Y., Hao R., A Gaussian-box modeling approach for urban air quality management in a northern Chinese city – I. model development, *Water Air Soil Pollution*, 2006.
18. City of Toronto, Traffic Data – <http://www.toronto.ca/transportation/publications/brochures/2006volmappm.pdf>, December, 2008.
19. Colls J., *Air Pollution an Introduction*, E&FN Spon, an imprint of Chapman & Hall, 70, 1997.
20. Cooper D., Alley F.C., *Air Pollution Control A Design Approach*, 3<sup>rd</sup> edition, 2002.
21. Derwent R.G., Middleton D.R., An Empirical Function for the Ratio NO<sub>2</sub>:NO<sub>x</sub>, *Clean Air*, The National Society for Clean Air, Brighton, 26, 3/4, 57-59, 1996.
22. Dobbins R.A., *Atmospheric Motion and Air Pollution*, 1979.
23. Environment Canada, General Guidance Document, Notice with Respect to Reporting of Information on Air Pollutants, Greenhouse Gases and Other Substances for the 2006 Calendar Year, Canada Gazette Part I under section 71 of the Canadian Environmental Protection Act 1999, December 8, 2007.
24. Environment Canada, Greenhouse Gas Emissions Reporting Technical Guidance on Reporting Greenhouse Gas Emissions, 2006.
25. Environment Canada Weather Network , [http://climate.weatheroffice.ec.gc.ca/climateData/canada\\_e.html](http://climate.weatheroffice.ec.gc.ca/climateData/canada_e.html) - 2007.
26. Environment Canada Weather Network , [http://climate.weatheroffice.ec.gc.ca/climateData/canada\\_e.html](http://climate.weatheroffice.ec.gc.ca/climateData/canada_e.html) - 2008.
27. Environment Canada Air Quality Services, [http://www.msc-smc.ec.gc.ca/aq\\_smog/on/on\\_e.cfm](http://www.msc-smc.ec.gc.ca/aq_smog/on/on_e.cfm) - 2008.



28. Environment Canada,  
[http://www.ec.gc.ca/pdb/querysite/results\\_e.cfm?opt\\_report\\_year=2007&opt\\_facility=ALL&opt\\_facility\\_name=&opt\\_npri\\_id=&opt\\_chemical\\_type=ALL&opt\\_cas\\_name=&opt\\_cas\\_num=&opt\\_province=&opt\\_postal\\_code=&opt\\_location\\_type=URBAN&opt\\_urban\\_center=590\\_ON&community1=&opt\\_industry=ALL&opt\\_naics4=&opt\\_csi2=&opt\\_csic=&opt\\_asic=](http://www.ec.gc.ca/pdb/querysite/results_e.cfm?opt_report_year=2007&opt_facility=ALL&opt_facility_name=&opt_npri_id=&opt_chemical_type=ALL&opt_cas_name=&opt_cas_num=&opt_province=&opt_postal_code=&opt_location_type=URBAN&opt_urban_center=590_ON&community1=&opt_industry=ALL&opt_naics4=&opt_csi2=&opt_csic=&opt_asic=) - NPRI database about the industries in Sault St. Marie, 2009.
29. Environmental Protection Act, Sulphur Content of Fuels, O.Reg. 361, 1970 amended in 1980, 1990 and 1999.
30. Environmental Commissioner of Ontario, 2007/08 Annual Report – Getting to K(No)w, 2008, page 57.
31. Fenger J., Urban Air Quality, *Atmospheric Environment*, 33, 4877-4900, 1999.
32. Fenger J., Air Pollution in the last 50 years – From Local to Global, 43, 13-22, 2009.
33. Golder D., Relations Among Stability Parameters in the Surface Layer, *Department of Meteorology*, 47-58, 1972.
34. Goyal, M. P. Singh and T.K. Bandyopadhyay, Environmental Studies of SO<sub>2</sub>, SPM and NO<sub>x</sub> over Agra, with various methods of treating calms, *Atmospheric Environment*, 28, 19, 3113-3123, 1994.
35. Hayes S.R., Moore G.E., Air Quality Model Performance: a Comparative Analysis of 15 Model Evaluations Studies, *Atmospheric Environment*, 1986.
36. Hemond H.F., Fechner-Levy E.J., *Chemical Fate and Transport in the Environment*, Second Edition, 2000.
37. Jacob, D, Heterogeneous Chemistry and Tropospheric O<sub>3</sub>, *Atmospheric Environment* 34, 2000.
38. Jerrett M., Arain A., Kanaroglou P., Beckerman B., Potoglou D., Sahuvaroglu T., Morrison J., Giovis C., A review and evaluation of intraurban air pollution exposure models., *Journal of Exposure Analysis and Environmental Epidemiology*, 15, 185-204, 2005.
39. Jerrett M., Arain M. A., Kanaroglou P., Beckerman B., Crouse D., Gilbert N.L., Brook J.R., Finkelstein N., Finklestein M. M., Modelling the Intraurban Variability of Ambient Traffic Pollution in Toronto, Canada. *Journal of Toxicology and Environmental Health*, A, 70, 200-212, 2007.
40. Karppinen A., Kukkonen J., Konttinen M., Härkönen J., Rantakrans E., Volkonen E., Koskentalo T., Elolähde T., The emissions, dispersion and chemical transformation of traffic-originated nitrogen oxides in the Helsinki metropolitan area, *International Journal Vehicle Design*, 20, 1-4, 1998.
41. Karppinen A., Kukkonen J., Elolähde T., Konttinen M., Koskentalo T., A modelling system for predicting urban air pollution: comparison of model predictions with the data of an urban measurement network in Helsinki, *Atmospheric Environment*, 32, 2000.
42. Kitabayashi K., Konishi S., Katatani A., A NO<sub>x</sub> Plume Dispersion Mode with Chemical Reaction in Polluted Environment, *JSME International Journal*, 49, 1, 2006.
43. Laskarzewska B., M. Mehrvar, "Atmospheric Chemistry in Existing Air Atmospheric Dispersion Models and Their Applications: Trends, Advances and Future in Urban Areas in Ontario, Canada and the World", *International Journal of Engineering*, Volume 3, Issue 1, 21-57, March 2009.
44. Lin X., Roussel P.B., Laszlo S., Taylor R., Melo O., Shepson P.B., Hastie D.R., Niki H., Impact of Toronto Urban Emissions on Ozone Levels Downtown, *Atmospheric Environment*, 30, 12, 2177-2193, 1996.
45. Mage D., Ozolins G., Peterson P., Webster A., Orthofer R., Vandeweerd V., Gwynne M., Urban Air Pollution in Megacities of the World, *Atmospheric Environment*, 30, 5, 681-686, 1996.
46. McMahon T., Denison P.J., Review Paper Empirical Atmospheric Deposition Parameters – A Survey, *Atmospheric Environment*, 13, 571-585, 1979.
47. McMullen R.W., The change of concentration standard deviations with distance, *JAPCA*, October 1975.
48. Milliez M., Carissimo B., Numerical simulations of pollutant dispersion in an idealized urban area for different meteorological conditions, 2006, *Boundary-Layer Meteorology*, 2007.
49. Ministry of the Environment New Zealand, Good Practice Guide for Atmospheric Modelling, June 2004.
50. Nagendra S.M.S, Khare M., Review Line Source Emission Modelling, *Atmospheric Environment*, 36, 2083-2098, 2002.
51. Ogawa Y., P.G. Diosey, K. Uehara and H. Ueda, Plume behaviour in stratified flows, *Atmospheric Environment*, 16 (6), 1419-1433, 1982.
52. Ontario Medical Association, The Illness Costs of Air Pollution, 2005-2006 Health and Economic Damage Estimates, June 2005.
53. Ontario Ministry of the Environment, Air Quality in Ontario 1999 Report, 2000.
54. Ontario Ministry of the Environment, Air Quality in Ontario 2000 Report, 2001.



55. Ontario Ministry of the Environment, Air Quality in Ontario 2001 Report, 2002.
56. Ontario Ministry of the Environment, Air Quality in Ontario 2002 Report, 2003.
57. Ontario Ministry of the Environment, Air Quality in Ontario 2003 Report, 2004.
58. Ontario Ministry of the Environment, Industrial Pollution Team, July 30 2004.
59. Ontario Ministry of the Environment, Air Quality in Ontario 2004 Report, 2005.
60. Ontario Ministry of the Environment, Air Dispersion Modeling Guideline for Ontario, July, 2005.
61. Ontario Ministry of the Environment, Green Facts – Ontario's Air Quality Index, May 2005.
62. Ontario Ministry of the Environment, Procedure for Preparing an Emission Summary and Dispersion Modelling Report, Version 2.0, PIBs # 3614e02, July 2005.
63. Ontario Ministry of the Environment, Step by Step Guide for Emission Calculation, Record Keeping and Reporting for Airborne Contaminant Discharge, 2001.
64. Ontario Ministry of the Environment, <http://www.oetr.on.ca/oetr/index.jsp> - O.Reg. 194/05 Industrial Emissions – Nitrogen Oxides and Sulphur Dioxide, 2005.
65. Ontario Ministry of the Environment, Air Quality in Ontario 2005 Report, PIBs6041, 2006.
66. Ontario Ministry of the Environment,  
<http://www.ene.gov.on.ca/envision/general/leadership/index.htm>  
– Environmental Leaders, 2009.
67. Ontario Ministry of the Environment, <http://www.ene.gov.on.ca/en/air/aqo/index.php>  
– 2009.
68. Ontario Ministry of the Environment,  
<http://www.airqualityontario.com/reports/summary.cfm> - MOE, AQI Network, 2007.
69. Ontario Ministry of the Environment, <http://www.airqualityontario.ca/> - MOE Air Quality Index, Historical Data, 2007.
70. Ontario Ministry of the Environment, Air Quality in Ontario 2007 Report, 2008.
71. Ontario Ministry of the Environment: <http://www.ene.gov.on.ca/envision/scb/>  
– SCB results, February 2009.
72. Ontario Ministry of Transportation, Provincial Highways Traffic Volumes (AADT Only) 2005, 2008.
73. Owen B., Edmunds H.A., Carruthers D.J., Singles R. J., Prediction of Total Oxides of Nitrogen and Nitrogen Dioxide Concentrations in a Large Urban Area Using a New Generation Urban Scale Dispersion Model with Integral Chemistry Model, Atmospheric Environment, 34, 2000.
74. Perkins H.O., Air Pollution, 1974.
75. Quelo D., Vivien Mallet and Bruno Sportisse, Inverse Modelling of NO<sub>x</sub> Emissions at Regional Scale Over Northern France. Preliminary Investigation of the Second-Order Sensitivity, Journal of Geophysical Research, DOI:10:1029. 2005
76. Scire, J.S., Strimaitis D.G., Yamartino R.J., Model formulation and user's guide for the CALPUFF dispersion model, Sigma Research Corp., 1990.
77. Seika M., Harrison R.M., Metz N., Ambient Background Model (ABM): Development of an Urban Gaussian Dispersion Model and Its Application to London, Atmospheric Environment, 32, 11, 1998.
78. Seinfeld J.H., Atmospheric Chemistry and Physics of Air Pollution, A Willey Interscience Publications, New York, 1986.
79. Shum Y.S., Loveland W.D., Hewson E.W., The use of artificial Activable trace Elements to Monitor Pollutants Source Strengths and Dispersal Patterns, JAPCA, November 1976.
80. Siemiatycki M., Traffic Jam Move: Move Over Megaprojects; small, creative options unlock the grid, Alternative Journal, 33:1, 2007.
81. The Association of Municipalities of Ontario:  
<http://www.yourlocalgovernment.com/ylg/muniont.html> - total number of municipalities in Ontario, February 2009.
82. Toronto Public Health, Air Pollution Burden of Illness from Traffic in Toronto, Problems and Solutions", November 2007.
83. Transport Canada,  
<http://www.tc.gc.ca/programs/environment/UTEC/CacEmissionFactors.aspx> - 2007.
84. University of Toronto, Greater Toronto Area Gordon Count Summary, 2002.
85. US EPA, User's Guide for the Industrial Source Complex (ISC3) Dispersion Models, EPA-454/B-95-003b, 1995.
86. US EPA, [http://www.epa.gov/scram001/dispersion\\_prefrec.htm](http://www.epa.gov/scram001/dispersion_prefrec.htm) - US EPA, Preferred / Recommended Models, 2007.



87. Wesely M.L., Parameterization of Surface Resistances to Gaseous Dry Deposition in Regional-Scale Numerical Models, *Atmospheric Environment*, 23, 6, 1293-1304, 1989.
88. Willmott, C.J., On the validation of models, *Physical Geography*, 1981.
89. Venkatram A., Horst T.W., Approximating dispersion from a finite line source. *Atmospheric Environment*, 40, 2401-2408, 2006.
90. Venkatram A., Isakov V., Pankratz D., Yuan J., Relating plume spread to meteorology in urban areas, *Atmospheric Environment*, 39, 371-380, 2005.
91. Vila-Guerau de Arellano, A. Dosio, J.-F. Vinuesa, A.A. M. Holtslang, S. Galmarini, The dispersion of chemically reactive species in the atmospheric boundary layer, *Meteorology and Atmospheric Physics*, Austria, 23-38, 2004.
92. Xie X., Huang Z., Wang J., Impact of building configuration on air quality in street canyon, *Atmospheric Environment*, 39, 4519-4530, 2005.
93. Yang R., Ciccone A., Morgen C., Modelling Air Pollution Dispersion in Urban Canyons of Downtown Toronto, *Air and Waste Management Association*, 2007.
94. Yuan J., Venkatram A., Dispersion within a model urban area, *Atmospheric Environment*, 39, 4729-4743, 2005.

## NOMENCLATURE

$a_1$	constant, 1.257 [ ]
$a_2$	constant, 0.4 [ ]
$a_3$	constant, $0.55 \times 10^{-4}$ [ ]
$c_2$	air units conversion constant, $1 \times 10^{-6}$ [cm <sup>2</sup> /μm <sup>2</sup> ]
$C$	concentration [g/m <sup>3</sup> ]
$D$	decay [s <sup>-1</sup> ]
$d_p$	particle diameter, m, or perpendicular distance [m]
$D_B$	Brownian diffusivity of the pollutant in air [cm <sup>2</sup> /s]
$F$	Buoyancy parameter [m <sup>4</sup> /s <sup>3</sup> ]
$g$	acceleration due to gravity, 981 [cm/s <sup>2</sup> ]
$H$	effective height, $H_s + \Delta H$ [m]
$\Delta H$	plume rise, usually due to buoyancy of hot emissions [m]
$H_s$	height of the stack [m]
$k$	von Karman constant, 0.4 [ ]
$L$	Monin-Obukhov length [m]
$Q_p$	source strength, mass flowrate of the pollutant [g/s]
$R$	precipitation rate [mm/hr]
$r_a$	aerodynamic resistance [s/cm]
$r_d$	deposition layer resistance [s/cm]
$rh(0)$	relative humidity [%]
$S_c$	Schmidt number [ ]
$SO_2$	Sulfur Dioxides
$S_{CF}$	slip correction factor [ ]
$S_t$	Stokes number [ ]
$T_{ref}$	absolute temperature [K]
$U$	wind speed at H [m/s]
$U_{dri}$	wind direction (degrees)
$u^*$	surface friction velocity [cm/s]
$z$	height above ground [m]
$z_d$	deposition reference [m]
$z_o$	surface roughness [m]
$\sigma_y$	sigma y, dispersion coefficient in y-direction [m]
$\sigma_z$	sigma z, dispersion coefficient in z-direction [m]
$v_d$	deposition velocity [cm/s]
$v_g$	gravitational settling velocity [cm/s]
$\nu$	viscosity of air, $\sim 0.15$ [cm <sup>2</sup> /s]
$\rho$	particle density [g/cm <sup>3</sup> ]
$\rho_{air}$	air density, $1.2 \times 10^{-3}$ [g/cm <sup>3</sup> ]
$\mu$	absolute viscosity of air, $1.81 \times 10^{-4}$ [g/cm/s]
$x_2$	constant, $6.5 \times 10^{-6}$ [ ]
$x_f$	downwind distance from the source (maximum) final plume rise [m]
$\Lambda$	scavenging ratio [ ]
$\lambda$	coefficient [hr/smm]



## ABBREVIATIONS

ARSUS	Air dispersion model for the Road Sources in Urban areaS is a Gaussian air dispersion based model developed for this thesis
AERMOD	the American Meteorological Society/Environmental Protection Agency Regulatory Model Improvement Committee's Dispersion Model
AADT	Annual Average Daily Traffic
AQFS	National Air Quality Forecast System
AQI	Air Quality Index
CEPA	Canadian Environmental Protection Act
CFD	Computational Fluid Dynamics
CHRONOS	Canadian Regional and Hemispheric Ozone and NO <sub>x</sub> System
GHG	Greenhouse Gases Release
GTA	Greater Toronto Area
HDCV	Heavy duty commercial vehicles
ISC-PRIME	Industrial Source Complex – Short Term Model [Version 3]-Plume Rise Model Enhancements
LDPV-A	Light-duty passenger automobiles
LDPV-T	Light-duty passenger trucks
LDCV	Light-duty commercial vehicles
MOE	Ontario Ministry of the Environment
MTO	Ontario Ministry of Transportation
NCEP	National Centers for Environmental Prediction
NO <sub>x</sub>	Nitrogen Oxides
NOAA	National Oceanic and Atmospheric Administration
NPRI	National Pollutant Release Inventory
OMA	Ontario Medical Association
O.Reg. 127/01	Ontario Regulation 127/01, entitled “ Airborne Contaminant Discharge Monitoring and Reporting”
O.Reg. 194/05	Ontario Regulation 194/05, entitled “Industrial Emissions – Nitrogen Oxides and Sulphur Dioxide”
O.Reg. 346	Appendix A to Ontario Regulation 346, referred to the air dispersion model of the Ontario Regulation 346
O.Reg. 419/05	Ontario Regulation 419/05, entitled “Air Pollution – Local Air Quality”
PM <sub>2.5</sub>	particulate matter with diameter less than 2.5 micrometers
SCB	Sector Compliance Branch
SO <sub>x</sub>	Sulfur Oxides often interchangeably used with SO <sub>2</sub>
STAC	Selected Targets Air Compliance department
SWAT	Environmental SWAT Team
Troposphere	10 km off the earth's surface includes biosphere
UTM	Universal Transverse Mercator coordinate system
US EPA	United States Environmental Protection Act
WRF	Weather Research and Forecasting